



Cell Wall Metabolism in *Bacillus subtilis*

Karzan Rafiq Sidiq

A thesis submitted for the degree of **Doctor of Philosophy**

Newcastle University

Faculty of Medical Sciences

Institute for Cell and Molecular Biosciences

April 2016

Abstract

Cell wall is a unique and essential component of bacterial cell. It defines cell shape and protects cell from bursting through its own internal osmotic pressure. It also represents a significant drain on the cells resources, particularly in Gram positives, where the wall accounts for more than 20 % of the dry weight of the cell, and approximately 50 % of “old” cell wall is degraded and new material made to permit cell growth. After the discovery of penicillin, there has been active study of bacterial cell wall structure and metabolism, as it represents the major target for antibacterial compounds. The biosynthetic pathways for cell wall precursors has been well investigated in bacteria generally, but the coordination of cell wall metabolic processes and the fate of turnover cell wall materials have only been well characterised in Gram-negative bacteria (e.g. *Escherichia coli*). In Gram-positive bacteria, it has generally been accepted that the old wall is released from the surface and lost to the environment during growth, with apparent recycling of this material during stationary phase for *Bacillus subtilis*. It is also known that the Gram-positive wall is subject to significant post-synthetic processing, involving the linkage of wall teichoic acids and the cleavage of molecules from the structure, e.g. D-alanine, although the function of these is unclear. Understanding the importance of these processes has relevance for both the pathogenicity and biotechnological use of bacteria, as well as for understanding bacterial cell biology. As it is known that the peptidoglycan fragments (e.g. muropeptides) induce the innate immune response in higher organisms and so act as a signal for infection, particularly for Gram-positive bacteria. Thus, understanding how they are generated and recycled by the bacteria may offer potential insights into novel therapeutics, also the accumulation of cell wall muropeptides should be avoided in biotechnological products. In this thesis, the D-alanine metabolism was manipulated to understand the mechanistic details of cell wall metabolism and D-alanine recycling in *B. subtilis*, using genetic, biochemical, bioinformatics and fluorescent microscopy approaches. Through these analyses, a D-alanine transporter (DatA, formerly YtnA) was identified by genetic screening. The roles of DatA and the carboxypeptidases, LdcB and DacA, in recycling of cell wall derived D-alanine have experimentally been confirmed. We also found that D-alanine aminotransferase (Dat) can act to synthesis D-alanine under certain conditions. From the data obtained a model for peptidoglycan assembly (coordinated synthesis and turnover) during growth of *B. subtilis* has been developed to take into account the various aspects of cell wall metabolism.

Acknowledgments

Firstly, I would like to express my sincere gratitude to my supervisor, Dr. Richard Daniel, for his continuous support, patience, motivation, enthusiasm, and immense knowledge. I really appreciated your guidance, valuable suggestions and always opened door of your office over the course of the research as well as writing of the thesis. Literally, I was a lucky PhD student for having you as a supervisor.

I am grateful to Prof. Bert van den Berg for his advice and for hosting me to over-produce and purify membrane protein in his laboratory, Newcastle University. My sincere thanks also go to Prof. David Thwaites and Dr. Noel Edwards for their trial to test D-alanine transport, by DatA, in *Xenopus* oocyte.

A big thank to Dr. Ling Juan Wu, which generously answered my questions and helped me with Time-lapse microscopy. Also, I thank Dr. Seoungjun Lee and Dr. Henrik Strahl for their help with TIRF microscopy.

I would also like to thank my mother, my siblings and my wife, Shokhan, for her great and precious social support and encouragement abroad.

I also thank my friends Dr. Hadi Mohammad and Dr. Adham Amin for their help and suggestions.

Finally, I must acknowledge my government, Kurdistan regional government-IRAQ, for funding my PhD study and offering me this golden opportunity in my academic life.

Kurdistan, your independence is my hope and dream.

Table of contents

Table of Contents	i
List of figures	v
List of tables	vii
Abbreviations	1
Chapter 1. Introduction	5
1.1 Peptidoglycan	7
1.1.1 Peptidoglycan precursor biosynthesis	7
1.1.2 Peptidoglycan biosynthesis	12
1.1.3 Modification of peptidoglycan	15
1.1.3.1 Swapping of D-alanine residues	15
1.1.3.2 Carboxypeptidation of peptidoglycan	18
1.1.4 Assembly and architecture of peptidoglycan	21
1.1.5 Peptidoglycan turnover	23
1.1.6 Peptidoglycan recycling	26
1.1.7 Roles of MreB isomers and LD-endopeptidases in cell shape maintenance and peptidoglycan synthesis.....	29
1.2 Teichoic Acids.....	31
1.2.1 Wall Teichoic Acid	31
1.2.2 Lipoteichoic Acid.....	33
1.2.3 Modification of teichoic acids.....	33
1.3 Amino acid uptake systems in bacteria	37
Chapter 2. Materials and methods	40
2.1 Solutions and Growth media	40
2.2 Bacterial strains collection	40
2.3 Plasmids.....	45
2.4 Media supplements.....	46
2.4.1 Amino acids, inducers and substrates	46
2.4.2 Antibiotics	47

2.5	Oligonucleotides.....	47
2.6	General methods.....	48
2.6.1	Extraction of genomic DNA (gDNA).....	48
2.6.2	Extraction of plasmid DNA.....	48
2.6.3	Polymerase chain reaction (PCR).....	48
2.6.4	Restriction digestion of DNA.....	48
2.6.5	Purification of PCR and restriction digestion products.....	48
2.6.6	Agarose gel electrophoresis.....	48
2.6.7	Purification of DNA band from agarose gel.....	49
2.6.8	Dephosphorylation of plasmid DNA.....	49
2.6.9	Ligation of DNA.....	49
2.6.10	DNA sequencing of cloned genes.....	49
2.6.11	Extraction of total RNA.....	49
2.6.12	Making complementary DNA (cDNA).....	49
2.6.13	Extraction of total cell protein and Polyacrylamide gel electrophoresis (SDS-PAGE).....	49
2.6.14	Coomassie staining of SDS-PAGE gel.....	50
2.6.15	Western blotting.....	50
2.6.16	Over-production and purification of membrane protein.....	51
2.6.17	Preparation of membrane vesicles.....	51
2.6.18	Transformation.....	52
2.6.18.1	Transformation of <i>B. subtilis</i>	52
2.6.18.2	Transformation of <i>E. coli</i>	52
2.6.19	Microscopy.....	53
2.6.19.1	Fluorescent Microscopy.....	53
2.6.19.2	Time-lapse microscopy.....	53
2.6.20	Immunofluorescence assay.....	53
2.7	Gene knockout (deletion) in <i>B. subtilis</i>	54
2.8	Plasmid constructs.....	55

2.9	Quantitative measurement of D-alanine in culture supernatant by RP-HPLC	57
2.9.1	Growth conditions	57
2.9.2	Culture sample processing	57
2.9.3	RP-HPLC analysis conditions	58
2.10	Radioactive [¹⁴ C] D-alanine labelling of cell wall	58
2.10.1	Radioactive incorporation assay	58
2.10.2	Radioactive depletion (turnover) assay	59
2.10.3	Measurement of radioactivity in culture supernatant	59
2.11	Cell wall labelling with fluorescent D-amino acid (FDAA)	60
2.11.1	Fluorescent D-amino acid incorporation assay	60
2.11.2	Fluorescent D-amino acid depletion (turnover) assay	60
2.11.3	Quantitative analysis of NADA labelled cells	61
Chapter 3.	Analysis of D-alanine metabolism in <i>B. subtilis</i>	62
3.1	Introduction	62
3.2	Results	65
3.2.1	Characterisation of D-alanine auxotroph <i>B. subtilis</i>	65
3.2.2	<i>B. subtilis</i> has almost equal amount of D-alanine in peptidoglycan and teichoic acids	67
3.2.3	Cell wall synthesis in the absence of carboxypeptidases	71
3.2.4	Identification of a D-alanine transporter in <i>B. subtilis</i>	75
3.2.4.1	A genetic screen for D-alanine transporter	75
3.2.4.2	Complementation of <i>datA</i>	79
3.2.4.3	<i>B. subtilis</i> transports exogenous D-alanine via DatA	83
3.2.5	D-alanine aminotransferase (Dat, formerly YheM) contributes to D-alanine synthesis in minimal medium	85
3.3	Discussion	88
Chapter 4.	Characterisation of D-alanine transporter (DatA)	92
4.1	Introduction	92
4.2	Results	95

4.2.1	Is <i>datA</i> gene a single transcription unit?	95
4.2.2	Conservation of DatA protein	97
4.2.3	Biochemical characterisation and substrate specificity of DatA.....	101
4.2.3.1	Membrane topology of DatA.	101
4.2.3.2	Expression of DatA protein in heterogeneous hosts.	104
4.2.3.3	L-alanine interferes in D-alanine transport.	107
4.2.3.4	Transport of D-cycloserine in <i>datA</i> strain.....	109
4.2.4	Recycling of cell wall derived D-alanine in <i>B. subtilis</i>	111
4.2.4.1	Cross feeding assay	111
4.2.4.2	RP-HPLC analysis of culture supernatant.....	113
4.2.4.3	Is there a second uptake system for D-alanine?	117
4.3	Discussion	119
Chapter 5. Peptidoglycan assembly in <i>B. subtilis</i>		123
5.1	Introduction	123
5.2	Results	125
5.2.1	Cell wall turnover in the absence of carboxypeptidases	125
5.2.2	Dynamics of peptidoglycan carboxypeptidation in <i>B. subtilis</i>	129
5.2.3	Role of penicillin binding proteins (PBPs) in ‘‘D-alanine swapping’’ ...	131
5.2.4	Peptidoglycan synthesis and turnover are coordinated.	136
5.2.5	Dynamics of peptidoglycan assembly in <i>B. subtilis</i>	138
5.2.6	Pattern of cell wall synthesis and turnover throughout generations of <i>B. subtilis</i> . 144	
5.3	Discussion	146
Chapter 6. General discussion and future directions.....		155
References.....		163
Appendices.....		187
Appendix A. Solutions and buffers		187
Appendix B. Growth media		190
Appendix C. Oligonucleotides		191
Appendix D. Distribution of DatA (formerly YtnA) homologous proteins.....		195

Appendix E. Transport of D-alanine by DatA protein translated in oocytes of <i>Xenopus laevis</i>	202
Publications.....	203

List of Figures

Figure 1.1 The structures of bacterial cell wall.....	6
Figure 1.2 Gram-positive peptidoglycan biosynthesis.....	10
Figure 1.3 Biosynthesis of D-alanine and D-glutamate in <i>B. subtilis</i>	11
Figure 1.4 D-alanine swapping in peptidoglycan of <i>E. coli</i> (A) and <i>B. subtilis</i> (B).....	17
Figure 1.5 Carboxypeptidation of peptidoglycan.....	20
Figure 1.6 Peptidoglycan hydrolases (Autolysins).	25
Figure 1.7 Peptidoglycan metabolism in <i>E. coli</i>	28
Figure 1.8 Mechanisms of teichoic acids modification with D-alanine	36
Figure 1.9 Solute transport across plasma membrane.....	39
Figure 3.1 Growth characteristics of wild type versus <i>alrA</i> strain.....	66
Figure 3.2 The <i>dltA-D</i> strain requires less D-alanine for growth.....	69
Figure 3.3 Growth and cell morphology	73
Figure 3.4 The growth curve and growth rate of D-alanine auxotroph strains	73
Figure 3.5 Cell wall modification by carboxypeptidases in vegetative <i>B. subtilis</i>	74
Figure 3.6 Growth and morphology of <i>datA</i> strain	77
Figure 3.7 Growth of KS30 and its parental strains on minimal and nutrient media.	78
Figure 3.8 Complementation of <i>datA</i> gene	81
Figure 3.9 Loss of D-alanine transport in <i>datA</i> strain.....	82
Figure 3.10 Role of DatA in the transport of D-alanine in <i>B. subtilis</i>	84
Figure 3.11 Growth of amino acid racemase mutants on minimal media (MM).....	87
Figure 4.1 The transcription profiles and expression of <i>datA</i> gene (formerly <i>ytnA</i>) in <i>B. subtilis</i>	94

Figure 4.2 Transcription analysis of <i>datA</i> gene	96
Figure 4.3 Phylogenetic distribution of DatA (formerly YtnA)	98
Figure 4.4 The sequence alignment of DatA and PRK11049 model.....	99
Figure 4.5 Membrane topology and localisation of DatA	103
Figure 4.6 D-alanine transport by membrane vesicles.....	106
Figure 4.7 Amino acid competition assay.....	108
Figure 4.8 D-cycloserine sensitivity of <i>datA</i> strain.....	110
Figure 4.9 Cross-Feeding Assay	112
Figure 4.10 Standard curve for D-alanine quantification in LB media.....	115
Figure 4.11 RP-HPLC analysis for D-alanine quantification in culture supernatants ..	116
Figure 4.12 Transport of D-alanine by <i>datA</i> strain in minimal media (MM).	118
Figure 5.1 Cell wall turnover in exponentially growing <i>B. subtilis</i>	127
.....	128
Figure 5.3 Localisation of DacA protein.....	130
Figure 5.4 Immunofluorescence microscopy of LdcB and DacA localisations.....	130
Figure 5.5 Peptidoglycan modification in carboxypeptidase mutant strains of <i>B. subtilis</i>	133
Figure 5.6 The effect of Pencillin G and D-alanine on peptidoglycan modification ...	134
Figure 5.7 NADA labelling of PBPs double mutant strains	135
Figure 5.8 Coordination of peptidoglycan synthesis and turnover in <i>B. subtilis</i>	137
Figure 5.9 Growth curves of <i>B. subtilis</i>	140
Figure 5.10 Time-lapse microscopic images of NADA labelled <i>B. subtilis</i>	140
Figure 5.11 Tracking of peptidoglycan assembly (coordination of peptidoglycan synthesis and turnover) in <i>B. subtilis</i>	141
Figure 5.12 Depletion of cell division proteins, FtsZ and FtsL, in <i>B. subtilis</i>	142
Figure 5.13 The effect of <i>lytE</i> deletion on cell wall turnover in <i>B. subtilis</i>	143

Figure 5.14 The NADA labelling of KS15 (<i>ΔdacA::spc</i>) strain throughout three generations	145
Figure 5.15 The proposed dynamics of peptidoglycan carboxypeptidation	147
Figure 5.16 A schematic model illustrates the dynamics of peptidoglycan assembly (coordinated cell wall synthesis and turnover) at the lateral cell wall of <i>B. subtilis</i>	152
Figure 5.17 Proposed mechanisms of peptidoglycan metabolic processes in the lateral cell wall of <i>B. subtilis</i>	153
Figure 5.18 A schematic diagram showing the pattern of peptidoglycan synthesis and turnover throughout generations of <i>B. subtilis</i>	154
Figure 6.1 Proposed D-alanine and peptidoglycan recycling pathways in <i>B. subtilis</i> ..	159

List of tables

Table 1.1 The list of identified penicillin-binding proteins (PBPs) of <i>B. subtilis</i> 168....	14
Table 2.1 Strains collection.....	40
Table 2.2 Plasmid constructs.....	45
Table 2.3 Amino acids, inducers and substrates	47
Table 2.4 Antibiotics details	47
Table 2.5 Pump and run parameters of RP-HPLC analysis.....	58
Table 3.1 The physical and chemical treatments of [^{14}C] labelled cells.....	70
Table 3.2 A selection of putative amino acids transport mutants in Japanese strains collection.....	76
Table 4.1 The properties of few proposed D-alanine transporter in bacteria.....	100

Abbreviations

ABC	ATP binding cassette
ATP	adenosine triphosphate
BSA	bovine serum albumin
<i>B. subtilis</i>	<i>Bacillus subtilis</i>
<i>C. crescentus</i>	<i>Caulobacter crescentus</i>
CAA	casamino acids
cDNA	complementary deoxyribonucleic acid
CH	casein hydrolysate
DAPI	4,6-diamidino-2-phenylindole
DDM	<i>n</i> -Dodecyl β -D-maltoside
dH2O	deionised water
DNA	deoxyribonucleic acid
DPM	disintegration per minute
DTT	dithiothreitol
<i>E. coli</i>	<i>Escherichia coli</i>
EDTA	ethylenediaminetetraacetic acid
e.g	<i>exempli gratia</i> (for example)
<i>et al.</i>	<i>et alii</i> (and others)
FDAA	Fluorescent D-amino acid
GalNAc	<i>N</i> -acetylgalactosamine
gDNA	genomic deoxyribonucleic acid
GFP	Green Fluorescent Protein
GlcNAc	<i>N</i> -acetylglucosamine

g	gram
h	hour / hours
H ⁺	proton / hydrogen ion
HMW	high molecular weight
HPLC	high performance liquid chromatography
IgG	Immunoglobulin gamma
IPTG	isopropyl β-D-1 -thiogalactopyranoside
kDa	kilo Dalton
kb	kilo base
kpsi	kilopound per square inch
LB	Luria-Bertani broth
L	litre
LMW	low molecular weight
LTA	lipoteichoic acid
M	molar
<i>m</i> -A2pm	<i>meso</i> -2,6-diaminopimelic acid
Mg ²⁺	magnesium ion
mg	milligram
ml	millilitre
μl	microlitre
MM	minimal medium
mm	millimeter
μm	micrometer
mM	millimolar

μM	micromolar
min	minute / minutes
ms	millisecond / milliseconds
MR	Marfeys's reagent (1-fluoro-2-4-dinitrophenyl-5-L-alaninamide)
MurNAc	<i>N</i> -acetylmuramic acid
MWCO	molecular weight cut-off
NA	nutrient agar
Na^{2+}	sodium ion
NaCl	sodium chloride
NADA	Boc-D-2,3-diaminopropionic acid
OD_{600}	optical density measured at a wavelength of 600 nm
Oligo / oligos	oligonucleotide / oligonucleotides
PAB	Penassay broth
PAGE	polyacrylamide gel electrophoresis
PMSF	phenylmethylsulfonyl fluoride
PBP	penicillin binding protein
PBS	phosphate buffered saline solution
PCR	polymerase chain reaction
PDB	protein database
PLP	pyridoxal 5'-phosphate
PTM	pre-transformation media
RNA	ribonucleic acid
RP-HPLC	reverse phase- high performance liquid chromatography
rpm	round per minute
SDS	sodium dodecyl sulfate
SMM	Spizizen minimal medium

sp. / spp.	species
<i>S. aureus</i>	<i>Staphylococcus aureus</i>
Na ⁺	sodium ion
SSC	sodium chloride-sodium citrate solution
TA	teichoic acid
UDP	undecaprenyl phosphate
C55-P	undecaprenyl phosphate derivative
WTA	wall teichoic acid
X-Gal	5-bromo-4-chloro-3-indolyl-β-D-galactopyranoside
°C	degree centigrade

Chapter 1. Introduction

Bacteria are prokaryotic unicellular microorganisms, whose cellular components are simpler comparing to complex eukaryotic cells. Bacterial cell is uniquely surrounded by a mesh-like structure, called cell wall, which maintains cell shape and prevents cell disruption due to turgor pressure (Koch, 2006; Muchová *et al.*, 2011). Based on the differences in their cell wall structure, bacteria are categorised into two major groups, Gram-negatives (e.g. *E. coli*) and Gram-positives (e.g. *B. subtilis*). The cell wall of Gram-negative bacteria (Figure 1.1A) consists of an outer membrane and at least a single layer of peptidoglycan (3-6 nm thick), located in a periplasmic space between inner and outer membranes (Matias *et al.*, 2003; Gan *et al.*, 2008). In contrast, the cell wall of Gram-positive bacteria (Figure 1.1B) is composed of multi-layered peptidoglycan (10-20 layers) without outer membrane (Foster and Popham, 2002). Gram-positive cell wall also contains two types of anionic polymers, which are wall teichoic acid (WTA) and lipoteichoic acid (LTA). The wall teichoic acid is attached to peptidoglycan, whereas lipoteichoic acid is anchored to cytoplasmic membrane at its base and extended through peptidoglycan (Neuhaus and Baddiley, 2003). Bacterial cell wall also has clinical importance, because peptidoglycan is the most suitable target of antibiotics (e.g. β -lactams) in Gram-positive pathogens. The structure and metabolism of bacterial cell wall have been investigated since the middle of 20th century (Martin, 1966). However, there are still outstanding questions regarding cell wall metabolism and peptidoglycan assembly in Gram-positive bacteria. Continuous investigations of cell wall will provide further insights for developing new antibacterial drugs and controlling of infections, caused by antibiotic-resistant bacteria. Besides, further understanding of cell wall metabolism is important for biotechnological applications. The focus of this study is to further understand cell wall metabolic processes in particular recycling of cell wall derived D-alanine and the dynamics of peptidoglycan assembly in *B. subtilis*, which is a Gram-positive, rod-shaped, aerobic, soil inhabitant and endospore-forming bacterium (Oggioni *et al.*, 1998; Tam *et al.*, 2006). Our current understanding of cell wall structure and metabolism in *B. subtilis* is reviewed in the following sections.

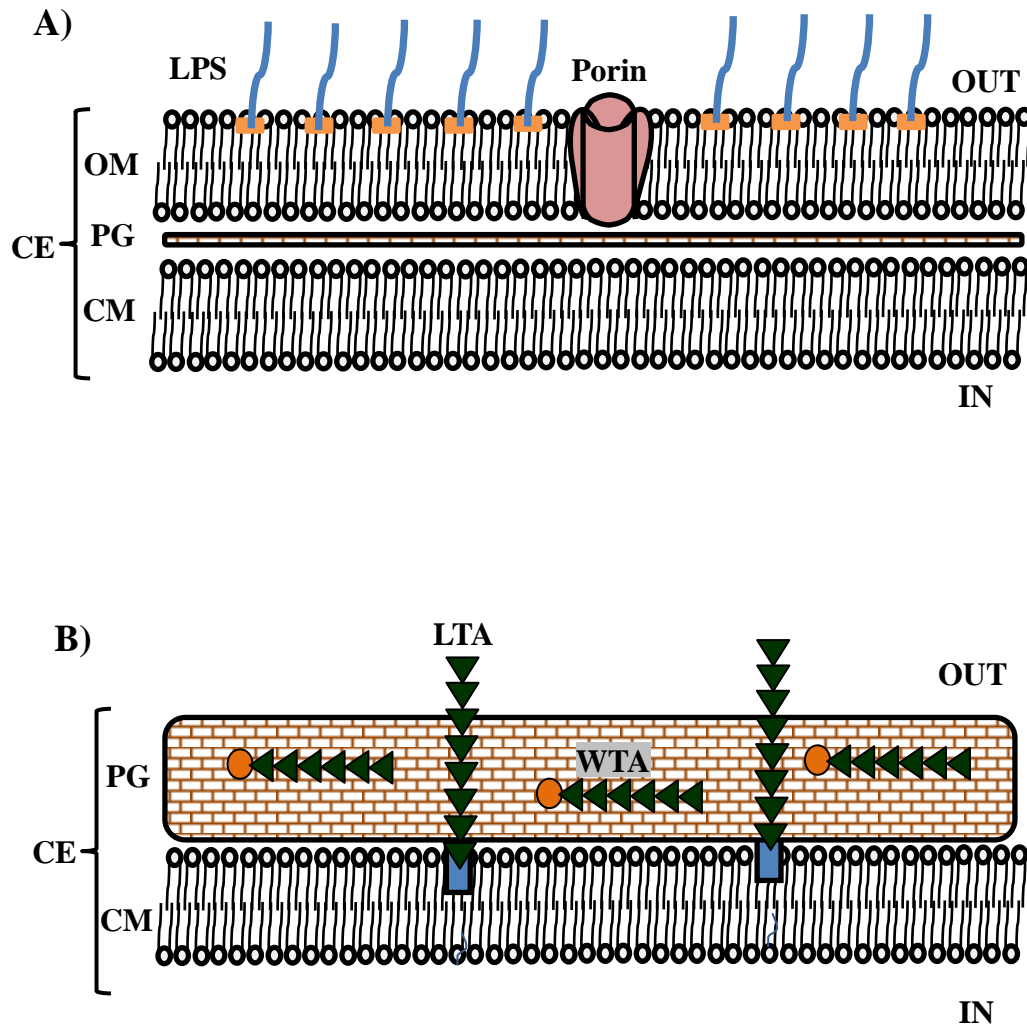


Figure 1.1 The structures of bacterial cell wall. A) Gram-negative cell wall (e.g. *E. coli*). B) Gram-positive cell wall (e.g. *B. subtilis*). See the text for details.

PG: peptidoglycan; CM: cell membrane; OM: outer membrane; CP: cell envelop;
 LPS: lipopolysaccharide; LTA: lipoteichoic acid; WTA: wall teichoic acid.

1.1 Peptidoglycan

Peptidoglycan (murein) consists of cross-linked glycan strands, which are arranged around bacterial cell membrane (Figure 1.2). The peptidoglycan of *B. subtilis* is 30-40 nm thick (Smith *et al.*, 2000) and 20 times thicker than the Gram-negative peptidoglycan (Shockman and Barrett, 1983). Although the chemical structure of murein is almost identical among bacteria, the glycan strands are slightly different with regard of *N* or *O* acetylation and stem peptide composition (Holtje, 1998). The glycan strands consist of alternating two aminosugars, *N*-acetylglucosamine (GlcNAc) and *N*-acetylmuramic acid (MurNAc), which are held together by β (1-4) glycosidic bonds (van Heijenoort, 2001). Peptide side chains extend from the lactyl groups of MurNAc residues. In *E. coli* and *B. subtilis*, the stem peptides comprise of L-alanine- D-glutamate- *meso*-2,6-diaminopimelic acid (*m*-A2pm)- D-alanine- D-alanine (van Heijenoort, 1994). However, the free carboxylic group of *m*-A2pm residues are amidated in the case of *B. subtilis* (Atrih *et al.*, 1999). The adjacent glycan strands are covalently cross-linked through the penultimate D-alanine residue (4th D-alanine residue) of one glycan strand and the *m*-A2pm residue of the adjacent glycan strand. However, some bacteria e.g *Staphylococcus aureus* has L-lysine instead of *m*-A2pm and the cross-links are mediated by a short peptide (Penta-glycine) (Vollmer *et al.*, 2008a).

1.1.1 Peptidoglycan precursor biosynthesis

The peptidoglycan precursor (lipid II) is synthesised via a complex sequence of enzymatic steps in cell cytoplasm (Figure 1.2) (van Heijenoort, 1994). Firstly, Undecaprenyl diphosphate-*N*-acetylglucosamine (UDP-GlcNAc) is synthesised from fructose 6-phosphate. This is followed by the synthesis of UDP-*N*-acetylmuramic acid (UDP-MurNAc) from UDP-GlcNAc, this reaction is catalysed by MurA and MurB enzymes. Secondly, the amino acids (L-alanine, D-glutamate, *m*-A2pm and D-alanine-D-alanine dimer) are attached to UDP-MurNAc one by one by the amino acid ligases (MurC, MurD, MurE, and MurF) respectively (Barreteau *et al.*, 2008). The D-alanine molecules are already dimerised by D-alanine-D-alanine ligase (Ddl) before linking to the premature peptidoglycan precursors (Walsh, 1989). Thirdly, Lipid I is formed when UDP-MurNAc- peptapeptide is covalently attached to plasma membrane via an undecaprenyl-phosphate molecule by MraY. Finally, the peptidoglycan building block (Lipid II) is yielded by MurG through joining Lipid I to a GlcNAc molecule (Bhavsar and Brown, 2006; Barreteau *et al.*, 2008).

Bacteria uniquely require two types of D-amino acids (D- alanine and D-glutamate) for synthesising peptidoglycan precursor, Lipid II (Holtje, 1998). D-amino acids are synthesised from the corresponding L-amino acids either by stereochemistic inversion of α -carbon, which is catalysed by amino acid racemase or epimerase (Figure 1.3A) (Yoshimura and Esak, 2003; Radkov and Moe, 2014) or stereospecific amidation of α -ketoacid, which is catalysed by D-amino acid aminotransferase (Figure 1.3B). These two mechanisms of D-alanine and D-glutamate production are reversible (Radkov and Moe, 2014). D-alanine is a crucial amino acid for cross-linking of glycan strands and maintaining the integrity of peptidoglycan (Dul and Young, 1973). *B. subtilis* synthesises D-alanine from L-alanine in a bidirectional reaction, which is catalysed by alanine racemase (Figure 1.3A) (Walsh, 1989). The alanine racemase enzyme needs pyridoxal 5'-phosphate (PLP) as a cofactor (Yoshimura and Esak, 2003; Radkov and Moe, 2014). The two characterised alanine racemases in *B. subtilis* are AlrA and AlrB, which are expressed during vegetative growth and sporulation respectively (Ferrari *et al.*, 1985; Pierce *et al.*, 2008). The D-alanine auxotroph *B. subtilis* (*alrA*), is unable to grow in common rich media, which are normally free of D-alanine. This is due to the inability to synthesise cell wall, which is followed by cell lysis. In contrast, it was reported that *alrA* null strain can grow in minimal medium (MM) without addition of D-alanine (Ferrari *et al.*, 1985). The second essential D-amino acid for peptidoglycan synthesis is D-glutamate (Kimura *et al.*, 2004). Before the discovery of glutamate racemases, it was thought that *B. subtilis* synthesises D-glutamate via transamination of D-alanine with α -ketoglutarate (Thorne *et al.*, 1955). However, it was reported that *B. subtilis* also produces D-glutamate from L-glutamate by at least two characterised glutamate racemases, RacE and YrpC (Ashiuchi *et al.*, 1998; Ashiuchi *et al.*, 1999). The *racE* gene is expressed in both rich medium and MM, but the expression of *yrpC* gene only occurs in MM. It was also experimentally confirmed that the *racE* gene is essential for growth in rich media (Kimura *et al.*, 2004). The glutamate racemases do not require PLP as a coenzyme (Yoshimura and Esak, 2003).

Bacteria apparently utilise D-amino acid aminotransferase in D-alanine and D-glutamate biosynthesis (Figure 1.3B) (Radkov and Moe, 2014). This enzymatic activity was historically detected in the cellular extract of *B. subtilis* (Thorne *et al.*, 1955) and *B. licheniformis* (Kuramitsu and Snoke, 1962). The D-alanine-D-glutamate aminotransferases were purified and characterised in *B. subtilis* (Martinez-Carrion and Jenkins, 1965) and *B. sphaericus* (Yonaha *et al.*, 1975). These enzymes obviously

catalysed the transamination from D-alanine and D-glutamate (amino donors) to α -ketoglutarate and pyruvate (amino acceptors) respectively (Figure 1.3B) (Yonaha *et al.*, 1975). The D-amino acid aminotransferases are effectively inhibited by D-cycloserine and Gabaculine compounds (Yonaha *et al.*, 1975; Soper and Manning, 1981). The complete genome sequence of *B. subtilis* showed *dat* (or *yheM*) gene, which encodes a putative D-alanine aminotransferase (Dat or YheM) (Kunst *et al.*, 1997). The Dat protein of *B. subtilis* showed 42 % sequence homology to Dat protein in *B. sphaericus* (Fotheringham *et al.*, 1998). More recently, it was reported that Dat did not recover the growth of a *B. subtilis* strain, which was mutated for both glutamate racemase genes (*racE* and *yrpC*), suggesting that Dat does not have significant role in D-glutamate synthesis (Kimura *et al.*, 2004). Whilst the physiological roles of D-alanine and D-glutamate racemases have been well understood in many bacteria, but the physiological functions of D-amino acid aminotransferases are still unclear.

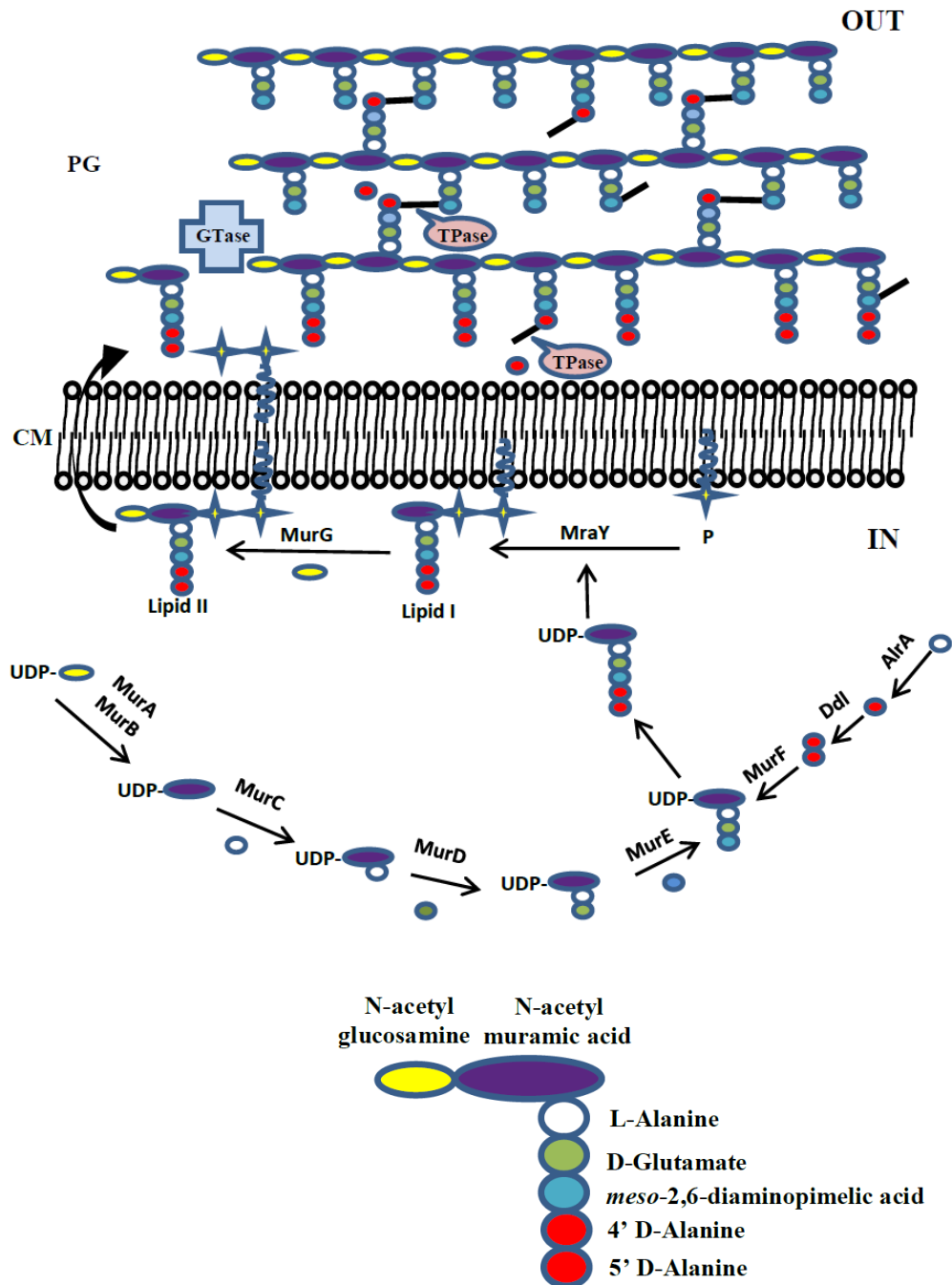
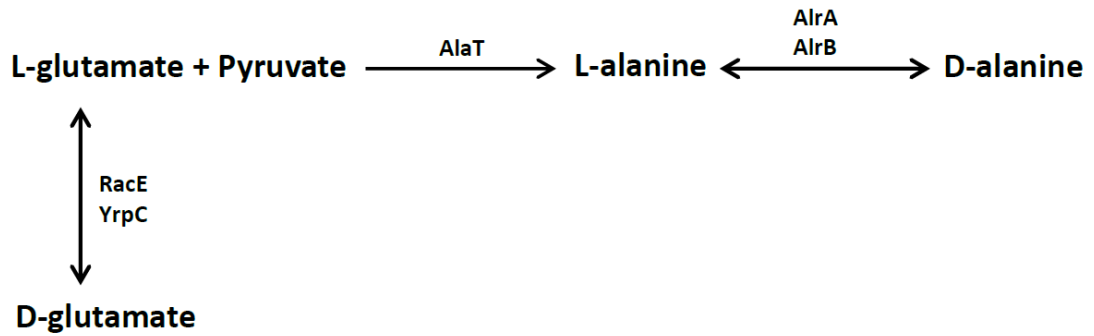


Figure 1.2 Gram-positive peptidoglycan biosynthesis. See the text for details. The idea of the figure is adapted from (Bhavsar and Brown, 2006) with some modification.

A)



B)

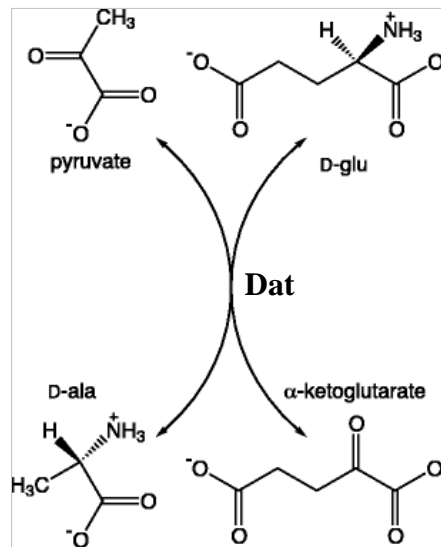


Figure 1.3 Biosynthesis of D-alanine and D-glutamate in *B. subtilis*. A) Synthesis of the D-amino acids (D-alanine and D-glutamate) by racemase enzymes. B) Synthesis of the D-amino acids by D-amino acid aminotransferase (Dat), the figure is copied from (Radkov and Moe, 2014). See the text for details of the figures.

1.1.2 Peptidoglycan biosynthesis

Peptidoglycan synthesis involves the formation of glycan strands (polymerisation of Lipid II), and then the cross-linking of the glycan strands (Figure 1.2). These two processes occur on the cell wall side of plasma membrane (van Heijenoort, 1994). The mature peptidoglycan precursor, Lipid II, is flipped out of the plasma membrane, where they are added to the reduced ends of the newly growing glycan strands by glycosyltransferases (Ward and Perkins, 1973). The glycan strands are cross-linked via their stem peptides to produce mature peptidoglycan (Sauvage *et al.*, 2008). In cross-linking reaction, the carboxyl group of 4th D-alanine residue of one stem peptide is usually attached to the amino group of *m*-A2pm on the adjacent stem peptide by transpeptidases (Vollmer *et al.*, 2008a). During transpeptidation, only penta-stem peptides serve as donor side chains and lose their terminal D-alanine residues (5th residue) upon cross-linking. However, tri-, tetra- and even penta-stem peptides function as acceptor peptide side chains (Holtje, 1998; Egan and Vollmer, 2013). Not all the stem peptides are cross-linked, and only about 30-40 % of them were found to be cross-linked in vegetative *B. subtilis* (Atrih *et al.*, 1999; Sekiguchi and Yamamoto, 2012). It was observed that the number of cross-bridges increases in the stationary growing cells of *B. subtilis* (Atrih *et al.*, 1999).

The polymerisation and cross-linking of glycan strands are carried out by penicillin-binding proteins (PBPs) (Figure 1.2) (McPherson and Popham, 2003; Wei *et al.*, 2003). The biochemical and genetic analyses have identified several PBPs in *B. subtilis* (Table 1.1). Apparently, the PBPs and their encoding genes are named in a complex system of nomenclature. The PBPs of *B. subtilis* 168 are classified into high molecular weight (HMW) and low molecular weight (LMW) PBPs. Here, we have only discussed HMW PBPs, but the LMW PBPs have been discussed in (section 1.1.3.2). The HMW PBPs are also categorised into class A and class B (Table 1.1) (Sauvage *et al.*, 2008). The class A HMW PBPs are bifunctional, which exhibit glycosyltransferase activity at N-terminal domain and transpeptidase activity at C-terminal domain. However, the class B HMW PBPs only catalyses transpeptidation reaction (McPherson *et al.*, 2001). As some of the class A and class B HMW PBPs are produced during sporulation, we have just focused on the vegetative PBPs. The complete genome sequence of *B. subtilis* revealed four proposed class A HMW PBPs genes (Table 1.1) (Kunst *et al.*, 1997). The deletion of all the four genes was not lethal in *B. subtilis*, suggesting that at least one glycosyltransferase (s) is still left to be discovered (McPherson and Popham, 2003). The

class A HMW PBPs also demonstrated functional redundancies in *B. subtilis* (Popham and Setlow, 1996; McPherson *et al.*, 2001). The two vegetative class A HMW PBPs are PBP1 and PBP4 (Popham and Setlow, 1996). PBP1 plays role in cell division (Scheffers and Errington, 2004) and its absence (*ponA* null) slows down growth rate and alters cell morphology (McPherson and Popham, 2003). The *ponA* mutant requires more divalent cation (Mg^{2+}) for having a better growth (Murray *et al.*, 1998). The immunofluorescence technique and GFP-tagging were used to examine the localisation of PBP1, it was observed that PBP1 is localised at the cell septum (Pedersen *et al.*, 1999; Scheffers *et al.*, 2004). The second class A HMW PBPs is PBP4, which plays role in cell wall synthesis during vegetative growth. The PBP4 is localised at the cell division septum and unevenly at the lateral cell edges (Scheffers *et al.*, 2004).

The class B HMW PBPs (Table 1.1) were also investigated in *B. subtilis*. Strikingly, PBP2b is the only essential PBP in *B. subtilis*. The PBP2b is required for cell wall synthesis at division site (Yanouri *et al.*, 1993; Daniel *et al.*, 1996; Daniel *et al.*, 2000). Fluorescence microscopy (immunofluorescence and GFP-tagging) showed that PBP2b is localised specifically to the cell septa in both vegetative and sporulating cells (Daniel *et al.*, 2000; Scheffers *et al.*, 2004). In addition, PBP2a and PbpH are mainly expressed during vegetative growth of *B. subtilis* (Murray *et al.*, 1997; Wei *et al.*, 2003). The lack of both PBP2a and PbpH is lethal, suggesting that they play redundant roles in lateral cell wall synthesis and rod shape determination (Wei *et al.*, 2003). The GFP tagged PBP2a and PbpH were seen at both the cell septum and the cylindrical part of the cell (Scheffers *et al.*, 2004). Moreover, PBP3 is identified as a member of class B HMW PBPs in *B. subtilis*. PBP3 is primarily produced during exponential growth and at lower level during sporulation (Murray *et al.*, 1996). The GFP-PBP3 was localised at the cell periphery in granular pattern (Scheffers *et al.*, 2004). The lack of PBP3 did not cause any detectable phenotypes during both vegetative growth and sporulation, so its role is unknown (Murray *et al.*, 1996).

Bacteria	PBP name	Encoding gene	Class	Molecular weight (kDa)		Predicted functional activity	Expression
<i>B. subtilis</i> 168	PBP1 ^φ	<i>ponA</i>	A	99.0	high	glycosyltransferase and transpeptidase	V and Spo
	PBP2c	<i>pbpF</i>		79.0			Spo
	PBP4	<i>pbpD</i>		70.0			V
	PBP2d	<i>pbpG</i>		71.0			Spo
	PBP3	<i>pbpC</i>	B	74.0		transpeptidase	V
	PBP2a	<i>pbpA</i>		79.0			V and Spo
	PBP2b	<i>pbpB</i>		79.0			V
	PBP4b	<i>pbpH</i>		76.0			V and Spo
	SpoVD	<i>spoVD</i>		71.0			Spo
	PBP4b	<i>yrrR (pbpI)</i>		65.0			Spo
	PBP5 (DacA)	<i>dacA</i>	C	48.0	low	carboxypeptidase	V
	PBP5* (DacB)	<i>dacB</i>		42.0			Spo
	PBP4a (DacC)	<i>dacC</i>		52.0			S
	DacF	<i>dacF</i>		43.0			Spo
	PBP4* ^φ	<i>pbpE</i>		51.0		V	
	PbpX ^φ	<i>pbpX</i>		43.0		V	
					endopeptidase	V	

Table 1.1 The list of identified penicillin-binding proteins (PBPs) of *B. subtilis* 168. The details of PBPs are shown in terms of name, encoding gene, classification, molecular weight, proposed function and the relevant growth stage. The proteins are classified as group A, B and C based on the predicted functions. V: vegetative growth, S: stationary phases, Spo: sporulation stage, φ: cell envelope stress proteins. The table is adapted from (Sauvage *et al.*, 2008) with some modification.

1.1.3 Modification of peptidoglycan

1.1.3.1 Swapping of D-alanine residues

Living organisms predominantly require L-amino acids for growth. However, D-amino acids are also found in both prokaryotic (e.g bacteria) and eukaryotic organisms (Yoshimura and Esak, 2003). The D-amino acids are produced *in vitro* by spontaneous racemisation (time-dependent geochemical reaction) and *in vivo* by enzymatic racemisation (Zhang and Sun, 2014). Bacteria normally release various D-amino acids during stationary growth. The D-amino acids prevent biofilm formation (Illana Kolodkin-Gal, 2010) and re-model the structural properties of peptidoglycan through active incorporation into the peptide side chains of the polymer (Lam *et al.*, 2009). The swapping of D-alanine on stem peptides was initially studied in Gram-negative bacteria (Figure 1.4A). HPLC analysis revealed that the supplemented D-methionine is incorporated into the position 4 of the peptide side chains in *E. coli*, *Vibrio cholera*, *Caulobacter crescentus* and *Pseudomonas aeruginosa* (Caparrós *et al.*, 1992; Lam *et al.*, 2009; Cava *et al.*, 2011). The swapping of fluorescently labelled D-amino acids with D-alanine residues at position 4 of stem peptides was recently re-confirmed in *E. coli* (Kuru *et al.*, 2012; Lebar *et al.*, 2014). The incorporation of D-methionine into peptidoglycan was also reported in stationary growing cells and even in β -lactams treated cells of *E. coli* (Tsuruoka *et al.*, 1984; Caparrós *et al.*, 1992). The exchange of 4th D-alanine residue with non-specific D-amino acids is catalysed in a poor substrate specificity reaction, but not all D-amino acids are incorporated (Caparrós *et al.*, 1992). In Gram-negative bacteria (e.g *E. coli* and *V. cholera*), the incorporation of D-amino acids into peptidoglycan might be endowed by a common (non-specific) enzymatic reaction, catalysed by penicillin-insensitive LD-transpeptidases (Figure 1.4A) (Caparrós *et al.*, 1992; Cava *et al.*, 2011).

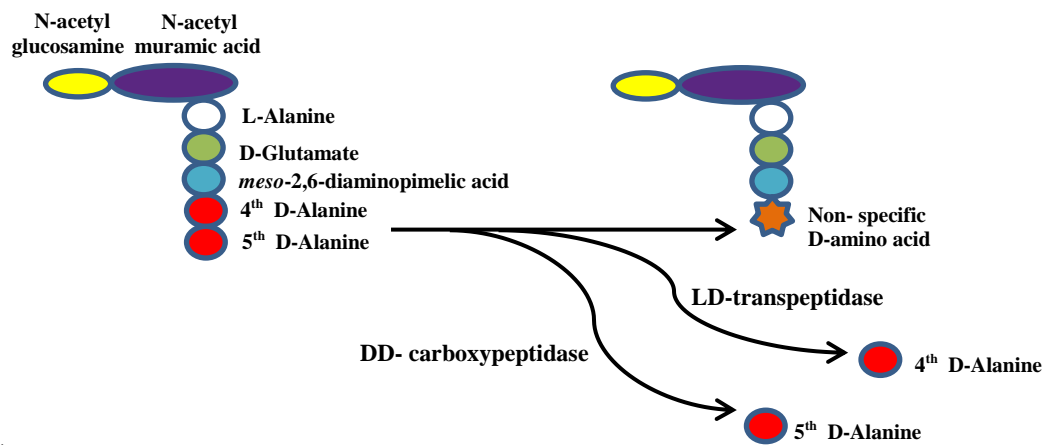
The accumulation of different D-amino acids was reported in stationary culture supernatant of *B. subtilis* (Lam *et al.*, 2009; Illana Kolodkin-Gal, 2010). It was shown that D-amino acids are usually incorporated into the peptidoglycan of *B. subtilis* during both exponential and stationary growth (Figure 1.4B) (Lam *et al.*, 2009). The incorporation of D-methionine into the 5th position of stem peptides was observed in *B. subtilis*, *Enterococcus faecalis* and *Staphylococcus aureus*. This swapping reaction was inhibited by penicillin G, but not by D-cycloserine, in *B. subtilis* (Cava *et al.*, 2011). The re-modelling of peptidoglycan with D-amino acids has inspired some of the researchers to develop fluorescent D-amino acid probes (FDAAs), ideal for labelling

peptidoglycan in live cells. The FDAAs are swapped extracellularly with D-alanine residues at position 5 of stem peptides in *B. subtilis* (Kuru *et al.*, 2012). This exchange reaction in peptidoglycan is catalysed by penicillin sensitive DD-transpeptidase (Figure 1.4B) (Cava *et al.*, 2011; Kuru *et al.*, 2012). Moreover, the usual trimming of terminal D-alanine residues by DD- carboxypeptidase (DacA) resulted in a very weak fluorescent signal in the cell wall of wild type *B. subtilis* (Kuru *et al.*, 2012).

The amidation of free carboxylic group of *m*-A2pm residues normally happen in lipid II of *B. subtilis*, but not in *E. coli* (Warth and Strominger, 1971; Atrih *et al.*, 1999; Bouhss *et al.*, 2008; Vollmer *et al.*, 2008a). Based on an *in vitro* experiment, it was reported that the amidation in lipid II is discriminated by the specificity of *B. subtilis* PBP1 and *E. coli* PBPA1 during cross-linking, that is to say the amidated stem peptides are only cross-linked by PBP1. This observation led to the development of new fluorescent probes (D-amino carboxamides), such as fluorescent-tagged D-Lysine carboxamide (FD-Lys-NH₂), which is amidated at its free carboxylic group. The FD-Lys-NH₂ nicely labelled the cell wall of wild type *B. subtilis*. There is a thought that the D-amino carboxamides might tolerate trimming by carboxypeptidases, so its fluorescent signal persists in wild type peptidoglycan (Lebar *et al.*, 2014). Moreover, analysis of mucopeptide identities in *B. subtilis* revealed that the terminal D-alanine residues were replaced by glycine in a small percentage of mucopeptides (Atrih *et al.*, 1999). This suggests that the L-amino acid (s) might also take part in the alteration of peptidoglycan stem peptides.

Recently, a few attempts have been done to identify the enzyme(s), which exchange the D-alanine residues with other D-amino acids in bacterial peptidoglycan. An *in vitro* study showed that the 5th D-alanine residues of lipid II was swapped with [¹⁴C] D-alanine by *E. coli* PBP1A, which is a PBP with glycosyltransferase and DD-transpeptidase activities. The DD-carboxypeptidase (DacA) was able to release the incorporated [¹⁴C] D-alanine residues (Lupoli *et al.*, 2011). It was also demonstrated that *E. coli* PBPA1 and *B. subtilis* PBP1 were able to incorporate the fluorescently labelled D-amino acid (D-Phe) into synthetic peptidoglycan *in vitro* (Lebar *et al.*, 2014).

A)



B)

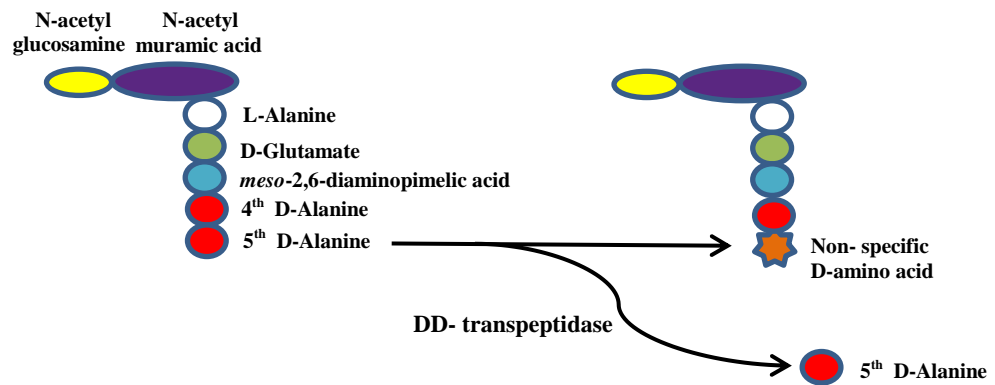


Figure 1.4 D-alanine swapping in peptidoglycan of *E. coli* (A) and *B. subtilis* (B). See the text for details.

1.1.3.2 Carboxypeptidation of peptidoglycan

Two types of carboxypeptidases have been identified in bacteria. The DD-carboxypeptidase cleaves the amide bond between the two D-alanine residues on peptide side chains and leave tetra-peptide side chains. Then, the LD-carboxypeptidase trims the 4th position D-alanine residues on tetra-peptide side chains to leave tri-peptide side chains in peptidoglycan (Figure 1.5) (Atrih *et al.*, 1999; Vollmer *et al.*, 2008b; Barendt *et al.*, 2011; Hoyland *et al.*, 2014). DD-carboxypeptidases are LMW PBPs, which have been investigated in different bacterial species. The DD-carboxypeptidases of *B. subtilis* 168 are PBP5 (DacA), PBP5* (DacB), PBP4a (DacC) and DacF (Table 1.1) (Sauvage *et al.*, 2008). DacA is the main DD-carboxypeptidase in vegetative growing cells, and it is probably a membrane bound enzyme. Peptidoglycan analysis revealed that the majority of muropeptides have penta-peptide side chains in *dacA* strain, whereas in wild type the muropeptides mostly have tri-peptide side chains (Atrih *et al.*, 1999). Despite having penta-stem peptides in peptidoglycan, *dacA* mutant did not apparently show any morphological abnormalities during exponential growth (Todd *et al.*, 1986). The rest of *B. subtilis* DD-carboxypeptidases are produced during post-exponential growth (stationary phase and sporulation) (Pedersen *et al.*, 1998; Popham *et al.*, 1999).

LD-carboxypeptidases have been identified in a few Gram-negative and Gram-positive bacteria, such as *E. coli* (Metz *et al.*, 1986; Ursinus *et al.*, 1992), *P. aeruginosa* (Korza and Bochtler, 2005), *Lactococcus lactis* (Courtin *et al.*, 2006), *Streptococcus pneumoniae* (Barendt *et al.*, 2011; Hoyland *et al.*, 2014), *Helicobacter pylori* (Sycuro *et al.*, 2012). *Novosphingobium aromaticivorans* (Das *et al.*, 2013) and *Campylobacter jejuni* (Friedrich *et al.*, 2014). The LD-carboxypeptidase (LdcA) of *E. coli* is cytosolic and plays role in peptidoglycan recycling by converting tetra-peptide (L-alanine-D-glutamate-*m*-A2pm-D-alanine) to tri-peptide (L-alanine-D-glutamate-*m*-A2pm), which is reused for *de-novo* synthesis of murein precursors. The *ldcA* mutant grows normally during exponential phase, whereas the cells grow slowly and start lysing during stationary phase (Templin *et al.*, 1999). In contrast, the LD-carboxypeptidase (DacB_{*spn*}) of *S. pneumoniae* is likely localised on the outside of cell membrane as a lipoprotein. It resides at the cell septum and over the entire cell surface. The lack of DacB_{*spn*} causes asymmetrical cell division, which results in different cell morphologies, such as very small round shaped cells and enlarged long cells (Barendt *et al.*, 2011). Also, the normal

helical shape of *C. jejuni* is changed to straight morphology in the absence of LD-carboxypeptidase (Δ *pgp2*) (Firdich *et al.*, 2014).

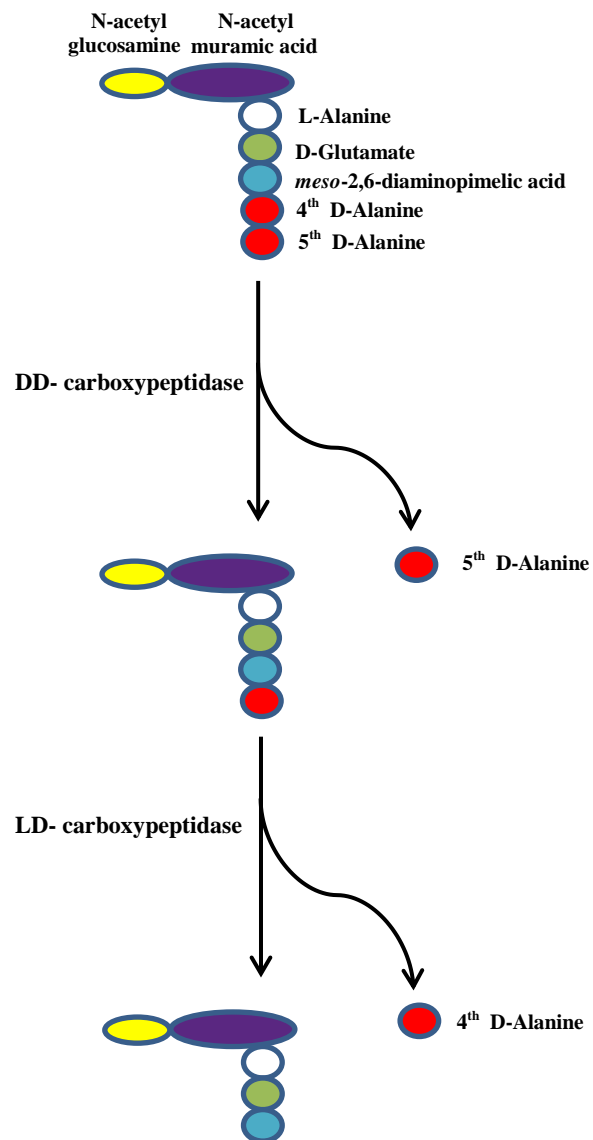


Figure 1.5 Carboxypeptidation of peptidoglycan. See the text for details.

1.1.4 Assembly and architecture of peptidoglycan

Radioactive labelling, autoradiography, electron microscopy and fluorescent microscopic techniques were used to study the cell wall assembly and/or architecture in bacteria. Generally, there are two concepts about murein architecture in rod-shaped bacteria. The first concept (layered murein model) assumes that the glycan strands horizontally run around the cylindrical part of the cell and parallel to the plasma membrane (Holtje, 1998; Vollmer and Holtje, 2001; Vollmer and Holtje, 2004). However, second concept (scaffold model) speculates that the glycan strands extend in a vertical manner, perpendicular to cytoplasmic membrane, where the cross-links are stress-bearing sites in peptidoglycan (Dmitriev *et al.*, 1999; Dmitriev *et al.*, 2003; Dmitriev *et al.*, 2005).

The cell wall of *B. subtilis* was initially studied at population level, using radioactive pulse-labelling experiments. A delay of one generation long or more was detected before the turnover of the pulse-labelled wall (Mauck *et al.*, 1971; Pooley, 1976a). This observation led to a suggestion that the cell wall of *B. subtilis* is a multi-layered structure. The new peptidoglycan layers are synthesised on the outer leaflet of cell membrane and subsequently moved outwards during growth. As the old peptidoglycan layers reach the cell surface, where they become labile to degradation by hydrolases. This suggestion was further experimentally supported by radioactive labelling experiments and illustrated in proposed models (Pooley, 1976a; Pooley, 1976b; Mobley *et al.*, 1984; Koch and Doyle, 1985a).

Several studies were also investigated murein assembly and architecture at cellular level. Mendelson (1976) studied the morphology and growth behaviour of a multiple mutant strain of *B. subtilis*, using phase contrast microscopy. He observed that the mutant cell were elongated and twisted around long axis of the cell. This observation let him to be first to propose a helical pattern model for bacterial cell growth. Mobley *et al.* (1984) used both autoradiography (labelling peptidoglycan with [1-³H] GlcNAc) and fluorescent microscopy (labelling teichoic acid with fluorescein- conjugated concanavalin A (ConA)) to study the pattern of cell wall synthesis and turnover in *B. subtilis*. Later, both immunoelectron and immunofluorescence microscopies were used by de Pedro *et al.* (1997) to study murein assembly and degradation in *E. coli*. The principle of the study was immunodetection of the periplasmic incorporation of D-cysteine into the murein. From these analyses, it was suggested that polymerisation of glycan strands happens at the cell septum and along the lateral wall, but the cell poles

are metabolically inert. Furthermore, uranium stained teichoic acids were examined by electron microscopy in *B. subtilis*. It was observed that the new cell wall material seemed to distribute uniformly along the inner part of cell cylinder, but no specific sites of incorporation were observed (Merad *et al.*, 1989). Recently, the peptidoglycan architecture in *B. subtilis* was described in a new coiled-coil model. This model was proposed based on high resolution atomic force microscopic examination of purified cell wall. It was observed that the outer surface of cell wall was rough due to turnover, but the inner surface showed cable- like structures (~50 nm width). It is thought that some of the glycan strands might be cross- linked to form a rope. The rope is twisted to form a cable, and then the cable is coiled around the short axis of the cell cylinder (Hayhurst *et al.*, 2008). However, the scaffold and coiled-coil models were contradicted, when the intact cell and purified sacculi of *B. subtilis* were examined by electron cryotomography and computational modelling. This recent study suggested that the glycan strands in Gram-positive cell wall are polymerised around the cell cylinder and parallel to the short axis of the cell (Beeby *et al.*, 2013), this is in agreement with the first concept (layered murein model) of peptidoglycan architecture.

The advancement of fluorescent microscopy and the introduction of various fluorescent probes into biological applications have started a new era in bacterial cytology. The advantage of some of the fluorescent probes is labelling and imaging of live cells without toxic effect. Daniel and Errington (2003) firstly used fluorescein- conjugated vancomycin, a cell wall inhibiting antibiotic, to examine the incorporation site of nascent peptidoglycan. The idea was binding of FL-vancomycin to the D-ala-D-ala portion of stem peptides in peptidoglycan. Later, Tiyanont *et al.* (2006) also used fluorescent analogues of vancomycin and ramoplanin to study peptidoglycan biosynthesis in *B. subtilis*. The fluorescent vancomycin was also used by Formstone and Errington (2005) and Kawai *et al.*, (2009) to study the role of MreB protein in peptidoglycan biosynthesis at the lateral cell wall of *B. subtilis*. The above fluorescent labelling studies observed the synthesis of new peptidoglycan at cell division site and helically around the long axis of the cell. However, the main limitation of fluorescent antibiotics was inability to study the dynamic of peptidoglycan assembly in live cells. More recently, fluorescent D-amino acids (FDAAs) were successfully used to label newly synthesised peptidoglycan in live bacteria. The FDAAs are not taken up by the cells but are swapped extracellularly with either terminal or penultimate D-alanine residues of stem peptides. The cell wall synthesis was studied in *E. coil* and *dacA* null

B. subtilis by using FDAA. It was seen that the synthesis of new peptidoglycan occurs at the cell septa and lateral wall. The super-resolution microscopy showed a circlet arrangement of peptidoglycan in the wall of *E. coli* (Kuru *et al.*, 2012). Thus, the recent electronic and fluorescent microscopic studies seem to support the first concept (layered murein model) of peptidoglycan architecture.

1.1.5 Peptidoglycan turnover

The cell wall of bacteria must undergo both anabolic (synthesis) and catabolic (degradation) processes during cell growth. Radioactive labelling was historically used to study the cell wall turnover and the effect of the lack of some peptidoglycan hydrolases (autolysins) on cell growth. Based on the inside-to-outside growth model, the new cell wall precursors are continually added to the innermost layers of peptidoglycan. Meanwhile, the old outermost layers of peptidoglycan are degraded by peptidoglycan hydrolases and released into the surrounding environment (Koch and Doyle, 1985a). Depending on bacterial species, about 25 % to 50 % of the old cell wall materials is turned over and released per generation (Mauck *et al.*, 1971; Pooley, 1976b; Goodell, 1985; Park and Uehara, 2008). The eubacteria generally require peptidoglycan hydrolases for normal growth. These enzymes generally include *N*-acetylmuramidases, lytic transglycosylases, β -*N*-acetylglucosaminidases, amidases, endopeptidases and carboxypeptidases (Figure 1.6), which are produced at different stages of growth. Each enzyme specifically cleaves a chemical bond in peptidoglycan to facilitate cell growth, peptidoglycan turnover, cell division, cell separation, motility and autolysis (Smith *et al.*, 2000; Vollmer *et al.*, 2008b). *B. subtilis* genome accommodates more than 35 genes, which encode putative peptidoglycan hydrolases, and about 70 % of these gene products have been characterised so far (Sudiarta *et al.*, 2010). The presence of large number of autolysins and their functional redundancies sometimes restrict our ability to precisely suggest the physiological role of some autolysins (Smith *et al.*, 1996). The murein hydrolases of *B. subtilis*, which have been supposed and/or proposed to play roles in cell wall turnover are *N*-acetylmuramidase-lytic transglycosylase (CwlQ ?) (Sudiarta *et al.*, 2010), β -*N*-acetylglucosaminidase (LytD), amidase (LytC) (Blackman *et al.*, 1998) and DL-endopeptidase (LytE) (Bisicchia *et al.*, 2007) (Figure 1.6).

The coordination of peptidoglycan synthesis and turnover in *E. coli* was already illustrated in a proposed three-for-one growth model, in which murein synthases and hydrolases synchronously work to degrade an old glycan strand and incorporate three new glycan strands instead. This means that murein hydrolysis does not occur randomly

(Holtje, 1998; Vollmer and Holtje, 2001). The physical interaction was also observed among peptidoglycan synthases and hydrolases in *E. coli*. However, the direct-interaction between peptidoglycan synthases and hydrolases may not be feasible in Gram-positive bacteria, because their cell wall is thick and grows according to inside-to-outside growth model (Vollmer *et al.*, 2008b). Mobley *et al.* (1984) used radioactive GlcNAc to study cell wall turnover in mutant strains of *B. subtilis*. They observed that cell wall turnover is notably reduced in autolysin deficient cells. Blackman *et al.* (1998) also showed that cell wall turnover is markedly reduced in *lytC* null mutant, labelled with radioactive GlcNAc. A greater reduction in cell wall turnover was observed in *lytC lytD* double mutant, comparing to *lytC* null (Blackman *et al.*, 1998). Bisicchia *et al.* (2007) reported that cell wall turnover is affected in *lytE* mutant *B. subtilis*. However, several studies have suggested cell elongation role for LytE (see section 1.1.1.7). In addition, the cell wall turnover was significantly recovered after addition of autolysate to a culture of turnover-deficient mutant of *B. subtilis* (Pooley, 1976b). These studies clearly demonstrated that cell wall synthesis and turnover are regulated in Gram-positive bacteria.

On the other hand, the effect of inhibition of cell wall synthesis on cell wall turnover was studied, using radioactive amino acids. It was observed that the cell wall turnover was considerably reduced in *B. subtilis* W-32 and *B. megaterium* KM in the presence of Actinomycin D and penicillin G respectively. It was suggested that cell wall turnover does not occur properly, while cell wall synthesis is inhibited (Mauck *et al.*, 1971). Thus, the above studies suggested that cell wall synthesis and turnover are apparently coordinated during cell growth.

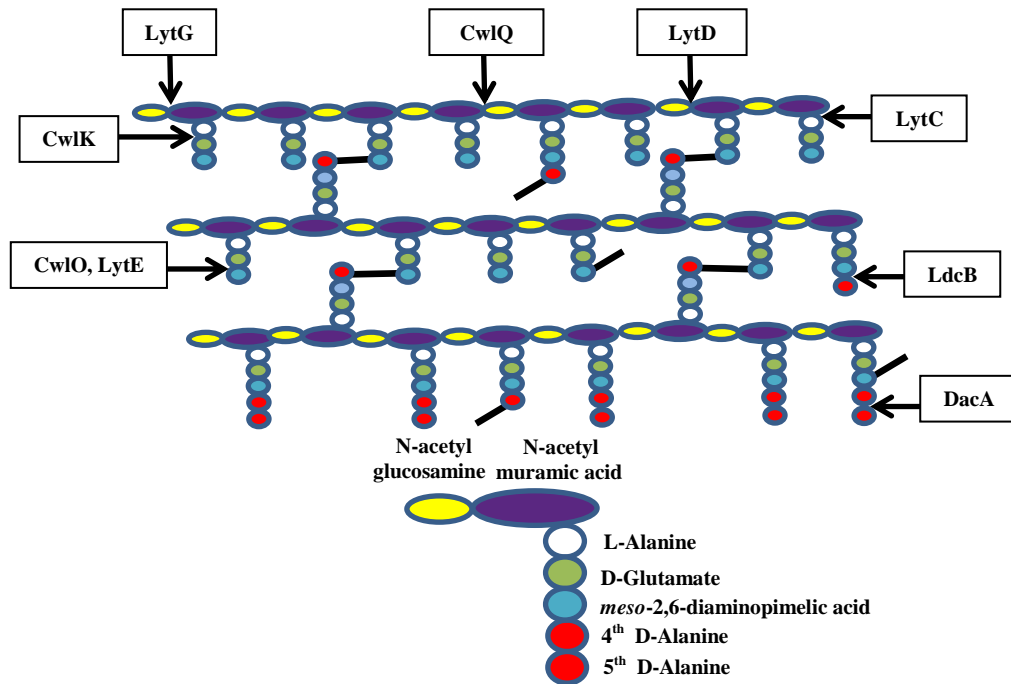


Figure 1.6 Peptidoglycan hydrolases (Autolysins). The eubacteria require peptidoglycan hydrolases for different growth processes, see the text. The vegetative hydrolases of *B. subtilis* are N-acetylmuramidase-lytic transglycosylase (CwlQ), endo- β -N-acetylglucosaminidase (LytD), Exo- β -N-acetylglucosaminidase (LytG) amidase (LytC), LD- endopeptidase (CwlK), DL-endopeptidases (CwlO and LytE), LD-carboxypeptidase (LdcB) and DD-carboxypeptidase (DacA).

1.1.6 Peptidoglycan recycling

The consequence of bacterial cell wall turnover is the release of fragments of the cell wall continuously in actively growing cells. So, cell wall turnover represents a significant drain of cellular resources, unless the released materials are recycled. Cell wall recycling pathways have been suggested in some bacterial species, such as *E. coli*, *B. subtilis* and *Clostridium acetabulyticum* (Park and Uehara, 2008; Litzinger *et al.*, 2010a; Reith and Mayer, 2011; Johnson *et al.*, 2013). It is also known that some bacteria exploit cell wall recycling as a strategy to sense the inhibition of cell wall synthesis by antibiotics and to regulate resistant mechanisms (e.g induction of β -lactamase and β -lactam resistant PBPs). It is also possible that pathogenic bacteria may recycle cell wall products to avoid activating of host innate immune response, which specifically responded to peptidoglycan fragments (Boudreau *et al.*, 2012; Johnson *et al.*, 2013; Bertsche *et al.*, 2015).

The fate of the cell wall turnover materials has been intensively studied in Gram-negative bacterium, *E. coli* (Figure 1.7) (Mayer, 2012). Murein recycling seems to be very efficient in *E. coli*, because only 6.0-8.0 % of degraded peptidoglycan was detected in culture media per generation (Goodell, 1985; Goodell and Schwarz, 1985). It is probable that the outer membrane plays important role as a mechanical barrier to contain the degraded cell wall materials in periplasmic space (Holtje, 1998; Litzinger *et al.*, 2010a). Thus, about 90 % of the cell wall turnover products is recycled in *E. coli* (Holtje, 1998). In *E. coli*, the lytic transglycosylases (SltY) and endopeptidases produce the main cell wall turnover products (anhydromuropeptide monomers (GlcNAc-anhMurNAc-peptide)), which can be directly transported to cytoplasm (Holtje, 1998; Park and Uehara, 2008) via a permease (AmpG) (Jacobs *et al.*, 1994). The recycled anhydromuropeptides are sequentially degraded in the cytoplasm by a group of muropeptide recycling enzymes, including a β -N-acetylglucosaminidase (NagZ) (Cheng *et al.*, 2000; Votsch and Templin, 2000), an amidase (AmpD) (Jacobs *et al.*, 1995) and a LD-carboxypeptidase (LdcA) (Templin *et al.*, 1999). The free tri-peptides and amino sugars (GlcNAc and anhMurNAc) are then used for *de novo* synthesis of peptidoglycan precursors (Park and Uehara, 2008; Reith and Mayer, 2011), but the amino sugars can also be used as energy source (Dahl *et al.*, 2004). Alternatively, the anhydromuropeptide monomers can be hydrolysed by an amidase (AmiD) in the periplasmic space to release the peptide side chains (Uehara and Park, 2007). The detached stem peptides can then be taken up via oligopeptide transport system

(Opp+MppA) (Park, 1993; Park *et al.*, 1998). The free amino sugars are also transported by phosphotransferase system, NagE and MurP (Park and Uehara, 2008; Reith and Mayer, 2011).

Unlike *E. coli*, the cell wall of Gram-positive bacteria has a thicker layer of peptidoglycan (Shockman and Barrett, 1983), which accounts for more than 20 % of total cell mass (Litzinger *et al.*, 2010a). So, Gram-positives would require a more efficient recycling pathway to keep their cell wall resources (Reith and Mayer, 2011). However, the loss of degraded cell wall materials was historically reported in *Bacillus spp.* (Chaloupka *et al.*, 1962; Mauck *et al.*, 1971; Blackman *et al.*, 1998). The rate and necessity of cell wall recycling are determined by nutritional status in the surrounding environment, so bacterial cell wall recycling may be repressed in rich media (Park and Uehara, 2008; Reith and Mayer, 2011). The peptidoglycan hydrolases such as *N*-acetylmuramidases, β -*N*-acetylglucosaminidases, amidase and endopeptidases might generate different sorts of peptidoglycan turnover products in *B. subtilis*. Moreover, muropeptide recycling pathway has been identified in *B. subtilis* (Figure 6.1). An ortholog of muropeptide permease (AmpG) is apparently absent in *B. subtilis* so far (Reith and Mayer, 2011). Instead, the muropeptides are hydrolysed extracellularly by secretory *N*-acetylglucosaminidase (NagZ) and amidase (AmiE) during stationary phase. The NagZ only cleaves the glycosidic bond in muropeptides and produce MurNAc-peptide (Litzinger *et al.*, 2010a; Litzinger *et al.*, 2010b). The AmiE cleaves the bond between MurNAc and L-alanine only in the muropeptides, which were already processed by NagZ (Litzinger *et al.*, 2010a). The detached peptide side chains are probably recycled through two oligopeptide permeases, Opp (LeDeaux *et al.*, 1997) and App (Koide and Hoch, 1994). The *opp* is expressed during exponential phase, whereas the expression of *app* is induced at the beginning of stationary growth. The Opp and App systems are specific for tetra- and penta-peptides, but Opp can also transport tripeptides (Koide *et al.*, 1999). Besides, phosphotransferase systems NagE and MurP may recover the released cell wall-derived amino sugars. The rescue of muropeptides by NagZ and AmiE is the first evidence of cell wall recovery pathway in Gram-positive bacteria (Litzinger *et al.*, 2010a). Thus, cell wall recycling pathways are apparently present in both Gram-negative and -positive bacteria.

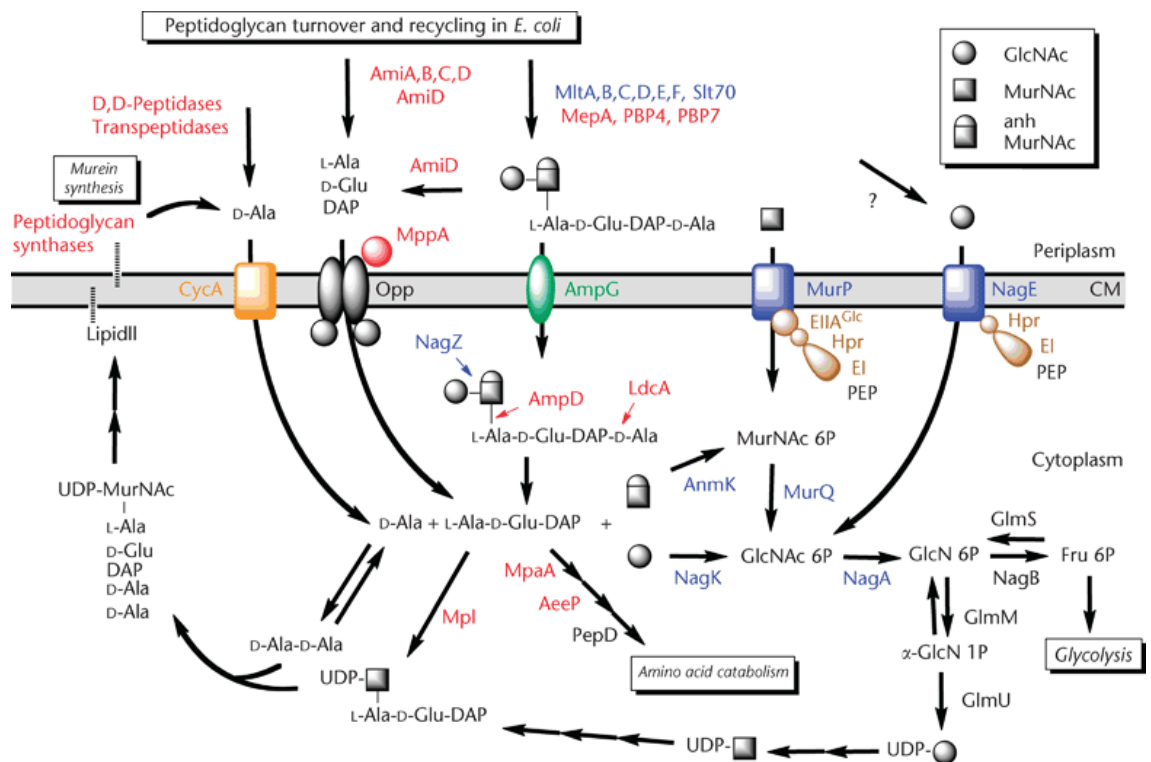


Figure 1.7 Peptidoglycan metabolism in *E. coli*. It shows comprehensive metabolic pathways of peptidoglycan synthesis, turnover and recycling in *E. coli*, as a Gram-negative model. The figure is copied from (Mayer, 2012). See the text for details.

1.1.7 Roles of MreB isomers and LD-endopeptidases in cell shape maintenance and peptidoglycan synthesis

The cytoskeleton proteins play key roles in controlling of cell shape and murein synthesis in both in Gram-negative and Gram-positive rod-shaped bacteria (Jones *et al.*, 2001; Carballido-Lopez and Errington, 2003b). The cytoskeleton proteins of *B. subtilis* are MreB, Mbl and MreBH (Figure 5.17) (Carballido-Lopez and Errington, 2003b). The *mreB* gene was firstly determined in *E. coli*, where synthetic mutations in *mreB* gene produced spherical cells, suggesting that MreB has role in rod shape determination (Doi *et al.*, 1988). The identification and characterisation of *mreB* gene in *E. coli* inspired the researchers to look for the gene homologs in Gram-positive bacteria. The *mreBCD* genes of *B. subtilis* were originally identified by Reeve *et al.* (1973) and characterised based on the sequence homologies to *mre* locus of *E. coli* by Varley and Stewart (1992). The inactivation of *mre* genes was lethal in *B. subtilis*, probably due to developing a morphological phenotype analogous to that of *E. coli* (Varley and Stewart, 1992). It was found that magnesium ion (Mg^{2+}) is required for stabilising the viability of *mreB* *B. subtilis*. When the *mreB* mutant was depleted for Mg^{2+} and monitored by time-lapse microscopy, the cells elongated normally, but the cell diameter was getting wider and followed by cell lysis (Formstone and Errington, 2005). The second *mreB* homolog gene, *mbl*, was identified in *B. subtilis* by Decatur *et al.* (1993). The insertional inactivation of *mbl* gene was not lethal but caused morphological changes, such as bloating and twisting of the cells (Abhayawardhane and Stewart, 1995). The third MreB homolog in *B. subtilis* is MreBH. The disruption of *mreBH* did not cause detectable morphological alterations (Carballido-Lopez and Errington, 2003b). However, another study reported that the depletion of MreBH increased cell diameter and changed cell morphology from rod to bent or vibrio shape (Soufo and Graumann, 2003). The *mreBH* mutant requires sufficient Mg^{2+} supplement to entirely recover its growth and morphological phenotypes (Carballido-Lopez *et al.*, 2006).

Additionally, the MreB isomers of *B. subtilis* were further characterised in terms of localisation and arrangement in bacterial cell. It was observed that the actin-like filaments (MreB, Mbl and MreBH) are co-localised as helical structures across the cylindrical part of the cell and presumably underneath the cell membrane (Jones *et al.*, 2001; Carballido-Lopez and Errington, 2003a; Carballido-Lopez *et al.*, 2006). Besides co-localisation, different experimental methods also showed probable physical interactions among the MreB proteins in *B. subtilis* (Defeu Soufo and Graumann, 2006;

Kawai *et al.*, 2009b). This observation led to a suggestion that MreB, Mbl and MreBH might assemble one heteropolymeric cord and function redundantly in cell wall synthesis (Carballido-Lopez *et al.*, 2006; Kawai *et al.*, 2009b).

The morphological and localisation studies proposed different possible functions for MreB isomers in *B. subtilis*. The MreB and Mbl proteins have distinct and complementary roles in controlling of cell shape. The MreB seemed to control cell diameter, while Mbl might be important for rod shape maintenance (Jones *et al.*, 2001; Formstone and Errington, 2005). In addition to its role in cell morphogenesis, it was proposed that MreB has role in chromosome segregation (Soufo and Graumann, 2003), this suggestion was soon contradicted by growing the *mreB* null in the presence of Mg^{2+} and staining the chromosome with fluorescent dye (Formstone and Errington, 2005). Moreover, the helical polymerisation of peptidoglycan specifically requires Mbl protein (Daniel and Errington, 2003). Whilst the helical insertion of new cell wall materials is directed by Mbl protein, the cell elongation happens as a consequence of both peptidoglycan and Mbl polymerisations in a helical pattern. The role of Mbl filaments in helical polymerisation of peptidoglycan was also illustrated in hypothetical models (Daniel and Errington, 2003; Carballido-Lopez and Errington, 2003a; Carballido-Lopez and Errington, 2003b). More recently, experimental data suggested that MreB and Mbl play redundant role in cell elongation and lateral cell wall synthesis. The lack of all the three MreB isomers resulted in the loss of peptidoglycan synthesis in lateral wall and the appearance of spherical shape phenotype (Kawai *et al.*, 2009b). The interactions of several PBPs with MreB, Mbl and to less extend MreBH were also reported in *B. subtilis* (Kawai *et al.*, 2009a; Kawai *et al.*, 2009b).

On the other hand, the MreB proteins are also found to have roles in the activity of some cell wall hydrolases. It has been reported that MreB and Mbl respectively control the function of LytE and CwlO, the two well characterised major DL-endopeptidases in *B. subtilis* (Figure 5.17) (Dominguez-Cuevas *et al.*, 2013). The LytE was localised at cell septum, cell pole and lateral cell wall, apparently in a helical pattern (Carballido-Lopez *et al.*, 2006; Hashimoto *et al.*, 2012), whereas CwlO was detected at the cell septum and lateral cell wall, seemingly in a helical pattern as well (Hashimoto *et al.*, 2012; Dominguez-Cuevas *et al.*, 2013). The localisation of CwlO and its regulation by Mbl are mediated by FtsEX, an ABC transporter complex (Dominguez-Cuevas *et al.*, 2013; Meisner *et al.*, 2013). In addition, the deletion of *mreBH* gene resulted in delocalisation of LytE at the lateral wall of *B. subtilis* suggesting that MreBH plays role in

cell morphogenesis by recruiting LytE to the lateral cell wall (Carballido-Lopez *et al.*, 2006). The absence of DL-endopeptidase activities of LytE and CwIO is lethal in *B. subtilis*. The depletion of CwIO in *lytE* null mutant resulted in the inhibitions of lateral cell wall synthesis and cell elongation (Bisicchia *et al.*, 2007). The roles of LytE and CwIO in cell elongation were further explained and displayed in hypothetical models. It was suggested that the two enzymes are localised to the lateral wall by the MreB proteins. Upon their localisation, LytE and CwIO start loosening the above layers of peptidoglycan and provide more space for insertion of new layers (Carballido-Lopez *et al.*, 2006; Hashimoto *et al.*, 2012; Dominguez-Cuevas *et al.*, 2013). Thus, the above proposed roles of MreB proteins in cell shape maintenance and cell wall metabolism may convincingly suggest collaborative strategies among MreB proteins, PBPs and some of the cell wall hydrolases for synchronising cell wall synthesis and turnover during growth.

1.2 Teichoic Acids

In addition to peptidoglycan, the cell envelop of Gram-positive bacteria contains anionic polymers, called teichoic acids. The two main types of teichoic acids are wall teichoic acid (WTA), which is covalently linked to peptidoglycan and lipoteichoic (LTA) acid, which is attached to plasma membrane and extends through peptidoglycan (Figure 1.8) (Neuhaus and Baddiley, 2003). The WTA and LTA are synthesised through separate pathways (Ward, 1981) and play several roles in Gram-positive bacteria. The teichoic acids are involved in biofilm formation, maintenance of cell morphology, membrane integrity, temperature stability of cells, cation homeostasis, providing scaffolds for cell wall hydrolases, facilitation of surface adhesion and resistance against antimicrobial peptides (Wecke *et al.*, 1996; Peschel *et al.*, 2000; Gross *et al.*, 2001; Abachin *et al.*, 2002; Neuhaus and Baddiley, 2003; Steen *et al.*, 2003; Kristian *et al.*, 2005; Kovacs *et al.*, 2006; Swoboda *et al.*, 2010). The presence of both WTA and LTA are essential for viability of *B. subtilis* (Schirner *et al.*, 2009). The structures and biosynthesis of WTA and LTA are discussed in the following sections.

1.2.1 Wall Teichoic Acid

The cell wall of *B. subtilis* 168 is composed of approximately equal quantities of peptidoglycan and teichoic acids, the majority of which is WTA (Foster and Popham, 2002). The WTA is a crucial cell wall component for rod shape maintenance in *B. subtilis*, suggesting that it play a role in cell elongation (Schirner *et al.*, 2009). The

WTA of *B. subtilis* 168 are classified into major and minor WTAs under non-phosphate-limiting conditions. The major WTA is composed of a base unit of *N*-acetylglucosamine- β -(1-4)-*N*-acetylmannosamine, which is attached to peptidoglycan and an extension part of poly(glycerol phosphate) chain, which consists of 45 to 60 glycerol phosphate residues (Figure 1.8) (Formstone *et al.*, 2008). The WTAs are synthesised on the cytoplasmic side of plasma membrane, where the *tagA*, *tagB*, *tagD*, *tagO*, *tagF*, *32va*, and *tagH* gene products are required for major WTA biosynthesis. The products of the first four genes (TagA, TagB, TagD and TagO) play roles in the synthesis of the linkage unit, whereas the products of the last three genes take part in chain polymerization (TagF) and membrane translocation (TagG, and TagH) of WTA (Bhavsar and Brown, 2006; Formstone *et al.*, 2008). Besides, an epimerase converts undecaprenyl-diphosphate-*N*-acetylglucosamine (UDP-GlcNAc) to undecaprenyl-diphosphate-*N*-acetylmannosamine (UDP-ManNAc), which is required for the linkage unit synthesis (Soldo *et al.*, 2002b).

Although the major and minor WTA share the same linkage unit, the extension part of minor WTA consists of poly (glucosyl *N*-acetylgalactosamine 1-phosphate) chain. The biosynthetic pathway of the minor WTA requires all the essential enzymes of the major pathway except TagF, instead GgaA and GgaB polymerises glucosyl *N*-acetylgalactosamine 1-phosphate repeats (Freymond *et al.*, 2006). Also, a different epimerase enzyme catalyses the synthesis of undecaprenyl-diphosphate-*N*-acetylgalactosamine (UDP-GalNAc) from UDP-GlcNAc for minor WTA (Estrela *et al.*, 1991). The GlcNAc moiety in WTA and the MurNAc moiety in peptidoglycan are covalently linked by a phosphodiester bond (Formstone *et al.*, 2008). Recently, fluorescent microscopic data suggested that the incorporation of WTAs into peptidoglycan probably occurs in a helical pattern around the cylindrical part of the cell (Formstone *et al.*, 2008). The WTAs of *B. subtilis* 168 are predominantly replaced by teichuronic acids under phosphate-limiting conditions (Soldo *et al.*, 1999; Bhavsar *et al.*, 2004). The composition of WTAs also seems to be different among Gram-positive bacteria. For instance, the extension parts of WTAs are composed of poly (ribitol-phosphate) chains in *B. subtilis* W23 and *S. aureus* (Brown *et al.*, 2010).

The first acting enzyme in the biosynthetic pathway of WTA is TagO (phosphotransferase) that catalyses the synthesis of undecaprenyl-GlcNAc (Soldo *et al.*, 2002a). Despite the growth dispensability of *tagO* mutation in *S. aureus* (D'Elia *et al.*, 2006a) and the suggestion that *tagO* gene is indispensable in *B. subtilis* (Soldo *et al.*,

2002a), a *tagO* null mutant of *B. subtilis* was constructed, which exhibited extremely slow growth with swollen and aggregated cell morphology. However, the later genes in WTA pathway are essential in *B. subtilis* (D'Elia *et al.*, 2006b).

1.2.2 *Lipoteichoic Acid*

The LTA of *B. subtilis* 168 is composed of a hydrophobic membrane linkage unit (diglucosyl-diacylglycerol) and an extended hydrophilic chain of Poly(glycerol phosphate) (Figure 1.8). Unlike WTA, the LTA chain polymerisation occurs on the cell wall side of plasma membrane, and predominantly at cell division site (Sekiguchi and Yamamoto, 2012). *B. subtilis* genome contains four homologous genes (*ltaS*, *yfnI*, *yqgS* and *yvgJ*), which are suggested to take part in LTA synthesis (Schirner *et al.*, 2009). The products of the first three genes are LTA polymerases and of the last gene is a LTA primase (Wormann *et al.*, 2011). It was suggested that there are functional redundancy among the LTA synthases, so the deletion of any one of these genes seems to be compensated by the expression of the others (Hashimoto *et al.*, 2013). Schirner *et al.* (2009) reported that LtaS is a major LTA synthase. The *ltaS* null mutant grows slower than wild type and produces long chainy cells. The *yfnI*, *yqgS* and *yvgJ* single mutants were not different from wild type in terms of growth rate and cell morphology. Even a triple mutant (*yfnI yqgS yvgJ*) strain was seemingly similar to wild type. In contrast, deletions of all the four *ltaS* paralogue genes resulted in a very slow cell division and sever cell separation defects. The functional redundancy between LTA synthases was further confirmed, when each of LtaS, YfnI and YqgS individually was able to synthesise LTA *in vitro* (Wormann *et al.*, 2011). Moreover, it was suggested that the lack of LTA affects divalent cation homeostasis, which is followed by the impairments of cell morphogenesis, cell separation and cell division (Schirner *et al.*, 2009).

1.2.3 *Modification of teichoic acids*

The glycerol phosphate residues of teichoic acids are usually modified with D-alanine. It is also known that glucose is attached to glycerol phosphate residues of WTA in a process, called glycosylation (Allison *et al.*, 2011). In this section, we only discussed the details of teichoic acids D-alanylation. Besides its crucial role in peptidoglycan synthesis, D-alanine is also a component of teichoic acids. It was shown that 9.0 % of WTA's and 44 % of LTA's glycerophosphate residues are substituted with D-alanine esters in *B. subtilis* (Perego *et al.*, 1995). The roles of teichoic acids and D-alanine esters have mostly been overlapped in literature. The suggested general roles of D-

alanyl esters of teichoic acids are regulation of autolytic enzymes activities, control of cation homeostasis in bacterial cell and determination the electromechanical features of Gram-positive cell wall (Neuhaus and Baddiley, 2003). The D-alanine esters of teichoic acids play some more roles in resistance against antibiotics (May *et al.*, 2005) and cationic antimicrobial peptides (Saar-Dover *et al.*, 2012), pathogen adhesion and virulence (Abachin *et al.*, 2002), protein secretion (Nouaille *et al.*, 2004), acid tolerance (Boyd *et al.*, 2000) and modulation of secretory protein folding (Hyyrylainen *et al.*, 2000).

The WTA and LTA are D-alanylated by the products of *dlt* operon, which consists of five genes (*dltA*, *dltB*, *dltC*, *dltD* and *dltE*) (Perego *et al.*, 1995). Based on the homology of some of the *dlt* gene products in *Lactobacillus casie* and *B. subtilis*, it was proposed that the products of *dltA* and *dltC* genes are D-alanine-D-alanyl carrier protein ligase (Dcl) and D-alanyl carrier protein (Dcp) respectively. However, DltB and DltD are an integral transport membrane protein and a membrane protein respectively (Figure 1.8) (Perego *et al.*, 1995; Neuhaus and Baddiley, 2003). The last gene of *dlt* operon (*dltE*) encodes an oxidoreductase with unknown role (Glaser *et al.*, 1993). Apart from *dltE* inactivation, the D- alanine esterification of both WTA and LTA were completely inhibited by insertional inactivation of each of the other four genes (*dltA-D*) in *B. subtilis*. Besides, it was reported that the expression of *dlt* operon is inhibited before the initiation of transition phase (sporulation) (Perego *et al.*, 1995). Disruption of *dlt* operon in *B. subtilis* did not cause alteration in cell growth, basic biochemical metabolisms and cell morphology. However, enhanced cell autolysis, slightly change in sporulation capability, change in cell motility and increased susceptibility to methicillin were observed in *dlt* mutant strain (Perego *et al.*, 1995; Wecke *et al.*, 1996; Wecke *et al.*, 1997).

In Gram-positive bacteria, the mechanisms of teichoic acids D-alanylation have been summarised in two proposed models, Fischer and colleagues model and Neuhaus and Baddiley model (Figure 1.8) (Reichmann *et al.*, 2013). In the former model, it was proposed that Dcl energises D-alanine molecule and then ligates the activated D-alanine to Dcp. The transmembrane protein (DltB) might mediate the transfer of D-alanine from Dcp to lipid-linked undecaprenyl phosphate (C₅₅-P) derivative. The final step requires the role of an outside membrane protein (DltD) which catalyses the transfer of D-alanine residues from C₅₅-P intermediates to poly(glycerophosphate) chains (Figure

1.8A) (Fischer, 1994; Heaton and Neuhaus, 1994; Perego *et al.*, 1995). Whilst there are some similarities between the two models, the role of C₅₅-P intermediate was omitted in the latter model. Besides, it was hypothesised that DltD is localised on the inner side of cell membrane and forms a platform, where activated D-alanine is attached to DcP by Dcl. The D-alanylation of LTA is terminated by membrane translocation of D-ala-Dcp through a membrane protein channel that assembled by DltB (Figure 1.8B) (Debabov *et al.*, 2000; Kiriukhin and Neuhaus, 2001; Neuhaus and Baddiley, 2003). The mechanism of D-alanine incorporation into teichoic acids was recently revised in *S. aureus*, the data were in support of Fischer and colleagues model (Reichmann *et al.*, 2013). The *in vivo* and *in vitro* studies suggested that LTA donates its D-alanyl esters to WTA, and the D-alanine ester substituents of LTA is compensated by *de novo* re-esterification (Haas *et al.*, 1984; Koch *et al.*, 1985b). A more recent study also showed that LTA is required for efficient D-alanylation of WTA in *S. aureus* (Reichmann *et al.*, 2013). However, it is controversial whether WTA acquires D-alanine esters directly by the roles of Dlt proteins or indirectly from LTA (Perego *et al.*, 1995).

The quantity of D-alanyl ester content of teichoic acids is affected by the pH of culture media. That is to say, the D-alanyl ester substitutions of teichoic acids are progressively increased at acidic pH but decreased at alkaline pH, this is due to the base catalysed hydrolysis of the labile ester linkages (Ellwood and Tempest, 1972; Archibald *et al.*, 1973; Koch *et al.*, 1985b; Hyyrylainen *et al.*, 2000). Shifting the pH of culture medium from 6.0 to 8.0 reduced the D-alanine content of WTA and LTA to 3.0 % and 9.0 % respectively in *S. aureus* (MacArthur and Archibald, 1984). The rate of teichoic acids D-alanylation could also vary through different stages of cell cycle (MacArthur and Archibald, 1984). It is also evident that the D-alanine ester content of teichoic acids are decreased with increasing of temperature (Hurst *et al.*, 1975) and NaCl concentration (Fischer and Rosel, 1980; Koch *et al.*, 1985b).

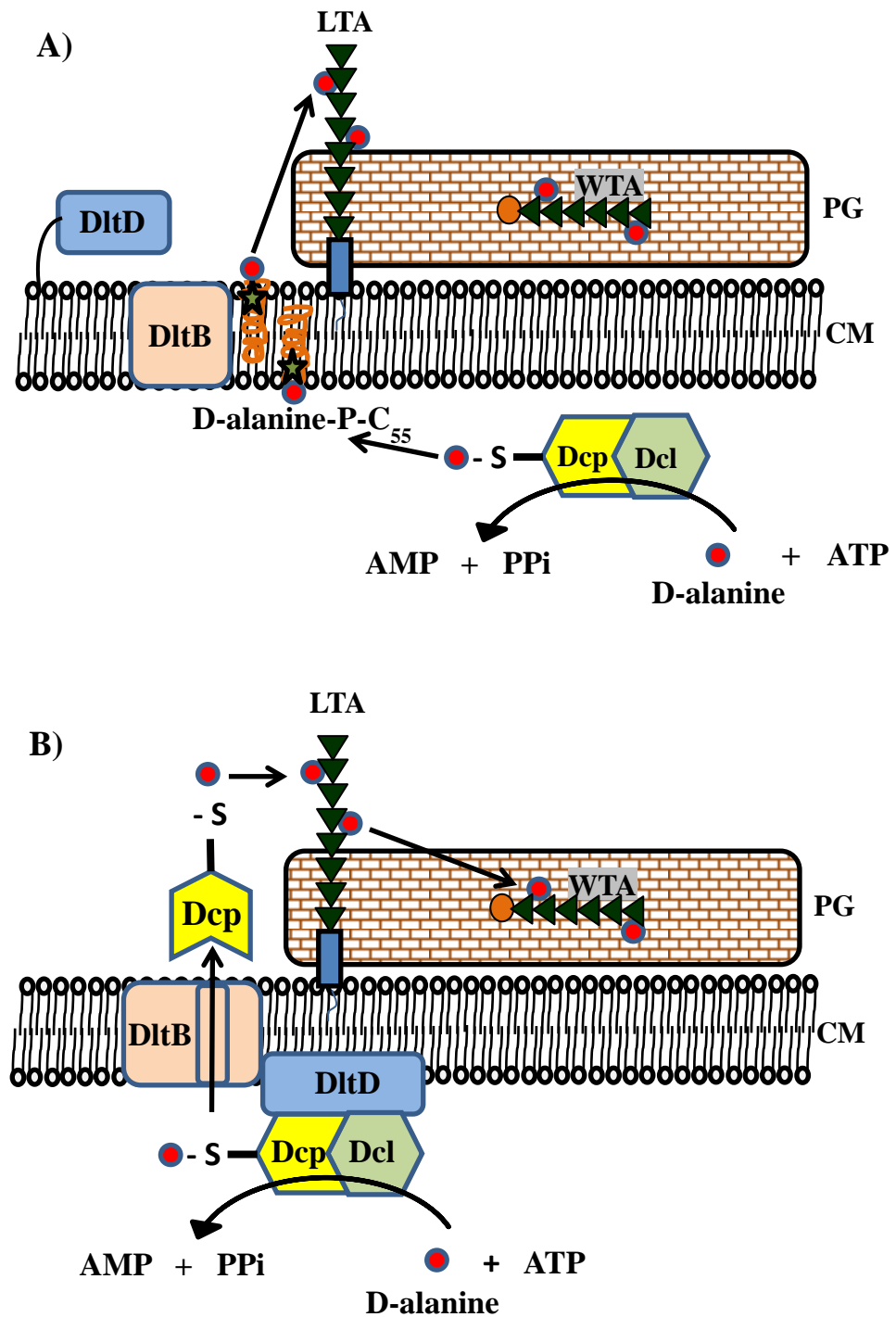


Figure 1.8 Mechanisms of teichoic acids modification with D-alanine. A) Fischer and colleague model, adapted from (Reichmann *et al.*, 2013) with some modification. B) Neuhaus and Baddiley model, adapted from (Neuhaus and Baddiley, 2003) with some modification. See the text for details.

PG: peptidoglycan; CM: cell membrane; LTA: lipoteichoic acid; WTA: wall teichoic acid; ATP: adenosine triphosphate; AMP: adenosine monophosphate; PPi: Phosphate.

1.3 Amino acid uptake systems in bacteria

Living organisms require amino acids for protein synthesis, energy production, nitrogen metabolism, cell wall synthesis and intercellular communication (Saier, 2000). L-amino acids are predominantly take part in the metabolisms of living organisms (Lam *et al.*, 2009). Bacteria obtain amino acids from *in vivo* and *in vitro* sources. In the former, the amino acids are synthesised from simple molecules or other amino acids in cytoplasm (Berg *et al.*, 2002). In the latter, the amino acids are taken up from surrounding environment abundantly through amino acid transporters (Saier, 2000).

Bacteria might be able to transport hydrophobic amino acid (e.g Tryptophan) by passive transport (diffusion), when the concentration of the amino acid is high in the surrounding environment (Figure 1.9A). However, cell membrane is a selective permeable barrier for most solutes, so the majority of the solutes (e.g amino acids) are actively transported by carrier proteins (Kramer, 1994). Bacteria can actively transport amino acids across cell membrane either by ATP binding cassette (ABC)- type uptake system (primary transport system) (Figure 1.9B) or secondary carriers (secondary transport system) (Figure 1.9C) (Hosie and Poole, 2001; Jung *et al.*, 2006). Nineteen families of the ABC-type transporters are present in prokaryotes, of which only two families are related to the transport of amino acids, including polar and apolar (hydrophobic) amino acids. However, 9 out of 11 families of secondary carriers for transporting of amino acids and their derivatives were found in bacteria. Therefore, most of the bacterial amino acid transporters are secondary carriers (permeases) (Saier, 2000). ABC-type uptake system is assembled by the products of more than one gene, which are composed of two integral membrane proteins (channel proteins), two cytoplasmic ATP binding cassette subunits and one or rarely two solute specific binding protein(s) (Hosie and Poole, 2001; Jung *et al.*, 2006). ABC-type uptake system depends on adenosine triphosphate (ATP) as an energy source for transporting of amino acids (Saier, 2000). In contrast, secondary carriers (permeases) usually comprise of a single polypeptide chain, which is integrated into the plasma membrane through its transmembrane alpha helical domains and arranged either as monomer or oligomer. The secondary carriers transport amino acids by electrochemical energy (sodium or proton-motive force) accumulated in the gradients of sodium or hydrogen ions (Saier, 2000; Jung *et al.*, 2006). Depending on the direction of gradients, secondary carriers are uniporter, symporter or antiporter. The uniporters usually transport amino acids, when the substrate's own gradient is directed inwards (Figure 1.9C1). The amino acid/cation

(H⁺ or Na⁺) symporters are the most frequent secondary carriers in bacteria. These symporters couple either H⁺ or Na⁺ with the amino acids during transport across the cell membrane (Figure 1.9C2). In contrast, the antiporters exchange two solutes across the cell cytoplasmic membrane (Figure 1.9C3) (Kramer, 1994). The active transport systems of the amino acids are highly substrate specific in bacteria (Cohen and Monod, 1957). However, the structurally related amino acids may still be transported by a single transporter. For instance, kinetic studies showed that alanine, glycine and serine have a common uptake system in bacteria (Oxender, 1972; Halpern, 1974).

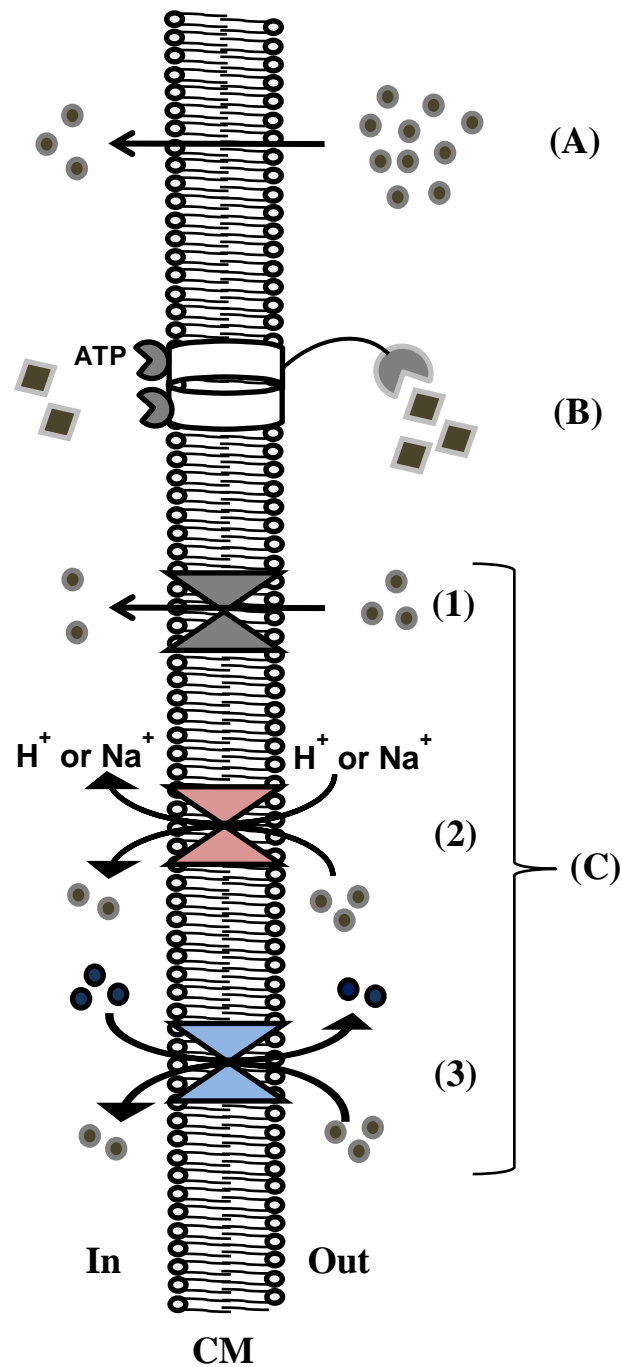


Figure 1.9 Solute transport across plasma membrane. A) Passive simple diffusion. B) Active ATP-binding cassette (ABC) transport system. C) Active secondary carriers: uniporter (C1), symporter (C2) and antiporter (C3). See the text for details.

Chapter 2. Materials and methods

2.1 Solutions and Growth media

The details of the solutions and media used in this study are listed in appendices A and B.

2.2 Bacterial strains collection

The bacterial strains were constructed by transformation. The details of the strains are shown in (Table 2.1). The abbreviations of antibiotic resistant genes, which were used for the strains selection, were *bla* (Ampicillin), *cat* (Chloramphenicol), *spc* (Spectinomycin), *kan* (Kanmycin), *neo* (Neomycine) *erm* (Erythromycin), *zeo* (Zeocine) and *ble* (Phleomycin). All the strains, once confirmed on having the correct genotype, were suspended in 20 % glycerol solution and kept at -80 °C.

Table 2.1 Strains collection

<i>B. subtilis</i> strains	Genotype	Construction or Source or Reference
168 CA	<i>trpC2 Bacillus subtilis</i>	Laboratory strains collection
RD180	<i>trpC2 ΔalrA::zeo</i>	Daniel, unpublished
KS11	<i>trpC2 ΔdltA-D::cat</i>	This work: deletion of <i>dltA-D</i> genes
KS12	<i>trpC2 ΔalrA::zeo ΔdltA-D::cat</i>	This work: RD180 transformed with gDNA of KS11
KS15	<i>trpC2 ΔdacA::spc</i>	This work: deletion of <i>dacA</i> gene
KS16	<i>trpC2 ΔalrA::zeo ΔdacA::spc</i>	This work: RD180 transformed with gDNA of KS15
KS17	<i>trpC2 ΔalrA::zeo ΔdacA::spc ΔdltA-D::cat</i>	This work: KS16 transformed with gDNA of KS11
KS18	<i>trpC2 ΔldcB::erm</i>	This work: deletion of <i>ldcB</i> gene
KS19	<i>trpC2 ΔalrA::zeo ΔldcB::erm</i>	This work: RD180 transformed with gDNA of KS18
KS20	<i>trpC2 ΔalrA::zeo ΔldcB::erm ΔdltA-D::cat</i>	This work: KS19 transformed with gDNA of KS11
KS21	<i>trpC2 ΔalrA::zeo + pLOSS*QalrA</i>	This work: pLOSS* <i>alrA</i> transformed into RD180
BKE30530	<i>trpC2 ΔytnA::erm</i> (This gene was re-designated <i>datA</i> in this work)	Bacillus genetic stock centre
KS22	<i>trpC2 ΔdatA::erm</i>	This work: 168CA transformed with gDNA of BKE30530

KS23	<i>trpC2 ΔdatA::erm ΔalrA::zeo</i> + <i>pLOSS*QalrA</i>	This work: KS21 transformed with gDNA of BKE30530
KS24	<i>trpC2 ΔldcB::erm ΔdltA-D::cat</i>	This work: KS18 transformed with gDNA of KS11
KS25	<i>trpC2 ΔdacA::spc ΔdltA-D::cat</i>	This work: KS15 transformed with gDNA of KS11
KS26	<i>trpC2 ΔdatA::erm amyE Ω (cat</i> <i>P_{spac} datA)</i>	This work: pKS1 transformed into KS22
KS27	<i>trpC2 ΔalrA::zeo amyE Ω (cat</i> <i>P_{spac} datA)</i>	This work: pKS1 transformed into RD180
KS28	<i>trpC2 ΔdatA::erm amyE Ω (spc</i> <i>P_{xyl} datA-gfp)</i>	This work: pKS2 transformed into KS22
KS29	<i>trpC2 ΔdatA::erm amyE Ω (spc</i> <i>P_{xyl} gfp-datA)</i>	This work: pKS3 transformed into KS22
KS30	<i>trpC2 ΔdatA::erm ΔalrA::zeo</i>	This work: KS22 transformed with gDNA of RD180
BKE31400	<i>trpC2 ΔalaT::erm</i>	Bacillus genetic stock centre
KS31	<i>trpC2 ΔalaT::erm</i>	This work: 168CA transformed with gDNA of BKE31400
BKE 17640	<i>trpC2 ΔalrB::erm</i>	Bacillus genetic stock centre
KS32	<i>trpC2 ΔalrA::zeo ΔalrB::erm</i>	This work: RD180 transformed with gDNA of BKE17640
BKE 34430	<i>trpC2 ΔracX::erm</i>	Bacillus genetic stock centre
KS33	<i>trpC2 ΔalrA::zeo ΔracX::erm</i>	This work: RD180 transformed with gDNA of BKE34430
BKE 26810	<i>trpC2 ΔyrpC::erm</i>	Bacillus genetic stock centre
KS34	<i>trpC2 ΔalrA::zeo ΔyrpC::erm</i>	This work: RD180 transformed with gDNA of BKE 26810
BKE10970	<i>trpC2 ΔyitF::erm</i>	Bacillus genetic stock centre
KS35	<i>trpC2 ΔalrA::zeo ΔyitF::erm</i>	This work: RD180 transformed with gDNA of BKE10970
KS36	<i>trpC2 ΔdatA::erm ΔdltA-D::cat</i>	This work: KS22 transformed with gDNA of KS11
KS38	<i>trpC2 ΔalaT (markerless)</i>	This work: pDR244 transformed into KS31

KS39	<i>trpC2 ΔalaT (markerless)</i> <i>ΔdatA::erm</i>	This work: KS38 transformed with gDNA of BKE30530
KS41	<i>trpC2 ΔdatA::erm amyE Ω (cat</i> <i>P_{spac} datA-ftsLRBS)</i>	This work: pKS6 transformed into KS22
KS42	<i>trpC2 ΔdatA::erm amyE Ω (cat</i> <i>P_{spac} datA-ftsL(RBS)) ΔalrA::zeo</i>	This work:KS41 transformed with gDNA of RD180
BKE34440	<i>trpC2 ΔpbpE::erm</i>	Bacillus genetic stock centre
KS49	<i>trpC2 ΔdacA::spc ΔpbpE::erm</i>	This work: KS15 transformed with gDNA of BKE34440
BKE04140	<i>trpC2 ΔpbpC::erm</i>	Bacillus genetic stock centre
KS56	<i>trpC2 ΔdacA::spc ΔpbpC::erm</i>	This work: KS15 transformed with gDNA of BKE04140
BKE31490	<i>trpC2 ΔpbpD::erm</i>	Bacillus genetic stock centre
KS57	<i>trpC2 ΔdacA::spc ΔpbpD::erm</i>	This work: KS15 transformed with gDNA of BKE31490
BKE27310	<i>trpC2 ΔpbpI::erm</i>	Bacillus genetic stock centre
KS58	<i>trpC2 ΔdacA::spc ΔpbpI::erm</i>	This work: KS15 transformed with gDNA of BKE27310
BKE13980	<i>trpC2 ΔpbpH::erm</i>	Bacillus genetic stock centre
KS59	<i>trpC2 ΔdacA::spc ΔpbpH::erm</i>	This work: KS15 transformed with gDNA of BKE13980
BKE23190	<i>trpC2 ΔdacB::erm</i>	Bacillus genetic stock centre
KS60	<i>trpC2 ΔdacA::spc ΔdacB::erm</i>	This work: KS15 transformed with gDNA of BKE23190
BKE10110	<i>trpC2 ΔpbpF::erm</i>	Bacillus genetic stock centre
KS61	<i>trpC2 ΔdacA::spc ΔpbpF::erm</i>	This work: KS15 transformed with gDNA of BKE10110
BKE37510	<i>trpC2 ΔpbpG::erm</i>	Bacillus genetic stock centre
KS62	<i>trpC2 ΔdacA::spc ΔpbpG::erm</i>	This work: KS15 transformed with gDNA of BKE37510
BKE18350	<i>trpC2 ΔdacC::erm</i>	Bacillus genetic stock centre
KS63	<i>trpC2 ΔdacA::spc ΔdacC::erm</i>	This work: KS15 transformed with gDNA of BKE18350
BKE15170	<i>trpC2 ΔspoVD::erm</i>	Bacillus genetic stock centre
KS64	<i>trpC2 ΔdacA::spc ΔspoVD::erm</i>	This work: KS15 transformed with gDNA of BKE15170

BKE25000	<i>trpC2 ΔpbpA::erm</i>	Bacillus genetic stock centre
KS65	<i>trpC2 ΔdacA::spc ΔpbpA::erm</i>	This work: KS15 transformed with gDNA of BKE25000
BKE22320	<i>trpC2 ΔponA::erm</i>	Bacillus genetic stock centre
KS66	<i>trpC2 ΔdacA::spc ΔponA::erm</i>	This work: KS15 transformed with gDNA of BKE22320
BKE16950	<i>trpC2 ΔpbpX::erm</i>	Bacillus genetic stock centre
KS67	<i>trpC2 ΔdacA::spc ΔpbpX::erm</i>	This work: KS15 transformed with gDNA of BKE16950
BKE234380	<i>trpC2 ΔdacF::erm</i>	Bacillus genetic stock centre
KS68	<i>trpC2 ΔdacA::spc ΔdacF::erm</i>	This work: KS15 transformed with gDNA of BKE234380
AG364	<i>trpC2 ΔpbpD ΔpbpF ΔponA ΔpbpG::Kan ΔdacA::zeo</i>	Guyet, unpublished
4001	<i>trpC2 pbpB^(S309A)</i>	Xu <i>et al.</i> , unpublished
4261	<i>trpC2 Δmbl::cat</i>	Schirner and Errington (2009)
KS69	<i>trpC2 ΔdacA::spc Δmbl::cat</i>	This work: KS15 transformed with gDNA of 4261
3427	<i>trpC2 ΔmreB::neo</i>	Laboratory strains collection
KS70	<i>trpC2 ΔdacA::spc ΔmreB::kan</i>	This work: KS15 transformed with gDNA of 3427
4262	<i>trpC2 ΔmrebH::erm</i>	Schirner and Errington (2009)
KS71	<i>trpC2 ΔdacA::spc ΔmrebH::erm</i>	This work: KS15 transformed with gDNA of 4262
AG547	<i>trpC2 ΔlytE::cat</i>	Guyet, unpublished
KS72	<i>trpC2 ΔdacA::spc ΔlytE::cat</i>	This work: KS15 transformed with gDNA of AG547
1059	<i>chr::pJSIZΔpble (P_{spac}-ftzZ ble)</i> <i>trpC2 amyE::(spc P_{xyl}-ftsZ-cfp)</i>	Feucht and Lewis (2001)
KS73	<i>trpC2 ΔdacA::spc chr::pJSIZΔpble (P_{spac}-ftzZ ble)</i>	This work: KS15 transformed with gDNA of 1059
804	<i>trpC2 Ω (ftsL::pSG441 aphA-3 P_{spac} pbpB)799 (φ105J506) cat P_{xyl}ftsL</i>	Daniel <i>et al.</i> (1998)

KS74	<i>trpC2</i> Ω (<i>ftsL</i> ::pSG441 <i>aphA-3</i> <i>P_{spac} pbpB</i>)799 (ϕ 105J506) <i>cat</i> <i>P_{xyl}ftsL</i> Δ <i>dacA</i> :: <i>spc</i>	This work: KS15 transformed with gDNA of 804
2085	<i>trpC2 dacA</i> ::pSG1493 (<i>cat P_{xyl}-gfp-dacA1-423</i>)	Scheffers <i>et al.</i> (2004)
BKE09670	<i>trpC2</i> Δ <i>dat</i> :: <i>erm</i>	Bacillus genetic stock centre
KS78	<i>trpC2</i> Δ <i>alrA</i> :: <i>zeo</i> Δ <i>dat</i> :: <i>erm</i>	This work::RD180 transformed with gDNA of BKE09670
<i>E. coli</i> strains	Genotype/Relevant features	Construction or Source or Reference
BL21(DE3)	<i>fhuA2 [lon] ompT gal</i> (λ DE3) <i>[dcm] ΔhsdS λ DE3 = λ sBamHIo</i> Δ <i>EcoRI-B</i> <i>int</i> ::(<i>lacI</i> :: <i>PlacUV5</i> :: <i>T7</i> <i>gene1</i>) <i>i21</i> Δ <i>nin5</i>	New England BioLabs®
KS46	BL21(DE3) + pET-28a(+) + <i>datA</i> - <i>His tag</i>	This work: pKS7 transformed into BL21(DE3)
KS47	BL21(DE3) + pET-28a(+) + <i>His tag-datA</i>	This work:pKS8 transformed into BL21(DE3)
C43(DE3)	additional induced mutations in BL21(DE3)	Miroux and Walker (1996)
KS48	C43(DE3) Ω pET-28a(+) + <i>datA</i> - <i>His tag N</i>	This work:pKS8 transformed into C43(DE3)
DH5 α	<i>fhuA2</i> Δ (<i>argF-lacZ</i>)U169 <i>phoA</i> <i>glnV44</i> Φ 80 Δ (<i>lacZ</i>)M15 <i>gyrA96</i> <i>recA1 relA1 endA1 thi-1 hsdR17</i>	New England BioLabs®
KS75	DH5 α + pGH19 Ω <i>data</i>	This work:pKS9 transformed into DH5 α
KS76	DH5 α + pGH19 Ω HA epitope- <i>datA</i>	This work:pKS10 transformed into DH5 α
KS77	DH5 α + pGH19 Ω <i>datA</i> -HA epitope	This work:pKS11 transformed into DH5 α

2.3 Plasmids

The following table shows the list of plasmids, which were used in this study. The details of the plasmids construction have been explained in (section 2.8).

Table 2.2 Plasmid constructs

Name plasmid	Relevant features	Construction	Source/Reference
pLOSS* <i>alrA</i>	<i>bla spc P_{spac} alrA - PdivIA-lacZ lacI rep pLS20*</i>	Insertion of <i>alrA</i> gene into <i>pLOSS*</i> vector	Daniel, unpublished
pPY18	<i>bla amyE3' cat P_{spac} lacI lacZ amyE5'</i>	-----	Duggin <i>et al.</i> (1999)
pKS1	<i>bla amyE3' cat P_{spac} dataA lacI lacZ amyE5'</i>	Insertion of <i>dataA</i> gene and its upstream 30 bases into <i>XbaI</i> cut pPY18	This work
pSG1154	<i>bla amyE3' spc P_{xyl} -gfp amyE5'</i>	-----	Lewis and Marston (1999)
pKS2	<i>bla amyE3' spc P_{xyl} dataA-gfp amyE5' (C-terminus)</i>	Insertion of <i>dataA</i> gene into <i>XhoI</i> and <i>EcoRI</i> cut pSG1154	This work
pSG1729	<i>bla amyE3' spc P_{xyl} gfp-amyE5'</i>	-----	Lewis and Marston (1999)
pKS3	<i>bla amyE3' spc P_{xyl} gfp-dataA amyE5' (N-terminus)</i>	Insertion of <i>dataA</i> gene into <i>XhoI</i> and <i>EcoRI</i> cut pSG1729	This work
pKS6	<i>bla amyE3' cat P_{spac} dataA-ftsL(RBS) lacI lacZ amyE5'</i>	Insertion of <i>dataA</i> gene and RBS of <i>ftsL</i> gene into <i>XbaI</i> and <i>BglII</i> cut pPY18	This work

pET-28a(+)	<i>lacI T7 promoter lac</i> operator RBS <i>His.tag T7.tag</i> <i>thrombin His.tag T7</i> terminator <i>Kan</i>	-----	Novagen®
pKS7	<i>pET-28a(+)</i> Ω <i>datA-His tag</i> (C-terminus)	Insertion of <i>datA</i> gene into <i>NcoI</i> and <i>BamHI</i> cut of pET-28a(+)	This work
pKS8	<i>pET-28a(+)</i> Ω <i>His tag- datA</i> (N-terminus)	Insertion of <i>datA</i> gene into <i>NheI</i> and <i>XhoI</i> cut of pET-28a(+)	This work
pDR244	<i>bla pACYC</i> <i>ori cre spc cop</i> <i>repF</i>	-----	Rudner, unpublished
pGH19	-----	-----	Liman et al. (1992)
pKS9	pGH19 Ω <i>data</i>	Insertion of <i>datA</i> gene into the <i>EcoRI</i> and <i>XbaI</i> of cut pGH19	This work
pKS10	pGH19 Ω HA epitope- <i>datA</i> (N-terminus)	Insertion of HA epitope- <i>datA</i> gene into the <i>EcoRI</i> and <i>XbaI</i> of cut pGH19	This work
pKS11	pGH19 Ω <i>datA</i> -HA epitope (C-terminus)	Insertion of HA epitope- <i>datA</i> gene into the <i>EcoRI</i> and <i>XbaI</i> of cut pGH19	This work

2.4 Media supplements

2.4.1 Amino acids, inducers and substrates

The amino acids, inducers and substrates (Table 2.3) were added to the media according to the strain genotypes and the purpose of the experiments.

Table 2.3 Amino acids, inducers and substrates

Supplement		Stock solution	Final concentration	Bacteria
Amino acids	Tryptophan	2.0 mg/ml	20 µg/ml	<i>B. subtilis</i>
	L-alanine	20 mg/ml	Various concentrations	
	Glycine	20 mg/ml		
	L-proline	20 mg/ml		
	D-alanine	20 mg/ml	450-500 µM	
	¹⁴ C-D-alanine	155.25 µg/ml	0.5-1.0 µM	<i>B. subtilis</i> and <i>E. coli</i>
	Boc-D-2,3-diaminopropionic acid (NADA)	25 mM	50 µM	<i>B. subtilis</i>
Inducers	IPTG	1.0 M	Various concentrations	<i>B. subtilis</i> and <i>E. coli</i>
	Xylose	25 %	0.5 %	<i>B. subtilis</i>
Substrate	X-gal	4.0 %	0.02 %	<i>B. subtilis</i>
	Starch	2.5 %	0.12 %	<i>B. subtilis</i>

2.4.2 Antibiotics

The details of the antibiotics, which were used in this study, are shown in the following table.

Table 2.4 Antibiotics details

Antibiotics	Stock solution	Final concentration	
		<i>B. subtilis</i>	<i>E. coli</i>
Ampicillin	50 mg/ml	---	100 µg/ml
Kanamycin	25 mg/ml	5 µg/ml	25 µg/ml
Chloramphenicol	10 mg/ml	5 µg/ml	---
Spectinomycin	100 mg/ml	50 µg/ml	---
Erythromycin	20 mg/ml	1.0 µg/ml	---
Lincomycin	50 mg/ml	25 µg/ml	---
Zeocine	100 mg/ml	10 µg/ml	---
Phleomycin	2.5 mg/ml	1.0 µg/ml	---
D-cycloserine	50 mg/ml	50 µg/ml	---
Penicillin G	100 mg/ml	100 µg/ml	---

2.5 Oligonucleotides

The oligonucleotides (oligos) were designed by using Clone Manager software and Primer 3 Output online tool. After designing, they were synthesised by Eurogentec-

Kaneka Corporation. Aliquots of 10 μ M were prepared from the stock solutions and usually stored at -20 °C. The oligos of this study are shown in appendix C.

2.6 General methods

2.6.1 Extraction of genomic DNA (gDNA)

The method developed by Ward and Zahler (1973) was used to extract gDNAs for transformation purpose. The DNeasy blood & tissue kit (QIAGEN) was used for extraction of gDNAs for PCR template. The isolated gDNA was usually stored at -20 °C.

2.6.2 Extraction of plasmid DNA

E. coli strains were grown in 5.0 ml of LB medium, containing the necessary antibiotic, at 37 °C overnight. The plasmid DNA was extracted from the cells by QIAprep® Spin Miniprep Kit (QIAGEN) according to the manufacturer's protocol. The plasmid DNA was stored at -20 °C.

2.6.3 Polymerase chain reaction (PCR)

The Q5™ High-Fidelity DNA polymerase (New England BioLabs®) was used in PCR throughout the study. The quantity of PCR components and the reaction conditions were according to the manufacturer's instructions.

2.6.4 Restriction digestion of DNA

Restriction enzymes and appropriate digestion buffers from different suppliers (e.g. promega, Roche and New England BioLabs®) were used to cut the PCR products and plasmids according to the manufacturer's instructions.

2.6.5 Purification of PCR and restriction digestion products

QIAquick PCR Purification Kit (QIAGEN) was used to clean up DNA in PCR reaction according to the manufacture's protocol.

2.6.6 Agarose gel electrophoresis

A 1.0 % of agarose gel (MELFORD *biolaboratories* Ltd.) was melted in 1.0 X TAE buffer. The solidified gel was submerged in 1.0 X TAE buffer in an electrophoresis tank. The DNA sample was mixed with DNA loading buffer and loaded into the agarose gel wells. The electrophoresis was run at 120 Volt for about 30-40 min. The gel was then soaked in 1.25 μ g/ml of ethidium bromide (Sigma) in 1.0 X TAE buffer for 15- 20 min. The DNA bands were visualised by UV transilluminator.

2.6.7 Purification of DNA band from agarose gel

Illustra GFX PCR DNA and Gel Band Purification Kit (GE healthcare life sciences) were used to purify DNA fragments from agarose gel according to the manufacture's protocol.

2.6.8 Dephosphorylation of plasmid DNA

Before ligation, the digested DNA plasmids were dephosphorylated by Thermo-sensitive alkaline phosphatase (TSAP, Promega), according to the manufacturer's instructions.

2.6.9 Ligation of DNA

The T4 DNA ligase (Roche) was used in the construction of knockout strains and cloning plasmid constructs (see sections 2.7 and 2.8). The ligation reaction contained the recommended quantities of T4 ligase and DNA according to the manufacturer's protocol. The ligation reactions were carried out at 4.0 °C for overnight.

2.6.10 DNA sequencing of cloned genes

The correct sequence of the cloned genes in plasmid constructs was verified by DNA sequencing. The sequencing process was done by a sequencing service, based in University of Dundee, UK.

2.6.11 Extraction of total RNA

The wild type strain (168CA) was grown in LB media to mid-exponential growth ($OD_{600} \sim 1.0$) at 37 °C. Total RNA was extracted from 1.0 ml the culture, using total RNA purification plus Kit (NORGEN Biotek Corp.) according to the manufacturer's protocol. The RNA extract was stored at -80 °C.

2.6.12 Making complementary DNA (cDNA)

The high capacity cDNA reverse transcription kit (Applied Biosystems™) was used for making cDNA according to manufacturer's protocol. The total RNA extract was used as template and non-specific random hexamers as primer. The cDNA was stored at -20 °C.

2.6.13 Extraction of total cell protein and Polyacrylamide gel electrophoresis (SDS-PAGE)

The bacterial cells were grown for an appropriate period in LB media (with or without inducers). One millilitre of the culture was pelleted and suspended in 200 µl of NuPAGE® LSD sample loading buffer. The bacterial total cell protein was extracted by sonication (SONICS vibra cell™). The pre-casted NuPAGE® Bis-Tris gel (NOVEX® by life

technologies) was submerged in 1.0 X NuPAGE[®] MES running buffer in an electrophoresis tank. The protein extract was heated at 70 °C for 10 min before loading. Depending on the OD₆₀₀ of the cultures, an appropriate amount (µl) of protein extracts were loaded into the gel wells. The electrophoresis was run at 150 Volt.

2.6.14 Coomassie staining of SDS-PAGE gel

The SDS-PAGE gel was fixed in fixation solution for 1.0 h. The Coomassie stain solution (1.0 % in ethanol) was diluted 1.0 in 10 with fixation solution. The gel was soaked in the stain for 1.0-2.0 h. The gel was then destained by incubating in water until the background was disappeared. The image of the stained protein gel was finally taken.

2.6.15 Western blotting

Wet Western blot method was used to transfer the protein bands from the gel to PVDF (Hybond P) membrane (GE Healthcare). The membrane was treated with methanol for 30 seconds and soaked in transfer buffer. The gel was put on two layers of wet chromatography paper (Fisher Scientific) in a tray, contained transfer buffer. The wet PVDF membrane was put on top of the gel and two layers of chromatography paper were put on the PVDF membrane. Any possible air bubbles were removed by rolling a plastic tube on the chromatography papers - gel - PVDF membrane sandwich. The sandwich was soaked in transfer buffer in a tank (TransBlot Cell, BioRad) and run at 20 mA (5-6 Volts) overnight. The sandwich disassembled and the membrane was rinse in PBS. The membrane was incubated in blocking buffer for 1.0 h. Primary antibody was added and incubated for 1.0 h. The membrane was washed with PBST (0.1% tween 20 in PBS) five times (four short time washing (5 min) and one long time washing (15 min)). The washed membrane was incubated again in blocking buffer for 30 min. Secondary antibody was added and incubated for 1.0 h. The membrane was washed with PBST as before. Then, the membrane was incubated with Pierce[®] ECL 2 western blotting substrate (Thermo Scientific), according to the manufacturer's protocol. The protein bands were visualised and imaged by Luminescent image analyser (imageQuant LAS 4000 mini, GE Healthcare). In this study, the primary antibodies, such as Rabbit anti-Gfp IgG (life technologies), Mouse anti-His IgG (Qiagen) and Guinea pig anti-LdcB IgG (Richard Daniel), were used. The primary antibodies were diluted 1.0 in 1000 with blocking buffer before using. Meanwhile, 1.0 in 2000 dilution of acetone precipitation purified rabbit polyclonal anti-DacA IgG (R. Daniel) was used. The secondary antibodies were anti-

rabbit IgG-, anti-mouse IgG- and anti-guinea pig IgG-Horse radish peroxidase (HRP) (Sigma[®]). These secondary antibodies were diluted 1.0 in 10000 with blocking buffer.

2.6.16 Over-production and purification of membrane protein

A 100 ml of LB medium plus an appropriate antibiotic was inoculated with *E. coli* strain, carried a plasmid copy of *His* tagged *datA* gene. The culture was incubated at 30 °C for overnight. The overnight culture was used to inoculate 5.0-10 L of LB medium, supplemented with kanamycin (25 µg/ml) and incubated at 37 °C until OD₆₀₀ 0.8. The culture was induced with 0.5-1.0 mM IPTG and incubated at 18, 22, 30 and 37 °C for 5 h and overnight. The induced culture was centrifuged at 6400 rpm, 4.0 °C for 20 min (Beckman coulter[®], Avanti[®] centrifuge J-26 XP, fixed angle rotor JLA-8.1000) The culture pellet was suspended in 60 ml of universal buffer and homogenised. The cells were disrupted by sonication (BRANSON digital sonifier[®]) three times at each of these strengths (10, 20, 30, 40, and 50 %). The period of each time of sonication was 20 seconds. In addition, French press (Constant cell disruption systems, constant systems limited, UK) was used to disrupt the cells at 23 kpsi. The disrupted cell suspension was centrifuged at 42000 rpm, 4.0 °C for 45 min (Beckman ultracentrifuge). The pellet was suspended in 30 ml of extraction buffer, homogenised and kept at 4.0 °C for 1.0 h with gentle stirring. The membrane extract was centrifuged at 50000 rpm, 4.0 °C for 30 min in Beckman ultracentrifuge. The purification was done manually by using a PD-10 column, containing Ni-NTA super flow resin (Qiagen). The Ni-NTA column was firstly equilibrated with column equilibration buffer. The supernatant was applied to the column, and the column was washed with 50 ml of column wash buffer. The protein was eluted in 3.0-10 ml of elution buffer. The diluted purified protein was concentrated to 500 µl by centrifugation, using a 50000 MWCO filter column.

2.6.17 Preparation of membrane vesicles

The membrane vesicle was prepared according to the methods, described in Konings and Freese (1972) and Wientjes *et al.* (1979). One litre of bacterial culture at OD₆₀₀ 1.5-2.0 was centrifuged for 10 min at 10000 X g and 4.0 °C (Beckman coulter[®], Avanti[®] centrifuge J-26 XP, fixed angle rotor F10BA-6X500y) The cell pellet was washed with 0.1 M potassium phosphate (pH 7.3) and suspended in protoplast formation buffer. The cell suspension was incubated at 30 °C for 45 min. Phase-contrast microscope was used to check that the majority of the cells turned to protoplasts. The protoplasts were pelleted for 20 min at 15000 X g and 4.0 °C. They were osmotically lysed by immediate

suspension in 0.1 M potassium phosphate (pH 7.3), and 10 µg/ml of deoxyribonuclease (DNAase, Sigma) was added. The cellular debris was removed by low speed centrifugation for 10 min at 15000 X g and 4.0 °C. The membrane vesicle in the supernatant was pelleted at 100000 X g for 1.0 h at 4.0 °C (Thermo Scientific WX ultracentrifuge, SureSpin™ 630 swinging Bucket Rotor). The membrane vesicles were suspended in 0.1 M potassium phosphate buffer (pH 6.6) at 5 mg protein per ml. The membrane vesicles were frozen in liquid nitrogen and kept at -80 °C. The D-alanine transport by membrane vesicles was studied at room temperature according to Konings and Freese (1972). The reaction mixture consisted of 0.5 µM (0.033 µCi/ml) of [1-¹⁴C] D-alanine and membrane vesicles in 0.05 M potassium phosphate buffer (pH 6.6) with and without 5.0 mM NaCl. A 100 µl of the mixture was filtered through cellulose nitrate membrane filter (Pore size 0.45 µm, diameter 25 mm, Whatman™) under vacuum every 10 min. The filter was washed with 0.05M potassium phosphate (pH6.6) and soaked in 2.0 ml of scintillation cocktail in a vial. The radioactivity in membrane vesicles was measured with a scintillation counter (HIDEX 300SL, reading period, 5.0 min per sample).

2.6.18 Transformation

2.6.18.1 Transformation of *B. subtilis*

The transformation of *B. subtilis* strains was fulfilled according to the method developed by Anagnostopoulos and Spizizen (1961) and modified by Young and Spizizen (1961). The transformed strains were checked for antibiotic resistance, and the gene knockouts were confirmed by PCR.

2.6.18.2 Transformation of *E. coli*

Fifty microliters of *E. coli* competence strains (DH5α, BL21 (DE3) and C43 (DE3)) were mixed with ligation mixture or plasmid DNA (~10 ng) and left on ice for 45 min. The transformation mixture was heat shocked by incubating at 42 °C for 2.0 min in a water bath. A 250 µl of LB medium was then added and incubated at 37 °C for 1.0 h. The transformation was selected on plates, containing an appropriate antibiotic. The plates were incubated at 37 °C for overnight. This transformation procedure was obtained from Current Protocol in Molecular Biology text book (Abusubel *et al.*, 2003).

2.6.19 Microscopy

2.6.19.1 Fluorescent Microscopy

For staining of cell membrane, FM5.59 fluorescent dye (Invitrogen) was used. A 40 μ l of cell culture was incubated with 1.0 μ l of FM5.59 stock (200 μ g/ml) for 3.0-5.0 min with shaking. The fluorescent D-amino acid (NADA) was also used for cell wall labelling. A multi-well slide was covered with a thin layer of 1.0 % agarose gel. A few microliters of the cells suspension was put on the agarose pad and let dry but not completely. The cell spot was covered with a cover slip and used in microscopic examination. For DNA staining, 2.0 μ l of DNA staining fluorescent dye DAPI (DAPI in antifade mountant, molecular Probes[®]) was added to dried cell spots on a slide. The images were acquired by either a Sony CoolSnap HQ2 cooled CCD camera (Roper scientific) attached to a Zeiss Axiovert M200 microscope or Qimaging Rolera Em-c2 cooled CCD camera attached to a Nikon Eclipse Ti microscope. The Metamorph[®] imaging software (MolecularDevices) was used to collect and process the microscopic images. The ImageJ program was used to apply scale bars to the images.

2.6.19.2 Time-lapse microscopy

The preparation of the microscopic slide for time-lapse microscopy was done according to a technique, described by de Jong *et al.* (2011). Fully NADA labelled live cells were pelleted and washed once with pre-warmed fresh PTM. The pellet was suspended in the same medium at OD₆₀₀ 0.05. A 2.0 μ l of the culture was spotted on the top of solid PTM (PTM + 1.0 % agarose), which was already mounted on the microscopic slide. The preparation of cell sample for time-lapse was performed as quickly as possible, and the experiment was done at 37 °C. The Nikon Eclipse Ti-U inverted epifluorescence microscope fitted with a Plan-Apochromat objective (Nikon DM 100x/1.40 Oil Ph3.0) and a CoolSnap HQ2 cooled CCD camera (Photometrics) was used to acquire the images of the live cells every 4.0 min at an exposure time of 80 milliseconds (ms). The light was transmitted from a 300 Watt xenon arc-lamp through a liquid light guide (Sutter Instruments). The images were collected by Frap-AI 7.7.5.0 Software (MAG Biosystems) and used to make movies by ImageJ program.

2.6.20 Immunofluorescence assay

The bacterial strain was grown in LB medium to mid-exponential phase (OD₆₀₀ ~ 1.0) at 37°C. A 0.5 ml of the culture was pelleted at 10000 rpm for 1.0 min (Thermo ScientificPico™ 17 Microcentrifuge, Fixed angle, 24 place rotor, RCF 17000). The pellet

was suspended in 0.5 ml of cell fixation solution (3.0 % paraformaldehyde in PBS) and held on ice for 30 min. The fixed cells were pelleted again and washed three times with PBS. The cells were finally suspended in GTE solution. A 20 μ l of the fixed cell suspension in GTE was spotted on a multi-well slide and left for 5.0 min at room temperature. After settling down of the cells on the slide, the excess solution was aspirated off and 20 μ l of 0.01 % poly lysine was added for 2.0 min. The excess poly lysine was aspirated off, and then the cells were treated with lysozyme in PBS solution (2 mg/ml) for 1.0 min at room temperature. The excess solution was removed and the cells spot was washed with PBS. The cells were rehydrated with PBS for 3.0 min. The cells spot was blocked with cell blocking solution (2.0 % Bovine serum albumin in PBS) for 15 min. The primary antibodies (Guinea pig anti-LdcB IgG and/or Rabbit anti-DacA IgG (provided by Richard Daniel)) were added at 1:1000 dilutions in cell blocking solution and incubated at 4.0 °C overnight. Next day, the cells spot was washes twice with PBST buffer and then 10 times with PBS. The secondary antibodies (Alexa Fluor[®] 594 anti-guinea pig IgG (H+L) (Molecular Probes[®]) and/or FITC conjugated anti-rabbit IgG (Sigma[®])) were added at 1:10000 dilution in cell blocking solution and incubated in a dark place for 1.0 h at room temperature. The cells spot was washed as before and mounted with 2.0 μ l of DNA staining fluorescent dye DAPI (DAPI in antifade mountant, molecular Probes[®]). The slide was finally covered with a cover slip and examined microscopically, using red (mcherry) filter and 1000 msec exposure time for detection of Alexa flour, but green (GFP) filter and 750 msec exposure time for FITC detection (see section 2.6.19.1 for microscope details and image processing).

2.7 Gene knockout (deletion) in *B. subtilis*

The desired genes were deleted by PCR amplification of a pair of 2.0 kilo base (kb) long concatameric DNA fragments. The produced fragments were complimentary to the upstream and downstream sequences, which are located outside of the reading frame of the deleted genes. We designed oKS01, oKS02, oKS03 and oKS04 oligos for deletion of *dltA-D* genes. The oKS01 and oKS02 oligos were used to amplify a 2.0 kb DNA fragment, complimentary to the DNA sequence at the upstream of *dltA* gene. The oKS03 and oKS04 oligos were used in the production of a 2.0 kb DNA fragment at the downstream of *dltD* gene. Although there is *Xba*I restriction site in the oKS02 and *Xba*I+*Bgl*III restriction sites in oKS3, but both the fragments were digested with *Bgl*III, because there was also a native *Bgl*III restriction site in the upstream fragment. After purification, appropriate quantities of the digested DNA fragments were ligated with a

chloramphenicol resistant cassette (*cat*), already digested with *Bam*HI. The ligation product was used in the transformation of *B. subtilis* 168CA strain. The correct knockout strain was confirmed by PCR and named KS11 (Δ *dlta-D::cat*).

The deletion of *dacA* gene was done by designing four oligos (oKS05, oKS06, oKS07 and oKS08). The oKS05 and oKS06 oligos were used to produce a 2.0 kb DNA fragment at the upstream of *dacA* gene, and oKS07 and oKS08 oligos used to amplify a 2.0 kb DNA fragment at the downstream of *dacA* gene. The oKS6 and oKS07 contained *Bam*HI restriction site, so the fragments were digested with *Bam*HI. The digested fragments were purified, and appropriate quantities of them were ligated with Spectinomycin resistant cassette (*spc*). The ligation product was transformed into *B. subtilis* 168CA strain. The correct knockout strain was confirmed by PCR and named KS15 (Δ *dacA::spc*).

The KS18 (Δ *ldcB::erm*) strain was constructed, using oKS09, oKS10, oKS11 and oKS12 oligos. The oKS09 and oKS10 oligos were used in PCR reaction to amplify a 2.0 kb DNA fragment at the downstream of *ldcB* gene, whereas oKS11 and oKS12 oligos were used in the PCR amplification of a 2.0 kb DNA fragment, complimentary to the DNA sequence at the upstream of *ldcB* gene. The 2.0 kb DNA fragments were digested with *Bam*HI, because the *Bam*HI restriction site was edited into the oKS10 and oKS11 oligos. The digested fragments were purified and appropriate amounts were ligated with erythromycin resistant cassette (*erm*). Finally, the competence *B. subtilis* 168CA strain was transformed with the ligation product. The correct transformant was checked by PCR.

2.8 Plasmid constructs

The pKS1 plasmid was constructed by inserting the *datA* gene coding sequence and its upstream 30 bases into the pPY18 vector. The *datA* gene was amplified by PCR using a pair of oligos (oKS21 and oKS22). The *datA* fragment and the pPY18 vector were cut with *Xba*I restriction enzyme separately. The digested *datA* fragment was purified and the digested pPY18 was dephosphorylated before ligation. The ligation mixture was transformed into *E. coli* DH5 α competent cells. The plasmid constructs were extracted from six randomly chosen transformed colonies, and they checked by restriction digestion and sequencing. The correct plasmid construct (pKS1) was inserted into the *amyE* locus on gDNA of *B. subtilis* by transformation. The lack of amylase activity was confirmed by growing the transformed cells on nutrient agar plates, supplemented with 0.12 % starch.

The KS2 and KS3 plasmids were constructed to express C- and N- termini GFP tagged *datA* respectively. The coding sequence of *datA* gene was amplified by PCR, using

oKS23 and oKS24 oligos. The amplified *datA* gene fragment was run in agarose gel electrophoresis and the desired band was cut out and purified by gel extraction kit. Then, the *datA* gene fragment and both pSG1154 (for C-terminus GFP tag) and pSG1729 (for N-terminus GFP tag) vectors were restriction digested with *XhoI* and *EcoRI*. The restriction digested vectors were dephosphorylated and ligated with the digested *datA* insert. The ligation mixture was transformed into *E. coli* DH5 α competent cells, and the plasmid constructs were checked as mentioned above. The correct pKS2 and pKS3 constructs were transformed into the *amyE* locus on gDNA of *B. subtilis*. The lack of amylase activity was also ensured.

The pKS6 plasmid was constructed by inserting of *datA* coding sequence into the pPY18 vector. The *datA* gene was amplified by PCR using a pair of oligos (oKS25 and oKS26). The ribosome binding site (RBS) of *ftsL* gene was edited to the upstream of start codon in the forward oligo (oKS25). The *datA* fragment and the pPY18 vector were cut with *XbaI* and *BgIII* restriction enzymes. The digested *datA* fragment was purified and the digested pPY18 was dephosphorylated before ligation. The ligation mixture was transformed into *E. coli* DH5 α competent cells. Six transformed colonies of *E. coli* were randomly chosen for plasmid extraction. The plasmid constructs were checked as mentioned previously. The correct pKS6 construct was introduced into the *amyE* locus on gDNA of *B. subtilis* by transformation. The lack of amylase activity was used to confirm correct insertion of the genetic construct.

The pKS7 and pKS8 plasmids were constructed to express C- and N- termini His tagged *datA* respectively. The coding sequence of *datA* gene was amplified by PCR, using two pairs of oligos (oKS27 and oKS28) for C-terminus His tag (oKS29 and oKS30) for N-terminus His tag. The *datA* gene fragments and the pET -28a(+) vector were restriction digested with *NcoI* and *BamHI* for C-terminus and with *NheI* and *XhoI* for N-terminus His tag. The restriction digested vectors were dephosphorylated and ligated with the corresponding *datA* inserts. The ligation mixture was transformed into *E. coli* DH5 α competent cells. The extraction and checking of the plasmid constructs were done as mentioned previously. The correct constructs were transformed into *E. coli* BL21(DE3) and *E. coli* C43 (DE3) strains.

The pKS9 plasmid was made for expressing *datA* gene in *Xenopus* oocyte. Both oKS71 and oKS72 oligos were used to amplify the coding sequence of *datA* gene by PCR. The second codon of *datA* gene was changed to GCA (an alanine specific codon), for keeping the optimal Kozak sequence (ACCATGG) at the beginning of the clone. The stop codon was also changed to TAA. The PCR product and pGH19 vector were restriction digested

with *EcoRI* and *XbaI*. The digested PCR product was purified and the digested pGH19 vector was dephosphorylated. Both the *datA* insert and the pGH19 were ligated. The ligation mixture was transformed into *E. coli* DH5 α competent cells. The pKS9 plasmid was linearised and cRNA was synthesised, using *in vitro* transcription (see appendix E). Besides, pKS10 and pKS11 were constructed to allow the expression of N- and C-termini HA-epitope tagged DatA protein respectively. The oKS72 and oKS73 oligos were used in the PCR amplification of N-terminus HA-epitope-*datA* recombinant gene. The oKS71 and oKS74 oligos were also used to amplify C-terminus HA-epitope-*datA* recombinant gene. Like pKS9, the pGH19 vector and the same restriction enzymes were used in the construction of pKS10 and pKS11.

2.9 Quantitative measurement of D-alanine in culture supernatant by RP-HPLC

2.9.1 Growth conditions

The bacterial strain was grown in 5.0 ml of LB broth at 30 C° for overnight. The overnight culture was diluted 1:10 with pre-warmed LB and was grown again for 2.0 h at 37 C°. After this incubation, the optical density at 600 nm (OD₆₀₀) of the culture was read. An appropriate volume of the culture was centrifuged at 6000 rpm for 3 min in a benchtop centrifuge (Universal 320, 35° angle rotor, 6 place, RCF 9,509). The pellet was suspended with pre-warmed LB broth to make culture with initial OD₆₀₀ 0.1 and incubated at 37 C°. The growth of the strain was monitored by reading OD₆₀₀, using a spectrophotometer (BECKMAN DU650).

2.9.2 Culture sample processing

Sample was taken from the culture at different time points and centrifuged at 6000 rpm for 5.0 min. The culture supernatant was filtered through sterile syringe filter (pore size 0.2 μ m, GILSON®) and then passed through spin column (Vivaspin 2.0 Hydrosart, 2000 MWCO, Generon Ltd.). For standard curve, the LB medium sample was filtered and passed through the spin column as well. The highly filtered culture supernatant was kept at 4.0 C° and used as sample for RP-HPLC detection of D-alanine. A 150 μ l of the super filtered culture supernatant was concentrated to 50 μ l by SpeedVac (SavantSPD131DDA SpeedVac concentrator, from Thermo Electron Corporation). A 150 μ l of Marfey's reagent (1.0 % Na-(2,4-Dinitro-5-fluorophenyl)-L-alaninamide in acetone, from Sigma) was added and mixed by vortex. Then, 40 μ l of sodium bicarbonate (1.0 M) was added and mixed to create an alkaline medium for the reaction. The mixture was heated for 1.0 h at 40 C° with shaking at 750 rpm (Thermomixer compact, Eppendorf). The mixture was

let to cool down and 25 μ l of HCl (2.2 M) was added to stop the reaction. The mixture was dried out by SpeedVac and suspended in 150 μ l of HPLC suspension solution (90 % of 0.05M Triethylamine phosphate (pH 3.0) and 10 % of Acetonitrile + 0.1 % Formic acid). The dried pellet was solubilised by glass stirring manually, and followed by 15 min vortexing (Thermomixer compact, Eppendorf). The suspension was finally filtered through 0.22 μ m centrifuge tube filter (cellulose acetate filter, from Costar) at 13000 rpm for 1.0 min, and the filtrate was use as sample for HPLC analysis.

2.9.3 RP-HPLC analysis conditions

The sample was run in Perkin Elmer series 200 HPLC machine. The column type was Spheri-5, RP-18, dimension 100 mm x 4.6 mm, particle size 5.0 μ m (Perkin Elmer) and the column guard was NewGuard RP-18, 7.0 μ m, 15 x 3.2 mm (Perkin Elmer). The solution A of the mobile phase was 0.05 M Triethylamine phosphate (pH 3.0) and the solution B was Acetonitrile + 0.1 % formic acid. The linear gradient was increasing of solution B from 10 % to 25 % in 40 min. The flow rate was 1.0 ml/min at 35 °C and the detection wave length was 340 nm, using S200 Diode array detector (DAD). After each run, the column was washed with solution D (water) and then with solution C (60 % methanol). The details of the run parameters are shown in (Table 2.5).

Table 2.5 Pump and run parameters of RP-HPLC analysis

Step	Time (min)	Flow (ml/min)	A	B	C	D	Curve	Sample volume(μ l)
0	0.5	1.00	90.0	10.0	0.0	0.0	0.0	150
1	1.5	1.00	90.0	10.0	0.0	0.0	0.0	
2	40.0	1.00	75.0	25.0	0.0	0.0	1.0	
3	25.0	1.00	60.0	40.0	0.0	0.0	1.0	
4	0.5	1.00	90.0	10.0	0.0	0.0	0.0	
5	20.0	1.00	90.0	10.0	0.0	0.0	0.0	
Total Run Time	87.00							

2.10 Radioactive [14 C] D-alanine labelling of cell wall

2.10.1 Radioactive incorporation assay

The bacterial strain was grown in LB broth with 450 μ M of D-alanine at 30 C° for overnight. The overnight culture was diluted 1:10 with pre-warmed LB broth,

supplemented with 450 μM of D-alanine and was let grow for 2.0 h at 37 $^{\circ}\text{C}$ on a shaker. An appropriate amount of the culture was pelleted at 6000 rpm for 3.0 min in a benchtop centrifuge (Universal 320, 35 $^{\circ}$ angle rotor, 6 place, RCF 9,509). The pellet was suspended in fresh LB broth to prepare 0.1 OD_{600} culture. The D-alanine auxotroph cultures contained 450 μM of D-alanine, including both radioactive (1.1 μM) and non-radioactive (449 μM) D-alanine in 1:400 ratio, the radioactivity in the culture was 0.065 $\mu\text{Ci/ml}$. The properties of radioactive [1- ^{14}C] D-alanine stock were specific activity: 58.6 mCi/mmol , concentration: 155.25 $\mu\text{g/ml}$; 0.1 mCi/ml , from HARTMANN ANALYTIC. In the meantime, another culture without radioactive D-alanine was used for monitoring growth curve in parallel of radioactive labelling. Both radioactive and non-radioactive cultures were grown at 37 $^{\circ}\text{C}$ with shaking at $n=100$ in shaking water bath (Thermo Scientific SWB25). A 100 μl of the radioactive culture was taken every 20 min for 2.0 h and filtered through cellulose nitrate membrane filter (Pore size 0.45 μm , diameter 25 mm, WhatmanTM) under vacuum. The filter was washed with 4 ml PBS buffer and let dry in a scintillation vial. Then, 2.0 ml of Ultima Gold scintillation cocktail (Perkin Elmer, Inc.) was added. The radioactivity (DPM) of the sample was measured with a scintillation counter (HIDEX 300SL, reading period 10 min per sample). The growth curve was simultaneously monitored by using a spectrophotometer (Thermo Scientific GENESYS 20).

2.10.2 Radioactive depletion (turnover) assay

At the end of the labelling assay (after 120 min), an appropriate amount of both the [1- ^{14}C] D-alanine labelled and non- labeled cell cultures were centrifuged at 6000 rpm for 2.0 min, using JENCONS-PLS minicentrifuge (Maximum speed/RCF: 6000 rpm/ 2000 xg; rotor: 6 x 1.5/ 2.0 ml). The cell pellets were suspended in fresh LB medium, containing only 450 μM of non-radioactive D-alanine. The initial OD_{600} of the cultures was ~ 0.1 . The culture of radioactive labelled cells was used for studying of cell wall turnover. The culture of non-radioactive cells was used for monitoring growth curve. The cultures were grown at 37 $^{\circ}\text{C}$ in shaking water bath and the same sampling technique was used as described above.

2.10.3 Measurement of radioactivity in culture supernatant

The initial radioactivity and the radioactivity left in the culture medium after 120 min of incubation was measured. At the onset (zero min) and the end (120 min) of radioactive labelling assay (section 2.10.1), a 100 μl of the culture was taken and centrifuged at 6000

rpm for 2.0 min in Jencons-*PLS* minicentrifuge (Maximum speed/RCF: 6000 rpm/ 2000 xg rotor: 6 x 1.5/ 2.0 ml). A 25 μ l of the culture supernatant was added to 2.0 ml of scintillation cocktail in a scintillation vial. The radioactivity was measured by the same scintillation counter as described above.

2.11 Cell wall labelling with fluorescent D-amino acid (FDAA)

2.11.1 Fluorescent D-amino acid incorporation assay

The bacterial strain was grown in LB broth at 30 °C with shaking for overnight. The overnight culture was diluted 1:10 with pre-warmed LB broth. The diluted culture was let grow for 2.0 h at 37 °C on a shaker. A 2.5 ml of the culture was pelleted at 6000 rpm for 3.0 min in a benchtop centrifuge (Universal 320, 35° angle rotor, 6 place, RCF 9,509). The pellet was suspended in 5.0 ml of pre-transformation media (PTM) and incubated for 2.0 h at 37°C. An appropriate amount of the culture was pelleted and suspended in fresh PTM to make a culture with OD₆₀₀ 0.1. Then, Boc-D-2,3-diaminopropionic acid (NADA) was added to the culture and incubated at 37 °C. Samples were taken at different time points and the cells were pelleted at 10000 rpm for 1.0 min (Thermo ScientificPico™ 17 Microcentrifuge, Fixed angle, 24 place rotor, RCF 17000). The cells were washed three times with 1.0 ml of cold PBS and fixed with cell fixation solution (3.0 % paraformaldehyde in PBS). The fixed cells were suspended in PBS for microscopic study (see section 2.6.19.1 for microscopy details).

Note: 25 mM of Mg²⁺ was added to the cultures of *ponA*, *mreB*, *mbl*, *mreBH* mutants.

2.11.2 Fluorescent D-amino acid depletion (turnover) assay

As explained above, the bacterial cells were labelled with NADA for 2.0 h at 37 °C. An appropriate amount of the fully labelled cells was pelleted and suspended in fresh PTM to make OD₆₀₀ 0.1 culture. The culture incubated at 37 °C and samples were taken at the beginning and every 20 min for 2.0 h. The cell samples were pelleted at 10000 rpm for 1.0 min (Thermo ScientificPico™ 17 Microcentrifuge, Fixed angle, 24 place rotor, RCF 17000). The cells were washed three times with 1.0 ml of cold PBS and fixed with cell fixation solution (3.0 % paraformaldehyde in PBS). The fixed cells were suspended in PBS for microscopic study (see section 2.6.19.1 for microscopy details). Cell wall turnover was also investigated in NADA labelled live cells by time-lapse microscopy (see 2.6.19.2 for details).

2.11.3 Quantitative analysis of NADA labelled cells

The Metamorph[®] imaging software (MolecularDevices) was used to collect and process the microscopic images of NADA labelled cells. All the images were acquired at a constant exposure time of 1000 msec, and using green (GFP) filter. The intensity of fluorescent (average of Gray level), which corresponds to the amount of NADA incorporated into the lateral cell wall, was measured by linescan tool (Scan width 6.0) of the Metamorph software. This software automatically generated the mean of fluorescent intensity in a selected area of the cell wall. Besides, ImageJ program was used to generate surface plot, showing differences in the distribution of fluorescent intensity throughout cell wall.

Chapter 3. Analysis of D-alanine metabolism in *B. subtilis*

3.1 Introduction

D-alanine is an essential amino acid for cell wall synthesis in bacteria. It participates in peptidoglycan cross-links, which are formed between the 4th D-alanine residue on one stem peptide (donor) and the *meso*-2,6-diaminopimelic acid (*m*-A2pm) residue on the adjacent stem peptide (acceptor) by transpeptidases (Vollmer *et al.*, 2008a). Only about 30-40 % of stem peptides are cross-lined in the peptidoglycan of *B. subtilis* (Atrih *et al.*, 1999; Sekiguchi and Yamamoto, 2012). The metabolic pathway of D-alanine has been studied for decades. However, the pathway has not been fully characterised in *B. subtilis*, so genetic manipulations in D-alanine metabolic pathway could be helpful to further understand D-alanine and cell wall metabolism in Gram-positive bacteria. *B. subtilis* synthesises D-alanine *in vivo* by the main alanine racemase, AlrA, which converts L-alanine to D-alanine and vice versa. When the alanine racemase gene (*alrA*) is deleted, D-alanine must be added to the growth medium. However, it was reported that D-alanine auxotroph strain (*alrA*) is able to grow in MM without D-alanine supplement, and addition of L-alanine to MM inhibited its growth (Ferrari *et al.*, 1985). It is unknown what gene product supports the growth of *alrA* strain in MM. A sporulation alanine racemase (AlrB) was also characterised in *B. subtilis*, but the physiological function of AlrB is still unclear (Pierce *et al.*, 2008).

Gram-positive bacteria also utilise D-alanine in the post-biosynthetic modification of teichoic acids, which are anionic polymers and second components of Gram-positive cell wall. The D-alanine molecules are added to the teichoic acids of *B. subtilis* by a four protein complex (DltA, B, C and D), encoded by *dlt* operon (Perego *et al.*, 1995). The deletion of any of the four *dlt* genes resulted in the complete absence of D-alanine in teichoic acids without causing any detectable growth and morphological defects (Perego *et al.*, 1995; Wecke *et al.*, 1996). The D-alanine esters of teichoic acids are spontaneously broken by the function of alkaline pH, whereas those of peptidoglycan are stable (Ellwood and Tempest, 1972; Archibald *et al.*, 1973; Koch *et al.*, 1985b; Hyyrylainen *et al.*, 2000). Therefore, the D-alanylation of teichoic acids can be avoided, while peptidoglycan carboxypeptidations are the main focus of investigation.

It was previously demonstrated that the D-alanine residues at positions 5 of stem peptides are trimmed by the main DD-carboxypeptidase (DacA) (Atrih *et al.*, 1999). It was thought that carboxypeptidases regulate the degree of cross-links in peptidoglycan

(Izaki *et al.*, 1968). However, the DacA of *B. subtilis* was inhibited by 6-aminopenicillanic acid and even its encoding gene was deleted without causing a significant change in the degree of peptidoglycan cross-linking, comparing to the wild type (Sharpe *et al.*, 1974; Atrih *et al.*, 1999). Lastly, it was proposed that DacA has a role in peptidoglycan maturation (Atrih *et al.*, 1999). Although the LD-carboxypeptidase activity was historically detected in the membrane extract of *B. sphaericus* (Arminjon *et al.*, 1977; Guinand *et al.*, 1979), more recently the LD-carboxypeptidase (LdcB, formerly YodJ) has been characterised in *B. subtilis*. This enzyme trims the uncross-linked D-alanine residues on the position 4 of peptide side chains, for still unclear reason. The HPLC analysis showed that the peptidoglycan of *ldcB* mutant mainly contains tetrapeptide side chains (Hoyland *et al.*, 2014). Despite the above hypotheses about the roles of DacA, the physiological roles of DacA and LdcB are unclear in *B. subtilis*.

More recently, studies have shown that soil and marine bacteria consume D-alanine and some other D-amino acids from the surrounding environment (Lam *et al.*, 2009; Azua *et al.*, 2014; Zhang and Sun, 2014). Besides these observations, the consumption of exogenous D-alanine by D-alanine auxotroph bacteria is evident that bacteria possess an uptake system for D-alanine transport. However, only few attempts have been done to identify and/or characterise D-alanine transporter in bacteria. The isolation of D-cycloserine resistant strains (*cycA*) of *E. coli* K-12 initiated the study of D-alanine transport in *E. coli* (Curtiss *et al.*, 1965; Russell, 1972; Cosloy, 1973). D-cycloserine compound is a structural analogue of D-alanine and acts as a competitive antagonist of D-alanine in bacterial cell wall biosynthesis (Shockman, 1959; Strominger, 1959; Zygmunt, 1962). It must actively be transported into the cells to inhibit bacterial growth (Oxender, 1972). The D-cycloserine resistant mutants (*cycA*) of *E. coli* K-12 showed nearly complete loss of D-alanine, D-serine, D-cycloserine and glycine transport, and partial loss of L-alanine transport (Wargel *et al.*, 1971; Cosloy, 1973; Robbins and Oxender, 1973). Moreover, a point mutation in *cycA* gene, encoding a L-alanine, D-alanine, glycine, D-serine transporter, provided partial resistance to D-cycloserine in *Mycobacterium bovis* BCG vaccine strains (Chen *et al.*, 2012). A *dagA* gene, which showed functional complementary to *cycA* of *E. coli*, was also identified in *Alteromonas haloplanktis*. It was suggested that DagA protein is a Na⁺ coupled D-alanine and glycine symporter (MacLeod and MacLeod, 1992). An alanine carrier protein (ACP) was also characterised in *Bacillus sp.* PS3 (thermophilic bacterium PS3). The transport of alanine

by ACP is driven by either Na^+ or H^+ (Kamata *et al.*, 1992). Furthermore, an alanine-sodium symporter (AgcS) was reported in an archaea bacterium, *Methanococcus maripaludis*, which transports both L- and D- alanine to permit them to be metabolised as a nitrogen source (Moore and Leigh, 2005). Recently, an ATP-binding cassette (ABC) transporter for D-alanine was characterised in *Salmonella enterica*. This pathogen has a *dalSTUV* operon, which encodes a periplasmic substrate (D-alanine)-binding protein (DalS), two membrane spanning permeases (DalT and DalV) and a cytoplasmic ATPase (DalU) (Osborne *et al.*, 2012). The properties of the above proposed D-alanine transporters are summarised in (Table 4.1). Thus, the gene(s), encoding D-alanine transporter(s), has not been identified in *B. subtilis*. The identification of such transporter could be helpful to understand some of the aspects of cell wall metabolism (e.g. roles of carboxypeptidation and the fate of the released D-alanine).

In this chapter, we characterised the growth of a *B. subtilis* D-alanine auxotroph (*alrA*) strain in LB and MM. This characterisation was exploited to determine the quantity of D-alanine in peptidoglycan and teichoic acids, to investigate the physiological functions of carboxypeptidases in cell wall metabolism, to identify a D-alanine transporter (Data) and finally to discover how *alrA* strain is able to grow in MM without D-alanine.

3.2 Results

3.2.1 Characterisation of D-alanine auxotroph *B. subtilis*.

A *B. subtilis* D-alanine auxotroph can be constructed through deleting the major alanine racemase gene (*alrA*). The lack of alanine racemase (AlrA) causes growth inhibition in the rich media, unless D-alanine is added. Since D-alanine is only needed in cell wall biosynthesis, the characterisation of D-alanine auxotroph strain could be an important point to start studying cell wall metabolism. To determine the growth rate and the optimal D-alanine concentration for the growth of *alrA* strain, the wild type (168CA) and RD180 ($\Delta alrA::zeo$) strains were grown in LB medium, supplemented with a range of D-alanine concentrations (88 μM –1500 μM). The OD_{600} was read, using a microplate reader (FLUOstar OPTIMA, BMG LABTECH). It was observed that 168CA strain grew at a constant growth rate in all the D-alanine concentrations (Figure 3.1A and B). In contrast, the growth rate of $\Delta alrA::zeo$ strains was generally slower than the wild type and was dependent on the concentration of D-alanine. The $\Delta alrA::zeo$ strain did not manage to grow in the presence of about 200 μM of D-alanine, but it showed optimal growth at about 450 μM of D-alanine (Figure 3.1A and B). Thus the optimal growth of *alrA* strain can be obtained by addition of 450-500 μM of D-alanine to LB media.

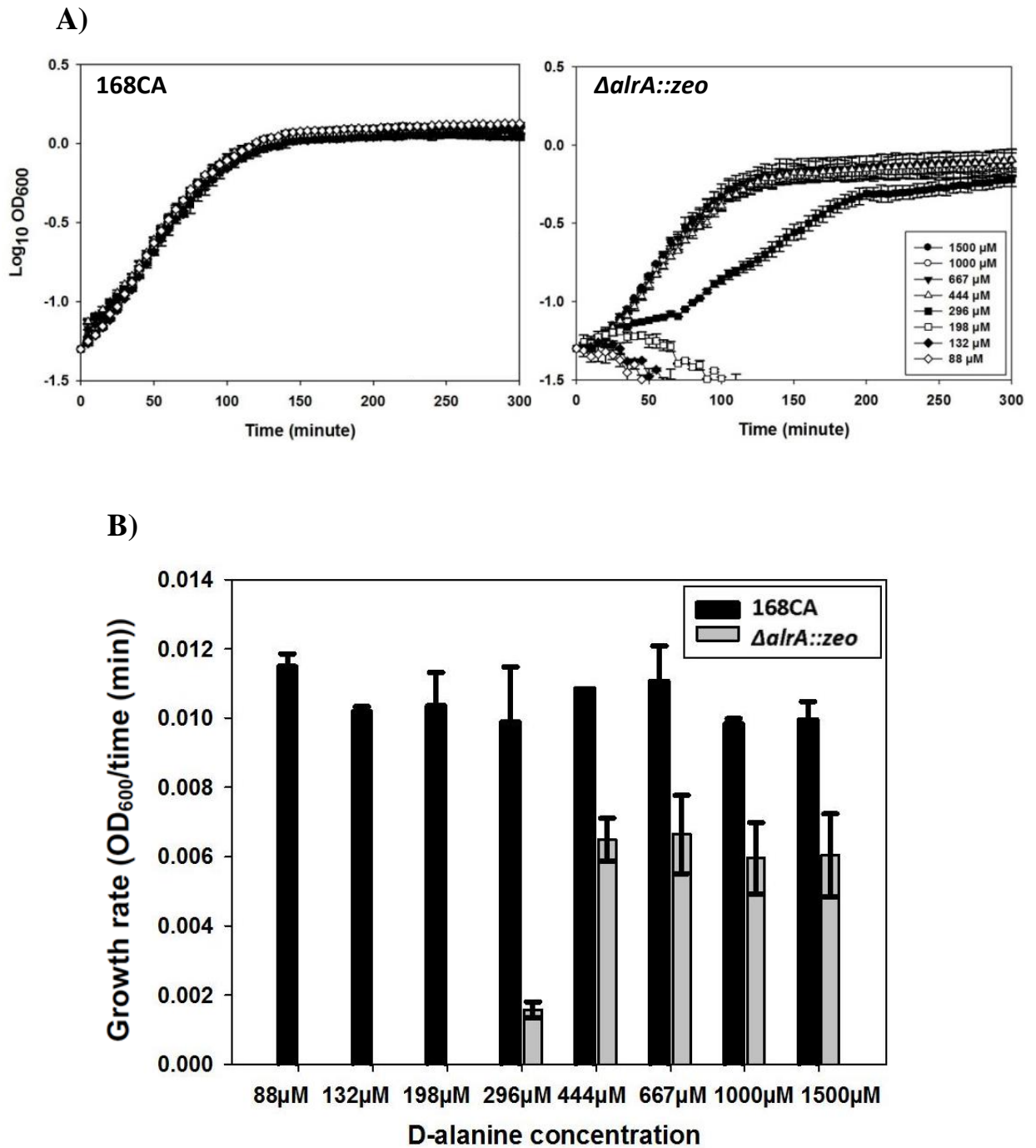


Figure 3.1 Growth characteristics of wild type versus *alrA* strain. A) The growth of wild type (168CA) and RD180 ($\Delta alrA::zeo$) strains in LB medium supplemented with different concentrations of D-alanine at 37 °C. The growth curves are generated from the data of two independent plate reader experiments and shown in Log_{10} . B) The growth rates of the strains were measured at three time point intervals (60-80, 80-100 and 100-120 min) of figure (A). The error bars represent the standard deviation of mean of growth rate in two independent experiments.

3.2.2 *B. subtilis* has almost equal amount of D-alanine in peptidoglycan and teichoic acids.

As D-alanine is a component of both peptidoglycan and teichoic acids, we wondered how much of cell wall D-alanine is in the teichoic acids, and does the deletion of *dlt* operon totally inhibit teichoic acid D-alanylation in live cells. The $\Delta alrA::zeo$ and KS12 ($\Delta alrA::zeo \Delta dltA-D::cat$) strains were firstly grown in LB medium, containing different concentration of D-alanine (88 μ M–1500 μ M). The growth curve of the strains was recorded by microplate reader at 37 °C. The $\Delta alrA::zeo \Delta dltA-D::cat$ strain managed to grow in the presence of about 200 μ M D-alanine and showed maximum growth rate at about 300 μ M. In contrast, it was observed that the $\Delta alrA::zeo$ strain was not able to grow at about 200 μ M and showed maximum growth rate at about 450 μ M (Figure 3.2A and B). The same results were obtained when the growth rate of $\Delta alrA::zeo$ and $\Delta alrA::zeo \Delta dltA-D::cat$ strains were studied in flask experiment, where the cell are supposedly provided with better oxygenation comparing to the small wells of microplate (data not shown). The above results showed that the *dltA-D* strain needs less D-alanine for cell wall biosynthesis than the wild type. To obtain more quantitative data, the D-alanine auxotroph strains, RD180 ($\Delta alrA::zeo$), KS12 ($\Delta alrA::zeo \Delta dltA-D::cat$), KS16 ($\Delta alrA::zeo \Delta dacA::spc$) and KS17 ($\Delta alrA::zeo \Delta dacA::spc \Delta dltA-D::cat$) were grown in LB medium, supplemented with 450 μ M D-alanine (including both radioactive and non-radioactive D-alanine in 1.0:400 ratio). The radioactive labelled strains were incubated for 2.0 h at 37 °C, and the cultures were pelleted and washed with cold PBS. Then, the radioactive labelled strains were treated chemically with sodium dodecyl sulphate (SDS) and sodium hydroxide (NaOH), and physically by boiling. The sodium dodecyl sulphate (SDS) destroys the cell membrane and the D-alanine esters in teichoic acids can be released by alkaline effect of NaOH. Thus the cells should only have D-alanine in peptidoglycan after treating with SDS and NaOH. The washed radioactive cell pellets of each of the above strains were suspended in H₂O, 2.5 % SDS and 2.5 % SDS + 200 mM NaOH separately and boiled at 100 °C for 15 min. A 100 μ l of the treated cells was filtration under vacuum and washed once with 4.0 ml PBS. The dried filters were put in scintillation vials, containing 2.0 ml of scintillation cocktail. The radioactivity (disintegration per minute (DPM)) was measured for both non-treated cells (control) and treated cells. As shown in (Table 3.1), the radioactivity of $\Delta alrA::zeo$ strain decreased by 9.52 %, 36.75 % and 47.5 % after boiling in H₂O, SDS and SDS + NaOH respectively. However, the KS12 ($\Delta alrA::zeo \Delta dltA-D::cat$) strain generally showed about 2.0-3.0 % reduction in radioactivity after

physical and chemical treatments. The KS16 ($\Delta alrA::zeo \Delta dacA::spc$) strain retained full radioactivity after boiling in H₂O and lost 4.0 % and 12 % of radioactivity after boiling in SDS and SDS + NaOH respectively. In contrast, the KS17 ($\Delta alrA::zeo \Delta dacA::spc \Delta dltA-D::cat$) strain did not lose any radioactivity (Table 3.1). Thus the 2.0-3.0 % of radioactivity, which is lost by KS12 ($\Delta alrA::zeo \Delta dltA-D::cat$) strain, represents the cytosolic D-alanine. The subtraction of 2.0-3.0 % of cytosolic [1-¹⁴C] D-alanine from the 47.5 % of the radioactivity, which is lost by RD180 ($\Delta alrA::zeo$) strain after SDS + NaOH treatment, is equal to the amount of D-alanine in teichoic acids and equate to 45 % of the total D-alanine incorporated into the teichoic acids by the cell population.

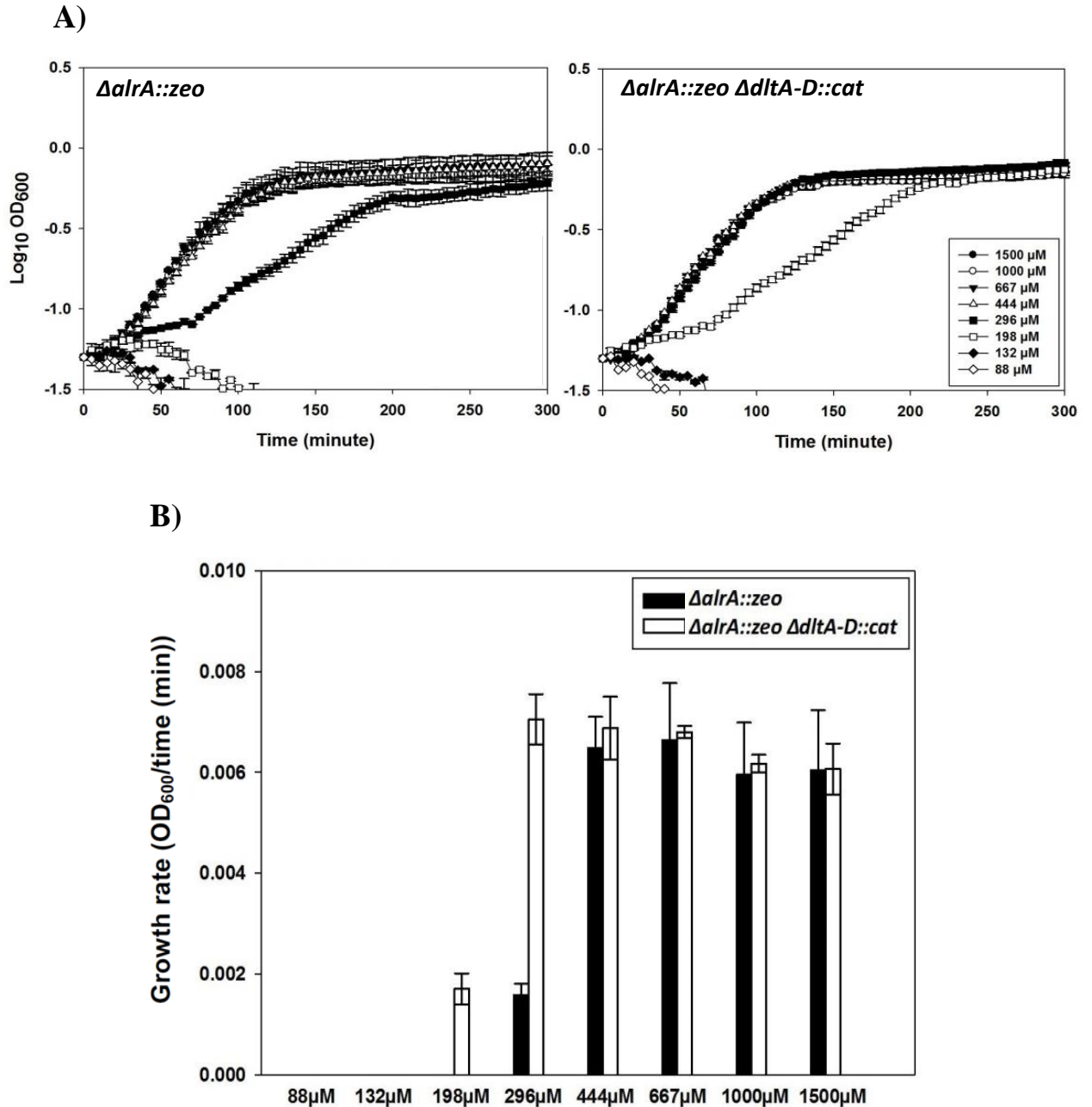


Figure 3.2 The *dltA-D* strain requires less D-alanine for growth. A) The growth curves of RD180 (*ΔalrA::zeo*) and KS12 (*ΔalrA::zeo ΔdltA-D::cat*) strains in LB medium, supplemented with different concentrations of D-alanine (88-1500μM) at 37°C. The growth curves were recorded by plate reader shown in Log₁₀ of OD₆₀₀. B) The growth rate of the the strains were measured at three time points intervals (60-80, 80-100 and 100-120 min) of figure (A). The error bars represent the standard deviation of mean of growth rate in two independent experiments.

Strains	Treatments	Boiled cells		
	Non-boiled cells	H2O	SDS	SDS+NaOH
	H2O (control)			
RD180 ($\Delta alrA::zeo$)	100 %	90.48 % (± 4.45)	63.25 % (± 1.27)	52.50 % (± 3.35)
KS12 ($\Delta alrA::zeo \Delta dltA-D::cat$)	100 %	96.90 % (± 5.92)	97.16 % (± 5.49)	98.34 % (± 9.5)
KS16 ($\Delta alrA::zeo \Delta dacA::spc$)	100 %	103.38 % (± 1.23)	96.09 % (± 3.66)	88.05 % (± 0.24)
KS17 ($\Delta alrA::zeo \Delta dacA::spc \Delta dltA-D::cat$)	100 %	100.07 % (± 0.13)	99.44 % (± 3.75)	101.28 % (± 3.04)

Table 3.1 The physical and chemical treatments of [$1-^{14}\text{C}$] labelled cells. It shows the percentage of radioactivity (DPM), left in the [$1-^{14}\text{C}$] labelled cells of RD180 ($\Delta alrA::zeo$), KS12 ($\Delta alrA::zeo \Delta dltA-D::cat$), KS16 ($\Delta alrA::zeo \Delta dacA::spc$) and KS17 ($\Delta alrA::zeo \Delta dltA-D::cat \Delta dacA::spc$) after boiling in water, 2.5 % SDS and 2.5 % SDS+ 200mM NaOH. The radioactivity (disintegration per minute (DPM)) was measured in 100 μl of the treated cell. The \pm value in the bracket expresses the standard deviation of mean of radioactivity percentage (% DPM) of three experimental replica (n=3.0). The background radiation was subtracted from the values.

3.2.3 Cell wall synthesis in the absence of carboxypeptidases.

Muropeptide analysis already suggested that uncross-linked D-alanine residues in the peptidoglycan of *B. subtilis* are usually trimmed by carboxypeptidases (LdcB and DacA) (Atrih *et al.*, 1999; Hoyland *et al.*, 2014). However, the functional requirement for the carboxypeptidation of peptidoglycan is unclear. There is a hypothesis about the role of the carboxypeptidases in recycling of peptidoglycan derived D-alanine provided that the rate of cell wall metabolism is not affected by the absence of the carboxypeptidases. The growth and morphology of KS15 ($\Delta dacA::spc$) and KS18 ($\Delta dlcB::erm$) strains were compared to wild type (168CA) strain during growth in LB medium at 37 °C. It was observed that 168CA, $\Delta dlcB::erm$ and $\Delta dacA::spc$ strains grow similarly and no change was seen in their growth (Figure 3.3A). The morphology of the mutant strains was similar to that of 168CA as well (Figure 3.3B). These observations might suggest that the above strains have sufficient *in vivo* source of D-alanine, which can be avoided in D-alanine auxotroph strains while the roles of the carboxypeptidases are being investigated. The effect of *ldcB* and *dacA* mutations was studied in D-alanine auxotroph strains, RD180 ($\Delta alrA::zeo$), KS16 ($\Delta alrA::zeo \Delta dacA::spc$) and KS19 ($\Delta alrA::zeo \Delta ldcB::erm$). These strains were grown in LB medium, supplemented with a range of D-alanine concentrations (88 μ M–1500 μ M). A microplate reader was used to monitor the optical density (OD₆₀₀) at 37 °C. The growth of the strains was altered according to the D-alanine concentrations (Figure 3.4A and B). All the three strains ($\Delta alrA::zeo$, $\Delta alrA::zeo \Delta dacA::spc$ and $\Delta alrA::zeo \Delta ldcB::erm$) did not manage to grow at the D-alanine concentrations below 200 μ M but grew similarly at saturated concentrations of 650 μ M and above. Interestingly, the growth of the strains was only discriminated at about 300 μ M and 450 μ M of D-alanine, at which the $\Delta alrA::zeo$ strain grew better than both $\Delta alrA::zeo \Delta dacA::spc$ and $\Delta alrA::zeo \Delta ldcB::erm$ strains. Also, the $\Delta alrA::zeo \Delta ldcB::erm$ strain grew better than $\Delta alrA::zeo \Delta dacA::spc$ (Figure 3.4B). Similar results were obtained when the strains were grown in flasks (data not shown).

In addition to the above experiments, the $\Delta alrA::zeo$, $\Delta alrA::zeo \Delta ldcB::erm$, $\Delta alrA::zeo \Delta dacA::spc$ strains were grown in LB medium, containing 450 μ M of D-alanine (including both radioactive [$1-^{14}$ C] and non-radioactive D-alanine in 1:400 ratio). Samples were taken from the cultures every 20 min for 2.0 h (see section 2.10.1 and 2.10.3 for method details). The amount of D-alanine taken up from the cultures and the amount incorporated into the cells were measured. The growth curves were also

monitored in parallel of the radioactive experiment. From these analysis, the $\Delta alrA::zeo \Delta dacA::spc$ strain took up and incorporated radioactive D-alanine more than $\Delta alrA::zeo \Delta ldcB::erm$ and $\Delta alrA::zeo$ strains. The $\Delta alrA::zeo \Delta ldcB::erm$ strain was also more radioactive than $\Delta alrA::zeo$ strain (Figure 3.5A). The amount of radioactive D-alanine consumed by $\Delta alrA::zeo$, $\Delta alrA::zeo \Delta ldcB::erm$, $\Delta alrA::zeo \Delta dacA::spc$ strains over 2.0 h of incubation were 4.07 %, 4.34 % and 9.23 % respectively (Figure 3.5B). In addition, the D-alanine substitution of teichoic acids was prevented in D-alanine auxotroph strains by deletion of *dlt* operon. The KS12 ($\Delta alrA::zeo \Delta dltA-D::cat$), KS20 ($\Delta alrA::zeo \Delta ldcB::erm \Delta dltA-D::cat$) and KS17 ($\Delta alrA::zeo \Delta dacA::spc \Delta dltA-D::cat$) strains were grown as above. The results (Figure 3.5A) were generally similar to those explained previously for $\Delta alrA::zeo$, $\Delta alrA::zeo \Delta ldcB::erm$, $\Delta alrA::zeo \Delta dacA::spc$ strains. Interestingly, the rate of cell wall metabolism was not apparently altered in the absence of carboxypeptidases (DacA and LdcB) (Figure 3.5A and 5.1). It was also observed that the rate of [$1-^{14}C$] D-alanine incorporation increased in $dltA-D^{+ve}$ strains with time, whereas it stayed almost constant in $dltA-D^{-ve}$ strains (Figure 3.5A).

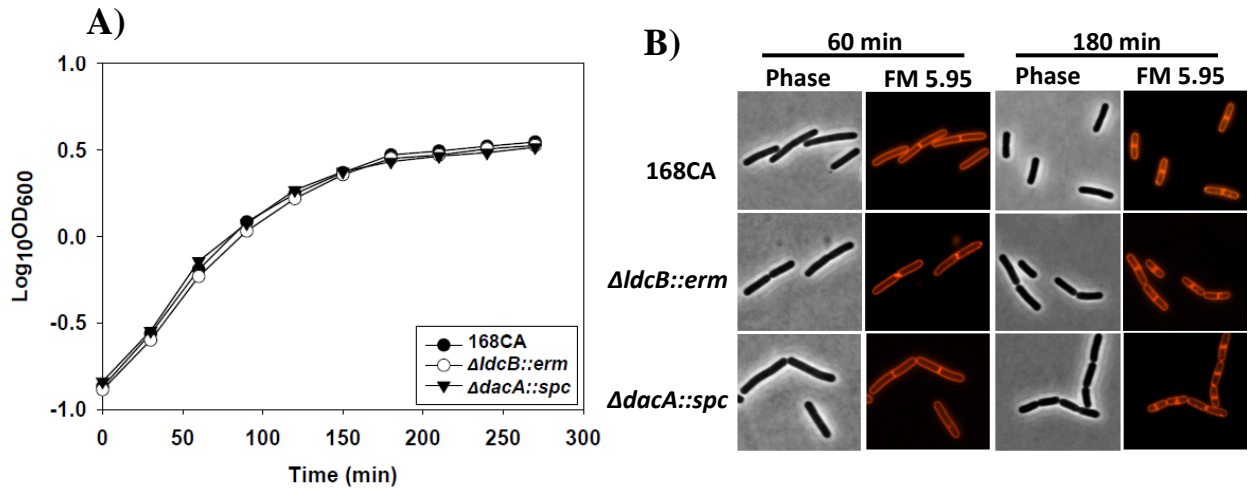


Figure 3.3 Growth and cell morphology. The growth of wild type (168CA) KS15 ($\Delta\text{dacA}::\text{spc}$) and KS18 ($\Delta\text{ldcB}::\text{erm}$) strains in LB medium at 37 °C. The growth curves are shown in Log_{10} of optical density (OD_{600}). B) The cell morphology of the same strains at 60 and 180 min of incubation and the cells were stained with fluorescent membrane dye (FM5.95). The scale bar is 6.0 μm .

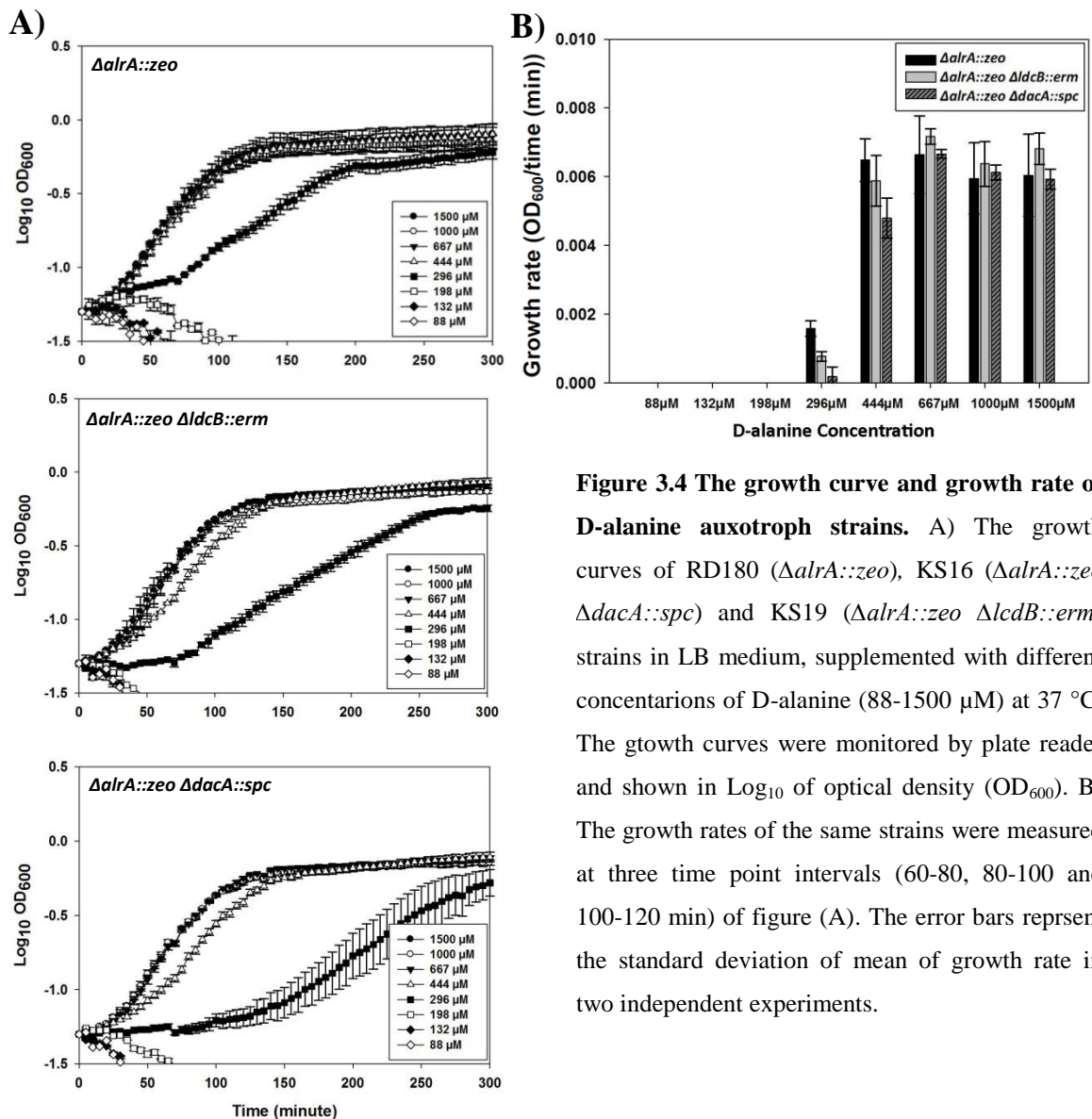


Figure 3.4 The growth curve and growth rate of D-alanine auxotroph strains. A) The growth curves of RD180 ($\Delta\text{alrA}::\text{zeo}$), KS16 ($\Delta\text{alrA}::\text{zeo}\ \Delta\text{dacA}::\text{spc}$) and KS19 ($\Delta\text{alrA}::\text{zeo}\ \Delta\text{ldcB}::\text{erm}$) strains in LB medium, supplemented with different concentrations of D-alanine (88-1500 μM) at 37 °C. The growth curves were monitored by plate reader and shown in Log_{10} of optical density (OD_{600}). B) The growth rates of the same strains were measured at three time point intervals (60-80, 80-100 and 100-120 min) of figure (A). The error bars represent the standard deviation of mean of growth rate in two independent experiments.

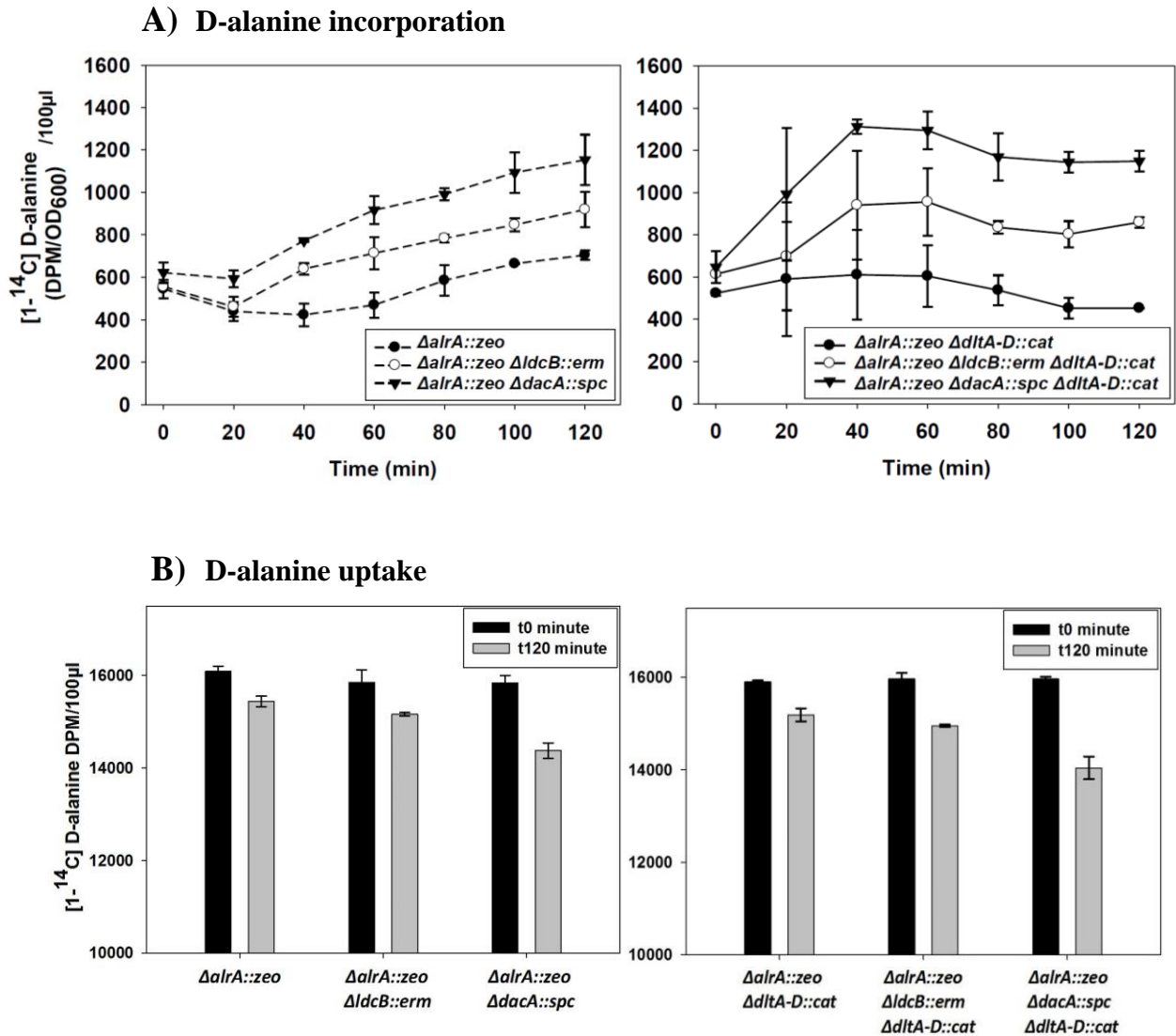


Figure 3.5 Cell wall modification by carboxypeptidases in vegetative *B. subtilis*. The RD180 ($\Delta alrA::zeo$), KS19 ($\Delta alrA::zeo \Delta ldcB::erm$), KS16 ($\Delta alrA::zeo \Delta dacA::spc$), KS12 ($\Delta alrA::zeo \Delta dltA-D::cat$), KS20 ($\Delta alrA::zeo \Delta ldcB::erm \Delta dltA-D::cat$) and KS17 ($\Delta alrA::zeo \Delta dacA::spc \Delta dltA-D::cat$) strains were grown at 37 °C in LB medium, supplemented with 450 μ M D-alanine (including both [$1-^{14}$ C] D-alanine and non-radioactive D-alanine in a ratio of 1.0::400). A) The amount of radioactive D-alanine incorporated into the cells at different time points. B) The amount of radioactive D-alanine taken up by the cells after 2.0 h of incubation. The radioactivity is measured as disintegrations per minute (DPM), and the background radiation was subtracted from the values. The error bars indicate the standard deviation of mean of radioactivity in two independent experiments.

3.2.4 Identification of a D-alanine transporter in *B. subtilis*.

3.2.4.1 A genetic screen for D-alanine transporter

D-alanine is usually taken up from culture medium by a D-alanine auxotroph strain, RD180 ($\Delta alrA::zeo$) (Figure 3.1A). We wondered what gene(s) encodes D-alanine transporter(s) in *B. subtilis*. The idea for identifying D-alanine transporter gene(s) was the creation of synthetic lethality (i.e the deletion of D-alanine transporter encoding gene would be lethal in *alrA* strain). The synthetic lethality of the double mutations could mean that D-alanine uptake system is lost and the double mutant strain cannot transport exogenous D-alanine. To test this idea, the genome of *B. subtilis* was searched for any putative amino acid transporter gene, using Blast search tool of online Subtilist database. Forty three non-essential genes were finally selected. The gDNAs were extracted from the 43 single mutant strains (Table 3.2) and used to transform 168CA and RD180 ($\Delta alrA::zeo$) strains. The transformants were selected on nutrient agar plates, containing erythromycin and 500 μ M D-alanine. The transformed colonies were checked for both erythromycin and zeocine resistance and D-alanine growth dependence. Consequently, it was found that only *alrA ytnA* double knockout is lethal, suggesting that D-alanine transport is lost in the absence of *ytnA* gene. In this study, *ytnA* gene has been renamed to *datA*, which stands for D-alanine transporter A. To investigate the effect of *datA* mutation on growth and morphology of *B. subtilis*, the 168CA and KS22 ($\Delta datA::erm$) strains were grown in LB medium at 37 °C and the growth curves were monitored until early stationary phase. Both the strains grew similarly (Figure 3.6A) and the $\Delta datA::erm$ strain was as normal as the 168CA in terms of morphology (Figure 3.6B).

It is known that *alrA* strain is able to grow in MM without D-alanine (Ferrari *et al.*, 1985). This observation gave us an idea to select *alrA datA* double knockout on MM. The gDNA of $\Delta alrA::zeo$ strain was used to transform KS22 strain ($\Delta datA::erm$) and the transformation was selected on MM, containing zeocine. We were able to collect transformants with both *alrA* and *datA* deletions, which were confirmed by PCR. The KS30 strain ($\Delta datA::erm \Delta alrA::zeo$) grows only in MM and seemed to grow slightly better in the presence of D-alanine (Figure 3.7). The growth of the strain was also inhibited by addition of L-alanine to MM. As expected, the $\Delta datA::erm \Delta alrA::zeo$ strain did not manage to grow on nutrient agar with and without D-alanine.

Strains	Geneotype
MGNA-C343	<i>trpC2</i> Δ <i>yfkT</i> ::pMUTIN4 (<i>erm</i>)
MGNA-B989	<i>trpC2</i> Δ <i>ycgH</i> ::pMUTIN4 (<i>erm</i>)
MGNA-B757	<i>trpC2</i> Δ <i>ywaA</i> ::pMUTIN4 (<i>erm</i>)
MGNA-C001	<i>trpC2</i> Δ <i>yckA</i> ::pMUTIN4 (<i>erm</i>)
MGNA-C394	<i>trpC2</i> Δ <i>yqiN</i> ::pMUTIN4 (<i>erm</i>)
MGNA-C383	<i>trpC2</i> Δ <i>yqiZ</i> ::pMUTIN4 (<i>erm</i>)
MGNA-C480	<i>trpC2</i> Δ <i>yqgT</i> ::pMUTIN4 (<i>erm</i>)
MGNA-A172	<i>trpC2</i> Δ <i>ytmL</i> ::pMUTIN4 (<i>erm</i>)
MGNA-B963	<i>trpC2</i> Δ <i>ybeC</i> ::pMUTIN4 (<i>erm</i>)
MGNA-B783	<i>trpC2</i> Δ <i>hutM</i> ::pMUTIN4 (<i>erm</i>)
MGNA-B940	<i>trpC2</i> Δ <i>ybgF</i> ::pMUTIN4 (<i>erm</i>)
MGNA-C381	<i>trpC2</i> Δ <i>yqiX</i> ::pMUTIN4 (<i>erm</i>)
MGNA-B939	<i>trpC2</i> Δ <i>ybgE</i> ::pMUTIN4 (<i>erm</i>)
MGNA-B914	<i>trpC2</i> Δ <i>yabM</i> ::pMUTIN4 (<i>erm</i>)
MGNA-C084	<i>trpC2</i> Δ <i>ydgF</i> ::pMUTIN4 (<i>erm</i>)
MGNA-C022	<i>trpC2</i> Δ <i>ycsG</i> ::pMUTIN4 (<i>erm</i>)
MGNA-A551	<i>trpC2</i> Δ <i>yurH</i> ::pMUTIN4 (<i>erm</i>)
MGNA-A736	<i>trpC2</i> Δ <i>ykbA</i> ::pMUTIN4 (<i>erm</i>)
MGNA-A031	<i>trpC2</i> Δ <i>yjoB</i> ::pMUTIN4 (<i>erm</i>)
MGNA-A468	<i>trpC2</i> Δ <i>yvbW</i> ::pMUTIN4 (<i>erm</i>)
MGNA-A012	<i>trpC2</i> Δ <i>ytgP</i> ::pMUTIN4 (<i>erm</i>)
MGNA-A909	<i>trpC2</i> Δ <i>yecA</i> ::pMUTIN4 (<i>erm</i>)
MGNA-A362	<i>trpC2</i> Δ <i>yjkB</i> ::pMUTIN4 (<i>erm</i>)
MGNA-A311	<i>trpC2</i> Δ <i>yobN</i> ::pMUTIN4 (<i>erm</i>)
MGNA-A173	<i>trpC2</i> Δ <i>ytmM</i> ::pMUTIN4 (<i>erm</i>)
MGNA-A230	<i>trpC2</i> Δ <i>aapA</i> ::pMUTIN4 (<i>erm</i>)
MGNA-B479	<i>trpC2</i> Δ <i>yhdG</i> ::pMUTIN4 (<i>erm</i>)
MGNA-C382	<i>trpC2</i> Δ <i>yqiY</i> ::pMUTIN4 (<i>erm</i>)
MGNA-A171	<i>trpC2</i> Δ <i>ytmK</i> ::pMUTIN4 (<i>erm</i>)
MGNA-C231	<i>trpC2</i> Δ <i>yfnA</i> ::pMUTIN4 (<i>erm</i>)
MGNA-B782	<i>trpC2</i> Δ <i>yxeM</i> ::pMUTIN4 (<i>erm</i>)
MGNA-A126	<i>trpC2</i> Δ <i>ytnA</i> ::pMUTIN4 (<i>erm</i>)
MGNA-A595	<i>trpC2</i> Δ <i>yusA</i> ::pMUTIN4 (<i>erm</i>)
MGNA-A596	<i>trpC2</i> Δ <i>yusC</i> ::pMUTIN4 (<i>erm</i>)
MGNA-A686	<i>trpC2</i> Δ <i>yhaG</i> ::pMUTIN4 (<i>erm</i>)
MGNA-C257	<i>trpC2</i> Δ <i>yflA</i> ::pMUTIN4 (<i>erm</i>)
MGNA-A659	<i>trpC2</i> Δ <i>yhcG</i> ::pMUTIN4 (<i>erm</i>)
MGNA-A653	<i>trpC2</i> Δ <i>yhcH</i> ::pMUTIN4 (<i>erm</i>)
MGNA-A655	<i>trpC2</i> Δ <i>yhcJ</i> ::pMUTIN4 (<i>erm</i>)
MGNA-A834	<i>trpC2</i> Δ <i>yoaC</i> ::pMUTIN4 (<i>erm</i>)
MGNA-A835	<i>trpC2</i> Δ <i>yoaD</i> ::pMUTIN4 (<i>erm</i>)
MGNA-A783	<i>trpC2</i> Δ <i>mtnK</i> ::pMUTIN4 (<i>erm</i>)
MGNA-A082	<i>trpC2</i> Δ <i>spoVG</i> ::pMUTIN4 (<i>erm</i>)

Table 3.2 A selection of putative amino acids transport mutants in Japanese strains collection. This was received from National BioResource Project, National Institute of Genetics (NIG), Japan. The pMUTIN4 vector (*bla erm P_{spac} lacZ lacI*) was genetically edited to be specifically inserted into the coding frame of the target gene. This resulted in the disruption of the gene function. These single knockouts were used in the identification of D-alanine transporter.

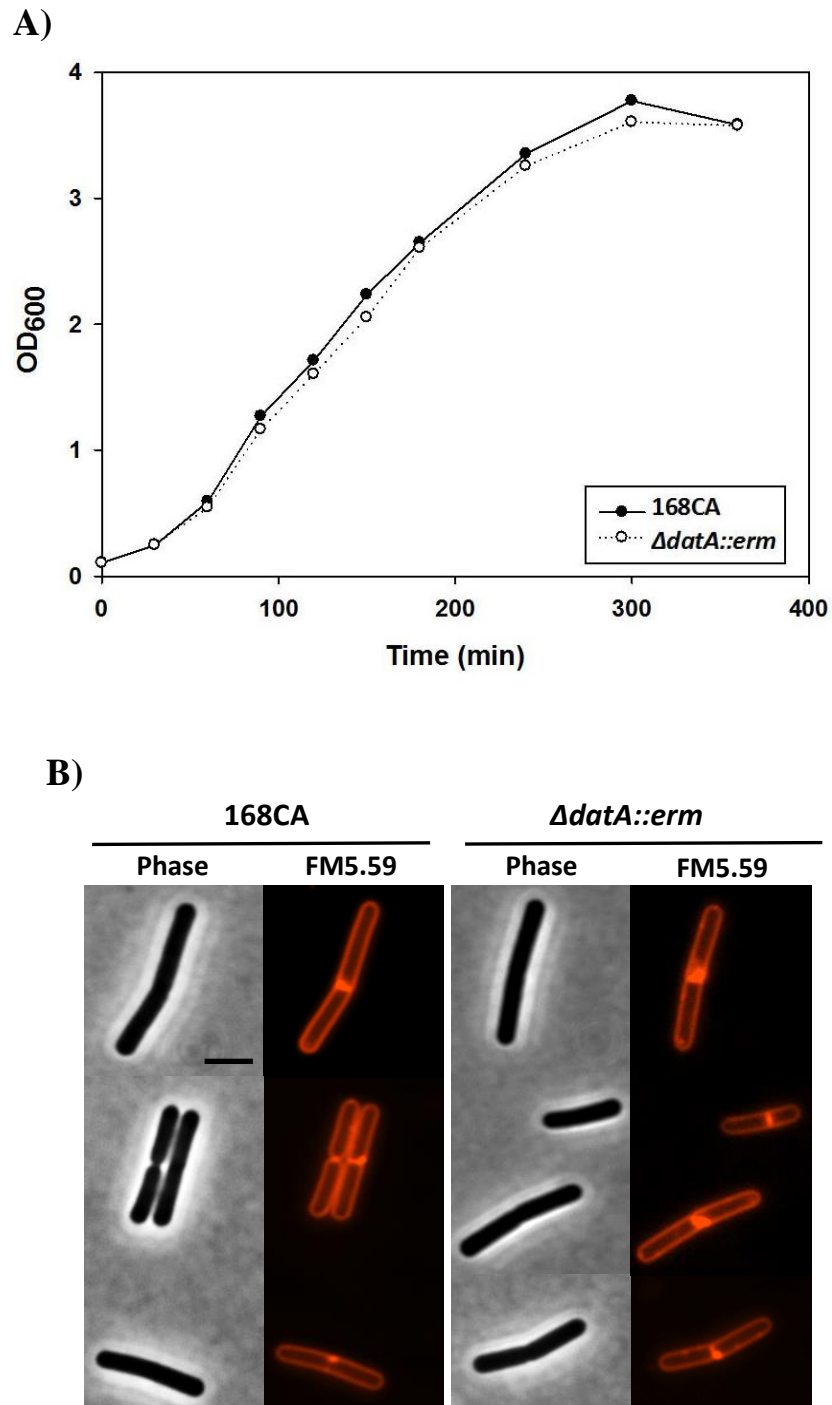


Figure 3.6 Growth and morphology of *datA* strain. A) The growth of 168CA and KS22 ($\Delta datA::erm$) strains in LB medium at 37 °C. B) The phase contrast and membrane dye (FM5.59) microscopic images of both the strains at mid exponential phase. The scale bar is 3.0 μm .

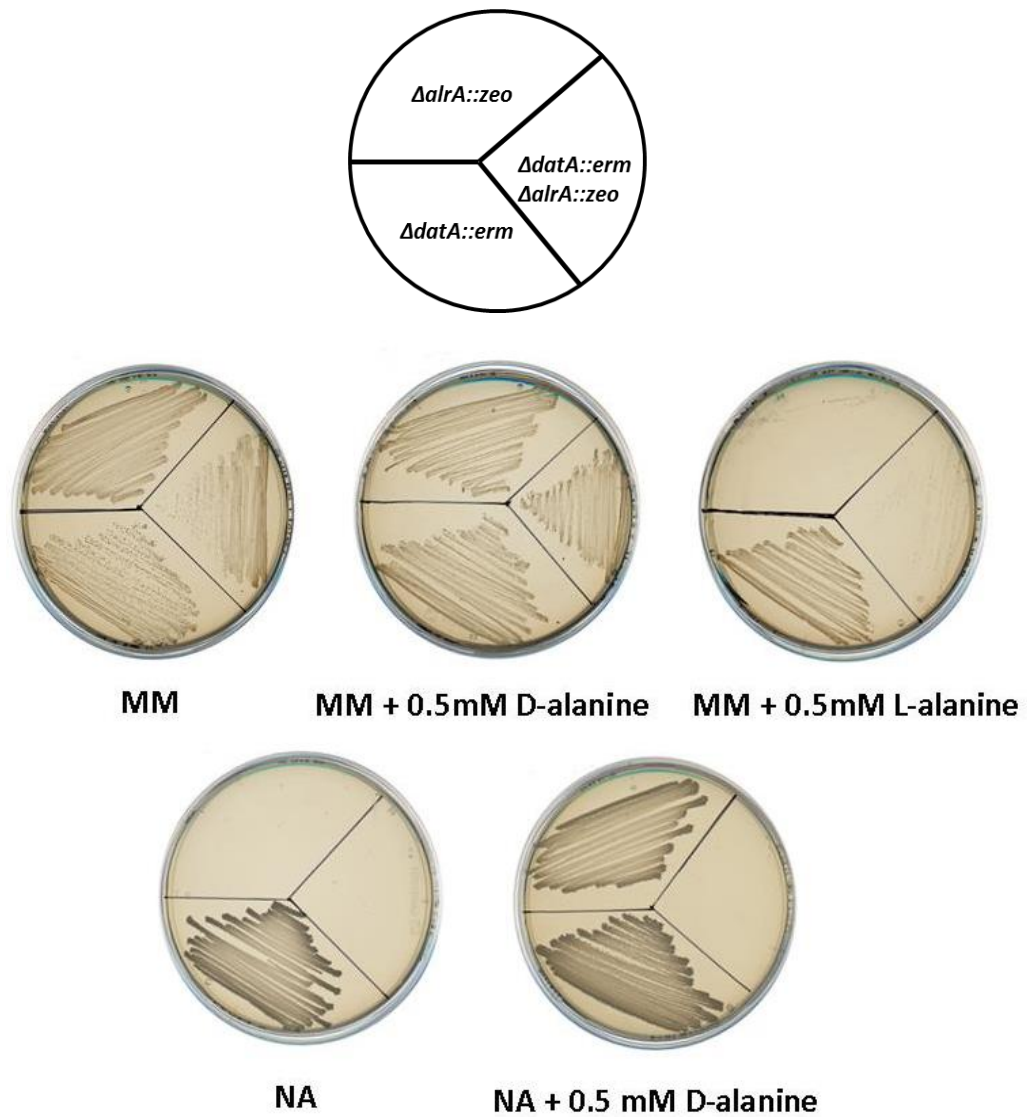


Figure 3.7 Growth of KS30 and its parental strains on minimal and nutrient media. The RD180 ($\Delta alrA::zeo$), KS22 ($datA::erm$) and KS30 ($\Delta datA::erm \Delta alrA::zeo$) strains were grown on minimal media (MM) for 48 h and on nutrient agar (NA) for 24 h at 37 °C. Some of the growth media were supplemented with 0.5 mM of L- alanine or D-alanine.

3.2.4.2 Complementation of *datA*.

Although our genetic screen suggested that DatA is involved in D-alanine transport, the genetic complementation of *datA* was required to eliminate possible polar effects of the knockout. The coding sequence of *datA* gene and 30 bases upstream, supposedly including the ribosome binding site (RBS), was cloned into pPY18 vector (*bla amyE3' cat P_{spac} lacI lacZ amyE5'*) to produce plasmid pKS1 (*bla amyE3' cat P_{spac} Ω datA lacI lacZ amyE5'*). The pPY18 vector contains an IPTG inducible promoter (*P_{spac}*) and *amyE* fragments for chromosomal integration of the vector. The pKS1 plasmid was inserted into the *amyE* locus of KS22 strain ($\Delta datA::erm$) by transformation. The produced strain, KS26 ($\Delta datA::erm amyE (cat P_{spac} \Omega datA)$), was again transformed with the gDNA of RD180 strain ($\Delta alrA::zeo$). The selection medium was nutrient agar, supplemented with 0.5 mM D-alanine and 1.0 mM IPTG. Despite the sequencing analysis confirmed the correct assembly of the DNA fragment and integration of *datA* gene into the *amyE* locus, attempts to delete *alrA* gene in $\Delta datA::erm amyE (cat P_{spac} \Omega datA)$ strain were not successful. On inspection of the *datA* coding sequence it was determined that the RBS sequence was particularly poor. Thus, the inability to complement *datA* null mutant with an inducible copy of the gene might be due to the poor translation of the cloned *datA* gene. To solve this potential problem, an optimised ribosome binding site (RBS), belongs to *ftsL* gene, was added to the upstream of *datA* coding sequence by PCR. The *datA-ftsL* (RBS) PCR product was inserted into the pPY18 vector to produce pKS6 (*bla amyE3' cat P_{spac} Ω datA-ftsL(RBS) lacI lacZ amyE5'*) construct. The pKS6 was inserted into the *amyE* locus of *datA::erm* strain by transformation to produce KS41 strain ($\Delta datA::erm amyE \Omega (cat P_{spac} datA-ftsL(RBS))$). We were finally able to transform KS41 strain with the gDNA of $\Delta alrA::zeo$ strain in the presence of IPTG and D-alanine. The produced strain, KS42 ($\Delta datA::erm amyE \Omega (cat P_{spac} datA-ftsL(RBS)) \Delta alrA::zeo$), required both D-alanine and IPTG for growth in nutrient agar (Figure 3.8). Thus this genetic complementation confirms that the loss of D-alanine transport in *alrA datA* strain was specifically due to the lack of DatA protein.

To generate further confirmatory genetic data regarding the role of DatA, we used the observation of Ferrari *et al.*, (1985), who reported that an $\Delta alrA$ strain maintains a plasmid copy of *alrA* gene in the absence of exogenous D-alanine. However, the stability of the plasmid was low when D-alanine was added to the growth medium. We exploited this observation for further confirmation of DatA as a D-alanine transport protein. The idea was if we delete *datA* gene in a strain, which is genotypically similar

to that of Ferrari *et al.*, (1985), the plasmid copy of *alrA* gene might be completely stable and conserved even in the presence of D-alanine. So, the RD180 ($\Delta alrA::zeo$) strain was transformed with a *pLOSS** $\Omega alrA$ construct (provided by R. Daniel) to produce KS21 strain ($\Delta alrA::zeo + pLOSS* \Omega alrA$). The *pLOSS** vector is an extra-chromosomal plasmid, which possesses a P_{spac} promoter and a β -galactosidase gene (*lacZ*) for hydrolysing 5-bromo-4-chloro-3-indolyl- β -D-galactoside (X-gal). The $\Delta alrA::zeo + pLOSS* \Omega alrA$ strain was then transformed with gDNA of BKE30530 strain ($\Delta ytmA (\Delta data)::erm$) to produce KS23 strain ($\Delta data::erm \Delta alrA::zeo + pLOSS* \Omega alrA$). The two strains ($\Delta alrA::zeo + pLOSS* \Omega alrA$ and $\Delta data::erm \Delta alrA::zeo + pLOSS* \Omega alrA$) were grown on plates of nutrient agar supplemented with X-gal and with and without D-alanine at 37 °C. The results showed that it is feasible for having a strain with *alrA data* double knockout on nutrient agar as long as it has a plasmid copy of *alrA* gene. It was seen that $\Delta alrA::zeo + pLOSS* \Omega alrA$ strain keeps the plasmid copy of *alrA* gene in the absence of D-alanine (Figure 3.9A). However, $\Delta alrA::erm + pLOSS* \Omega alrA$ cells started losing their plasmids in the presence of 450 μ M of D-alanine (Figure 3.9B). When the concentration of D-alanine was doubled (900 μ M), the *pLOSS* $\Omega alrA$* plasmid was lost by almost all the $\Delta alrA::zeo + pLOSS* \Omega alrA$ cells (Figure 3.9C). In contrast to KS21, the cells of KS23 strain ($\Delta data::erm \Delta alrA::zeo + pLOSS* \Omega alrA$) conserved their plasmids in the absence and the presence of D-alanine (Figure 3.9A, B, C). This means that the $\Delta data::erm \Delta alrA::zeo + pLOSS* \Omega alrA$ strain completely rely on plasmid copy of *alrA* gene for *in vivo* synthesis of D-alanine.

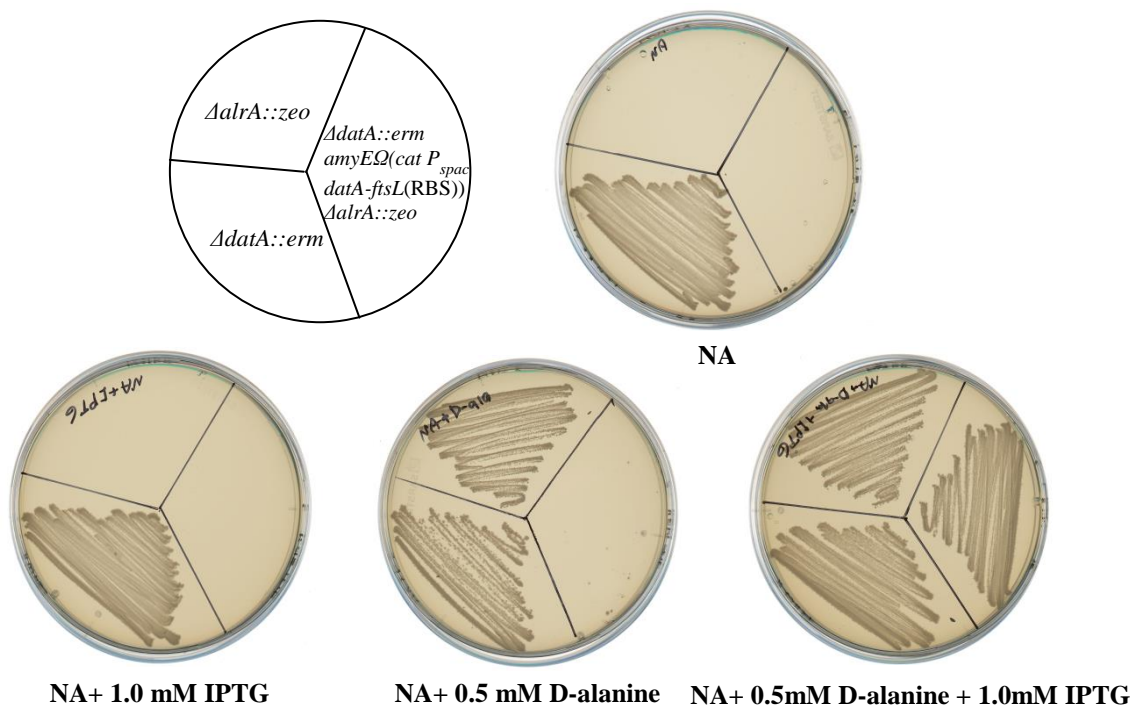


Figure 3.8 Complementation of *dataA* gene. Growth of KS22 ($\Delta dataA::erm$), RD180 ($\Delta alrA::zeo$) and KS42 ($\Delta dataA::erm amyE \Omega (cat P_{spac} dataA-ftsL(RBS)) \Delta alrA::zeo$) strains on nutrient agar (NA) plates with and without 1.0 mM IPTG and 0.5 mM D-alanine. The plates were incubated at 37 °C overnight.

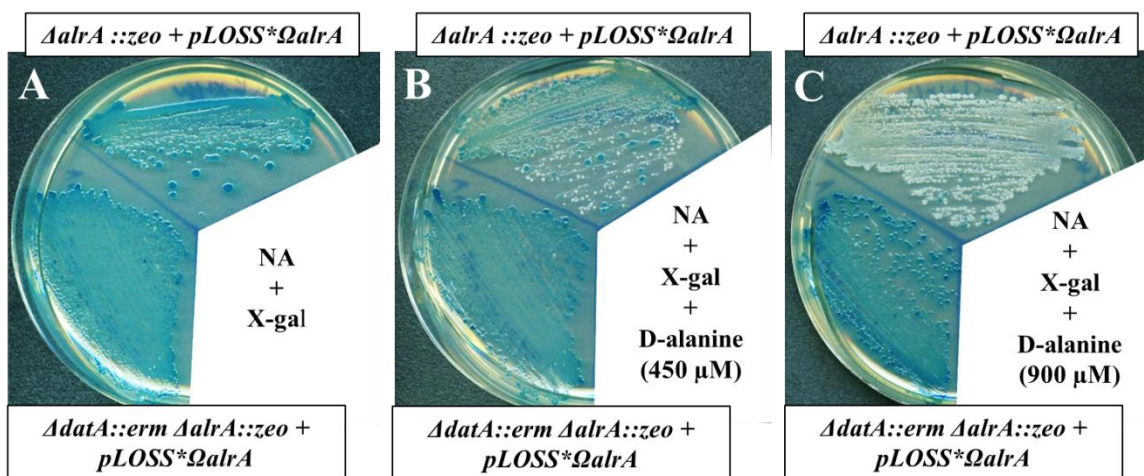


Figure 3.9 Loss of D-alanine transport in *dataA* strain. The growth of KS21 ($\Delta alrA::zeo + pLOSS^* \Omega alrA$) and KS23 ($\Delta alrA::zeo \Delta dataA::erm + pLOSS^* \Omega alrA$) strains on nutrient agar (NA) plus X-gal (A), X-gal and 450 μ M of D-alanine (B) and X-gal and 900 μ M of D-alanine (C) at 37 °C overnight. The blue colonies indicate that the $pLOSS^* \Omega alrA$ plasmid is conserved in the cells, whereas the cells produced white colonies after losing the plasmid.

3.2.4.3 *B. subtilis* transports exogenous D-alanine via Data.

In the previous experiments, the D-alanine auxotroph strain (*alrA*) was used to investigate D-alanine transport in *B. subtilis* and it was found that Data is required for D-alanine transport. We wondered whether exogenous D-alanine is usually taken up by wild type strain, using *datA* null as a control strain. Therefore, the transport of [$1\text{-}^{14}\text{C}$] D-alanine was studied in 168CA and KS22 ($\Delta\text{datA}::\text{erm}$) strains. The strains were grown in LB medium plus 1.0 μM (0.065 $\mu\text{Ci/ml}$) of [$1\text{-}^{14}\text{C}$] D-alanine and the growth curves were also monitored in parallel. Samples were taken from the radioactive cultures at the beginning (t_0) and after 120 min (t_{120}) of incubation and centrifuged at 6000 rpm for 2.0 min in JENCONS-PLS minicentrifuge (Maximum speed/RCF: 6000rpm/2000 xg; rotor: 6x 1.5/2.0 ml). The culture supernatants were used for D-alanine uptake measurement. To measure D-alanine incorporation into the cells, the cell pellets were rinsed with PBS and suspended in appropriate amount of PBS. Despite their similar growth it was observed that 168CA strain took up about 15 % of D-alanine from the medium, whereas no D-alanine was taken up by $\Delta\text{datA}::\text{erm}$ strain after 2.0 h of incubation (Figure 3.10A). The incorporation of [$1\text{-}^{14}\text{C}$] D-alanine was also observed into the cells of 168CA, but $\Delta\text{datA}::\text{erm}$ strain did not incorporate D-alanine within 2.0 h of incubation (Figure 3.10B). This result confirms that Data is required for usual transport of D-alanine in *B. subtilis*. Moreover, it was also observed that the amount of the incorporated [$1\text{-}^{14}\text{C}$] D-alanine into 168CA strain was less than the amount of the D-alanine, which was consumed from the medium by 168CA (Figure 3.10A and B).

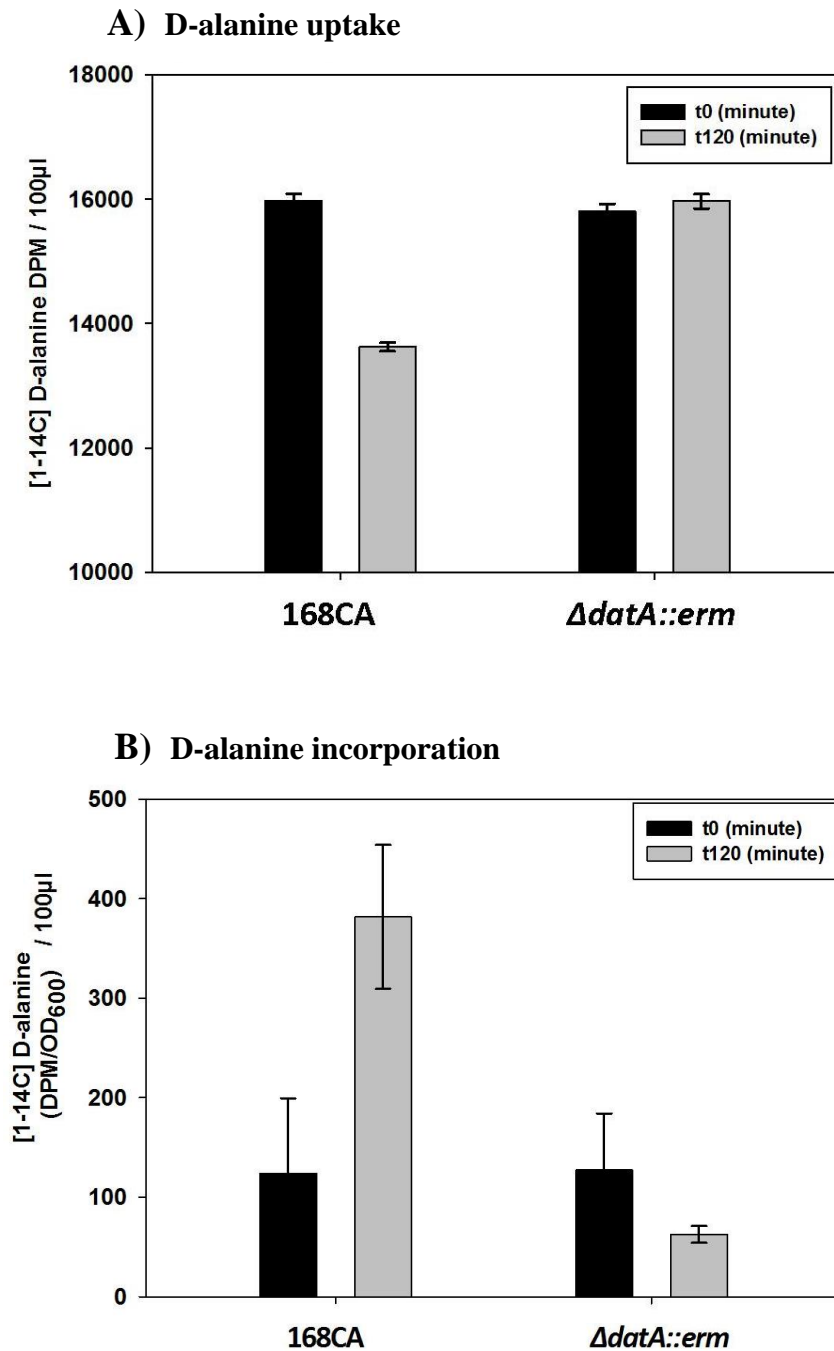


Figure 3.10 Role of DatA in the transport of D-alanine in *B. subtilis*. The D-alanine uptake (A) and D-alanine incorporation (B) were studied in wild type (168CA) and KS22 ($\Delta datA::erm$) strains. The strains were grown in the presence of 1.0 μ M of [1-¹⁴C] D-alanine in LB medium at 37 °C. The radioactivity, disintegration per minute (DPM), was measured in the culture supernatants and in the cells at the beginning (t0) and after 120 min (t120) of incubation. The error bars represent the standard deviation of mean of radioactivity (DPM) of two independent experiments and three replicas in each experiment. The background radiation was subtracted from the values.

3.2.5 *D-alanine aminotransferase (Dat, formerly YheM) contributes to D-alanine synthesis in minimal medium*

It had already been observed that *alrA* strain is able to grow in D-alanine free MM, but addition of L-alanine inhibited growth (Ferrari *et al.*, 1985). We hypothesised that the exposure of *alrA* strain to L-alanine for long time may induce suppressor mutations in genes, which encode L-alanine transporter and/or transcriptional regulator of the unknown gene, which its product catalyses D-alanine synthesis in MM. In these cases, the produced strains might have ability to grow in the presence of L-alanine in MM and in the absence of D-alanine in rich medium. The identification of the unknown gene that supports the growth of *alrA* in MM was firstly tried by exploiting the growth inhibitory effect of L-alanine to obtain suppressor mutations. The $\Delta alrA::zeo$ strain was grown in MM to mid exponential phase at 37 °C. To this culture, 1.0 mM of L-alanine was added and kept growing overnight. The overnight culture was grown on MM plates with and without 10 mM L-alanine for 48 h. Then, six independent L-alanine insensitive strains of $\Delta alrA::zeo$ were selected and grown on nutrient agar. These L-alanine insensitive strains were able to grow on nutrient agar without D-alanine (data not shown). The gDNA of the strains were sequenced by Wipac research group, using Miseq platform. The genome sequencing result of each strain was analysed by CLC genomics workbench (Version 7.5). The location of the mutations on the genome was identified by using The Microscope Platform database (<http://www.genoscope.cns.fr/agc/microscope/home/>). Through these analyses, it was observed that the deletion and substitution of single nucleotides happened in more than two genes in each strain. The point mutations in cardiolipin synthase encoding gene (*clsA*) (substitution of Thymidine (T) by Guanidine (G) produced a stop codon (TAG)) and in transcription termination factor encoding gene (*rho*) (deletion of Thymidine (T) resulted in the alteration of frame reading of *rho* gene) seemed to be common in all the L-alanine insensitive *alrA* strains (data not shown). However, the products of these two genes apparently play no direct role in transport and metabolism amino acid. Thus, this route of investigation did not help us understand how *alrA* strain could grow in MM

As a second alternative way to investigate the growth of *alrA* strain in MM, we used synthetic lethality approach, which is caused by double genes knockout. The hypothesis was if an enzyme catalyses D-alanine production in MM, the deletion of its encoding gene could inhibit the growth of *alrA* strain in MM. To test this hypothesis, the *B. subtilis* relevant databases (*SubtiWiki*, *Subtilist*, *SubCyc*) were searched for any

suspected genes that have either putative or functionally characterised roles in D-amino acid metabolism. We chose the genes that encode sporulation D-alanine racemase (AlrB), glutamate racemase (YrpC), two putative amino acid racemases (RacX and YitF) and D-alanine aminotransferase (Dat). The gDNAs of BKE17640 ($\Delta alrB::erm$), BKE26810 ($\Delta yrpC::erm$), BKE34430 ($\Delta racX::erm$), BKE10970 ($\Delta yitF::erm$) and BKE09670 ($\Delta dat::erm$) strains were transformed into RD180 ($\Delta alrA::zeo$) strain to generate double mutants. These strains (KS32 ($\Delta alrA::zeo \Delta alrB::erm$), KS34 ($\Delta alrA::zeo \Delta yrpC::erm$), KS33 ($\Delta alrA::zeo \Delta racX::erm$), KS35 ($\Delta alrA::zeo \Delta yitF::erm$) and KS78 ($\Delta alrA::zeo \Delta dat::erm$)) were grown on MM at 37 °C to determine if growth is impossible under these conditions. From this analysis, only $\Delta alrA::zeo \Delta dat::erm$ strain was unable to grow on MM (Figure 3.11).

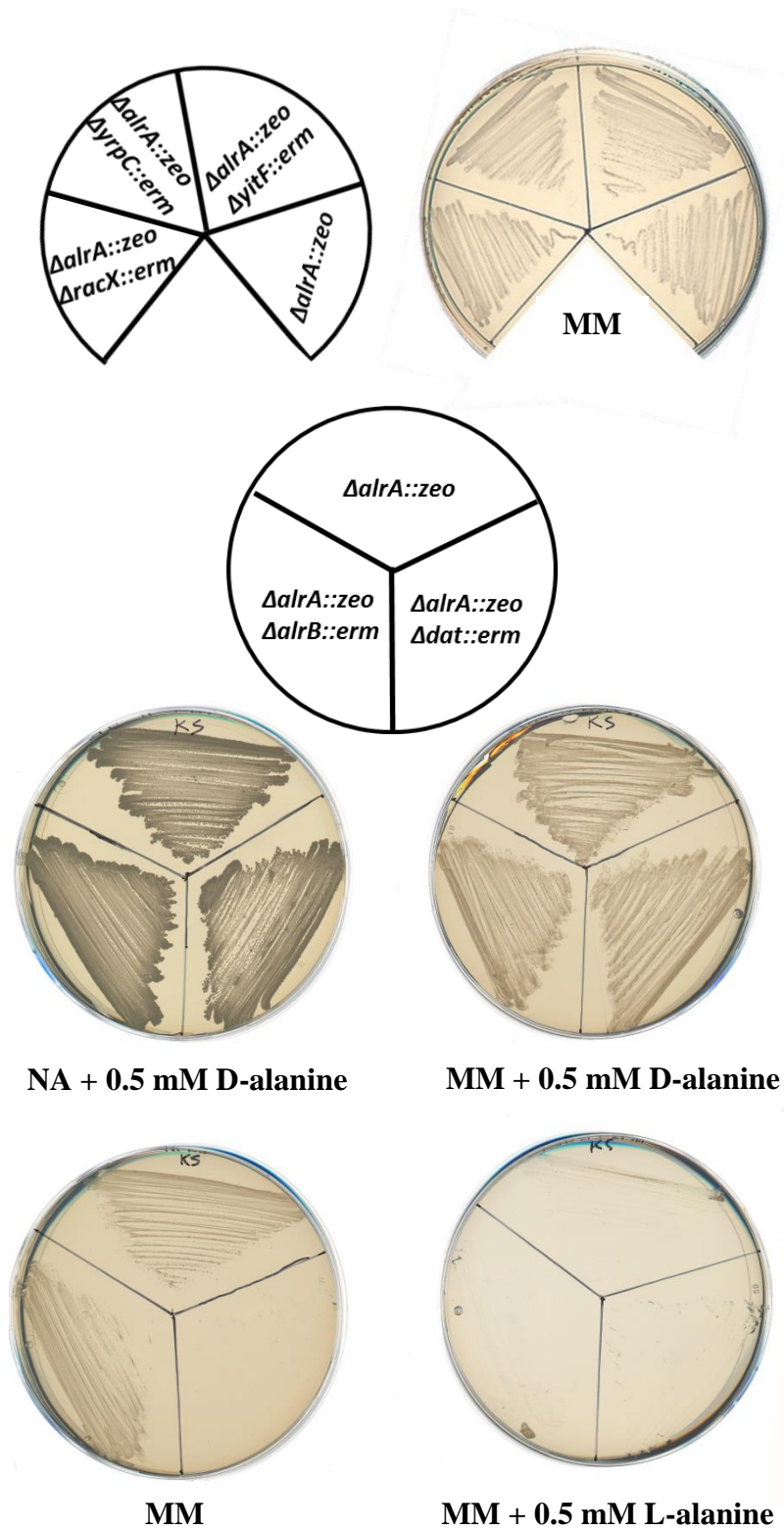


Figure 3.11 Growth of amino acid racemase mutants on minimal media (MM). The D-alanine auxotroph strains, RD180 ($\Delta alrA::zeo$), KS32 ($\Delta alrA::zeo \Delta alrB::erm$), KS33 ($\Delta alrA::zeo \Delta racX::erm$), KS34 ($\Delta alrA::zeo \Delta yrpC::erm$), KS35 ($\Delta alrA::zeo \Delta yitF::erm$) and KS78 ($\Delta alrA::zeo \Delta dat::erm$) were grown on nutrient agar (NA) and MM, with and without L- and D-alanine, at 37°C for 36 hours.

3.3 Discussion

In this chapter, D-alanine metabolism was exploited as a way to investigate cell wall metabolic processes in *B. subtilis*. Through these analyses, we identified a D-alanine transporter and it was also found that a D-alanine aminotransferase (Dat) acts to synthesise D-alanine under certain growth conditions. As a starting point, D-alanine auxotroph strain (*alrA*) was characterised in terms of optimal growth requirement of D-alanine. The characterisation was performed in rich media to avoid the slow growth rate of the strain in MM and because it was reported that *alrA* is able to grow in MM without D-alanine (Ferrari *et al.*, 1985). We found that the *alrA* strain requires about 500 μM of D-alanine for optimal growth in rich medium, and the strain usually grows slower than the wild type (see section 3.2.1). This result suggests that *B. subtilis* possesses an uptake system for D-alanine which is able to supply the cell wall metabolism with sufficient D-alanine from extracellular source. As D-alanine is also a component of teichoic acids, we took the advantage of deletion of *dlt* operon to prevent the D-alanylation of teichoic acids and determine the percentage of D-alanine in peptidoglycan. The results showed that *dltA-D*^{-ve} strain requires less D-alanine for cell wall synthesis than the wild type (*dltA-D*^{ve+}) (see section 3.2.2). The radioactive results also demonstrated that the deletion of *dltA-D* genes totally removes D-alanine from teichoic acids and that peptidoglycan and teichoic acids of *B. subtilis* contain almost equal amount of D-alanine (see section 3.2.2). These data suggest the presence of high levels of D-alanine in teichoic acids during exponential growth. The absence of D-alanine in teichoic acids is important to investigate the roles of carboxypeptidases in peptidoglycan metabolism.

It is known that the uncross-linked D-alanine residues on position 4 and 5 of stem peptides are cleaved by LD-carboxypeptidase (LcdB) and DD-carboxypeptidase (DacA) respectively. We investigated the effect of lack of carboxypeptidase activities on growth and peptidoglycan metabolism. It was observed that the *dacA* and *ldcB* strains grow as much as the wild type in LB medium (see section 3.2.3), suggesting that the consequences of *dacA* and *ldcB* mutations are not detectable in D-alanine prototroph strains, where the *in vivo* source of D-alanine (AlrA) supplies the cells with enough quantity of D-alanine. However, the deletion of *dacA* and *ldcB* genes in a D-alanine auxotroph strain (*alrA*) clearly showed differences in the growth rate of the strains (see section 3.2.3). The differences can be detected only in narrow range of D-alanine concentrations (300 - 450 μM), where the growth rate of *alrA* strain was higher than

that of *alrA dacA* and *alrA ldcB* double mutants, besides the *alrA ldcB* strain showed intermediate growth rate. These results might hypothesise that the trimmed 5th and 4th D-alanine residues by DacA and LdcB may be recycled in *alrA* strain. However, the 5th D-alanine residues are available for recycling in the case of *ldcB* strain and no D-alanine is released from the peptidoglycan of *dacA* strain. We also further investigated the role of carboxypeptidases in cell wall metabolism, using radioactive (¹⁴C) D-alanine labelling. The results showed that the cell wall of *dacA* strain is more radioactive than the cell wall of wild type and *ldcB* strain. Again, *ldcB* strain showed intermediate radioactivity (see section 3.2.3). The interpretation of these observations is that the *dacA* mutant holds more D-alanine in its peptidoglycan than *ldcB* mutant, and *ldcB* mutant possesses more D-alanine in its peptidoglycan comparing to the wild type. This is consistent with (Atrih *et al.*, 1999; Hoyland *et al.*, 2014). The same differences were again observed when *ldcB* and *dacA* genes were deleted in *dltA-D^{-ve}* strains (see section 3.2.3). Interestingly, the lack of carboxypeptidase activities did not affect the rate of cell wall synthesis. This supports our above hypothesis regarding the role of carboxypeptidases in D-alanine recycling rather than regulation of peptidoglycan cross-links. Moreover, it was observed that the incorporation rate of radioactive D-alanine increased in *dltA-D^{ve+}* strains with time, while it was constant in the *dltA-D^{ve-}* strains (Figure 3.5A). This observation could be consistent with a study, which observed rapid increase in the D-alanine content of WTA in *B. subtilis* during exponential phase (Hyyrylainen *et al.*, 2000).

We previously observed that *alrA* strain takes up the supplemented D-alanine in culture medium. As D-alanine is an essential component of bacterial cell wall, the identification of its transporter could be quite useful in bacterial cell wall investigations. The online Subtilist database was firstly searched to identify the putative amino acid transporters in *B. subtilis* (see section 3.2.4.1 for the hypothesis). The *alrA* strain was transformed with gDNAs, carrying mutations in a suspected amino acid transporter. The results showed that *alrA ytnA* strain is unable to grow in LB medium, supplemented with D-alanine (see section 3.2.4.1). The lethal effect of the double mutations suggests the loss of D-alanine transport in the absence of *ytnA* gene (this gene is re-designated *datA* in this work). Based on Ferrari *et al.* (1985) observation *alrA* strain grows in MM without D-alanine, so we were able to isolate a viable double mutant on MM (see section 3.2.4.1). The *alrA datA* strain is only able to grow on MM and seemed to grow slightly better in the presence of D-alanine. However, it did not grow upon the addition of L-alanine to

MM. This may also suggest that the usual L-alanine content of rich medium inhibits the growth *alrA* and *alrA datA* strains. Thus, the above results suggested that DatA is a D-alanine transporter in *B. subtilis* and L-alanine is still transported by *datA* strain.

The role of DatA in D-alanine transport was further investigated, using genetic complementation (see section 3.2.4.2). An inducible copy of *datA* gene was able to restore the growth of *alrA datA* strain in rich medium, containing D-alanine. This result strongly suggests that DatA protein is required for D-alanine transport in *B. subtilis*. Furthermore, it was already observed that an *alrA* strain depended on a plasmid copy of *alrA* gene in the absence of exogenous D-alanine, but the plasmid was lost upon addition of D-alanine to the culture medium (Ferrari *et al.*, 1985). Based on this observation we hypothesised if *datA* gene is deleted, the plasmid copy of *alrA* gene should be kept in the presence and absence of D-alanine. The effect of *datA* mutant was investigated in *alrA* strain by observing the stability of *pLOSS** plasmid, which carried a constitutively expressed copy of *alrA* gene (see section 3.2.4.2). It was observed that the *pLOSS* Ω alrA* is required for *alrA* growth in rich medium, whereas the *pLOSS* Ω alrA* is lost in the presence of D-alanine in rich medium. However, the *pLOSS* Ω alrA* was kept by *alrA datA* strain in the presence and absence of D-alanine in the medium. This result suggests that D-alanine transport is absent in *alrA datA* strain and the strain only depends on the *pLOSS* Ω alrA* for D-alanine production *in vivo*. More experimental evidence about the role of DatA in D-alanine transport was obtained, when the wild type and *datA* strains were grown in LB medium, supplemented with radioactive (^{14}C) D-alanine (see section 3.2.4.3). The wild type cells showed the transport (15 %) and incorporation of exogenous D-alanine, whereas *datA* strain did not take up and incorporate D-alanine within 2.0 h of incubation (see section 3.2.4.3). These observations suggested that despite having an *in vivo* source of D-alanine, wild type cells usually takes up exogenous D-alanine via DatA. There was also a significant difference between the amount of radioactive D-alanine transported and the amount incorporated in wild type *B. subtilis*, suggesting that a large amount of the transported D-alanine is utilised as energy source. Together, the above experimental data confirmed that DatA has high specificity to D-alanine, because DatA is able to discriminate D-alanine from other amino acids in rich medium. The details of DatA characterisation is in chapter 4.

Ferrari *et al.* (1985) previously observed that *alrA* strain is able to grow in MM without D-alanine supplement, but L-alanine supplement inhibited the growth. The same

consequence has been observed in this study, so we were curious to identify the gene product that catalyses D-alanine production in *alrA* strain in MM. The hypothesis was the addition of L-alanine to MM might induce suppressor mutations in genes that encode L-alanine transport system and/or transcriptional regulator of the gene, which supplies the *alrA* strain with D-alanine. So, suppressor mutations in the assumed genes may give the ability to *alrA* strain to resist L-alanine and grow without D-alanine in rich medium. We firstly tried to make suppressor mutations in *alrA* strain by exploiting the growth inhibitory effect of L-alanine (see section 3.2.5). We collected six strains of L-alanine insensitive *alrA*, which were able to grow in rich medium without D-alanine. However, the sequencing results of these six strains showed some point mutations in some genes (e.g. *rho*, encodes transcription termination factor and *clsA*, encodes cardiolipin synthase), which apparently do not have direct roles in the transport and metabolism of amino acids (see section 3.2.5). Alternatively, the creation of synthetic lethality was tried through synchronising the deletion of two defined genes, one of them was *alrA* and the other gene was either characterised or predicted to be involved in metabolising of D-amino acids. The *B. subtilis* online databases were hopefully checked for any possible genes and we selected five genes, which were predicted to have such activity. The *alrA* strain was transformed with the null mutation of the five genes (see section 3.2.5). Through this analysis, only *dat alrA* strain was not able to grow in MM, suggesting that the D-alanine aminotransferase (Dat) contributes to D-alanine synthesis in MM when the main alanine racemase (AlrA) is absent. This result also gave us a clue to explain why L-alanine inhibits the growth of *alrA* strain in MM and rich media. The reason is probably the interference of L-alanine in the metabolic activity of Dat enzyme, because L-alanine is the stereoisomer of D-alanine and Dat produces D-alanine from D-glutamate in a reversible reaction. The available L-alanine may push Dat enzyme to convert L-alanine to D- or L-glutamate rather than making D-alanine from D-glutamate (Thorne *et al.*, 1955). Due to the matter of time we were not able to further investigate cell wall metabolism of *B. subtilis* in MM, but this finding would solve the problem of future studies which are going to investigate alanine or cell wall metabolism in MM.

Chapter 4. Characterisation of D-alanine transporter (DatA)

4.1 Introduction

In chapter 3, we have found that DatA (formerly YtnA) is involved in D-alanine transport in *B. subtilis*. The characterisation of DatA protein could be really useful for further understanding the properties of amino acid transporters and the mechanisms of amino acid transport in living organisms generally. The primary data about *datA* gene has been shown on the specialized online databases, *SubtiWiki*, *SubtiList* and *BsubCyc*. The *datA* gene is 1389 base pairs (bp) long and located at 3124.70 kilo base (kb) of *B. subtilis* genome. The *asnB* and *ytpA* genes are located at the upstream and downstream of *datA* gene respectively (Figure 4.1A) (Kunst *et al.*, 1997). It was thought that *datA* is co-transcribed with its upstream gene, *asnB* (Yoshida *et al.*, 1999). However, northern blotting analysis did not show transcriptional connection between *asnB* and *datA* genes (Sierro *et al.*, 2008). This seems to be supported by the Genbank entry (AF008220), which suggests the presence of a terminator at the end of *asnB* gene. Moreover, microarray analysis (Nicolas *et al.*, 2012) showed that the transcription of *datA* seems to start from the promoter of *metK* gene and apparently did not terminate completely at its own terminator (Figure 4.1A). Thus the transcription of *datA* gene as a single transcription unit is controversial. In addition, the level of gene expression suggests that *datA* is expressed during vegetative growth (Figure 4.1B). The *datA* gene encodes a 50 kilo Dalton (kDa) membrane protein, comprising of 463 amino acids, which is similar to proline transporter (Kunst *et al.*, 1997). However, its neighbour genes have different suggested functions. The *asnB* gene is encoded to an asparagine synthase (Yoshida *et al.*, 1999) and YtpA protein has phospholipase activity, which is required for the production of Bacilysocin antibiotic in *B. subtilis* 168 (Tamehiro *et al.*, 2002).

The amino acids are actively transported either by ABC transporters or secondary carriers (permeases), but the majority of amino acid transporters are secondary carriers in bacteria (Saier, 2000). The permeases have common structural features, such as possession of 10-12 alpha helical transmembrane domains, each hydrophobic domain contains about 20 amino acid residues and only a few of them are charged residues, the helical hydrophobic membrane domains are linked together through hydrophilic loops, which are relatively long on the cytoplasmic side of the membrane, the carboxy- and amino- termini are cytoplasmic and the presence of a surplus of positively charged amino acid residues (Arginine, lysine, Histidine) in the cytoplasmic loops (Poolman and

Konings, 1993). It has been demonstrated that substrate heterogeneity is common among amino acid uptake system, and kinetic studies suggest that alanine, glycine, serine and D-cycloserine share a common uptake system in bacteria (Oxender, 1972; Halpern, 1974).

The accumulation of different D-amino acids has been reported in the stationary culture supernatant of *B. subtilis* (Lam *et al.*, 2009). Interestingly, D-alanine was not detected despite the fact that it is normally trimmed in peptidoglycan by carboxypeptidases and is also spontaneously released from teichoic acids in alkaline growth condition. Thus, the tracking of the fate of released D-alanine molecules may provide interesting insights into the field of cell wall recycling in Gram-positive bacteria.

In this chapter the suggested D-alanine transporter (DatA) is characterised in terms of gene transcription, membrane topology, substrate specificity, phylogeny and distribution. We have also shown the roles of DatA and carboxypeptidases (dacA and LdcB) in the recycling of cell wall-derived D-alanine.

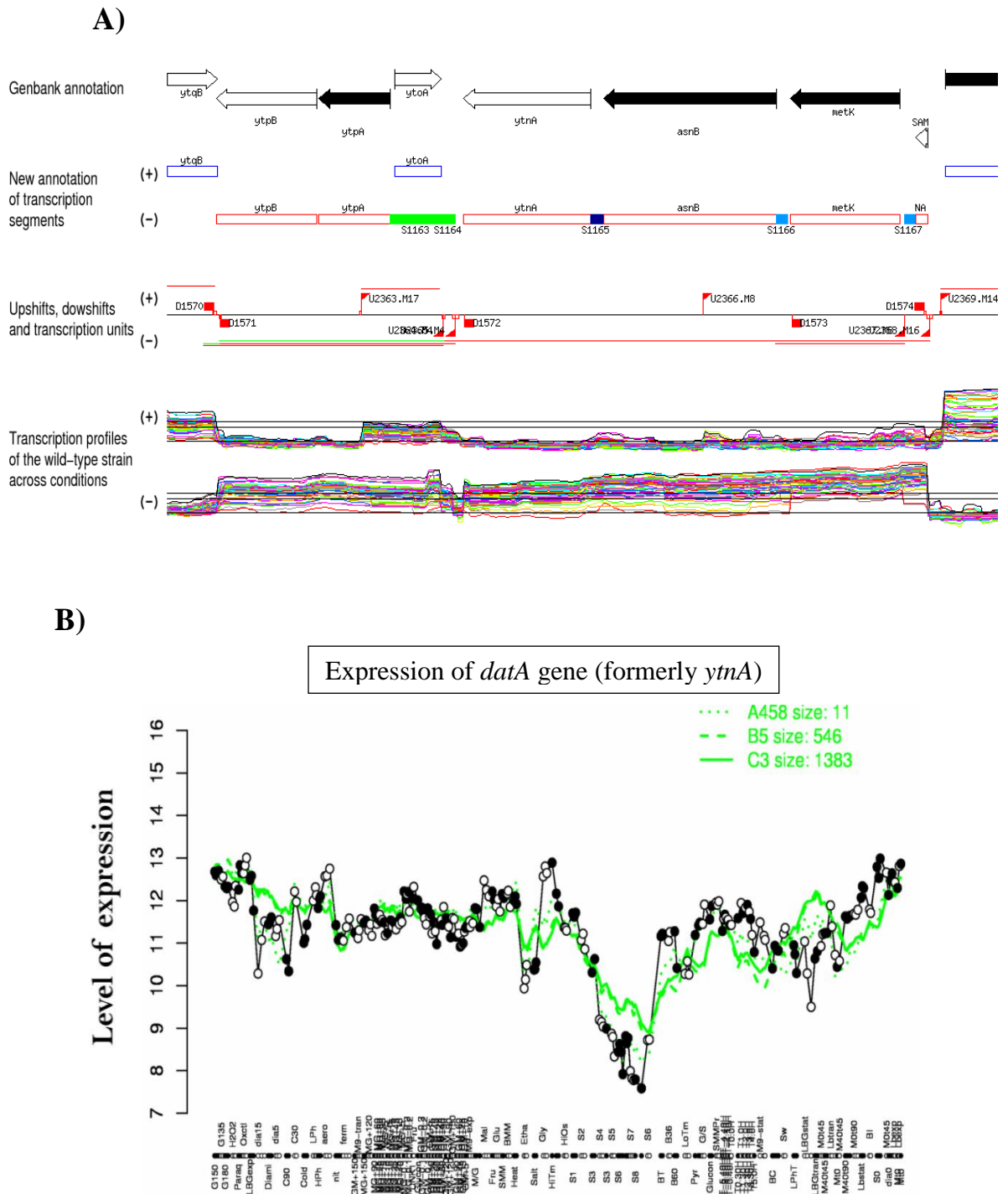


Figure 4.1 The transcription profiles and expression of *datA* gene (formerly *ytnA*) in *B. subtilis*. A) It shows gene annotations in a region of the chromosome, where *datA* gene is located. The microarray analysis shows the transcription profiles of *datA* and its neighbour genes in different growth conditions. The location of suggested promoters and terminators are also revealed (Nicolas *et al.*, 2012). B) The expression profile of *datA* gene across different growth conditions. The figures are adapted from *SubtiWiki* database 2.0/ Expression Data Browser.

4.2 Results

4.2.1 *Is data gene a single transcription unit?*

As the transcriptional regulation of *datA* gene was still unclear (see section 4.1) and because we did not manage to genetically complement *datA*, where an inducible copy of *datA* gene was cloned with its native ribosome binding site (RBS) (see section 3.2.4.2). We decided to determine if *datA* is transcribed with its neighbour genes. The *B. subtilis* was grown in LB medium to mid-exponential growth at 37 °C. The genomic DNA (gDNA) and total RNA were extracted from the cells. The total RNA extract was checked for gDNA contamination, before making complementary DNA (cDNA) by using random hexamers. In the meantime 16 pairs of oligos (oKS38 - oKS69) were designed to amplify short and long DNA fragments, located inside and between the upstream and downstream genes of *datA* (Figure 4.2A). The gDNA was firstly used as the PCR template to check whether the oligos produce the expected fragments. As shown in (Figure 4.2Bi), all the oligos worked perfectly and produced the expected fragments. However, using cDNA as PCR template showed no bands for SAM-*pckA* (lane 15), *datA*-SAM (lane23) and *ytoA-metK* (lane 25). Besides, thin bands for *ytqB-ytpB* (lane 2), *ytoA-datA* (lane 8), *ytqB-ytoA* (lane18), *ytpB-datA* (lane 20) and *ytoA-asnB* (lane21) were observed (Figure 4.2Bii). The thin bands particularly for large fragments could be the effect of mRNA degradation, which results in low copy number of cDNA. This problem was improved through increasing the number of PCR cycles from 25 to 32 cycles. To conclude, the comparison of the bars 8, 10, 19 and 20 and 22 in (Figure 4.2A) to the corresponding lanes in (Figure 4.2Bii) clearly showed that *datA* is co-transcribed with its upstream genes, *metK* and *asnB* and downstream genes, *ytpA* and *ytpB*.

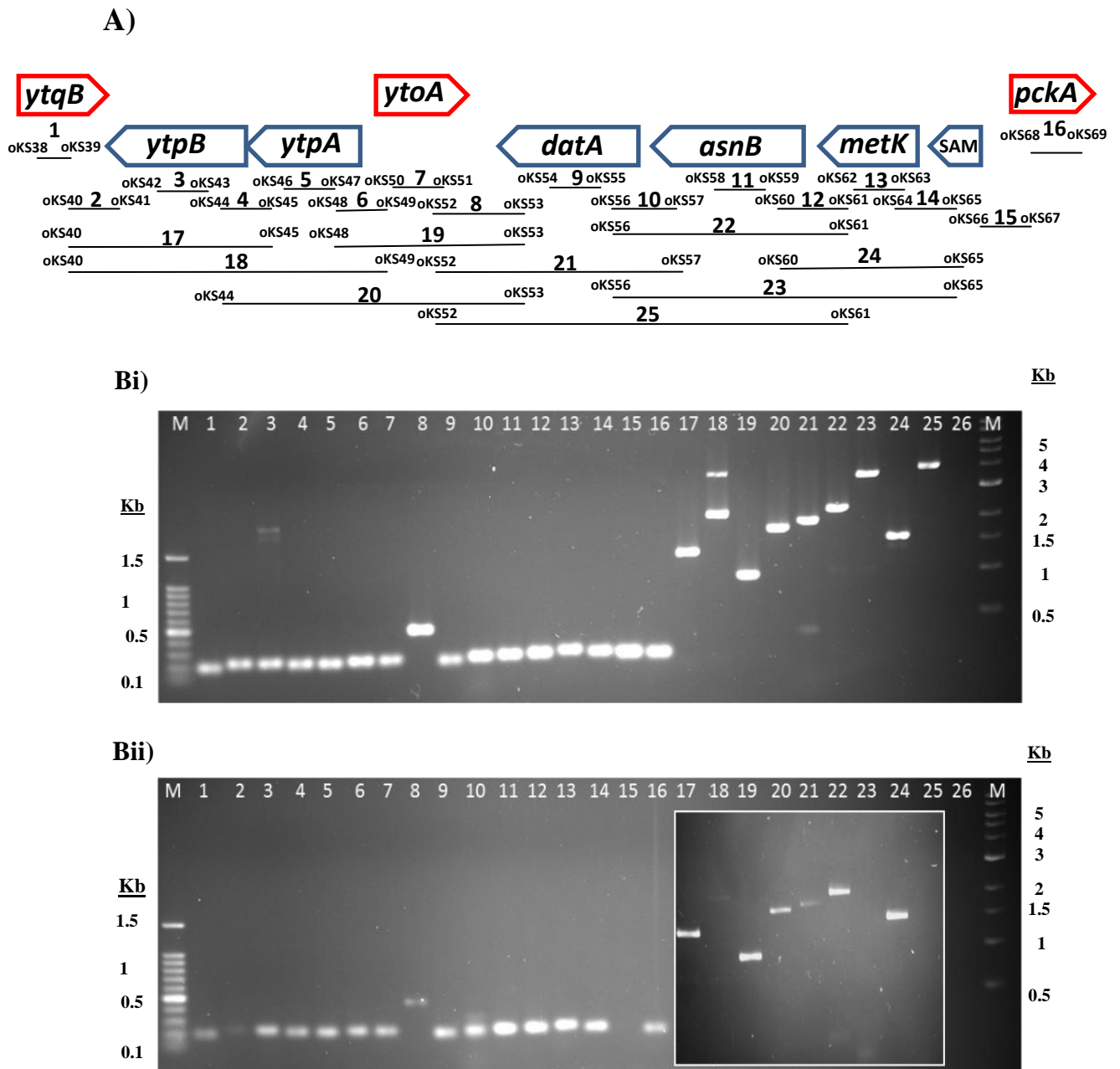


Figure 4.2 Transcription analysis of *dataA* gene. A) The *dataA* gene and some of its upstream and downstream genes were amplified by PCR. The numbered bars represent the corresponding fragments of the DNA, which were amplified with specific pairs of oligos (oKS38-oKS69). The images of agarose gel show products of PCR reactions (25 cycles), using gDNA (Bi) and cDNA (Bii) as templates. The lane numbers correspond to the numbered bars in the figure (A). The lane 26 is negative control, in which total RNA was used as template for amplifying bar 9. The white bordered square in figure (Bii) is 32 cycles PCR reaction.

4.2.2 Conservation of DatA protein

The STRING 9.1 and National Centre for Biotechnology information (NCBI BLAST) databases were used to determine the conservation of proteins homologous to DatA and their percentage of identity in other organisms. The STRING 9.1 database showed a wide range of distribution of DatA-like proteins throughout bacterial kingdom and even in some eukaryotes. However, the proteins showed different percentage of identities to DatA as well as different putative functions (Figure 4.3 and appendix D). The high identities were shown by YtnA (89 %), GK3461 (79.8 %) and BcerKBAB4_0608 (75 %) proteins of *Bacillus amyloliquefaciens*, *Geobacillus spp.* and *Bacillus weihenstephanensis* respectively. The DatA homologous proteins were also found in clinically important members of Enterobacteriaceae (53-58 % identity), Pseudomonadaceae (45-69.8 % identity), Brucellaceae (43-44 % identity), Bordetella (34-35 % identity), Streptococcaceae (31.7-39 % identity), Campylobacteraceae (34-44 % identity), Helicobacteraceae (34% identity), Staphylococcaceae (50-51 % identity), Listeria (55 % identity), Bacillaceae (75 % identity), Clostridiaceae (36-60 % identity) and Corynebacterineae (33-52 % identity). Interestingly, the DatA homologs are suggested to be putative D-alanine/D-serine/glycine permease in *Xanthomonas spp.*, *Stenotrophomonas maltophilia*, *Brucella melitensis*, *Acidovorax citrulli*, *Delftia acidovorans*, *Comamonas testosteroni*, *Streptococcus thermophiles*, *Clostridium botulinum Eklund* and *Mycobacterium spp.* The full details about the bacterial species, proteins name, putative functions and identity rate are shown in appendix D. In addition, the NCBI BLAST revealed a significant conservation of DatA sequence, 72-100 % identity, among the members of Bacillaceae and Paenibacillaceae families. The NCBI BLAST search also showed homology between DatA and PRK11049, which is a computationally derived sequence representing a conserved putative D-alanine/D-serine/glycine permease (CycA) in a diverse collection of bacterial *spp.* (Figure 4.4). DatA seems to share good amino acid sequence identity (~ 48.0 % identity) with PRK11049 model even in non-membranous domains. Furthermore, we analysed the properties of the proposed D-alanine transporters in bacterial species (Table 4.1). The DatA protein seems to show a reasonable percentage of sequence identity to CycA protein in *E. coli* (41.7 %) and *Mycobacterium bovis* BCG (35.4 %), so DatA could be a member of the amino acid transporter family in amino acid-polyamine-organocations superfamily (Table 4.1). Moreover, no similarity was found between the genetic context of DatA and the DatA-like proteins, using STRING 9.1 database.

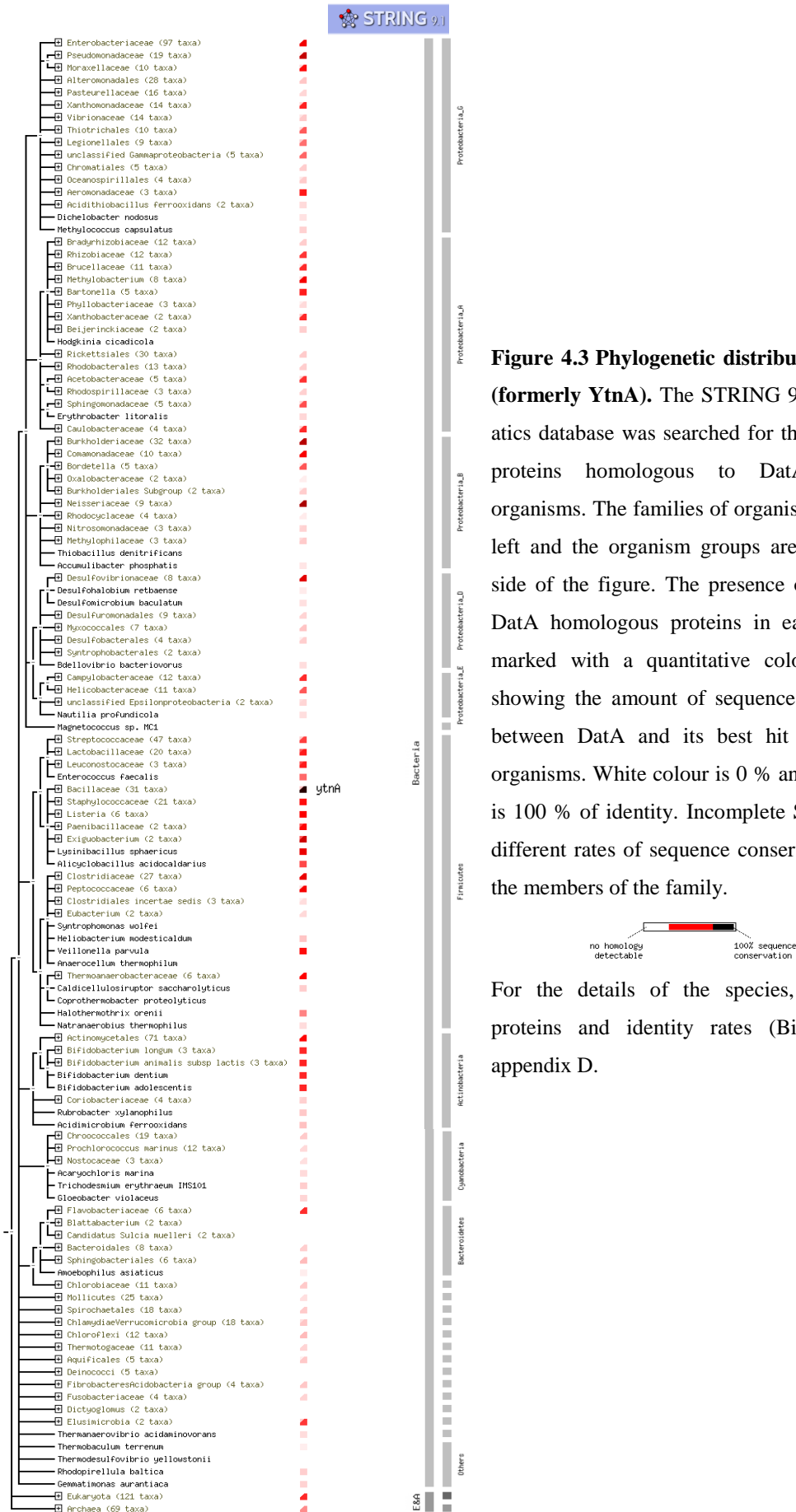


Figure 4.3 Phylogenetic distribution of DatA (formerly YtnA). The STRING 9.1 bioinformatics database was searched for the presence of proteins homologous to DatA in other organisms. The families of organisms are on the left and the organism groups are on the right side of the figure. The presence or absence of DatA homologous proteins in each family is marked with a quantitative coloured square, showing the amount of sequence conservation between DatA and its best hit in the other organisms. White colour is 0 % and dark brown is 100 % of identity. Incomplete Square means different rates of sequence conservation among the members of the family.

For the details of the species, homologous proteins and identity rates (Bit score) see appendix D.

```

          10      20      30      40      50      60      70      80
DatA   N  4  QKQELH RGL EERHIS LMSL GAAIGVGLFLGSASAIQLAGPGILVAY AASGLVMFFIMRALGEMAIQKPVAGSFSRYARDY 83
Cdd:PRK11049 14 AEQSLRRNLTNRHIQLIAIGGAIGTGLFMGSGKTIISLAGPSIIFVYMIIGFMLFFVMRAMGELLNSNLEYKSFSDFAIDL 93
          90      100     110     120     130     140     150     160
DatA   84  LGPLAGYL TGVN YWFLWVVT CMAEITAVGIYMGFWFPDVPNWIWAL SALVIMTGVN FLAVKAYGELEFWFALIKIVAILS 163
Cdd:PRK11049 94 LGPWAGYF TGTW YWFCWVVTGIADVVAITAYAQFWFPDLSDWVASLAVLLLLSLNLATVKMFGEMEFWFAMIKIVAIVA 173
          170     180     190     200     210     220     230     240
DatA   164 MIAVGL LMI IAG-VGNGGIATGISNLWNNGGFPHGLKGVLLSLQVMVFAYLGIEMIGVTAGEVKNPQKSLAKAIDTVFW 242
Cdd:PRK11049 174 LIVVGLVMVAMHFQSPTGVEASFAHLWNDGGMFPKGLSGFFAGFQIAVFAFVGLIELVGTAAETKDFEKS LPRAINSIPI 253
          250     260     270     280     290     300     310     320
DatA   243 RILIFVYV GALFVIMS IYPWQEIGSQSPFVLT FQKVGIPSAAGIINFVVLTAALSSCNSGIFSTGRMLFNLAEQKEAPQA 322
Cdd:PRK11049 254 RIIMFYV FALIVIMS VTPWSSVVPDKSPFVELFVLVGLPAAASVIN FVVLTS AASSANSVGFSTSRMLFGLAQEGVAPKA 333
          330     340     350     360     370     380     390     400
DatA   323 YGQLTKGGIPGRAVLASAGALLVGVLLNYVVP--AKVFTWVT SIATFGAIWTWAIILLSQIKYRKS I KPEEKKQLKYKMP 400
Cdd:PRK11049 334 FAKLSKRAVPARGLTFSCICLLGGVLLYVNPsvIGAF TLVTVSAILFMFVW TIIILCSYLVRKQ-RPHLHEKSIYKMP 412
          410     420     430     440
DatA   401 LFFFTSYVSLAFLAFVVIIMAYSPDTRVAVIIGPIWFLI LLAVY 444
Cdd:PRK11049 413 LGKLMCWVCMAFFAFVLVLLTLEDDTRQALIVT PLWFIALGLGY 456 C

```

Figure 4.4 The sequence alignment of DatA and PRK11049 model. The alignment was automatically generated by NCBI BLAST and shows the regions of amino acid sequence similarity (red letters) between DatA protein and CycA protein. The PRK11049 model represents a conserved putative D-alanine/D-serine/glycine permease (CycA) in a collection of different bacterial species. The TMHMM server 2.0 was used to determine the transmembrane domains, which are bolded and underlined on the aligned proteins sequences.

Bacteria	Protein name	Function	Transporter		No. of Transmembrane domains	Identity to DatA (%)	Reference
			Superfamily	Family			
<i>E. coli</i>	CycA	D-serine/D-alanine/ Glycine/D-cycloserine permease	2.A.3 Amino acid - polyamines - organocation (APC)	2.A.3.1 Amino acid transporter	12	41.7	(Wargel <i>et al.</i> , 1970; Wargel <i>et al.</i> , 1971; Robbins and Oxender, 1973)
<i>Mycobacterium bovis</i> BCG	CycA	D-serine/L- and D-alanine /Glycine/ D-cycloserine transporter			12	35.4	(Chen <i>et al.</i> , 2012)
<i>Altromonas Haloplanktis</i>	DagA	Sodium-linked D-alanine/ glycine symporter		2.A.25 Alanine or glycine::cation symporter (AGCS)	11	24.7	(MacLeod and MacLeod, 1992)
<i>Bacillus sp.</i> PS3	ACP	Sodium/Proton-dependent alanine carrier protein			10	26.0	(Kamata <i>et al.</i> , 1992; Kanamori <i>et al.</i> , 1999)
<i>Methanococcus maripaludis</i> (Archea)	AgcS	L- and D-alanine: sodium symporter			11	24.6	(Moore and Leigh, 2005)
<i>Salmonella enterica</i>	DalS	Periplasmic substrate (D-alanine)-binding protein	3.A.1 ATP-binding cassette (ABC) transporter	3.A.1.3 Polar amino acid transporter (PAAT)	-----	-----	(Osborne <i>et al.</i> , 2012)
	DalU	Cytoplasmic ATPase			-----		
	DalT	Membrane spanning			4		
	DalV	transport channel proteins			5		

Table 4.1 The properties of few proposed D-alanine transporter in bacteria. The transporter family and superfamily were obtained from transporter classification database (TCDB), and the TMHMM Server V 2.0 was used to generate the number of transmembrane domains. The percentage of identity was determined by using SIM-alignment tool in ExPASy, a Swiss institute of bioinformatics resource portal. The selected parameters in SIM-alignment tool were comparison matrix: BLOSUM100, number of alignments computed: 1, gap open penalty: 0 and gap extension penalty: 0. The protein sequences, used in TMHMM server 2.0 and SIM-alignment tool, were obtained from online Uniport database[©] 2002-2016.

4.2.3 Biochemical characterisation and substrate specificity of DatA

4.2.3.1 Membrane topology of DatA.

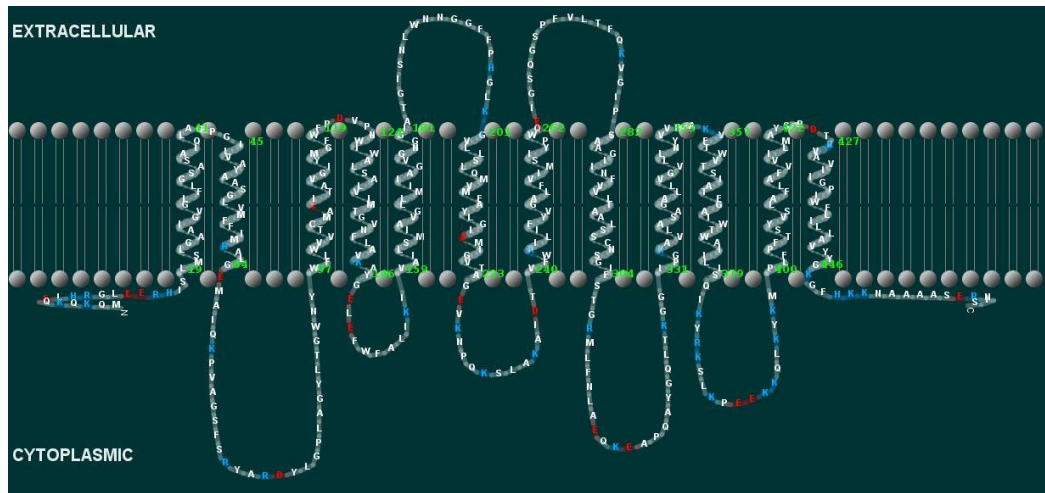
We used prediction bioinformatics tools to characterise DatA protein in terms of its membrane topology and number of transmembrane helices. The protein sequence of DatA was firstly copied from online *SubtiWiki* database and inputted into the TMHMM Server V 2.0 to generate some predicted membrane properties of DatA protein. The data of TMHMM Server V 2.0 was used to produce a two-dimensional visual representation of DatA protein in cell membrane, using TransMembrane protein Representation in two Dimensions software ([http:// bioinformatics.biol.uoa.gr/ TMRPres-2D/](http://bioinformatics.biol.uoa.gr/TMRPres-2D/)) (Figure 4.5A). According to the output data of TMHMM Server V 2.0, DatA protein possesses 12 alpha helical transmembrane helices and there are approximately 20 amino acid residues in each of the transmembrane domains, where the majority of the amino acid residues are uncharged. DatA protein also has five cytoplasmic hydrophilic loops, two extracellular hydrophilic loops and cytosolic carboxy (C)- and amino (N)- termini. The cytoplasmic hydrophilic loops are longer than the extracellular loops and contain positively charged amino acids (e.g lysine (K), arginine (R) and histidine (H) (Figure 4.5A).

We also investigated the predicted crystal structure of DatA to gain some primary information about the protein's structure. The Protein Data Bank (PDB) (<http://www.rcsb.org/pdb/home/home.do>) was searched for structurally solved DatA-like proteins. This identified Arginine:Agmatine antiporter (AdiC) in *E. coli* O157:H7 (Figure 4.5B) as having strong similarity to DatA. The alignment properties of DatA and AdiC were **length:** 325, **identities:** 76/325 (23 %), **positives:** 138/325 (42 %) and **gaps:** 25/325 (8 %). AdiC is a member of amino acid, polyamine and organocation (APC) superfamily of transporters (Casagrande *et al.*, 2008) and possesses 12 alpha helical transmembrane domains, which are integrated into the cell membrane as dimers (Figure 4.5B) (Fang *et al.*, 2009; Gao *et al.*, 2009). AdiC protein is generally similar to sodium-solute symporters in terms of structural folding (Gao *et al.*, 2010).

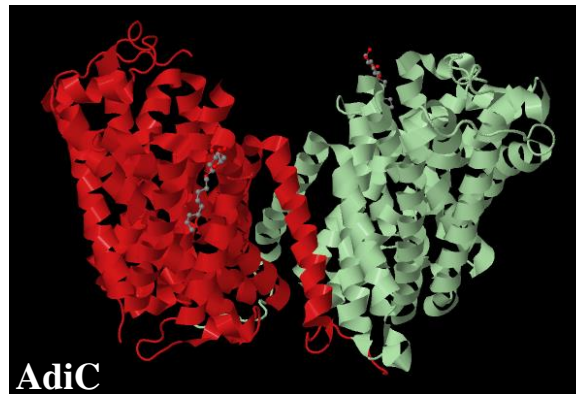
To test these bioinformatics predictions, the localisation of DatA protein was studied by fluorescent microscopy, using green fluorescent protein (GFP) tagging. The cloning vectors pSG1154 (*bla amyE3' spc P_{xyl} -gfp amyE5'*) and pSG1729 (*bla amyE3' spc P_{xyl} gfp- amyE5'*) were respectively used to construct C-terminus (pKS2: *bla amyE3' spc P_{xyl} datA-gfp amyE5'*) and N-terminus (pKS3: *bla amyE3' spc P_{xyl} gfp-datA amyE5'*)

GFP tagged DatA. The pKS2 and pKS3 constructs were separately introduced into the *amyE* locus of KS22 (*datA::erm*) strain by transformation, resulting in KS28 ($\Delta datA::erm amyE \Omega (spc P_{xyl} datA-gfp)$) and KS29 ($\Delta datA::erm amyE \Omega (spc P_{xyl} gfp-datA)$) strains. The KS28 and KS29 strains were grown on nutrient agar, supplemented with 0.5 % xylose and incubated at room temperature overnight. The cells were mounted on a slide and examined by fluorescent microscope. It was seen that only N- terminus GFP-DatA gave fluorescent signal, which seemed to be localised to the cytoplasmic membrane (Figure 4.5C). The Western blot analysis also showed the protein band of N-terminus GFP-DatA (data not shown). Despite the correct cloning and sequencing of KS28 strain ($\Delta datA::erm amyE \Omega (spc P_{xyl} datA-gfp)$), the C-terminus DatA-GFP was not detected in both fluorescent microscopy and Western blotting for unknown reason. To check the functionality of N-terminus GFP tagged DatA, the KS29 strain ($\Delta datA::erm amyE \Omega (spc P_{xyl} gfp-datA)$) was transformed with the gDNA of RD180 ($\Delta alrA::zeo$) in the presence of D-alanine and xylose. However, no transformants were obtained from the cross, indicating that GFP tag might impair the transport activity of DatA.

A)



B)



C

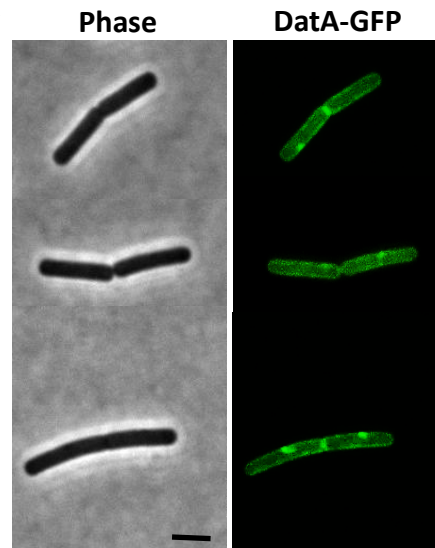


Figure 4.5 Membrane topology and localisation of DatA. A) The predicted membrane topology and transmembrane helices of DatA in two-dimensional graphical model, generated by TMHMM Server V 2.0 and TMRPres2D softwares. The coloured residues (Blue:positive, red:negative and gray:uncharged residues) show the electrostatic potential feature of the protein. B) Homodimeric assembly of structurally characterised Arginine:Agmatine antiporter (AdiC) in *E. coli*, 3.0Å resolution, copied from (Gao *et al.*, 2010). C) Fluorescent microscopic images of KS29 strain ($\Delta datA::erm amyE \Omega(spc pxyl gfp-datA)$), which was grown on nutrient agar plates, containing 0.5 % of xylose and 0.5 mM of D-alanine, and incubated at room temperature overnight. The scale bar is 3.0 μm .

4.2.3.2 Expression of *Data* protein in heterogeneous hosts.

It was found necessary to investigate the substrate specificity of DatA protein *in vitro* (e.g. liposomes). The *data* gene was firstly amplified by PCR and inserted into pET-28a(+) vector to generate pKS7 (C-terminus His-tagged *data*) and pKS8 (N-terminus His-tagged *data*) constructs. The pKS7 and pKS8 constructs were transformed into *E. coli* BL21 to make KS46 strain (*E. coli* BL21+ *pET-28a(+)*Ω *C His-tagged data*) and KS47 strain (*E. coli* BL21+ *pET-28a(+)*Ω *N His-tagged data*) respectively. The strains were grown in large scale LB media (5-10 L) and induced with IPTG (0.5-1 mM). The total cellular protein extract and the purified membrane fraction were analysed in stained SDS-PAGE and Western blot analysis (see section 2.6.16 for methods details). Despite the perfect cloning procedures and sequencing analysis, we did not manage to have purified DatA protein at different temperature degrees (18, 22, 30 and 37 °C) and at different periods of IPTG induction (5 h and overnight).

It was known that the expression of DatA did not seem to work in *E. coli* BL 21(DE3), but it worked well in the living cells of *B. subtilis* (see section 3.2.4.2). This observation was used as a control to investigate the transport of D-alanine in the membrane vesicles of *B. subtilis* and *E. coli* C43(DE3), which was suggested to be a good expression system for toxic membrane proteins (Miroux and Walker, 1996). The *B. subtilis* strains, KS22 ($\Delta dataA::erm$) and KS41 ($\Delta dataA::erm amyE \Omega (cat P_{spac} dataA-ftsL(RBS))$), were grown in LB medium at 37 °C. The cultures were induced with 0.5 mM IPTG at OD₆₀₀ 0.5. The cells were harvested for preparing membrane vesicles at OD₆₀₀ 1.5. The membrane vesicles were suspended in potassium phosphate buffer. The transport of [¹⁴C] D-alanine by *B. subtilis* membrane vesicles was performed in the presence and absence of 5.0 mM NaCl (see section 2.6.17 for method details). The membrane vesicles of *dataA::erm* strain were not able to take up radioactive D-alanine (Figure 4.6A). However, D-alanine uptake by membrane vesicles of ($\Delta dataA::erm amyE \Omega (cat P_{spac} dataA-ftsL(RBS))$) strain reached peak after 10 min of incubation, and then it seemed that the accumulated D-alanine started to leak out (Figure 4.6B). The leakage of lysine was already observed in the membrane vesicles of *B. subtilis* (Konings and Freese, 1972), this is probably due to the loss of membrane integrity. Although the membrane vesicles were prepared from cells grown in LB medium, which usually contains NaCl, the transport of D-alanine into the membrane vesicles seemed to be facilitated by 30 % in the presence of 5.0 mM NaCl (Figure 4.6B). Before investigating D-alanine uptake in the membrane vesicles of *E. coli* C43(DE3) and KS 48 (*E. coli* C43+ *pET-28a(+)*Ω *N His-tagged data*),

the strains were grown in LB medium and the culture of (*E. coli* C43+ *pET-28a(+)* Ω *N His-tagged datA*) strain was induced with different concentrations of IPTG at OD₆₀₀ 0.5. This experiment helped us to harvest the *E. coli* cells for making membrane vesicles at an appropriate time before the cells are affected by the expressed DatA (Figure 4.6C). The preparation of *E. coli* C43 membrane vesicles and the transport of D-alanine were done as previously (see section 2.6.17). It was seen that the membrane vesicles of *E. coli* C43 were able to transport D-alanine (Figure 4.6D). The maximum uptake of D-alanine was observed after 10 min of incubation and stayed constant thereafter. In contrast, the expression of DatA protein impaired D-alanine transport in (*E. coli* C43+ *pET-28a(+)* Ω *N His-tagged datA*) strain (Figure 4.6E).

As the expression of DatA and its transport activity were not possible in living cells and in membrane vesicles of *E. coli*, we thought about the investigation of DatA transport activity in *Xenopus laevis* oocyte, which is a popular eukaryotic expression system for structural and functional studies of transport membrane proteins (Sigel, 2010). The *datA* gene was cloned into an eukaryotic expression vector (pGH19) and then DatA encoding cRNA was made by *in vitro* transcription system. The cRNA was microinjected into the oocytes, where the cRNA is translated to DatA protein. The transport of radioactive D-alanine into the oocytes was examined. However, the transport of D-alanine was not observed in the oocytes (possibly contain DatA) compared to the control oocytes (without DatA) at pH 5.5 and 7.0 (this work was done by Dr. Noel Edwards and Prof. David Thwaites in their lab., based in medical school, Newcastle University (see appendix E for method details)). Thus, from three different approaches it was difficult to directly confirm that DatA alone acts to take up D-alanine in heterogeneous hosts. However, it is obvious that DatA is required for D-alanine transport in *B. subtilis*.

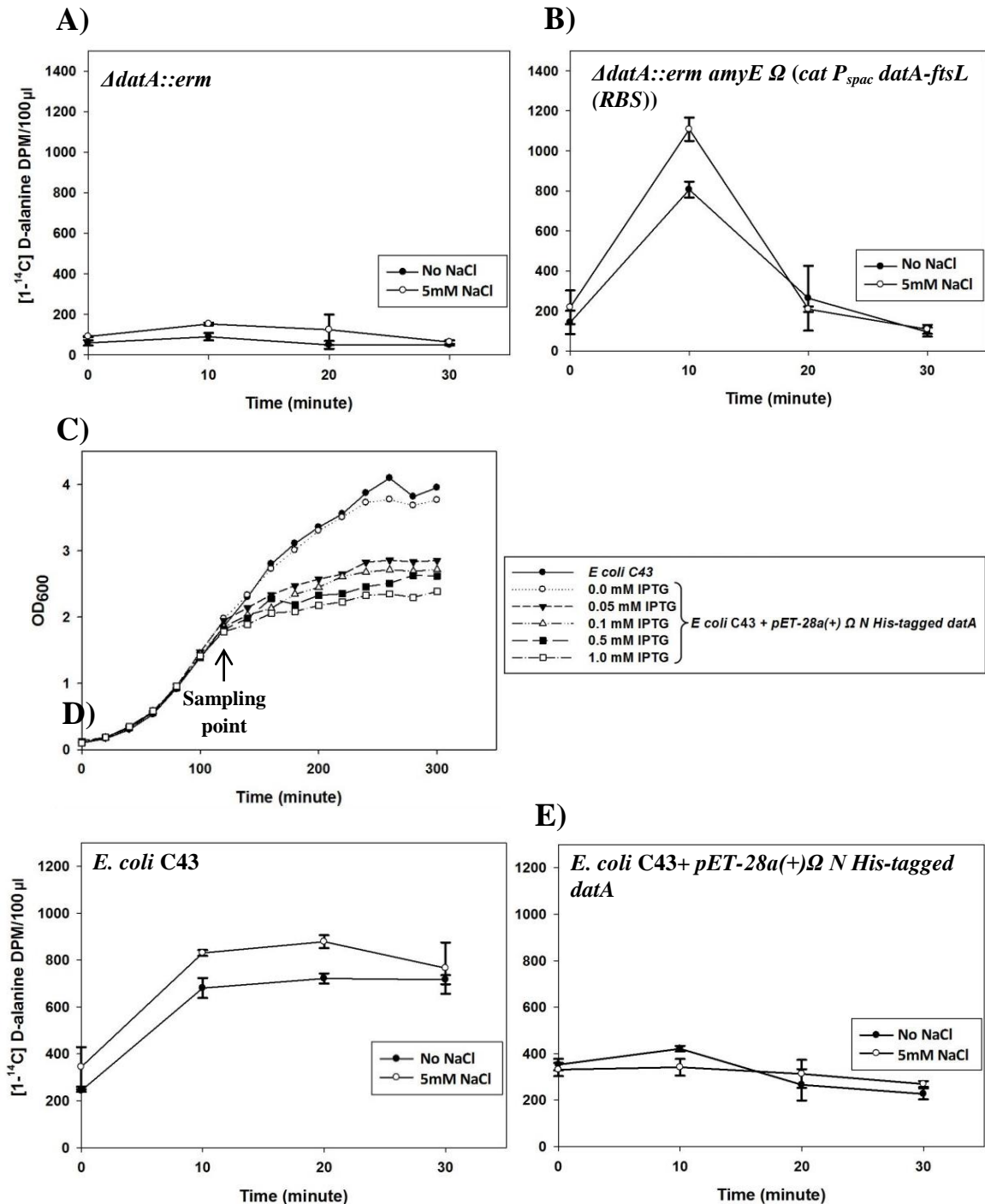
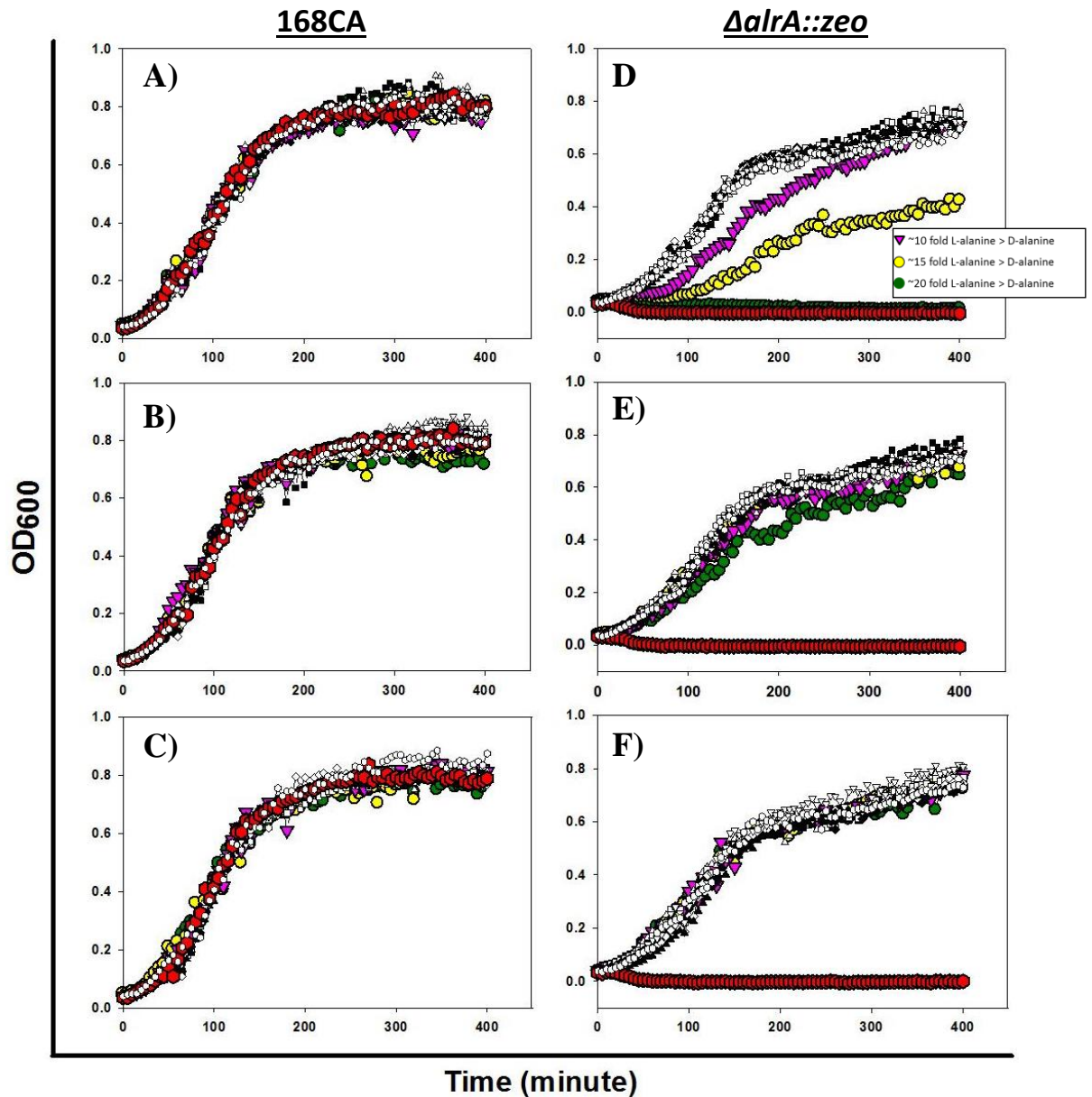


Figure 4.6 D-alanine transport by membrane vesicles. A and B) The transport of radioactive [$1\text{-}^{14}\text{C}$] D-alanine by membrane vesicles of *B. subtilis* KS22 ($\Delta datA::erm$) and KS41 ($\Delta datA::erm amyE \Omega (cat P_{spac} datA-ftsL(RBS))$). C) The growth of *E. coli* C43 and KS48 (*E. coli* C43+ $pET\text{-}28a(+)\Omega N$ His-tagged *datA*) in LB medium with and without different concentrations of IPTG at 37 °C. D and E) The [$1\text{-}^{14}\text{C}$] D-alanine uptake by membrane vesicles of *E. coli* C43 and KS48 (*E. coli* C43+ $pET\text{-}28a(+)\Omega N$ His-tagged *datA*). The mixture of D-alanine transport assay contained membrane vesicle in 0.05 M potassium phosphate, 0.5 μM [$1\text{-}^{14}\text{C}$] D-alanine and ± 5.0 mM NaCl. The error bars indicate the standard deviation of mean of radioactivity (DPM) of three experimental replica ($n=3$). The background radiation was subtracted from the values.

4.2.3.3 L-alanine interferes in D-alanine transport.

After the failure of *datA* expression in *E. coli* (section 4.2.3.2), we did amino acid competition assay. The idea of this *in vivo* assay was growing *alrA* strain in the presence of D-alanine and a low molecular weight amino acid such as L-alanine, glycine and L-proline. If the growth of *alrA* strain is inhibited by a combination of D-alanine and one of the above amino acids, it could mean that D-alanine uptake system is not only specific to D-alanine. This trial might indirectly provide at least primary knowledge about the substrate specificity of D-alanine transporter in *B. subtilis*. The 168CA and RD 180 ($\Delta alrA::zeo$) strains were grown in LB medium, supplemented with 450 μ M of D-alanine and a range of L-alanine, Glycine and L-proline concentrations (0.0098 mM – 5.0 mM) separately. The growth of the strains was monitored at 37 °C, using microplate reader. It was observed that the growth of 168CA was not affected by the supplemented L-alanine:D-alanine, Glycine:D-alanine and L-proline:D-alanine (Figure 4.7A, B and C). The $\Delta alrA::zeo$ strain also grew similarly in the presence of supplemented Glycine:D-alanine and L-proline:D-alanine (Figure 4.7E and F). However, the growth of $\Delta alrA::zeo$ strain was affected by the supplemented L-alanine:D-alanine (Figure 4.7D). As LB medium normally contains L-alanine, we worked out how much L-alanine can interfere with D-alanine transport. The calculation of L-alanine content in tryptone and yeast extract, the two main ingredients of LB medium, was done depending on DifcoTM and BBLTM manual (Zimbro *et al.*, 2009). We found that LB medium itself contains about 3-4 mM of free L-alanine. Taking all L-alanine into account, the growth of $\Delta alrA::zeo$ strain was reduced when L-alanine concentration was 10 fold higher than D-alanine, but the growth was totally inhibited when the ratio of L-alanine to D-alanine was 20:1 (Figure 4.7D). Thus L- and D-alanine might be transported via a common transporter.



●	450 μ M D-alanine + 5 mM L-alanine	450 μ M D-alanine + 5 mM Glycine	450 μ M D-alanine + 5 mM L-Proline
○	450 μ M D-alanine + 2.5 mM L-alanine	450 μ M D-alanine + 2.5 mM Glycine	450 μ M D-alanine + 2.5 mM L-Proline
▼	450 μ M D-alanine + 1.25 mM L-alanine	450 μ M D-alanine + 1.25 mM Glycine	450 μ M D-alanine + 1.25 mM L-Proline
△	450 μ M D-alanine + 0.625 mM L-alanine	450 μ M D-alanine + 0.625 mM Glycine	450 μ M D-alanine + 0.625 mM L-Proline
■	450 μ M D-alanine + 0.3125 mM L-alanine	450 μ M D-alanine + 0.3125 mM Glycine	450 μ M D-alanine + 0.3125 mM L-Proline
□	450 μ M D-alanine + 0.1563 mM L-alanine	450 μ M D-alanine + 0.1563 mM Glycine	450 μ M D-alanine + 0.1563 mM L-Proline
◆	450 μ M D-alanine + 0.078 mM L-alanine	450 μ M D-alanine + 0.078 mM Glycine	450 μ M D-alanine + 0.078 mM L-Proline
◇	450 μ M D-alanine + 0.039 mM L-alanine	450 μ M D-alanine + 0.039 mM Glycine	450 μ M D-alanine + 0.039 mM L-Proline
▲	450 μ M D-alanine + 0.0195 mM L-alanine	450 μ M D-alanine + 0.0195 mM Glycine	450 μ M D-alanine + 0.0195 mM L-Proline
▽	450 μ M D-alanine + 0.0098 mM L-alanine	450 μ M D-alanine + 0.0098 mM Glycine	450 μ M D-alanine + 0.0098 mM L-Proline
●	0.0 μ M D-alanine + 0.0049 mM L-alanine	0.0 μ M D-alanine + 0.0049 mM Glycine	0.0 μ M D-alanine + 0.0049 mM L-Proline
○	450 μ M D-alanine	450 μ M D-alanine	450 μ M D-alanine
	A&D	B&E	C&F

Figure 4.7 Amino acid competition assay. The inhibitory effect of supplemented L-alanine (A&D), glycine (B&E) and L- proline (C&F) on D-alanine transport in 168CA (A, B, C) versus RD180 (Δ alrA::zeo) strain (D, E, F). The strains were grown in LB medium at 37 C°. The growth curves are shown in optical density (OD₆₀₀). Note: LB medium initially contains about 3.0-4.0 mM of free L-alanine.

4.2.3.4 Transport of D-cycloserine in *datA* strain.

D-cycloserine is a compound that structurally mimics D-alanine (Shockman, 1959; Strominger, 1959; Zygmunt, 1962). It interferes with alanine racemase activity and blocks conversion of L-alanine to D-alanine (Roze and Strominger, 1966). D-cycloserine also inhibits the formation of D-alanine dimer by D-alanyl-D-alanine ligase (Neuhaus and Lynch, 1964). Previous studies suggested that D-cycloserine is transported via D-alanine uptake system (CycA) in *E. coli* K-12 (Wargel *et al.*, 1970; Wargel *et al.*, 1971; Robbins and Oxender, 1973) and *M. tuberculosis* (David, 1971). We wondered whether D-cycloserine is also transported by DatA in *B. subtilis*. The *datA* strain must be resistant to D-cycloserine, if DatA protein is specific to the transport of this compound as well. To test this hypothesis, the 168CA and KS22 ($\Delta datA::erm$) strains were grown in PAB medium at 30 °C overnight. A serial dilution (1.0 in 4.0) of the overnight cultures was prepared and 10 µl of each of the diluted culture was spotted on nutrient agar plates, with and without D-cycloserine. D-alanine was present in some of the plates to see whether competition between D-alanine and D-cycloserine rescues the cells from growth inhibition. The plates were incubated at 37 °C overnight. As shown in (Figure 4.8), both 168CA and KS22 ($\Delta datA::erm$) strains grew normally in the absence of D-cycloserine and in the presence or absence of D-alanine. In contrast, the growth of the strains was inhibited by D-cycloserine, and the $\Delta datA::erm$ strain was slightly more sensitive to D-cycloserine than 168CA. Also, D-alanine supplement did not change the sensitivity of the strains against D-cycloserine. Thus D-cycloserine is not transported via DatA, suggesting that D-alanine and D-cycloserine apparently do not have a common uptake system in *B. subtilis*.

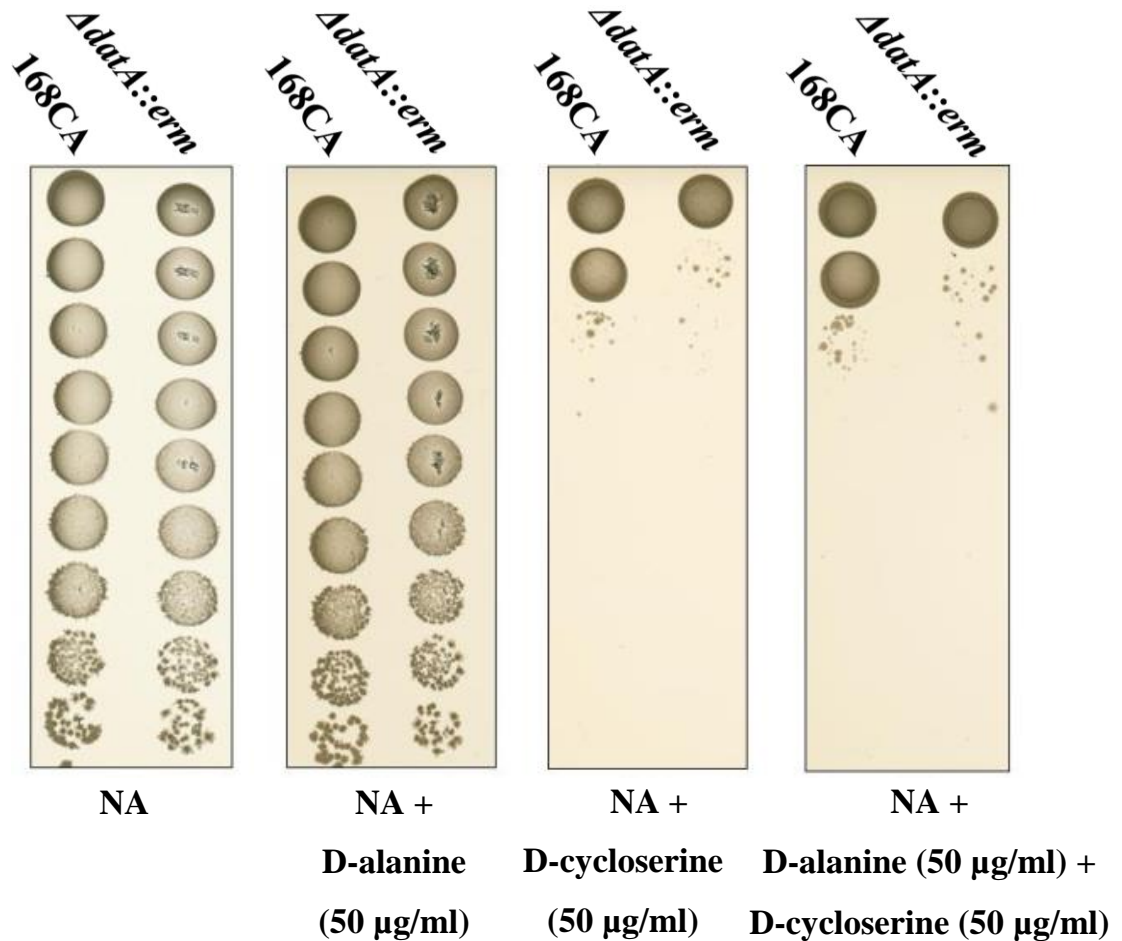


Figure 4.8 D-cycloserine sensitivity of *datA* strain. The 168CA and KS22 ($\Delta datA::erm$) strains were grown in PAB medium at 30 °C overnight. Serial dilutions (1.0 in 4.0) of the overnight cultures were prepared. A 10 μl of each of the diluted culture was spotted on nutrient agar (NA) plates, with and without D-alanine (50 $\mu\text{g/ml}$) and D-cycloserine (50 $\mu\text{g/ml}$). The plates were left at room temperature for drying out the culture spots and then incubated at 37 °C overnight.

4.2.4 Recycling of cell wall derived D-alanine in *B. subtilis*

As explained in the introduction section of chapter 3.0, D-alanine is known to be released from peptidoglycan by carboxypeptidases (DacA and LdcB) and to be spontaneously released from teichoic acids by the action of alkaline pH. However, little is known about the fate of the released amino acids. To determine if DatA has a role in the recycling of D-alanine, both qualitative and quantitative methods were employed.

4.2.4.1 Cross feeding assay

In this assay, the D-alanine auxotroph (*alrA*) strain was grown closely next to wild type and *datA* strain on a solid medium. The hypothesis was the released D-alanine molecules from the cell wall of wild type might be recycled and no D-alanine would be available to support the growth of *alrA* strain. In contrast, *datA* strain should not be able to retake up its cell wall D-alanine and the accumulated D-alanine might be enough to allow the growth of *alrA* strain. The D-alanine donor strains (wild type (168CA), KS11 ($\Delta dltA-D::cat$), KS22 ($\Delta datA::erm$) and KSS36 ($\Delta dltA-D::cat \Delta datA::erm$)) were grown on nutrient agar plates for 3.0 h at 37 °C. Then, the D-alanine auxotroph (recipient) strains (RD180 ($\Delta alrA::zeo$) and KS12 ($\Delta alrA::zeo \Delta dltA-D::cat$)) were streaked closely parallel to the D-alanine donor strains and incubated for a further 23 h. In so doing it was found that the 168CA strain did not support the growth of $\Delta alrA::zeo$ and $\Delta alrA::zeo \Delta dltA-D::cat$ strains (Figure 4.9A), whereas $\Delta datA::erm$ strain did permit the growth of recipient strains (Figure 4.9B). To differentiate between D-alanine from peptidoglycan metabolism and that released from teichoic acids, the same analysis was done, using $\Delta dltA-D::cat$ and $\Delta dltAD::cat \Delta datA::erm$ as D-alanine donor strains and $\Delta alrA::zeo$ and $\Delta alrA::zeo dltA-D::cat$ as D-alanine recipient strains (Figure 4.9C and D). Again, the same results were observed as explained above. Although this method provided no indication of the amount of D-alanine released by normal growth, the results clearly suggested that cell wall derived D-alanine is recycled via DatA (Figure 6.1).

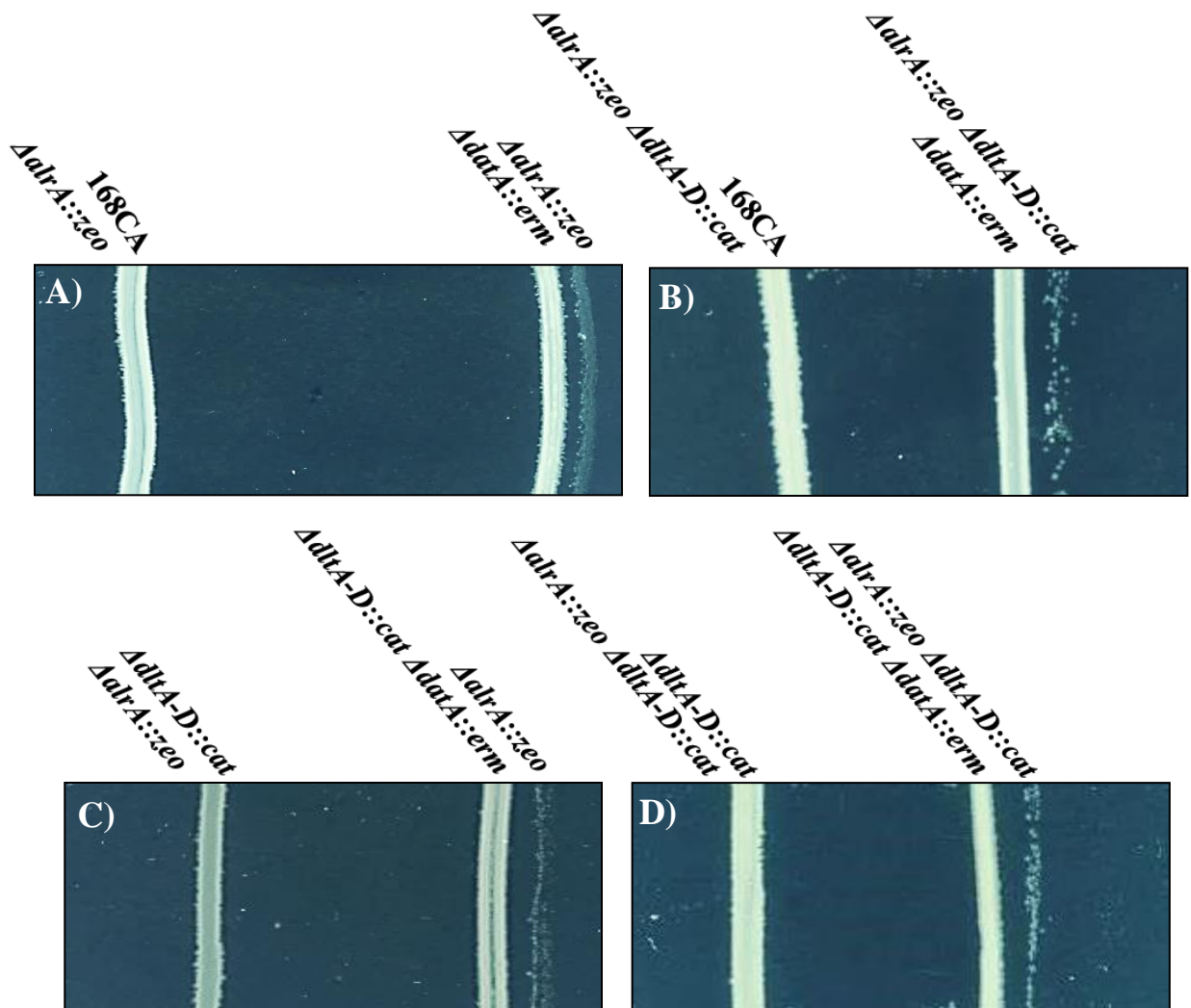


Figure 4.9 Cross-Feeding Assay. The 168CA, KS11 (*ΔdltA-D::cat*), KS22 (*ΔdatA::erm*) and KSS36 (*ΔdltA-D::cat ΔdatA::erm*) strains (D-alanine donors) and RD180 (*ΔalrA::zeo*) and KS12 (*ΔalrA::zeo ΔdltA-D::cat*) strains (D-alanine recipients) were used in this assay. The D-alanine donor strains were firstly streaked on nutrient agar plates and incubated for 3 h at 37 °C. Later, the D-alanine recipient strains were streaked closely parallel to the donor strains and kept incubating for a further 23 h. The total incubation time was 26 h.

4.2.4.2 RP-HPLC analysis of culture supernatant

To provide a more quantitative measurement of released D-alanine, Reverse Phase- High performance liquid chromatography (RP-HPLC) was used to analyse culture supernatant of *B. subtilis*. Pre-column derivatisation of amino acids by Marfey's reagent (MR) was the principle to permit detection and differentiation between L- and D-amino acids. Marfey's reagent is 1-fluoro-2,4-dinitrophenyl-5-L-alanine amide that reacts with primary amines. The MR derivatives of D-amino acids are different from corresponding L-amino acids derivatives in the strength of intramolecular bonding. The D-amino acid-MR derivatives having stronger intramolecular interactions, resulting in lower polarity compared to the corresponding MR derivatives of L-amino acids. Therefore, the derivatised L-amino acids elute much sooner than the derivatised D-amino acids in RP-HPLC (Marfey, 1984).

A standard curve was initially generated by using serial dilutions of D-alanine in LB medium (Figure 4.10A and B). The samples were processed and prepared to HPLC analysis according to the Marfey manufacturer's instructions with some modifications (see sections 2.9.2 and 2.9.3 for methods details). Having defined the sensitivity of the system, the 168CA, KS22 ($\Delta datA::erm$), KS11 ($\Delta dltA-D::cat$), and KS36 ($\Delta dltA-D::cat \Delta datA::erm$) strains were grown in LB medium at 37 °C (see section 2.9.1 and Figure 4.11A). Samples were taken at different growth phases (corresponding to 90, 180, 390 min and after overnight (O/N) incubation). The samples were centrifuged and the culture supernatants were processed for HPLC analysis (see methods sections 2.9.2 and 2.9.3). Comparing the HPLC results of 168CA to those of $\Delta datA::erm$ strain (Figure 4.11B), D-alanine was clearly detected in the culture supernatants of both the strains during exponential growth (90 and 180 min), with a greater amount of D-alanine detected at 180 min of incubation than that seen at 90 min. It was also evident that the $\Delta datA::erm$ strain released more D-alanine into its culture supernatant than 168CA at 90 and 180 min. Surprisingly, D-alanine was not detectable easily in the culture supernatants of 168CA and $\Delta datA::erm$ when sampled in stationary phase (390 min and O/N of incubation) (Figure 4.11B). It was also evident that a significant proportion of the amino acid content of the medium had been consumed by this stage (Figure 4.11B). To differentiate peptidoglycan derived D-alanine from that released from teichoic acids, the D-alanylation of teichoic acids was also prevented, using *dltA-D*^{-ve} strains. The culture supernatants of KS11 ($\Delta dltA-D::cat$) and KS36 ($\Delta dltA-D::cat \Delta datA::erm$) strains were compared at 180 min of incubation. The $\Delta dltA-D::cat \Delta datA::erm$ strain

accumulated higher D-alanine (331.2 μM) in its culture supernatant than the *$\Delta\text{dltA-D}::\text{cat}$* strain (135.2 μM) (Figure 4.11C). Interestingly, the D-alanine quantity (231 μM) in the culture supernatant of 168CA at 180 min (Figure 4.11B) was about twice of D-alanine (135.2 μM) in the *$\Delta\text{dltA-D}::\text{cat}$* culture supernatant (Figure 4.11C). The *$\Delta\text{data}::\text{erm}$* and *$\Delta\text{dltA-D}::\text{cat } \Delta\text{data}::\text{erm}$* strains also showed almost equal amount of D-alanine, 326 μM and 331.2 μM respectively at 180 min of incubation (Figure 4.11B and C). Thus these results clearly showed that D-alanine is usually released from cell wall and re-utilised during both exponential and stationary growth phases.

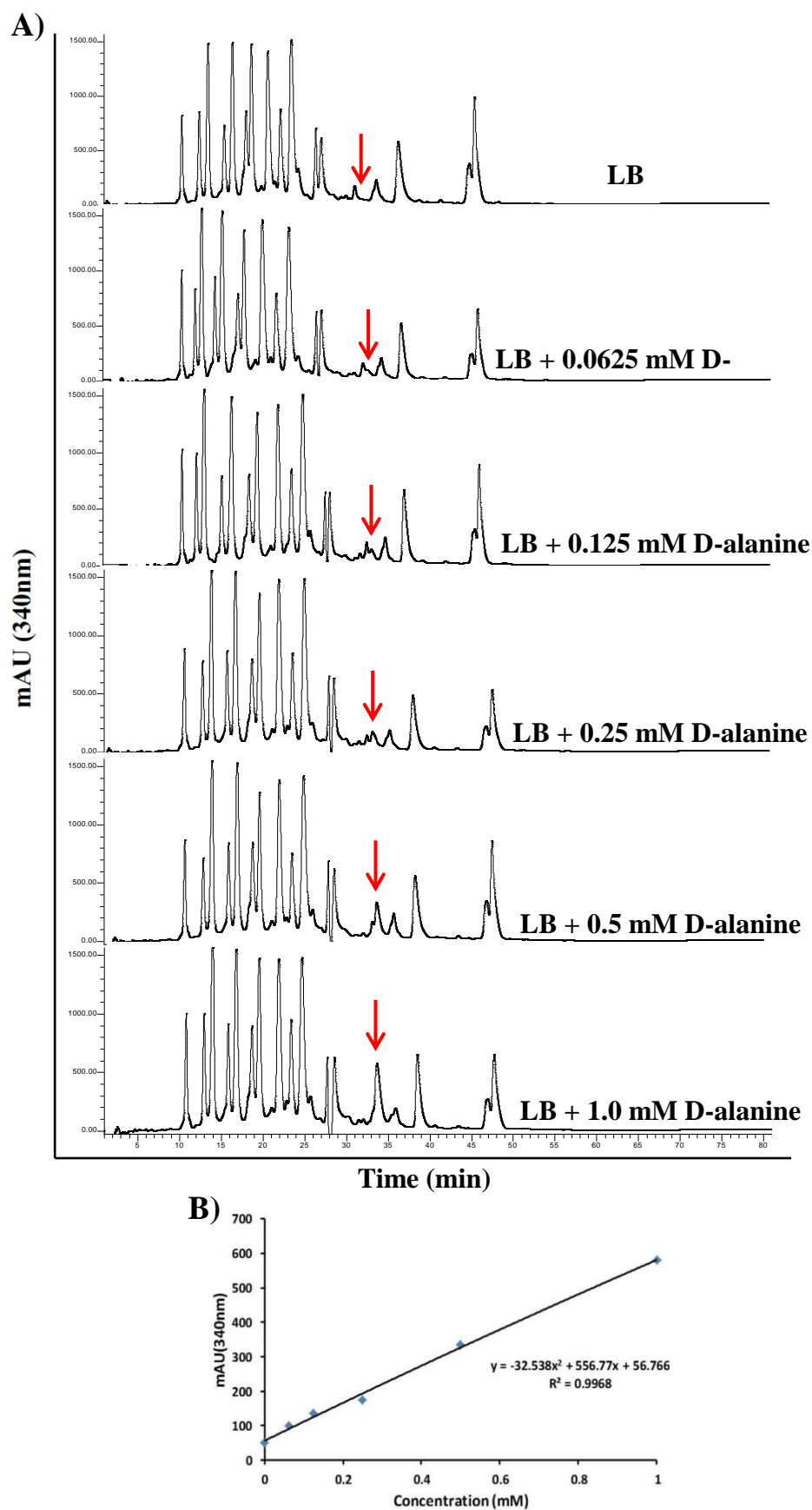


Figure 4.10 Standard curve for D-alanine quantification in LB media. A) The RP-HPLC analysis of 2000 MWCO filtered LB medium with and without D-alanine (mM). The red arrows indicate the D-alanine peaks, which were raised around 34 min. B) A standard curve was generated from the data of figure (A) for quantitative determination of D-alanine.

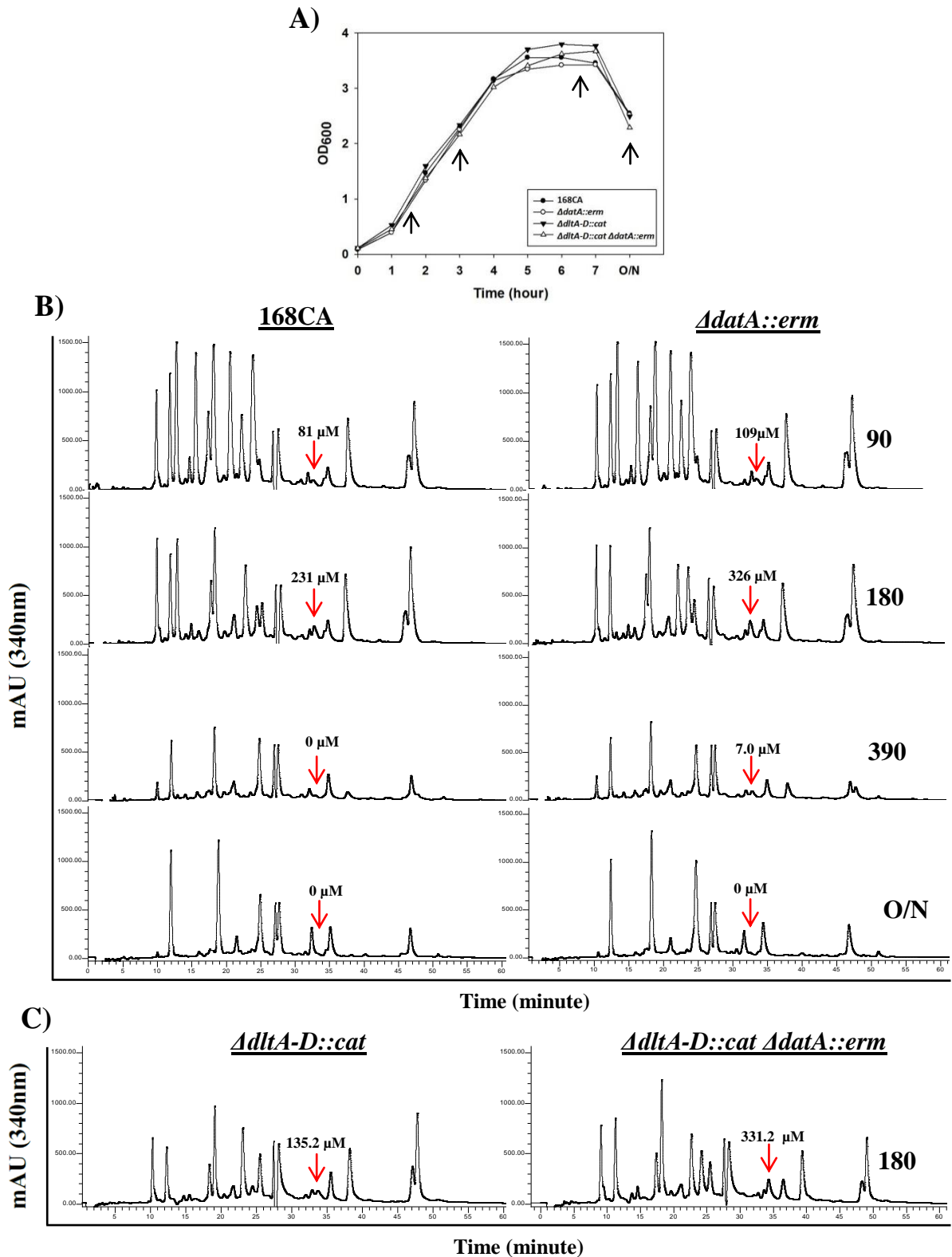


Figure 4.11 RP-HPLC analysis for D-alanine quantification in culture supernatants. A) The growth curve of 168CA, KS22 ($\Delta datA::erm$), KS11 ($\Delta dltA-D::cat$) and KS36 ($\Delta dltA-D::cat \Delta datA::erm$) strains in LB medium at 37 °C. The black arrows represent the time points, when the samples were taken for RP-HPLC analysis. B) The RP-HPLC analysis of 2000 MWCO filtered culture supernatants of 168CA and KS22 ($\Delta datA::erm$) strains at different time points (90, 180, 390 min and O/N). C) The RP-HPLC analysis of KS11 ($\Delta dltA-D::cat$) and KS36 ($\Delta dltA-D::cat \Delta datA::erm$) strains at 180 min of incubation. The red arrows indicate D-alanine peaks, which appeared at around 34 min.

4.2.4.3 Is there a second uptake system for D-alanine?

Our previous data suggested that DatA is the sole D-alanine transporter, when *B. subtilis* is grown in rich medium (see sections 3.2.4.1, 3.2.4.2 and 3.2.4.3). However a little better growth of KS30 strain ($\Delta alrA::zeo \Delta datA::erm$) on D-alanine supplemented MM (Figure 3.7) and the disappearance of D-alanine in the stationary culture of KS22 strain ($\Delta datA::erm$) (Figure 4.11B) suggested that D-alanine is still transported in *datA* strain. These observations were further investigated in MM. The 168CA and $\Delta datA::erm$ strains were firstly grown for 240 min in MM, containing 1.0 μM (0.065 $\mu\text{Ci/ml}$) of radioactive [$1\text{-}^{14}\text{C}$] D-alanine. The radioactivity in culture supernatant and the incorporation of radioactive D-alanine into the cells were measured at the onset (t_0) and the end of the experiment (t_{240}). Unlike in rich media, the 168CA and $\Delta datA::erm$ strains showed efficient uptake of D-alanine in MM, 96 % and 93 % respectively (Figure 4.12A). Again, unlike in rich media D-alanine was incorporated into $\Delta datA::erm$ cells nearly as much as of 168CA in MM (Figure 4.12B). It was also observed that the amount of incorporated radioactive D-alanine is much lower than the amount transported into the cells (Figure 4.12A and B). We also took the advantage of poor growth phenotype, caused by *alaT* mutation, to further investigate D-alanine transport in *datA* strain in MM. The AlaT is a poorly characterised protein with putative alanine transaminase activity. It is thought that AlaT catalyses the synthesis of L-alanine from pyruvate and glutamate (A). The deletion of *alaT* gene does not have detectable effect on growth in rich medium, but the lack of AlaT causes the cells to struggle to grow in MM. The hypothesis was the addition of L- and D-alanine to MM may provide better growth to *alaT* strain, but the deletion of *datA* gene in the *alaT* strain might block D-alanine transport. The KS22 ($\Delta datA::erm$), KS31 ($\Delta alaT::erm$) and KS39 ($\Delta datA::erm \Delta alaT::markerless$) strains were grown on nutrient agar and MM at 37 °C overnight. As shown in (Figure 4.12C), all the three strains grew normally on nutrient agar, whereas only $\Delta datA::erm$ showed growth on MM. When D-alanine and L-alanine were added to MM, both $\Delta alaT::erm$ and $\Delta datA::erm \Delta alaT::markerless$ strains regained ability to grow on MM. Thus the above investigations showed that *datA* strain is able to transport D-alanine in poor growth medium.

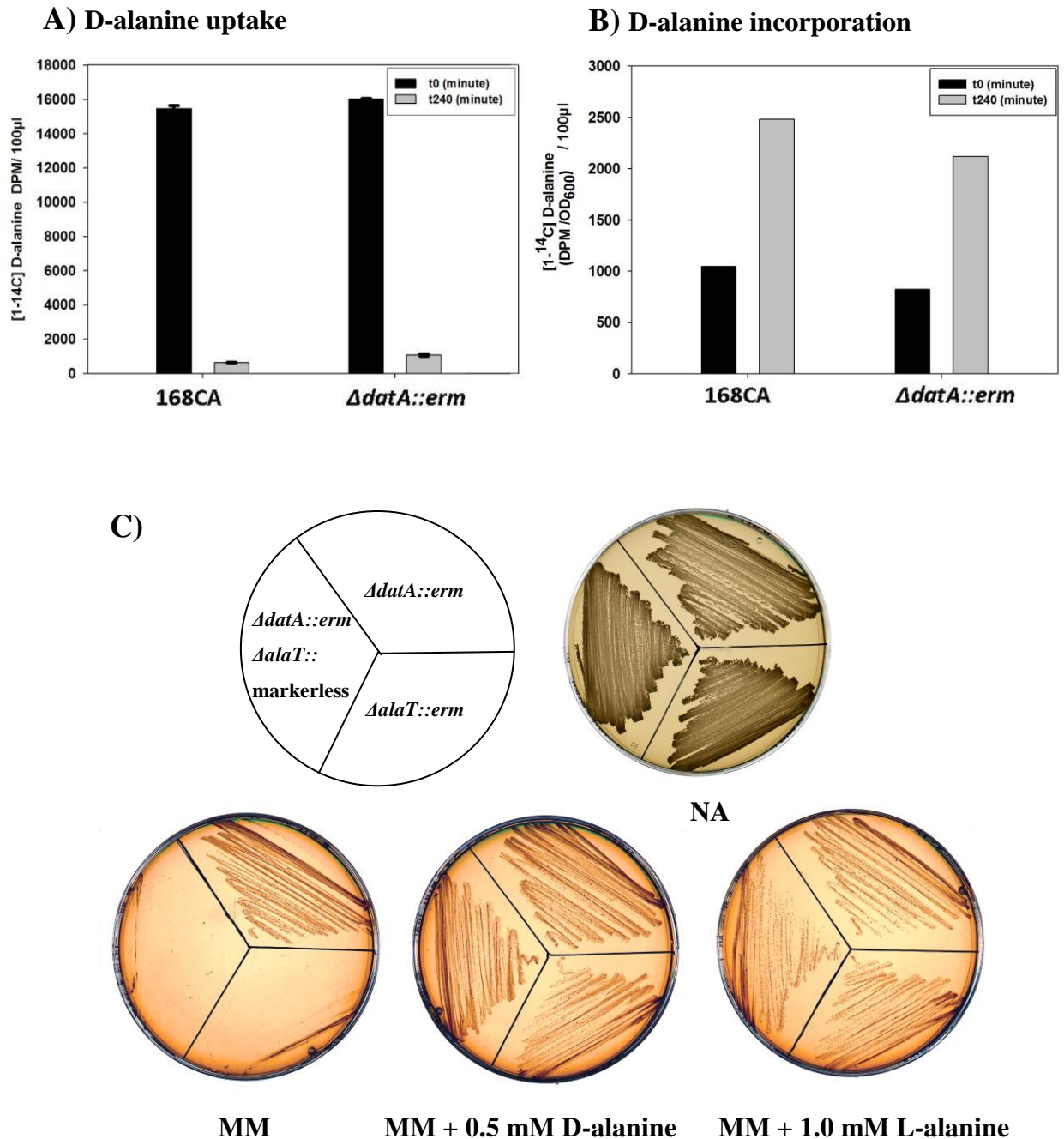


Figure 4.12 Transport of D-alanine by *datA* strain in minimal media (MM). D-alanine uptake (A) and D-alanine incorporation (B) into the 168CA and KS22 (*datA::erm*) strains. The strains were grown in MM, supplemented with (1.0 μ M) radioactive [1- 14 C] D-alanine at 37 °C. The radioactivity (DPM) in the culture supernatants and in the cells were measured at the beginning (t0) and after 240min (t240) of incubation. The radioactivity represents three experimental replicas (n=3) at each time point in one experiment. The background radioactivity is subtracted from the data. C) The growth of KS22 (*ΔdatA::erm*), KS31 (*ΔalaT::erm*) and KS39 (*ΔdatA::erm ΔalaT::* markerless) strains on nutrient agar (NA) and MM with and without D- and L-alanine at 37 °C for 24 h.

4.3 Discussion

In this chapter the identified D-alanine transporter (DatA) has been characterised and its role in D-alanine recycling has been investigated. We revised the transcription profile of *datA* gene, using real-time PCR (see section 4.2.1). The results showed that *datA* is apparently co-transcribed with its upstream genes, *asnB* and *metK*, and downstream genes, *ytpA* and *ytpB*. This result is consistent with Yoshida *et al.* (1999), who thought that *datA* is possibly co-transcribed with the *asnB* gene. However, the result contradicts a previous northern blotting analysis, where no transcriptional connection between *datA* and *asnB* genes was detected (Sierra *et al.*, 2008). Our result potentially explains why a cloned copy of *datA* gene did not work with its native RBS (see section 3.2.4.2). The reason might be related to the initiation of translation of the DatA-encoding mRNA, which may be unable to efficiently bind ribosomes as a single transcription unit (monocistronic mRNA). That is to say, the translation of upstream genes may normally promote the translation of *datA* as a part of a polycistronic mRNA. Moreover, the upstream (*asnB*) and downstream (*ytpA*) genes of *datA* did not show any direct relation to D-alanine metabolism and amino acid transport (see section 4.1).

The bioinformatics databases were searched to identify proteins that have sequence homology to DatA protein. This investigation could be useful in structural and functional studies of DatA as well as in discovery of D-alanine transporter in other bacteria. The phylogenetic analyses revealed that the DatA-like proteins are putative or characterised amino acid transporters in many bacterial species (see section 4.2.2), but DatA is highly conserved in the members of Bacillaceae family. Interestingly, a few of the proteins homologous to DatA were putative D-alanine/D-serine/glycine permeases (CycA) in a group of diverse bacterial species. The DatA protein showed a good percentage of amino acid sequence identity to CycA proteins in *E. coli* K-12 and *Mycobacterium bovis* BCG (Table 4.1), supporting the D-alanine transport role of DatA and suggesting that DatA is a member of amino acid transporter family, which is included in amino acid-polyamine-organocations superfamily. Moreover, the bioinformatics data showed that the genetic context of *datA* is absent in the other bacterial species, suggesting that the *datA* gene locus is unique to the *Bacillus spp.*

The properties of DatA protein has been investigated, using bioinformatics tools and GFP tag. DatA protein predictably contains 12 alpha helical transmembrane helices and two extracellular hydrophilic loops, which might have specificity to D-alanine (see section 4.2.3.1). The general predicted properties of DatA are quite similar to those of the amino

acid permeases (Table 4.1). Also, based on its identity to the structurally characterised Arginine:Agmatine antiporter (AdiC) of *E. coli*, DatA protein might be present in the cell membrane as a dimer (see section 4.2.3.1). The sub-cellular localisation of DatA protein seemed to confirm the above bioinformatics to some degree, because the GFP tagged DatA apparently localised to the cell membrane (see section 4.2.3.1). However, the GFP-DatA recombinant protein was not functional to be able to complement *datA* mutant, suggesting that GFP tag might affect the correct membrane localisation of DatA protein. This also caused the GFP signal was not seen obviously at the cell membrane.

We wanted to investigate the amino acid specificity of DatA *in vitro* (e.g liposomes). The study of transport activity in liposomes requires purified transport protein, but the attempts to over-produce His-tagged DatA protein in *E. coli* BL21(DE3) was not successful (see section 4.2.3.2). We then tried to investigate D-alanine transport in the membrane vesicles of *E. coli* C43(DE3), suggested to be a good strain for production of toxic membrane proteins (Miroux and Walker, 1996). However, the transport of D-alanine seemed to be totally impaired in the membrane vesicles of an *E. coli* C43(DE3) strain, which carried an inducible copy of *datA* gene on a plasmid (see section 4.2.3.2). These problems are commonly encountered during overexpression of highly hydrophobic membrane proteins in *E. coli*, probably due to either poor overexpression or toxicity that causes host cell death (Grisshammer and Tate, 1995; Miroux and Walker, 1996). Alternatively, the transport of D-alanine by DatA was studied in *Xenopus laevis* oocyte, which is a popular eukaryotic expression model for structural and functional studies of transporters (Sigel, 2010). Again, we did not observe the D-alanine transport activity of DatA, possibly translated in *Xenopus laevis* oocytes (see section 4.2.3.2). It is suggested that some prokaryotic proteins are proven difficult to be translated in oocytes, and the GC content of the transporter gene should be about 50 %. The *Xenopus laevis* oocytes have mostly worked very well for the transporters, whose encoding genes have 49-56 % GC content (E-mail contact with prof. David Thwaites). However, the GC content of DatA encoding gene is 45 %. As the bioinformatics showed identity between DatA and AdiC, a homodimeric Arginine:Agmatine antiporter in *E. coli* (see section 4.2.3.1), one more possibility might be difficulty in the assembly of DatA transporter as homodimers in the cell membrane of the above heterogeneous hosts. Thus these limitations did not allow us to investigate the specificity of DatA in prokaryotic and eukaryotic expression systems.

An amino acid competition assay was eventually done as an *in vivo* investigation to indirectly examine the specificity of D-alanine transporter (see section 4.2.3.3). The idea of this assay was addition of an amino acid and D-alanine simultaneously to a culture of

D-alanine auxotroph (*alrA*) strain. If the growth of *alrA* is inhibited by the supplemented amino acid, it presumably means that the transport of D-alanine is prevented by the supplemented amino acid, in other words D-alanine and the supplemented amino acid have the same uptake system. The interference of some LMW amino acids such as L-alanine, glycine and proline into D-alanine transport was investigated in LB medium (see section 4.2.3.3). We observed that only L-alanine inhibits the growth of *alrA* strain, suggesting that both L- and D-alanine have a common transporter in *B. subtilis*. Moreover, the studies already suggested a common uptake system for D-alanine and D-cycloserine in *E. coli* K-12 (CycA) (Wargel *et al.*, 1970; Wargel *et al.*, 1971; Cosloy, 1973; Robbins and Oxender, 1973) and *M. tuberculosis* (David, 1971). These suggestions made us to investigate the specificity of DatA to D-cycloserine (see section 4.2.3.4). The hypothesis was if D-cycloserine is transported by DatA, the deletion of *datA* gene must provide resistance against this compound. In contrast to *E. coli* and *M. tuberculosis*, our data showed that D-cycloserine inhibits the growth of *datA* strain, suggesting that D-cycloserine is not transported by D-alanine transporter (DatA) in *B. subtilis*. Again, the addition of D-alanine to the culture medium did not reduce the D-cycloserine sensitivity of wild type and *datA* strain. This again suggests that D-alanine and D-cycloserine have separate uptake system in *B. subtilis*.

In the previous chapter, our data hypothesised that the released D-alanine molecules from cell wall might be recycled. This hypothesis was further investigated by a cross-feeding assay (see section 4.2.4.1), which is a qualitative method in which *alrA* strain was streaked next to wild type and *datA* strain on a solid medium. Following incubation the growth of *alrA* strain was supported by *datA* strain. This means that the released D-alanine molecules from cell wall (peptidoglycan and teichoic acids) are usually recycled, whereas in the case of *datA* mutant the proposed D-alanine transporter (DatA) is absent and the released D-alanine accumulates in the surrounding environment. Besides, the D-alanylation of teichoic acids was prevented through deletion of *dltA-D* to investigate the fate of the D-alanine residues, which are released from peptidoglycan by the carboxypeptidases (DacA and LdcB). It was observed that *dltA-D* did not support the growth of *alrA* strain, but *datA dltA-D* strain did. These observations suggested that DacA and LdcB trim the uncross-linked D-alanine residues to be recycled via DatA in *B. subtilis* (Figure 4.9 and 6.1). In addition, RP-HPLC was used as a quantitative method to investigate D-alanine recycling in *B. subtilis* (see section 4.2.4.2). The results revealed that the cell wall derived D-alanine molecules are released into the culture supernatant of both wild type and *datA* strain during exponential growth, but the

quantity of D-alanine was detectably higher in the culture supernatant of *datA* strain. Interestingly, the amount of D-alanine in the culture media of both wild type and *datA* strain was found to disappear on entry into stationary phase, which is consistent with (Lam *et al.*, 2009). When the *dltAD*^{-ve} strains were tested during exponential growth, the *datA dltA-D* double mutant strain accumulated more D-alanine than *dltA-D* strain in its culture supernatant. Again, the results of HPLC analysis suggested that *B. subtilis* recycles the cell wall derived D-alanine molecules via DatA (Figure 4.11 and 6.1). However, the disappearance of D-alanine in the stationary cultures of *datA* strain could suggest that D-alanine is still transported. This is consistent with our previous data showed a little better growth of *datA* strain in MM, supplemented with D-alanine (see section 3.2.4.1).

We further investigated the transport of D-alanine in *datA* strain by growing the wild type and *datA* strains in MM, supplemented with radioactive (¹⁴C) D-alanine (see section 4.2.4.3). It was found that both wild type and *datA* strains almost similarly transported and incorporated D-alanine. Moreover, we exploited the poor growth phenotypic effect of *alaT* mutation, which potentially reduces the ability of *B. subtilis* to make L-alanine *in vivo*. The *alaT* strain grows normally in rich media (usually contains L-alanine), but the strain grows very slowly on MM. Therefore, we deleted *datA* gene in *alaT* strain to test D- and L-alanine transport in the absence of DatA protein (see section 4.2.4.3). It was found that *datA alaT* mutant was able to transport D- and L-alanine in MM. The above experimental observations together suggested that the transport of D-alanine in *datA* strain can only be detected in MM and in exhausted cultures of rich media during stationary phase. Interestingly, it was observed that *datA alaT* strain happily grows in rich medium, suggesting that L-alanine is efficiently transported in the absence of DatA protein. This also suggests the transport of L- and D-alanine through different uptake systems in *B. subtilis* (more discussion in chapter 6).

Chapter 5. Peptidoglycan assembly in *B. subtilis*

5.1 Introduction

Peptidoglycan is the stress-bearing structure in the cell wall of Gram-positive bacteria (e.g. *B. subtilis*). The peptidoglycan metabolic processes are synthesis, modification, turnover and recycling. These processes have generally been well investigated in Gram-negative model bacterium, *E. coli*. However, apart from peptidoglycan synthesis other metabolic processes are less understood in *B. subtilis*. Cell wall growth was initially studied in *B. subtilis* at population level, using radioactive labelling isotopes (^3H and ^{14}C GlcNAc and D-glutamate). The radioactive studies have consistently showed the pattern of peptidoglycan synthesis and turnover in models, suggesting that the new peptidoglycan layers are incorporated into the inner most layers by PBPs, meanwhile the stretched old peptidoglycan layers are degraded at the cell surface by hydrolases (Pooley, 1976a; Pooley, 1976b; Koch and Doyle, 1985a). Few attempts were previously made to visualise the growth of *B. subtilis* cell wall, using autoradiography and electron and fluorescent microscopies (Mobley *et al.*, 1984; Merad *et al.*, 1989). These studies demonstrated that the insertion of new cell wall material and the degradation of old cell wall occur uniformly along the cell cylinder, but the cell poles are metabolically less active. Moreover, the recent developments in peptidoglycan labelling fluorescent probes have offered a great progress in bacterial cell wall studies. The fluorescent microscopic studies increasingly suggested that the synthesis of new peptidoglycan occurs at cell division site and in a helical pattern around the cylindrical part of the cell (Daniel and Errington, 2003; Tiyanont *et al.*, 2006; Kuru *et al.*, 2012). This helical polymerisation is guided by actin-like proteins (MreB, Mbl and MreBH) (Kawai *et al.*, 2009a; Kawai *et al.*, 2009b) and facilitated by DL-endopeptidases (CwlO and LytE), which are hypothesised to play role in cell elongation through providing enough space for insertion of new peptidoglycan layers at the inner part of cell wall (Hashimoto *et al.*, 2012; Dominguez-Cuevas *et al.*, 2013). A sophisticated coordination between peptidoglycan synthesis and turnover is crucial for cell wall strength, cell shape maintenance and cell elongation (Popham, 2013). The coordination of peptidoglycan synthesis and turnover has already been proposed in *E. coli* (three-for-one growth model) (Holtje, 1998; Vollmer and Holtje, 2001). However, the mechanistic details of peptidoglycan assembly during growth have not been elucidated in Gram-positive bacteria.

B. subtilis usually modifies its peptidoglycan by swapping the 5th D-alanine residues on some of the stem peptides with other D-amino acids. It is suggested that penicillin-sensitive DD-transpeptidase(s) catalyses “D-alanine swapping” (Cava *et al.*, 2011; Kuru *et al.*, 2012). However, the physiological purpose of D-alanine swapping is unclear and enzyme(s) catalyses this swapping reaction has not been identified in *B. subtilis*. The identification of D-alanine swapping enzyme could be important to further understand how this bacterium controls the percentage of peptidoglycan cross-links. In addition, the involvement of carboxypeptidases in what is so-called cell wall maturation has already been proposed in *B. subtilis* (Atrih *et al.*, 1999), but understanding the dynamics of peptidoglycan carboxypeptidation might improve our understanding about cell wall assembly in Gram-positive bacteria.

In this chapter, radioactive D-alanine and fluorescent D-amino acids were used to understand the mechanistic details of cell wall assembly (coordination between cell wall synthesis and turnover) in *B. subtilis*. Besides, the identification of D-alanine swapping catalytic enzyme(s) and the fate of the released cell wall material were investigated in exponentially growing *B. subtilis*.

5.2 Results

5.2.1 Cell wall turnover in the absence of carboxypeptidases

The radioactive D-alanine and fluorescently labelled D-amino acid (FDAA) were used to investigate cell wall turnover and the effect of lack of carboxypeptidases on this catabolic process. The [1-¹⁴C] D-alanine labelled cells of RD180 ($\Delta alrA::zeo$), KS16 ($\Delta alrA::zeo \Delta dacA::spc$) and KS19 ($\Delta alrA::zeo \Delta ldcB::erm$) strains were taken at 120 min of the radioactive labelling experiment (described in section 3.2.3). The radioactive cells were washed and suspended in fresh LB medium (OD₆₀₀ 0.1), which contained 450 μ M of non-radioactive D-alanine. To measure radioactivity in the cells, culture samples were taken every 20 min for 2.0 h. The cells were filtered under vacuum and washed with PBS (see sections 2.10.2 for method details). It was observed that the level of [1-¹⁴C] D-alanine incorporated into the cell population gradually reduced and reached minimum level after 80 min of incubation (Figure 5.1). The third generation cells were no longer radioactive (generation time of *alrA* strain was 40 min in LB medium, containing 450 μ M D-alanine at 37 °C in shaking water bath). We also observed that the D-alanine composition of cell wall varied according to the genotypes. The $\Delta alrA::zeo$ strain showed lowest level of radioactivity, comparing to the other two strains. However, the $\Delta alrA::zeo \Delta dacA::spc$ strain was more radioactive than both $\Delta alrA::zeo$ and $\Delta alrA::zeo \Delta ldcB::erm$ strains. Interestingly, the differences in cell wall D-alanine content did not altered the rate of cell wall turnover in the strains. In addition, peptidoglycan turnover was investigated in *dltA-D*^{-ve} strains, which lack D-alanine in teichoic acids. The [1-¹⁴C] D-alanine labelled cells of KS12 ($\Delta alrA::zeo \Delta dltA-D::cat$), KS20 ($\Delta alrA::zeo \Delta ldcB::erm \Delta dltA-D::cat$) and KS17 ($\Delta alrA::zeo \Delta dacA::spc \Delta dltA-D::cat$) were collected at 120 min of the radioactive labelling experiment (described in section 3.2.3). The strains were grown in LB medium, supplemented with 450 μ M of non-radioactive D-alanine. The the cell samples were taken, filtered under vacuum and washed with PBS. The radioactivity was measured in the cells (see sections 2.10.2 for method details). Although these strains requires D-alanine only for peptidoglycan synthesis, the rates of peptidoglycan turnover in the $\Delta alrA::zeo \Delta dltA-D::cat$, $\Delta alrA::zeo \Delta ldcB::erm \Delta dltA-D::cat$ and $\Delta alrA::zeo \Delta dacA::spc \Delta dltA-D::cat$ strains were generally similar to those explained previously for $\Delta alrA::zeo$, $\Delta alrA::zeo \Delta ldcB::erm$ and $\Delta alrA::zeo \Delta dacA::spc$ strains (Figure 5.1).

Peptidoglycan turnover was also visualised and investigated by taking the advantage of extracytoplasmic incorporation of fluorescent D-amino acids (FDAA) into the

peptidoglycan. The *dacA* strain was used in this investigation, because its peptidoglycan contains a significant amount of penta-stem peptides and their 5th D-alanine residues are sufficiently swapped with Boc-D-2,3-diaminopropionic acid (NADA), a type of FDAA). The $\Delta dacA::spc$ strain was grown in PTM, supplemented with 50 μ M NADA. Cell samples were taken every 20 min and fixed in 3.0 % paraformaldehyde before microscopy (see section 2.11.2 for method details). It was observed that the fluorescent signal firstly disappeared at the cell division site and gradually decreased at the lateral cell wall (Figure 5.2A). The cylindrical part of the cells showed minimum fluorescence after 100 min of growth (Figure 5.2), which is consistent with the above radioactive result (the generation time of *dacA* strain was 35 min in PTM). However, the cell poles kept the fluorescence throughout the growth. Interestingly, the images at 40 and 60 min showed that the glycan strands apparently arranged parallel to the short axis of the cell (Figure 5.2A). To have better visualisation of glycan strands arrangement in cell wall, the total internal reflection fluorescence (TIRF) microscope was used to examine the cells at 40 min of NADA depletion. The TIRF image showed stripy cell wall pattern (Figure 5.2B). Moreover, the radioactive and fluorescent results clearly showed that the degraded old cell wall is released to the culture medium during exponential growth phase.

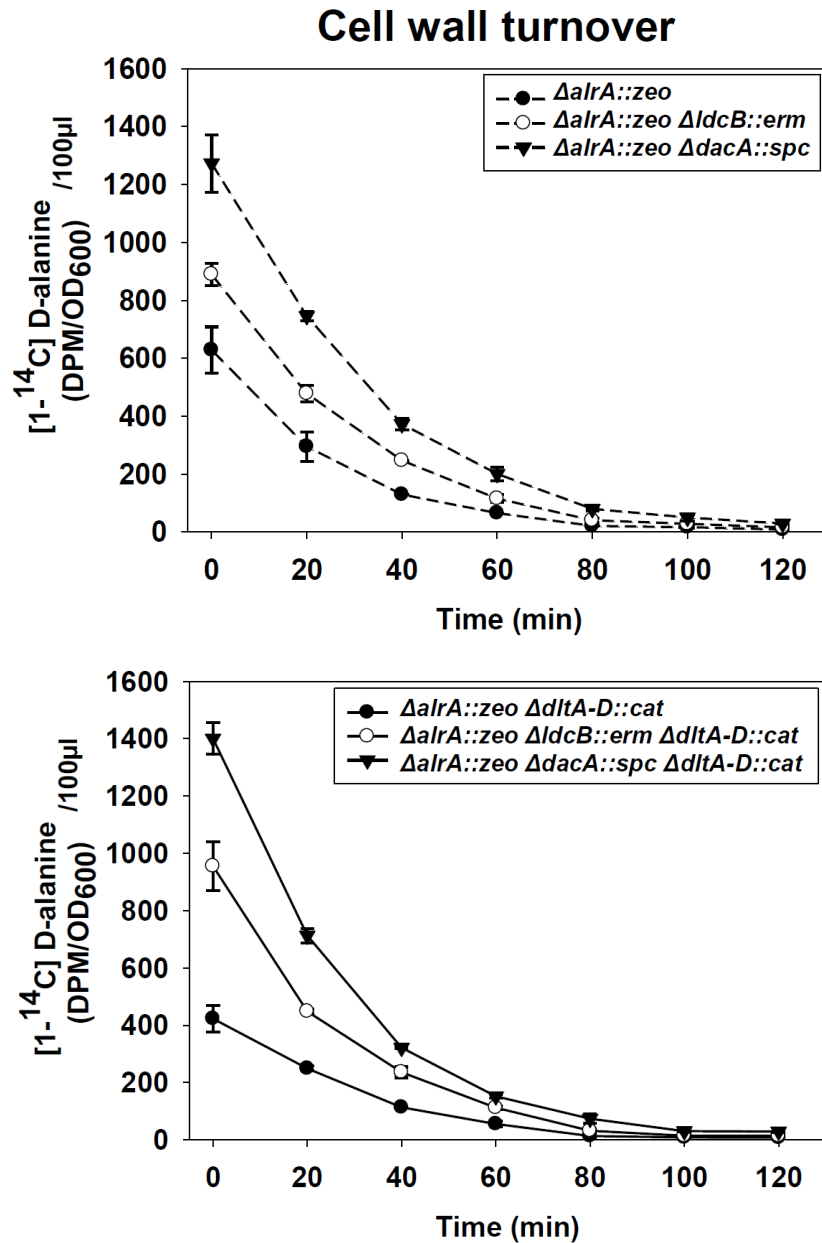
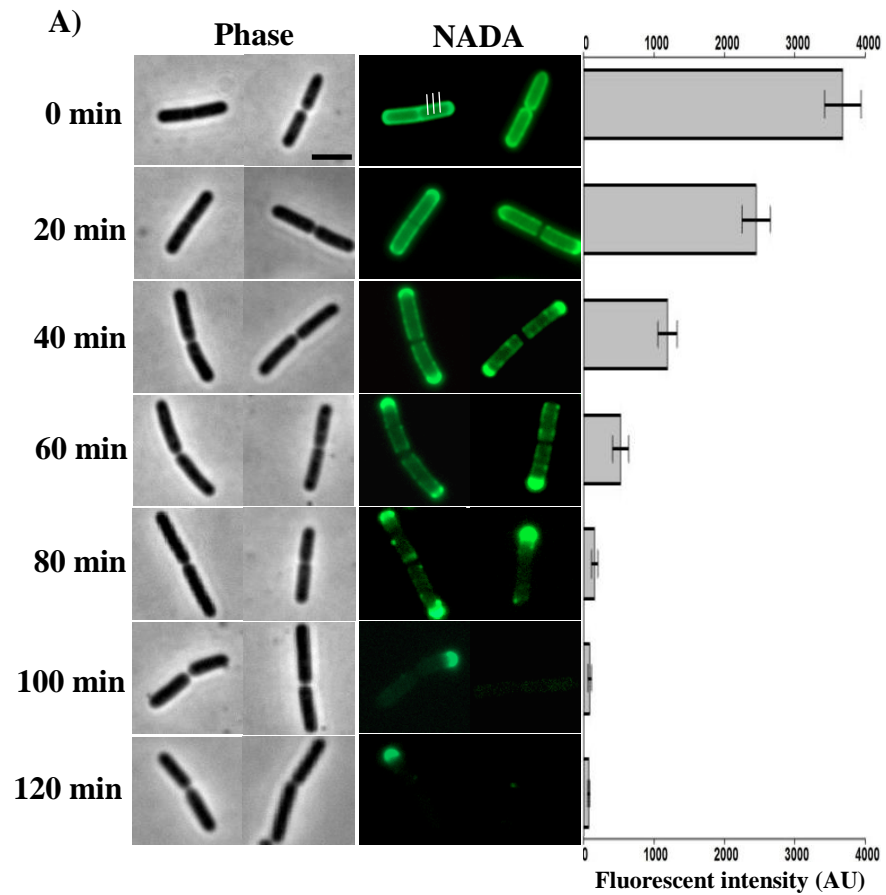


Figure 5.1 Cell wall turnover in exponentially growing *B. subtilis*. The [1-¹⁴C] D-alanine labelled RD180 ($\Delta alrA::zeo$), KS19 ($\Delta alrA::zeo \Delta ldcB::erm$), KS16 ($\Delta alrA::zeo \Delta dacA::spc$), KS12 ($\Delta alrA::zeo \Delta dltA-D::cat$), KS20 ($\Delta alrA::zeo \Delta ldcB::erm \Delta dltA-D::cat$) and KS17 ($\Delta alrA::zeo \Delta dacA::spc \Delta dltA-D::cat$) strains were grown at 37 °C in LB medium plus 450 μ M D-alanine for 2.0 h. Culture samples were taken for measuring radioactivity in the cells (see sections 2.10.2 for method details). The error bars indicate the standard deviation of mean of radioactivity in two independent experiments. The background radiation was subtracted from the values.



B)

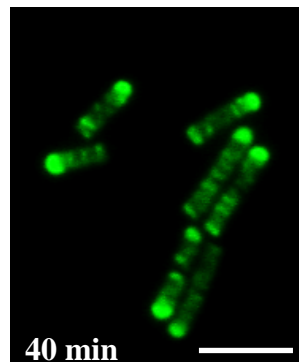


Figure 5.2 Peptidoglycan turnover in *B. subtilis*. A) The KS15 ($\Delta dacA::spc$) strain was grown in PTM, contained 50 μM of NADA. After 2.0 h of incubation at 37 $^{\circ}\text{C}$, the labelled cells were washed with fresh PTM and suspended in fresh medium with an initial OD_{600} 0.1. A) The microscopic images of fixed cells in 3.0 % formaldehyde at different time points, the scale bar is 3.0 μm . The amount of NADA released (peptidoglycan turnover) from the lateral cell wall also measured by linescan tool of Metamorph software (see section 2.11.3 for details). The three white lines crossed the wall of KS15 strain ($\Delta dacA::spc$) indicate the site of fluorescent measurement. The error bar is the standard deviation of mean of Gray level average in 50 cells of one experiment. The background fluorescent was subtracted from the values. B) The TIRF microscopic image of KS15 ($\Delta dacA::spc$) cells at 40 min of figure (A). The scale bar is 5 μm .

5.2.2 Dynamics of peptidoglycan carboxypeptidation in *B. subtilis*.

Examining the localisation of carboxypeptidases probably help us to explain how peptidoglycan is undergone carboxypeptidation. It was previously determined that DacA-GFP was localised at cell division site (Scheffers *et al.*, 2004). However, we observed that only about one fourth of DacA is fused to GFP in 2085 strain (*dacA::pSG1493 (cat P_{xyl}-gfp-dacA¹⁻⁴²³)*), using DacA specific antibody in a Western blot analysis of total cell lysate (Figure 5.3A). This suggested that GFP tagging does not show the complete localization of DacA protein in the cell. Therefore, we used immunofluorescence assay to examine the localisation of LdcB and DacA in 168CA, KS18 (*AldcB::erm*) and KS15 (*ΔdacA::spc*) strains (see section 2.6.20 for method details). The immunofluorescence of 168CA strain showed that LdcB protein is greatly localised at cell division site and extended decreasingly towards the poles probably in a helical pattern around the cylindrical part of the cell (Figure 5.4A). However, the *ΔdacA::spc* strain showed irregular localisation of LdcB proteins (Figure 5.4C). This is probably due to the unexposed substrates for LdcB in *ΔdacA::spc* strain. The DacA protein was also localised at cell division site and lateral cell wall in 168CA (Figure 5.4A) and *AldcB::erm* strain (Figure 5.4B). However, *ΔdacA::spc* strain unexpectedly showed fluorescent signal along its lateral cell wall (Figure 5.4C). A Western blot analysis of 168CA and *ΔdacA::spc* cellular lysates, using anti-DacA IgG, also showed non-specific multiple bands (data not shown). The binding of anti-DacA IgG to some other non-specific proteins, obliged us to re-test the localisation of GFP tagged DacA, using 2085 strain (*dacA::pSG1493 (cat P_{xyl}-gfp-dacA¹⁻⁴²³)*). This strain was grown to mid exponential growth in LB medium, containing 0.5 % xylose. It was observed that DacA-GFP is clearly localised at the cell division site and thinly distributed along the lateral cell wall (Figure 5.3B).

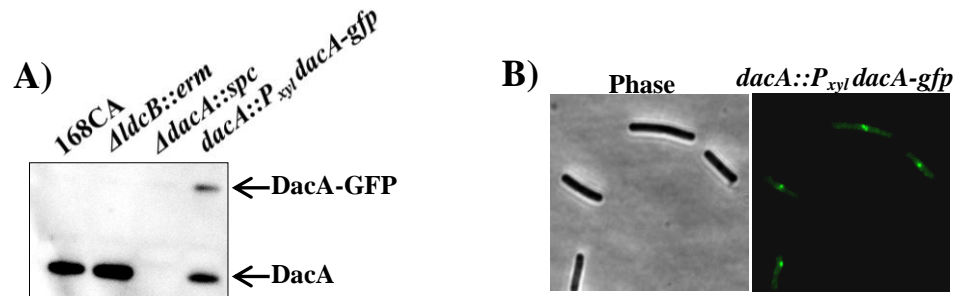


Figure 5.3 Localisation of DacA protein. A) Western blot of DacA protein in different strains, using rabbit anti-DacA IgG as primary antibody and anti-rabbit IgG-peroxidase as secondary antibody. B) The fluorescence microscopic image of 2085 strain (*dacA::pSG1493 (cat P_{xyl}-gfp-dacA¹⁻⁴²³)*), which has GFP tagged DacA protein. The expression of DacA-GFP was induced with 0.5 % Xylose in LB medium.

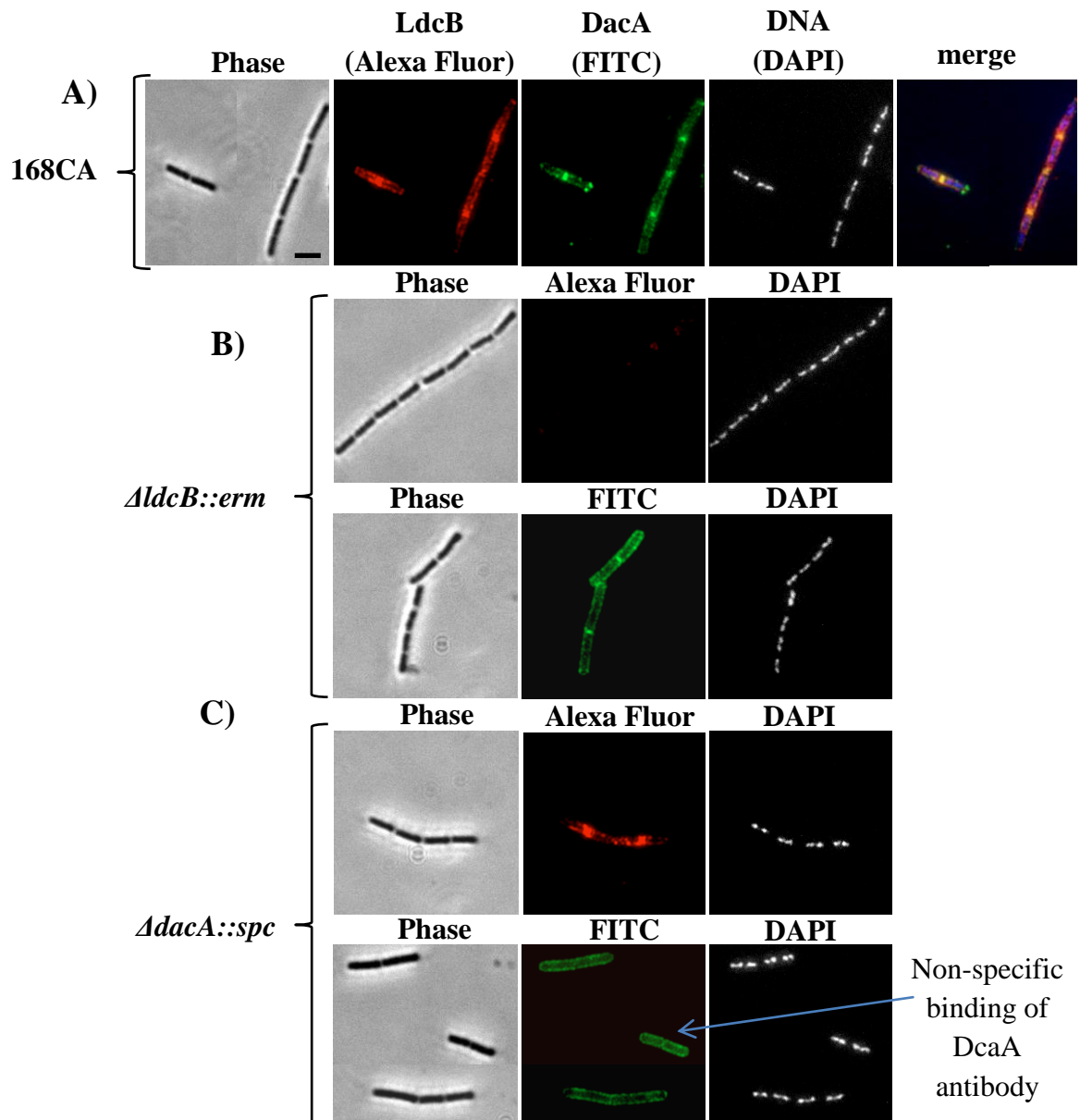


Figure 5.4 Immunofluorescence microscopy of LdcB and DacA localisations. Immunofluorescence microscopic images of LdcB and DacA localisation in 168CA (A), KS18 (*AldcB::erm*) (B) and KS15 (*AdacA::spc*) (C) strains. The Alexa Fluor (red fluorescence) represents LdcB protein and FITC (green fluorescence) represents DacA protein. The genomic DNA was stained with DAPI. The scale bar is 3 μ m.

5.2.3 Role of penicillin binding proteins (PBPs) in “D-alanine swapping”

It is known that some of the 5th D-alanine residues are exchanged with non-specific D-amino acids in the peptidoglycan of *B. subtilis*. However, only the 4th D-alanine residues are subjected to swapping in *E. coli* (Cava *et al.*, 2011; Kuru *et al.*, 2012). As the 4th D-alanine residues are usually trimmed by LdcB in *B. subtilis*, we wondered whether the exposed 4th D-alanine residues are swapped in *ldcB* mutant strain. The 168CA, KS18 ($\Delta ldcB::erm$) and KS15 ($\Delta dacA::spc$) strains were grown at 37 °C in PTM, supplemented with 50 μ M NADA. Samples were taken at different time points, and the cells were washed and fixed in 3.0 % paraformaldehyde (see section 2.11.1 for method details). The image of the fixed cells was taken by fluorescent microscope. The 168CA strain showed the lowest fluorescent intensity in its lateral cell wall compared to $\Delta ldcB::erm$ $\Delta dacA::spc$ strains. The lateral cell wall of $\Delta ldcB::erm$ strain was a little bit more fluorescent than 168CA but significantly less fluorescent than $\Delta dacA::spc$ strain (Figure 5.5B and B). It was also observed that the fluorescent intensity in the lateral cell wall of the strains was increased with time. This means that the old peptidoglycan layers (non-fluorescent) were successively replaced by the new layers (fluorescent layers) (Figure 5.5).

It has been suggested that penicillin sensitive DD-transpeptidases play role in D-alanine exchange in *B. subtilis* (Cava *et al.*, 2011; Kuru *et al.*, 2012). To identify what PBP(s) catalyses the swapping reaction in peptidoglycan, we firstly ensured the inhibitory effect of penicillin G (penG) on D-alanine swapping. Also, the effect of supplemented D-alanine on the rate of NADA swapping was examined. The 168CA and KS15 ($\Delta dacA::spc$) strain were grown in PTM with and without 100 μ g/ml penG for 2.0 min, and then 50 μ M of fluorescent D-amino acid (NADA) was added. In addition, $\Delta dacA::spc$ strain was grown in the presence of 500 μ M D-alanine and 50 μ M NADA (ratio 10:1) at 37 °C. Cell samples were taken at different time points, washed with PBS and fixed with 3.0 % paraformaldehyde before microscopy (see section 2.11.1 for method details). We observed that penG inhibited the incorporation of NADA into peptidoglycan, but the presence of D-alanine in the culture did not affect the rate of NADA incorporation (Figure 5.6).

After ensuring that the incorporation of NADA is catalysed by penicillin-sensitive enzyme(s), the single mutant strains of all known PBPs, KS15 ($\Delta dacA::spc$), BKE23190 ($\Delta dacB::erm$), BKE18350 ($\Delta dacC::erm$), BKE234380 ($\Delta dacF::erm$), BKE25000 ($\Delta pbpA::erm$), 4001 ($pbpB^{(S309A)}$), BKE04140 ($\Delta pbpC::erm$), BKE31490

($\Delta pbpD::erm$), BKE34440 ($\Delta pbpE::erm$), BKE10110 ($\Delta pbpF::erm$), BKE37510 ($\Delta pbpG::erm$), BKE13980 ($\Delta pbpH::erm$), BKE27310 ($\Delta pbpI::erm$), BKE16950 ($\Delta pbpX::erm$) and BKE22320 ($\Delta ponA::erm$), ($\Delta spoVD::erm$) were grown for 15 min in PTM, supplemented with 50 μ M of NADA at 37 °C. The culture of *ponA* strain contained 25 mM of Mg^{2+} as well. The cells were fixed with 3.0 % paraformaldehyde before microscopic examination (see section 2.11.1 for method details). The microscopic images showed that all the single *pbp* mutants obviously incorporated NADA into the cell division site (data not shown). To obviously see differences in the rate of D-alanine swapping and to generate quantitative data, the vegetative *pbp* genes were knocked out in $\Delta dacA::spc$ strain. The double mutant strains were labelled with NADA as above, and the labelled cells were processed for microscopic study (see section 2.11.1 for method details). As shown in (Figure 5.7), the double *pbp* mutants differently labelled their peptidoglycan with NADA. It was observed that the lack of PBP2a (*pbpA*), PBP3 (*pbpC*), PBP4 (*pbpD*), PBP4* (*pbpE*) and PBP1 (*ponA*) decreased the rate of NADA incorporation. In contrast, ($\Delta dacA::spc \Delta pbpH::erm$) strain was solely hyper-labelled. Even AG364 strain ($\Delta pbpD \Delta pbpF \Delta ponA \Delta pbpG::Kana \Delta dacA::zeo$), which lacked all the known class A PBPs, was still able to modify peptidoglycan with NADA. Thus D-alanine swapping was not totally inhibited by the absence of a particular PBP.

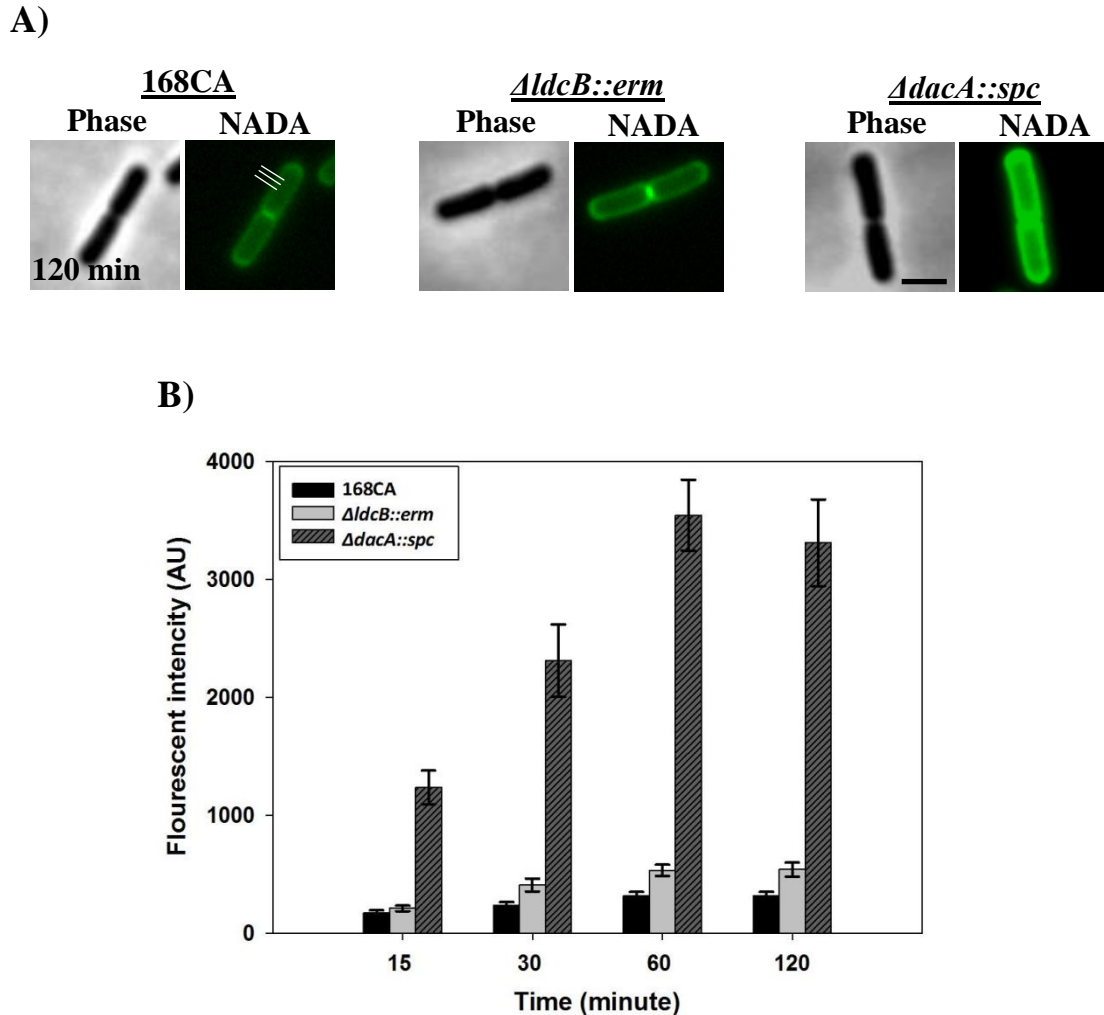


Figure 5.5 Peptidoglycan modification in carboxypeptidase mutant strains of *B. subtilis*. The 168CA, KS18 ($\Delta ldcB::erm$) and KS15 ($\Delta dacA::spc$) strains were grown at 37 °C in PTM, containing 50 μ M of NADA. The cells were washed with PBS and fixed in 3.0 % paraformaldehyde at different time points. A) The microscopic images of the cells after 120 min of NADA labelling. B) The amount of NADA incorporated into the lateral cell wall (three white lines crossed the 168CA cell in figure (A)) was measured by linescan tool of Metamorph software (see section 2.11.3 for details). The three lines crossed the cell shaft of 168CA indicate the site of fluorescent measurement. The error bar is the standard deviation of mean of Gray level average in 50 cells in two independent experiments. The background fluorescent was subtracted from the values. The scale bar is 2.0 μ m.

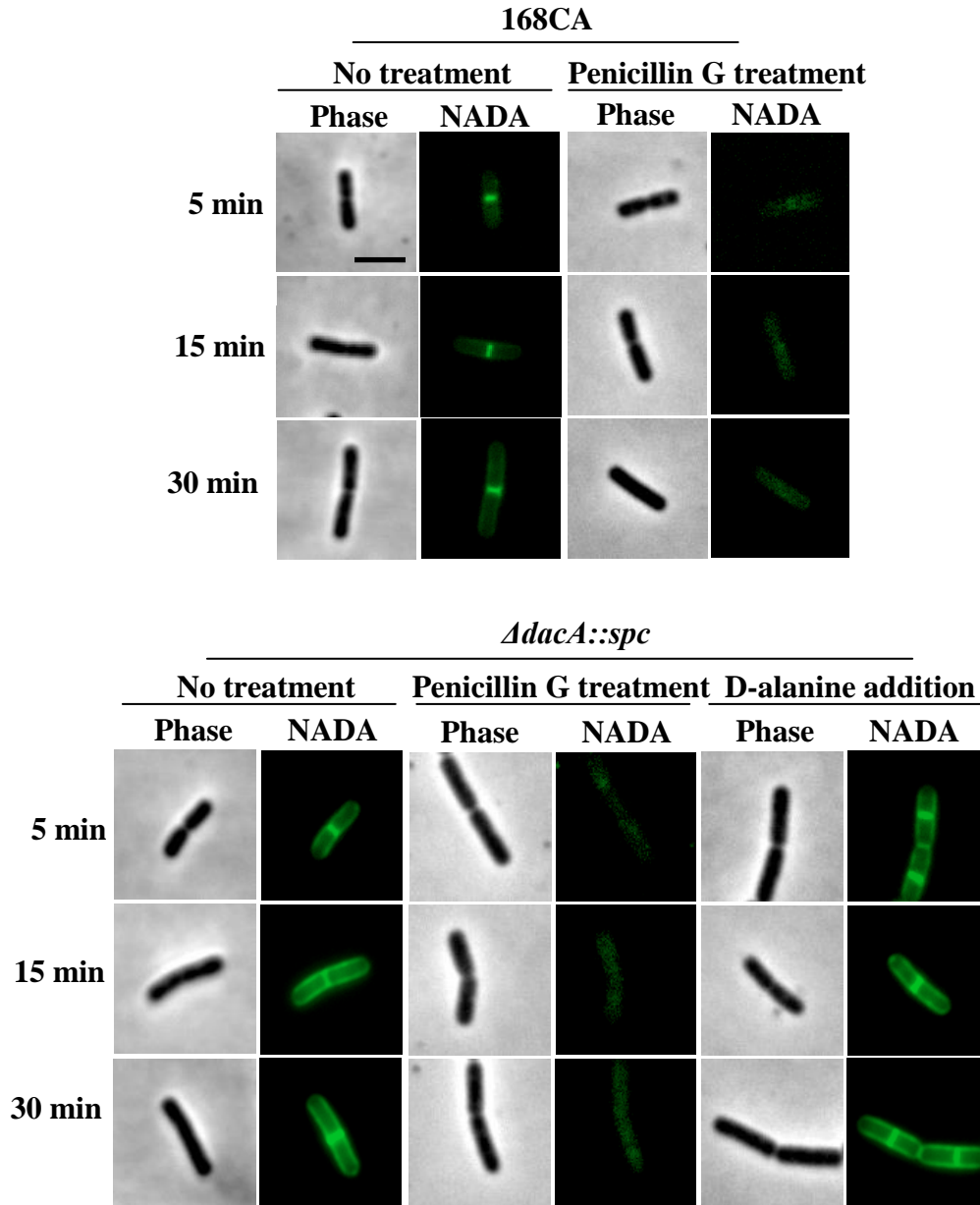


Figure 5.6 The effect of Penicillin G and D-alanine on peptidoglycan modification. The 168CA and KS15 (*ΔdacA::spc*) strains were treated with penG (100 μg/ml) for 2.0 min in PTM, after that 50 μM of NADA was added. KS15 (*ΔdacA::spc*) was also grown in the presence of 500 μM of D-alanine and 50 μM of NADA. The strains were grown at 37 °C and samples were taken at different time points. The cells were washed with PBS and fixed in 3.0 % paraformaldehyde (see section 2.11.1 for method details). The scale bar is 3.0 μm.

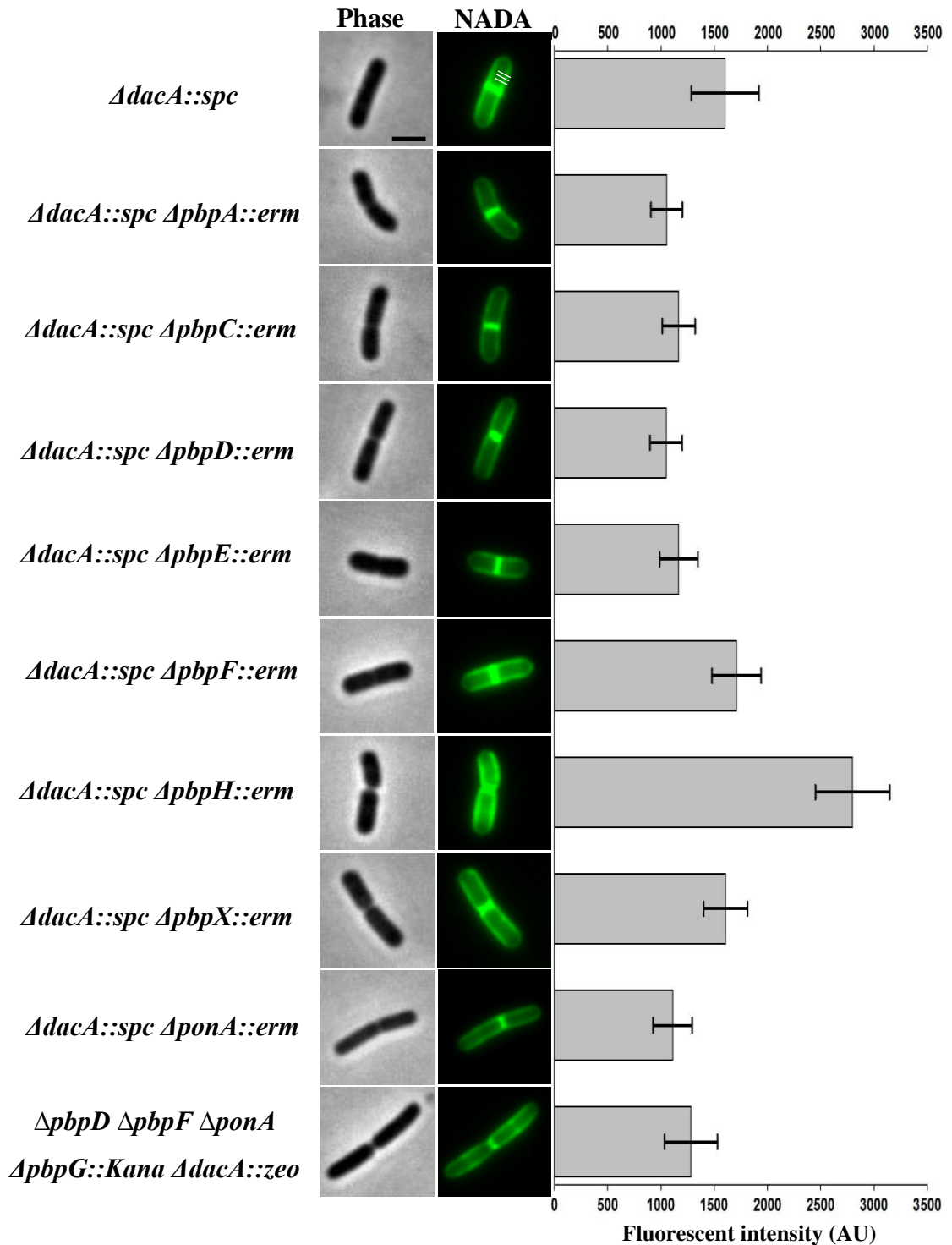


Figure 5.7 NADA labelling of PBPs double mutant strains. The KS15 (*ΔdacA::spc*), KS65 (*ΔdacA::spc ΔpbpA::erm*), KS56 (*ΔdacA::spc ΔpbpC::erm*), KS57 (*ΔdacA::spc ΔpbpD::erm*), KS49 (*ΔdacA::spc ΔpbpE::erm*), KS61 (*ΔdacA::spc ΔpbpF::erm*), KS59 (*ΔdacA::spc ΔpbpH::erm*), KS67 (*ΔdacA::spc ΔpbpX::erm*), KS66 (*ΔdacA::spc ΔponA::erm*) and AG364 (*ΔpbpD ΔpbpF ΔponA ΔpbpG::Kana ΔdacA::zeo*) strains were labelled with 50 μ M of NADA for 15 min. The cells were fixed before microscopic examination. The amount of fluorescent in the lateral cell wall was also measured by linescan tool of Metamorph software (see section 2.11.3 for fluorescent quantitative analysis). The three lines crossed the cell shaft of KS15 strain (*ΔdacA::spc*) indicate the site of fluorescent measurement. The error bar is the standard deviation of mean of Gray level average in 50 cells per strain. The background fluorescent was subtracted from the values. The scale bar is 2.0 μ m.

5.2.4 Peptidoglycan synthesis and turnover are coordinated.

The cell wall labelling fluorescent probe (NADA) was used to visualise the coordination of peptidoglycan synthesis and turnover in *B. subtilis* at cellular level. The fully NADA labelled $\Delta dacA::spc$ strain was grown in PTM with and without 100 $\mu\text{g/ml}$ of penG. The samples were taken every 20 min for 2.0 h. The cells were washed with PBS and fixing in 3.0 % paraformaldehyde (see section 2.11.2 for method details). It was seen that the fluorescent signal gradually disappeared in the lateral cell wall in the absence of PenG and about 2.0 % of fluorescence left after 2.0 h of incubation. However, the cell poles maintained the fluorescence (Figure 5.8A and B). Interestingly, the inhibition of peptidoglycan synthesis by penG kept the fluorescent signal in the lateral cell wall of the survived cells (Figure 5.8A, B and C). The highest percentage of fluorescent intensity (~27 %) was lost during first 20 min, but the persistence of the fluorescent signal in the cell wall was almost stabilised beyond 20 min of incubation.

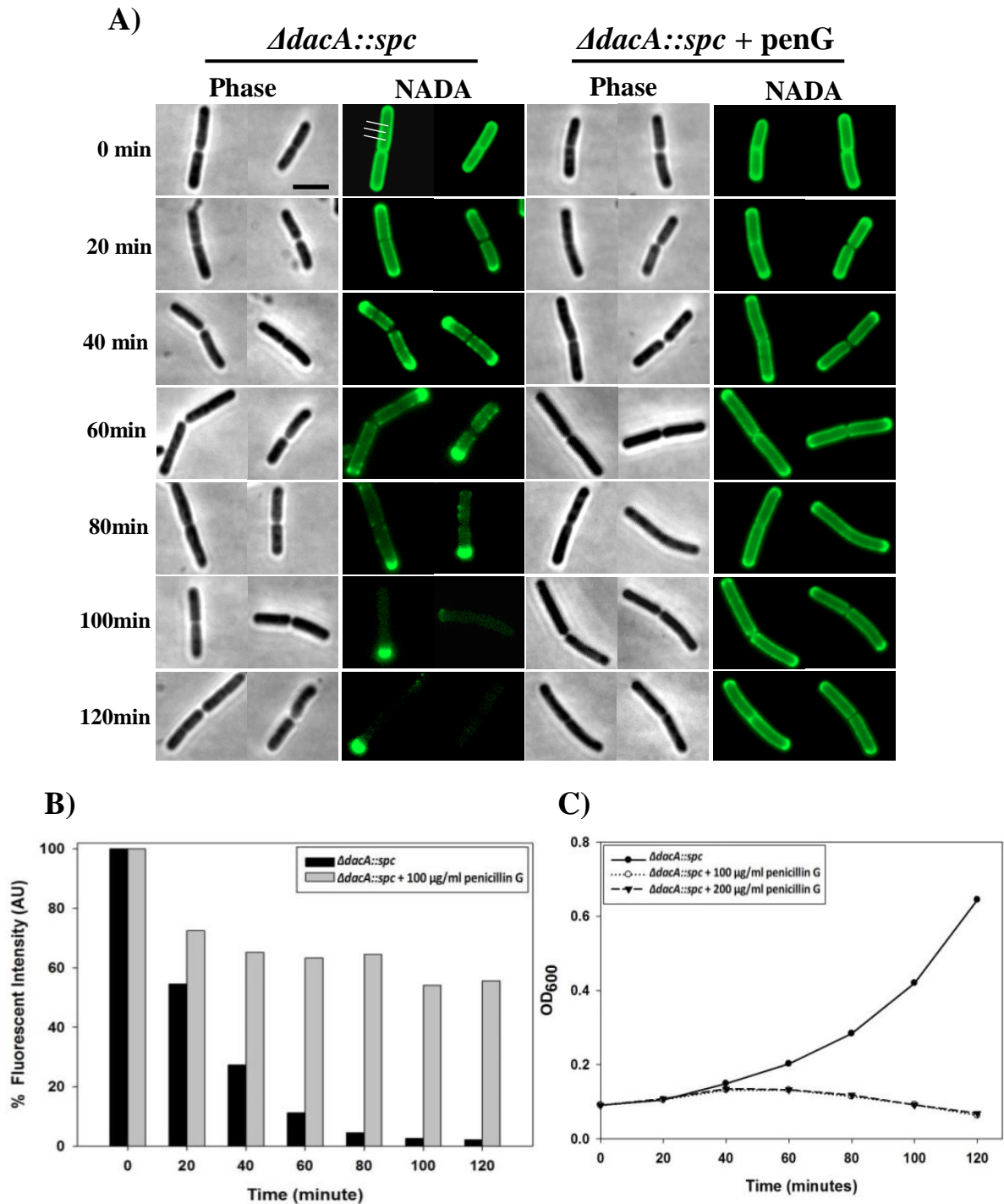


Figure 5.8 Coordination of peptidoglycan synthesis and turnover in *B. subtilis*. A) The KS15 (*ΔdacA::spc*) strain was labelled with NADA in PTM (see section 2.11.1 for details). After 2.0 h of incubation at 37 °C, the labelled cells were washed with fresh PTM and suspended (OD₆₀₀ 0.1) in fresh PTM medium with and without 100 μM of penG. Samples of cells were taken, washed with PBS and fixed in 3.0 % formaldehyde (see section 2.11.2 for details). B) The percentage of NADA released (peptidoglycan turnover) from the lateral cell wall was measured by linescan tool of Metamorph software (see section 2.11.3). The percentage (%) represents the mean of Gray level average in 50 cells in one experiment. The three lines crossed the cell wall of *dacA* strain at zero time represents the site, where the cell wall fluorescent was measured. C) The growth curve of KS15 (*ΔdacA::spc*) strain in the presence and absence of penG in PTM at 37 °C. The scale bar is 3.0 μm.

5.2.5 Dynamics of peptidoglycan assembly in *B. subtilis*.

Our previous data suggested that peptidoglycan synthesis occurs in a helical pattern (Figure 5.2A and B) and peptidoglycan synthesis and turnover are co-ordinated (Figure 5.8A and B). However, the mechanistic details of peptidoglycan assembly during cell elongation have not been understood. The slowdown of growth rate was helpful to closely investigate peptidoglycan assembly (the generation time of *dacA* strain was 35 min in PTM) (Figure 5.9). We firstly used time-lapse microscopy to visualise cell wall synthesis and turnover in live cells. The KS15 ($\Delta dacA::spc$) strain was grown in PTM, containing 50 μ M NADA, at 37 °C for 2.0 h. The fully NADA labelled cells were collected by centrifugation, washed once with fresh pre-warmed medium and added to an agarose pad on a microscopic slide (see section 2.6.19.2 for method details). The images of the live cells were automatically taken every 4 min intervals. It was observed that new peptidoglycan (non-fluorescent) was incorporated at division site and moved towards the cell poles (Figure 5.10 and movie 5.1). In the meantime, the corresponding old peptidoglycan (fluorescent) was degraded and disappeared like waves from the cell division site towards the poles. The incorporation of new peptidoglycan to the division site was not immediately seen at the beginning of cell elongation (Figure 5.10). This is probably due to the multi-layered peptidoglycan of *B. subtilis*. Although the time-lapse microscopy provided a live view of peptidoglycan assembly in defined cells, the frequent exposure of the cells to the microscopic light source caused photobleaching of NADA. To get more obvious images of peptidoglycan assembly, we tracked the time-course of peptidoglycan assembly in fixed cells. The $\Delta dacA::spc$ strain was grown in PTM in the presence of 50 μ M of NADA at 37 °C. Samples were taken at different time points (2, 10 and 30 min), washed with PBS and fixed in 3.0 % paraformaldehyde (see section 2.11.1 for details). It was observed that the cells started incorporating new peptidoglycan precursor into the cell division site very quickly and increasing of fluorescent intensity in the lateral wall was time-dependent (Figure 5.11A). To see differences in the distribution of fluorescent signal in the entire cell wall, surface plots were generated by using ImageJ software. The surface plots obviously reveal uneven distribution of fluorescence intensity in the cell wall, the area of cell cylinder close to cell division site was more fluorescent than the area close to the cell poles. On the other hand, the depletion of NADA in fully labelled cells was examined (Figure 5.11B). The same pattern of cell wall synthesis and turnover was observed as explained for NADA incorporation.

To investigate the roles of essential cell division proteins (FtsZ and FtsL) in peptidoglycan assembly at the lateral cell, the KS73 ($\Delta dacA::spc$ *chr::pJSIZ* $\Delta pble$ (P_{spac} -*ftzZ ble*)) and KS74 ($\Delta dacA::spc$ Ω (*ftsL::pSG441 aphA-3 P_{spac} pbpB*)799 ($\phi 105J506$) *cat P_{xyI}.ftsL*) strains were grown in PTM for 2.0 h in the presence of IPTG and xylose respectively. The strains were depleted for FtsZ and FtsL by growing them in fresh PTM without the inducers (IPTG and xylose). The depletion of FtsZ lasted 100 min but of FtsL was 120 min. Soon after the depletion of FtsZ and FtsL, 50 μ M of NADA was added to the cultures and kept growing for 30 min. The cells were washed, fixed and prepared for microscopic study (see section 2.11.1 for details). The results showed the incorporation of NADA into the lateral cell wall, but no fluorescent signal was seen at the cell division site (Figure 5.12).

The proposed role of DL-endopeptidase (LytE) in cell wall turnover was also investigated, using NADA labelling. The KS15 ($\Delta dacA::spc$) and KS72 ($\Delta dacA::spc$ $\Delta lytE::cat$) strains were grown in the presence of NADA for 2.0 h. The fully labelled cells were used to investigate cell wall turnover (see section 2.11.2 for method details). As shown in (Figure 5.13), the absence of LytE did not apparently cause any problem in cell wall turnover. Moreover, we revised the proposed roles of actin-like MreB proteins in cell wall biosynthesis. The effect of lack of MreB (KS70: $\Delta dacA::spc$ $\Delta mreB::neo$), Mbl (KS69: $\Delta dacA::spc$ $\Delta mbl::cat$) and MreBH (KS71: $\Delta dacA::spc$ $\Delta mreBH::erm$) on peptidoglycan synthesis was studied, using NADA labelling. It was observed that the pattern of peptidoglycan synthesis is not altered in the absence of anyone of MreB proteins (data not shown), this is consistent with Kawai *et al.* (2009b), who used fluorescent vancomycin to investigate the role roles of MreB proteins in cell wall synthesis.

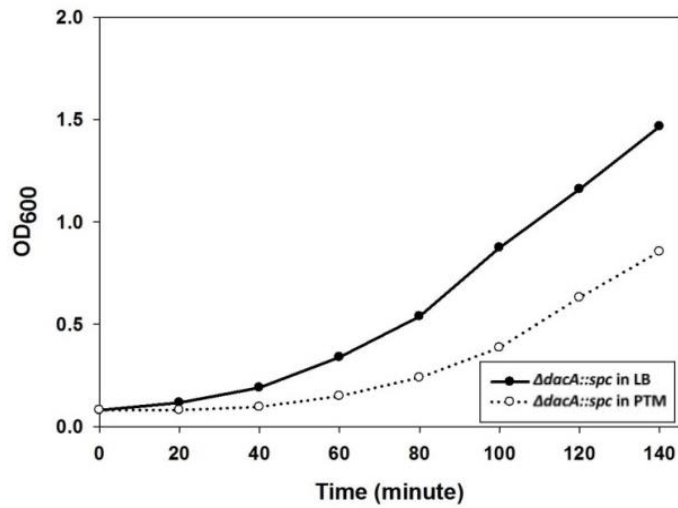


Figure 5.9 Growth curves of *B. subtilis*. The growth of KS15 strain ($\Delta dacA::spc$) was compared in LB and PTM media at 37 °C.



Figure 5.10 Time-lapse microscopic images of NADA labelled *B. subtilis*. The KS15 strain ($\Delta dacA::spc$) was grown in PTM, contained 50 μM of NADA. After 2.0 h of incubation at 37 °C, the labelled cells were washed with PTM and suspended in fresh medium. The fully NADA labelled cells was put on a pad of agarose solidified PTM on a microscopic slide and grown at 37 °C. The images of live cells were taken every 4 minutes at exposure time of 80 ms (see section 2.6.19.2 for method details). The scale bar is 2.0 μm .

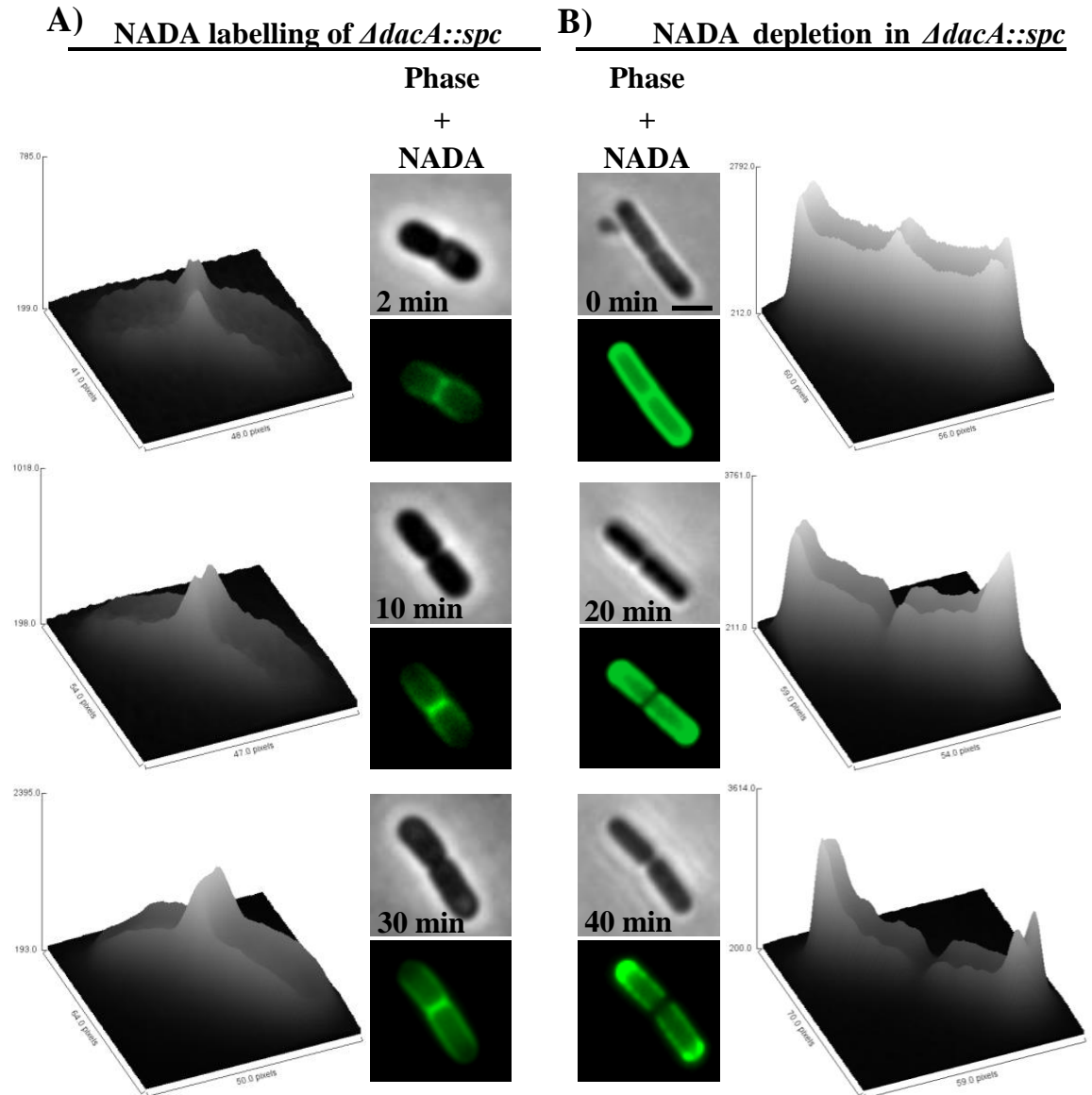


Figure 5.11 Tracking of peptidoglycan assembly (coordination of peptidoglycan synthesis and turnover) in *B. subtilis*. A) The KS15 ($\Delta dacA::spc$) strain was grown in PTM, containing 50 μM of NADA at 37 °C (see section 2.11.1). B) The fully labelled KS15 ($\Delta dacA::spc$) cell was depleted from NADA in PTM (see section 2.11.2). The surface plots of the cells were generated by ImageJ software. The surface plots show the distribution of fluorescent intensity in cell wall. The scale bar is 2.0 μm .

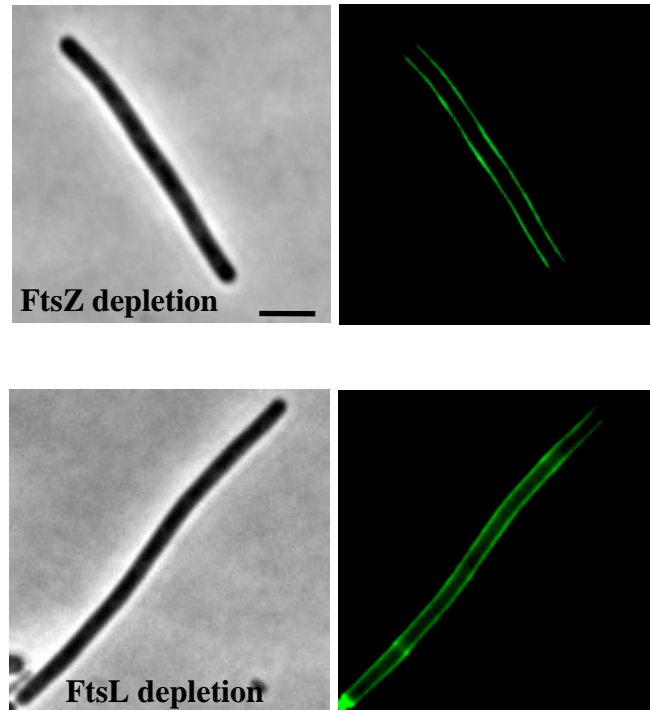


Figure 5.12 Depletion of cell division proteins, FtsZ and FtsL, in *B. subtilis*. The FtsZ and FtsL proteins were firstly depleted in KS73 ($\Delta dacA::spc$ $chr::pJSIZ\Delta pble$ ($P_{spac-ftzZ ble}$)) and KS74 ($\Delta dacA::spc \Omega$ ($ftsL::pSG441 aphA-3 P_{spac pbpB}$)799 ($\phi 105J506$) $cat P_{xyl ftsL}$) strains. The depleted strains were grown in PTM, containing 50 μ M NADA, for 30 min. The cells were washed with PBS and fixed in 3.0 % paraformaldehyde before microscopic study (see section 2.11.1). The scale bar is 3.0 μ m.

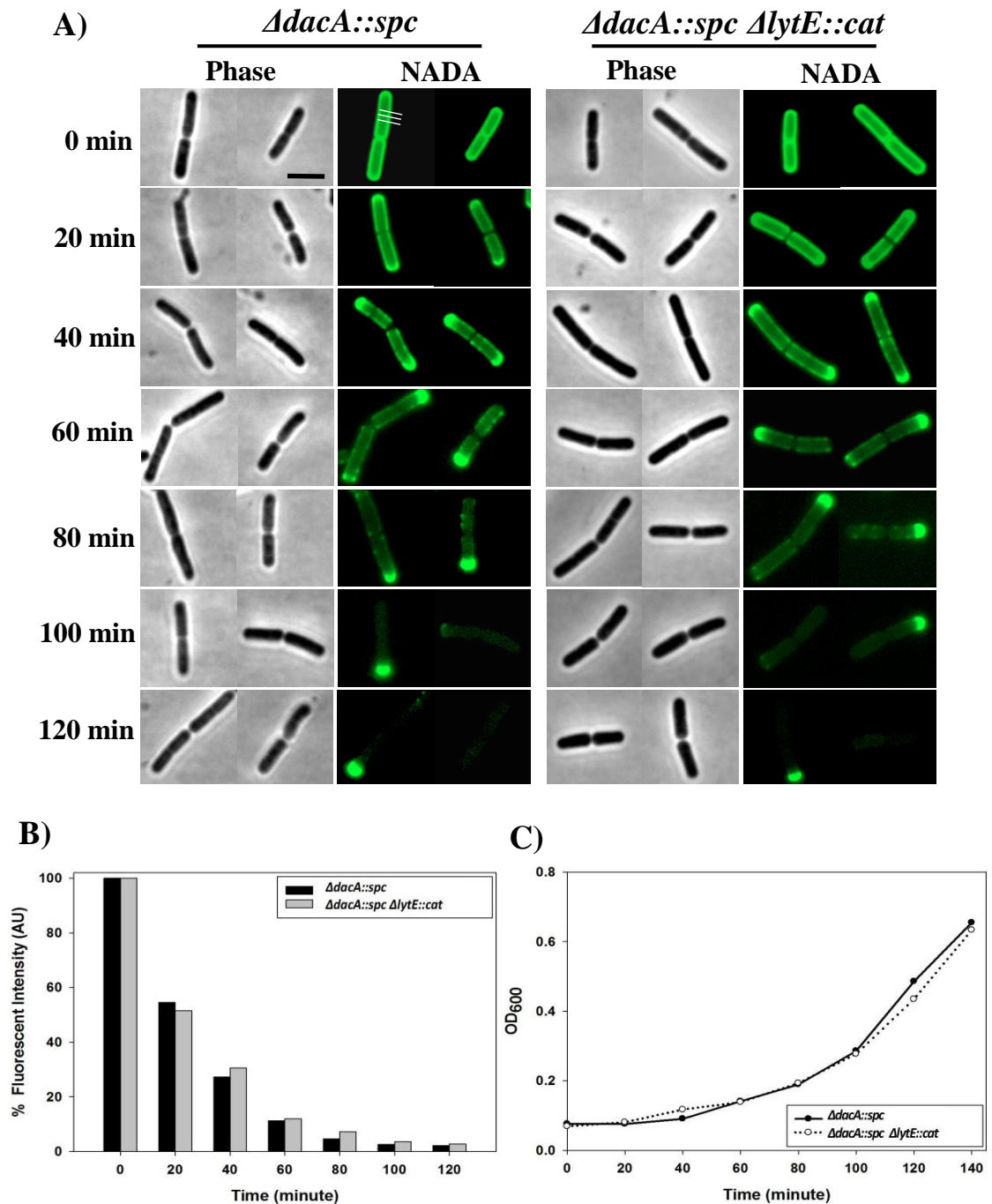


Figure 5.13 The effect of *lytE* deletion on cell wall turnover in *B. subtilis*. A) KS15 (*ΔdacA::spc*) and KS72 (*ΔdacA::spc ΔlytE::cat*) strains were grown in PTM, containing 50 μM of NADA. After 2.0 h of incubation at 37 °C, the labelled cells were washed with fresh PTM and suspended (OD₆₀₀ 0.1) in fresh medium. The cells were washed with PBS and fixed in 3.0 % formaldehyde. B) The percentage of released NADA (as a result of peptidoglycan turnover) from the lateral cell wall was also measured by linescan tool of Metamorph software (see section 2.11.3). The percentage (%) represents the mean of Gray level average in 50 cells in one experiment. The three lines crossed the cell wall of *dacA* null at zero time image represents the site, where the linescan measurement tool was placed. C) The growth curve of KS15 (*ΔdacA::spc*) and KS72 (*ΔdacA::spc ΔlytE::cat*) strains in PTM at 37 °C. The scale bar is 3.0 μm.

5.2.6 *Pattern of cell wall synthesis and turnover throughout generations of B. subtilis.*

We previously observed that the complete replacement of old peptidoglycan layers with new layers takes about three generations (Figure 5.1 and 5.2A). We wanted to understand the pattern of cell wall synthesis and turnover throughout generations of *B. subtilis*. The KS15 ($\Delta dacA::spc$) strain was labelled with NADA in PTM. Cell samples were taken at different time points, washed with PBS and fixed in 3.0 % paraformaldehyde before microscopic study (see section 2.11.1 for method details). It was observed that the fluorescence increased unevenly along the cylindrical part of the cell and the cells showed different patterns of NADA labelling throughout generations (the generation time of *dacA* strain was 35 min in PTM) (Figure 5.14). The first generation of cells was supposedly born at around 30 min of incubation, when the cells were mostly at two stages of growth, early and late stage cells. The early stage cells were mature cells, with one new pole (fluorescent) and one old pole (non-fluorescent). The late stage cells were actually older than the early stage cells and they were dividing to give the second generation cells. The second generation cells were born at around 60 min, when the cells were at two stages of growth as well. The early stage second generation cells were mature cells and of two types. The first type of early stage second generation cells had one old pole and one new pole, whereas the second type of early stage cells possessed two new poles. The late stage second generation cells were older than the early stage cells and were dividing to be the third generation cells. Finally, the third generation cells were born at around 100 min. The lateral cell wall of third generation cells was totally fluorescent. This could mean that the cell wall completely consists of new peptidoglycan layers, but one fourth of third generation cells still kept one pole from initial mother cell.

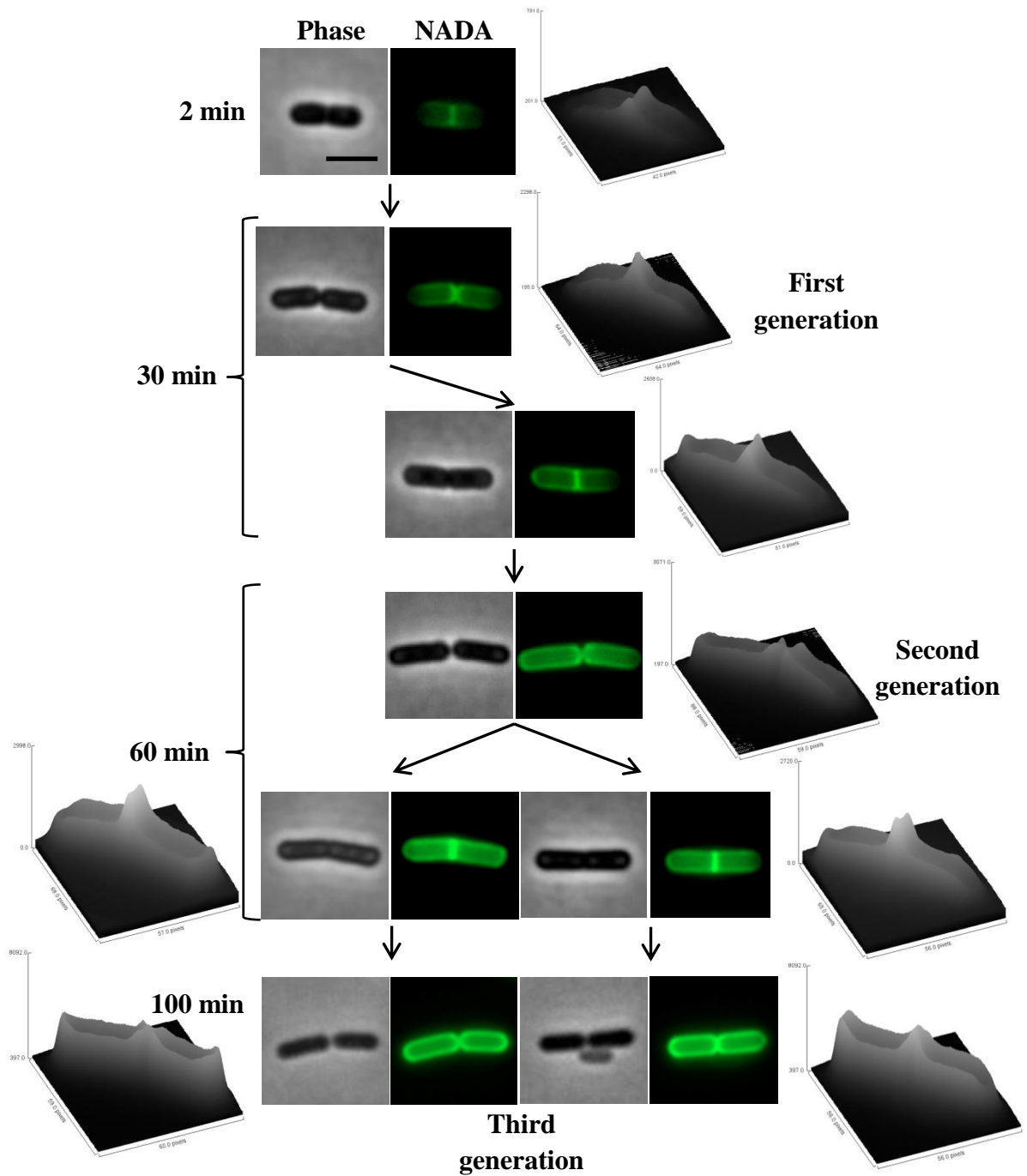


Figure 5.14 The NADA labelling of KS15 (*AdacA::spc*) strain throughout three generations. See the text for details. The surface plot of each cell image was generated by ImageJ software. The surface plots show the distribution of fluorescent intensity in cell wall. The scale bar is 3.0 μm .

5.3 Discussion

In this chapter, we investigated the peptidoglycan metabolic processes in *B. subtilis*. The investigation led to the development of a model illustrating the mechanistic details of peptidoglycan assembly in such Gram-positive bacterium. Cell wall turnover and the effect of carboxypeptidases in this catabolic process were firstly studied during exponential growth, using radioactive (^{14}C) D-alanine and fluorescently labelled D-amino acids (FDAA) (see section 5.2.1). The radioactive labelling and fluorescent microscopy both suggested that the old layers of peptidoglycan are completely replaced by new layers in the lateral cell wall of third generation cells. The radioactive results also showed that cell wall turnover occurs normally in the absence of the carboxypeptidases (DacA and LdcB). This observation supports the proposed roles of carboxypeptidases in D-alanine recycling. Besides, similar rates of cell wall turnover was observed in *dltA-D*^{-ve} strains and *dltA-D*^{ve+} strains, suggesting that either D-alanine esters of teichoic acids are spontaneously released or teichoic acids undergo turnover as much as peptidoglycan. The microscopic images showed that cell wall synthesis and turnover coordinately commence at the cell division site and continues along the lateral cell wall, whereas cell wall metabolism apparently does not occur at the cell poles. Also, the peptidoglycan layers are apparently arranged in helical pattern around the cell shaft and this is the first obvious visualisation of peptidoglycan turnover and glycan strand arrangement in a Gram-positive bacterium. Moreover, the old cell wall material was released into the culture medium, indicating that cell wall recycling apparently does not occur during exponential growth as suggested by the radioactive assay (see section 5.2.1). The fate of released cell wall products is further discussed in chapter 6.

It is known that the uncross-linked D-alanine residues in peptidoglycan are trimmed by the carboxypeptidases in *B. subtilis*. However, the dynamics of peptidoglycan carboxypeptidation has not been explained. We studied the localisation of DacA and LdcB to understand the dynamics of carboxypeptidation in peptidoglycan, using immunofluorescent microscopy (see section 5.2.2). The results showed that LdcB is localised at the division site and distributed, probably in a helical pattern, along the cylindrical part of the cell. Although it was clear that DacA localised at cell division site, the non-specific binding of anti DacA IgG limited our ability to see DacA at the lateral cell wall. This limitation obliged us to re-examine the localisation of GFP-tagged DacA, which was already observed at division site (Scheffers *et al.*, 2004). We again

observed that GFP-DacA is localised at the cell division site and thinly distributed at the lateral cell wall. However, our western blot analysis showed that only about one fourth of DacA were tagged with GFP (see section 5.2.2), so a clear localisation of DacA proteins may not be seen due to the GFP-DacA cleavage. Overall, DacA and LdcB are concentrated at cell division site and distributed in the lateral cell wall, where new peptidoglycan is present. With regard to the dynamics of peptidoglycan carboxypeptidation, we suggest that new peptidoglycan is processed by carboxypeptidases (DacA and LdcB) very soon after synthesis (Figure 5.5). The DacA firstly binds to the newly synthesised peptidoglycan layers to trim the 5th D-alanine residues, and then LdcB acts relatively quickly to cleave off the uncross-linked 4th D-alanine residues (see Figure 5.15).

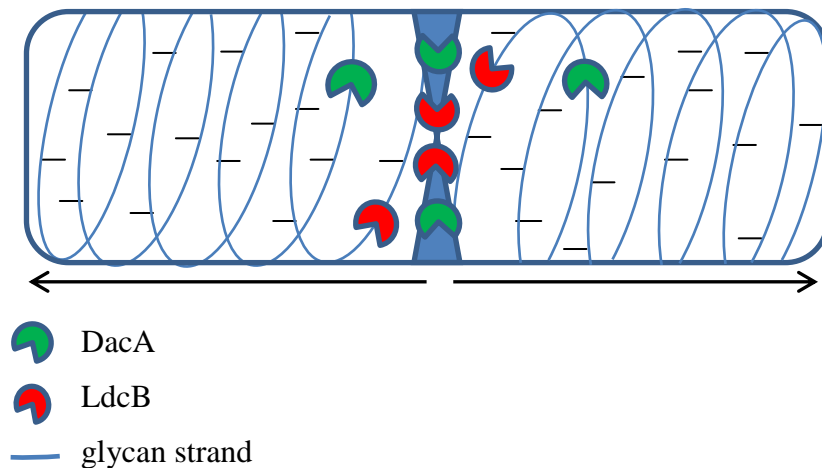


Figure 5.15 The proposed dynamics of peptidoglycan carboxypeptidation. The figure represents a vegetative cell of *B. subtilis*. The new glycan strands are synthesised at cell division site and are extended towards the cell poles by coiling around the cell shaft. After cross-linking of the newly growing glycan strands, DD-carboxypeptidase (DacA) firstly binds to the new strands at cell division site and slides towards the cell poles, to trim the D-alanine residues at position 5 of stem peptides. When the 4th D-alanine residues are exposed, LD-carboxypeptidase (LdcB) is quickly localised and follows DacA to release the uncross-linked D-alanine residues at position 4. The arrow represents the direction of glycan strand polymerisation.

It is already shown that the 5th D-alanine residues on some of the stem peptides are swapped with some other D-amino acids in *B. subtilis* (Lam *et al.*, 2009; Cava *et al.*, 2011; Kuru *et al.*, 2012). The number of 5th D-alanine residues in peptidoglycan of *dacA* strain is theoretically equal to the number of 4th D-alanine residues in the peptidoglycan of *ldcB* strain. We used NADA labelling to investigate “D-alanine swapping” in *ldcB* strain, which abundantly have tetra-peptide side chain in peptidoglycan (see section 5.2.3). The *ldcB* strain showed a slightly higher rate of D-alanine exchange than the wild type. However, the rate of D-alanine exchange in *ldcB* strain was significantly lower than seen in the *dacA* strain. This suggests that the 4th D-alanine residues are not exchanged, but the lack of LdcB might slightly reduce the efficiency of DacA in trimming of 5th D-alanine residues, that is why the fluorescent signal is slightly higher in the lateral cell wall of *ldcB* strain.

In addition to above, it is suggested that D-alanine swapping in peptidoglycan is catalysed by DD-transpeptidase (Cava *et al.*, 2011; Kuru *et al.*, 2012). The DD-transpeptidation reaction is usually catalysed by penicillin-binding proteins (PBPs) (Sauvage *et al.*, 2008). To determine if there is a specific PBP(s) doing D-alanine exchange, the *pbp* mutant strains were grown in the presence of NADA (see section 5.2.3). The result showed that the rate of NADA incorporation was not abolished in anyone of the *pbp* single mutants, suggesting that D-alanine swapping may not be catalysed by a specific PBP. Interestingly, the lack of PBP2a, PBP3, PBP4, PBP4* and PBP1 individually caused detectable reduction in the fluorescent intensity in lateral cell wall, suggesting that these PBPs play redundant role in D-alanine swapping. The role of PBP1 in catalysing 5th D-alanine exchange was already reported in an *in vitro* study (Lebar *et al.*, 2014). In contrast, the rate of D-alanine exchange significantly increased in a *pbpH* strain (see section 5.2.3). This might be consistent with the suggested redundant roles of PBP2a and PBP4 in lateral cell wall synthesis (Wei *et al.*, 2003). That is to say the activity of PBP2a, which seemingly play role in D-alanine swapping, may increase to compensate the lack of PBP4. Once the writing up of this thesis was started, a paper was published by Fura *et al.* (2015), who used fluorescently labelled D-lysine and cytometry to identify PBP(s) that exchanges D-alanine residues in the peptidoglycan of *B. subtilis*. Consistent with our results, they observed that D-alanine swapping occurred in all single *pbp* mutants and the incorporation of fluorescent D-lysine was significantly higher in *pbpH* null strain. They also proposed that PBP4 is primarily in charge of swapping process in *B. subtilis*. However, our results suggested

that PBP2a, PBP3, PBP4, PBP4* and PBP1 are potentially capable of incorporating unnatural D-amino acids into the *B. subtilis* peptidoglycan. Moreover, the addition of D-alanine in a ratio of 10:1 of NADA did not affect peptidoglycan modification with NADA, suggesting that the natural D-alanine may not be swapped with the D-alanine residues on the stem peptides.

The cell wall of bacteria normally undergoes anabolic (synthesis) and catabolic (turnover) processes during growth. We wanted to find out whether cell wall turnover is a random process or if it occurs coordinately with cell wall synthesis. The cell wall turnover was studied in fluorescently labelled cell wall in the presence of penicillin G (see section 5.2.4). The result showed a significant reduction in cell wall turnover, while cell wall synthesis is inhibited by penG. The highest rate of cell wall turnover was only observed at the beginning, this was expected because the cells were actively growing and the addition of penG may not inhibit cell wall synthesis immediately. This result suggests that cell wall synthesis and turnover depend on each other and the coordination of the two processes is required for normal growth. Our result is also consistent with Mauck *et al.* (1971), who studied the relationship between cell wall synthesis and turnover in *B. subtilis* and *B. megaterium* KM at population level, using cell wall inhibition antibiotics and radioactive isotopes. However, the possible drawback of Mauck *et al.* (1971) study was loss of radioactivity as a result of cell lysis due to the action of the antibiotic. Although it is clear that cell wall synthesis and turnover are coordinated in thick peptidoglycan of Gram-positive bacteria, the mechanistic details of such coordination have not been understood.

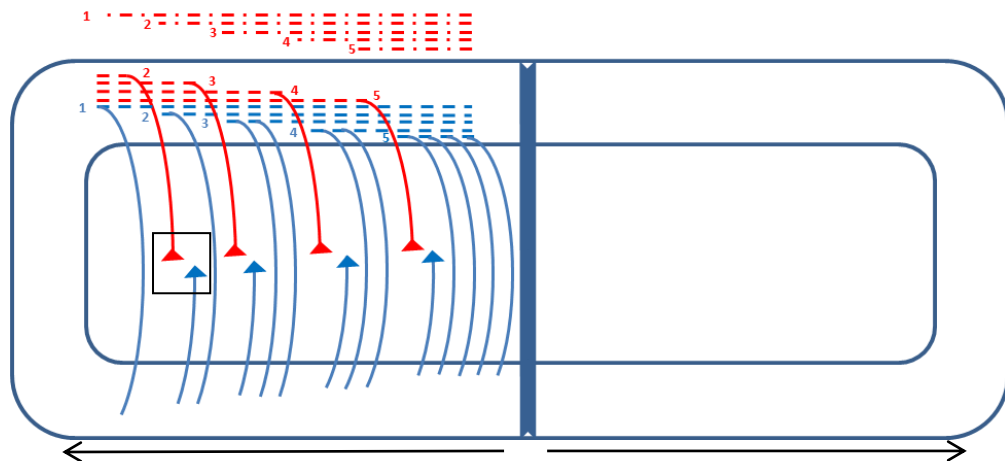
Unlike radioactive isotopes, electron microscopies and fluorescently labelled antibiotics, the FDAA can be used to visualise the dynamics of cell wall assembly at single cell level during growth of *B. subtilis*. We used this useful advantage of FDAA to understand peptidoglycan assembly in *B. subtilis*. The *dacA* strain was used in the following investigations due to its good labelling with FDAA. The cells of *dacA* strain were labelled with NADA in PTM, a medium in which the cells grow slower than in usual rich medium. This strategy was helpful to visualise the time-course of cell wall assembly in fixed and live cells. Firstly, peptidoglycan assembly was studied in live cells, using time lapse microscopy (see section 5.2.5). It was observed that the new peptidoglycan is incorporated into the cell division site and continues along the lateral cell wall possibly in a helical pattern. In the meantime the corresponding old peptidoglycan is co-ordinately degraded. One drawback of time-lapse microscopy was

gradual inactivation of the fluorescent probe (NADA) upon frequent exposure to the light source (photobleaching). Secondly, peptidoglycan synthesis and turnover were investigated in FDAA labelled cells after fixation in paraformaldehyde. Although the results showed the same observation as of time-lapse microscopy, the fixation of the cells was useful to analyse the distribution of fluorescence in cell wall, using surface plot tool of ImageJ software. This single cell analysis led to the development of a model, explaining the dynamics of peptidoglycan assembly in the cylindrical part of Gram-positive rod cell (Figure 5.16 and 5.17). According to our model, the polymerisation of new glycan strands successively starts at the cell division site and move around the cylindrical part of the cell towards the cell poles. That is to say, several new peptidoglycan layers are incorporated close to the cell membrane in a cascade manner and are extended around the cell shaft in helical patterns. Meanwhile, the corresponding outermost layers of old peptidoglycan are coordinately degraded and released to the surrounding environment (Figure 5.16 and 5.17). The model also shows how cell wall thickness and cell diameter are controlled during growth. To further test our model, the FDAA labelling was also used to see the effect of essential cell division proteins (FtsZ and ftsL) in peptidoglycan synthesis at lateral cell wall (see section 5.2.5). The result showed that the lack of FtsZ and FtsL only inhibits peptidoglycan synthesis at the cell division site. Moreover, a radioactive study already suggested that LytE, a DL-endopeptidase, plays role in peptidoglycan turnover (Bisicchia *et al.*, 2007). However, it is mostly suggested that LytE plays role in cell elongation (Carballido-Lopez *et al.*, 2006; Hashimoto *et al.*, 2012; Dominguez-Cuevas *et al.*, 2013). Therefore, we revised the proposed role of LytE in cell wall turnover, using NADA labelling (see section 5.2.5). It was observed that cell wall turnover was not affected in the absence of LytE. This observation supports the proposed role of LytE in cell elongation. In addition to the understanding of peptidoglycan assembly in individual cell, we investigated the pattern of peptidoglycan synthesis and turnover through generations of *B. subtilis* (see section 5.2.6). It was observed that the new and old peptidoglycan layers are unevenly distributed along the cylindrical part of the cells, suggesting that cell wall synthesis and turnover occur correspondingly and at different rates along the cylindrical part of the cell (see section 5.2.6 and Figure 5.18 for description).

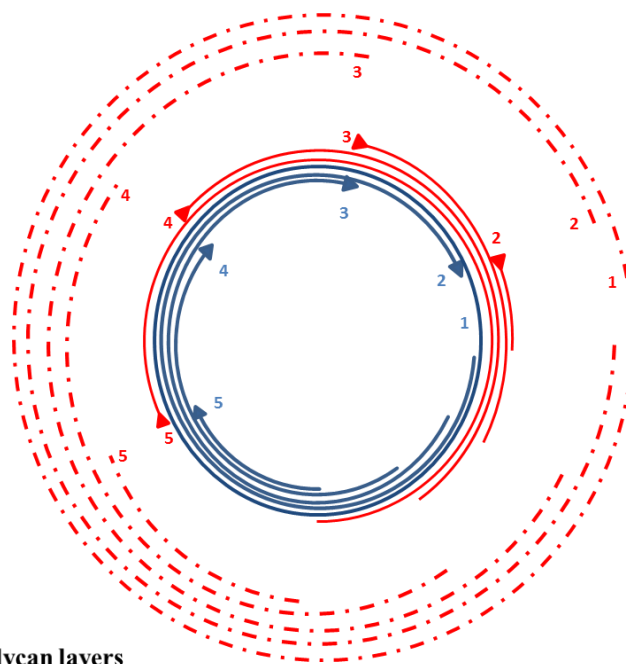
Thus our data in (Figure 5.1, 5.2, 5.8, 5.10, 5.11 and 5.14 and movie 5.1) led to the development of a comprehensive model illustrates the mechanistic details of

peptidoglycan assembly (coordinated peptidoglycan metabolism) in individual cell and throughout generations of *B. subtilis* (see Figure 5.16, 5.17 and 5.18).

A)



B)



- Old peptidoglycan layers
- New peptidoglycan layers
- - - Released peptidoglycan
- ▲ Peptidoglycan hydrolases
- ▲ Peptidoglycan synthases

Figure 5.16 A schematic model illustrates the dynamics of peptidoglycan assembly (coordinated cell wall synthesis and turnover) at the lateral cell wall of *B. subtilis*. A) a schematic cartoon shows the longitudinal view of an actively growing cell. The peptidoglycan synthases polymerize new glycan strands (blue layers) successively at the inner part of cell wall, starting at the cell division site towards the cell pole. Meanwhile, the corresponding old glycan strands (red layers) were degraded at the outermost layers of peptidoglycan by hydrolases. The digits represent the order of synthesis and degradation of peptidoglycan layers. The arrows display the direction of glycan strand polymerisation. B) It represents the left polar view of the cell in figure (A). It clarifies how bacterial cell evenly keeps the thickness of peptidoglycan along the cylindrical part of the cell, this is crucial for maintaining of rod shape and resisting turgor pressure. The black square in figure (A) represents an area that shown in details in (Figure 5.17).

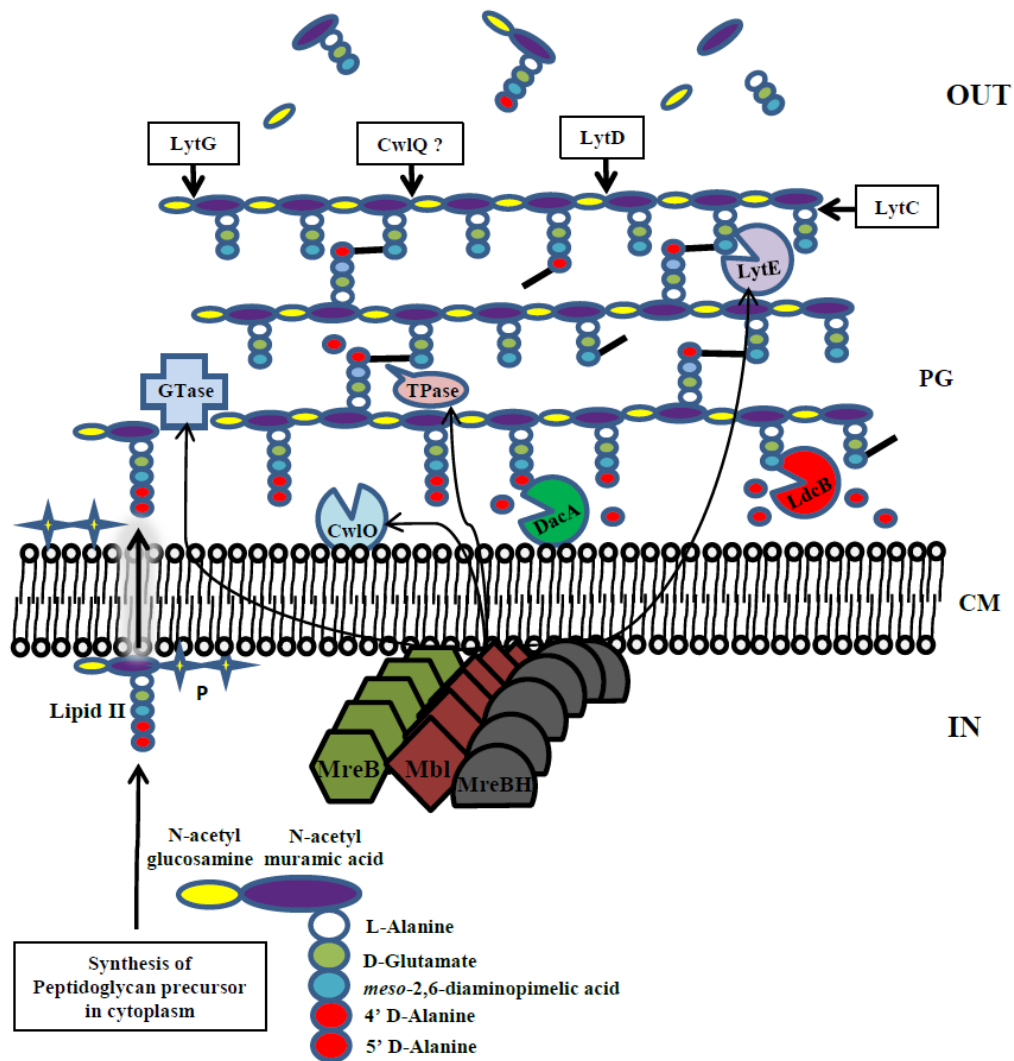


Figure 5.17 Proposed mechanisms of peptidoglycan metabolic processes in the lateral cell wall of *B. subtilis*. It shows a comprehensive mechanism of peptidoglycan metabolism during vegetative growth. The mature peptidoglycan precursor (lipid II) is membrane translocated and added to the newly growing glycan strand at the innermost layers of peptidoglycan by glycosyltransferase (GTase). The transpeptidase (TPase) cross-links about 30-40 % of stem peptides, possibly in the same strand and with the stem peptides of the upper layer. The new peptidoglycan layer is processed by carboxypeptidases (DacA and LdcB) soon after cross-linking. The cell must maintain its normal diameter during growth, so DL-endopeptidases (LytE and CwlO) may loosen the already synthesised peptidoglycan layers to provide space for insertion of new peptidoglycan layers. The cell morphogenesis proteins (MreB isomers) are also essential in directing peptidoglycan synthases (GTase and TPase) and DL-endopeptidases (LytE and CwlO). Meanwhile, the peptidoglycan hydrolases (Exo-glucosaminidase (LytG), Muramidase (still unknown), Endo-glucosaminidase (lytD) and Amidase (LytC)) degrade old peptidoglycan at the outermost layers to facilitate cell growth. The roles of MreB proteins in directing the PBP and DL-endopeptidases are adapted from (Dominguez-Cuevas *et al.*, 2013). CM: plasma membrane; PG: Peptidoglycan; P: Phosphate

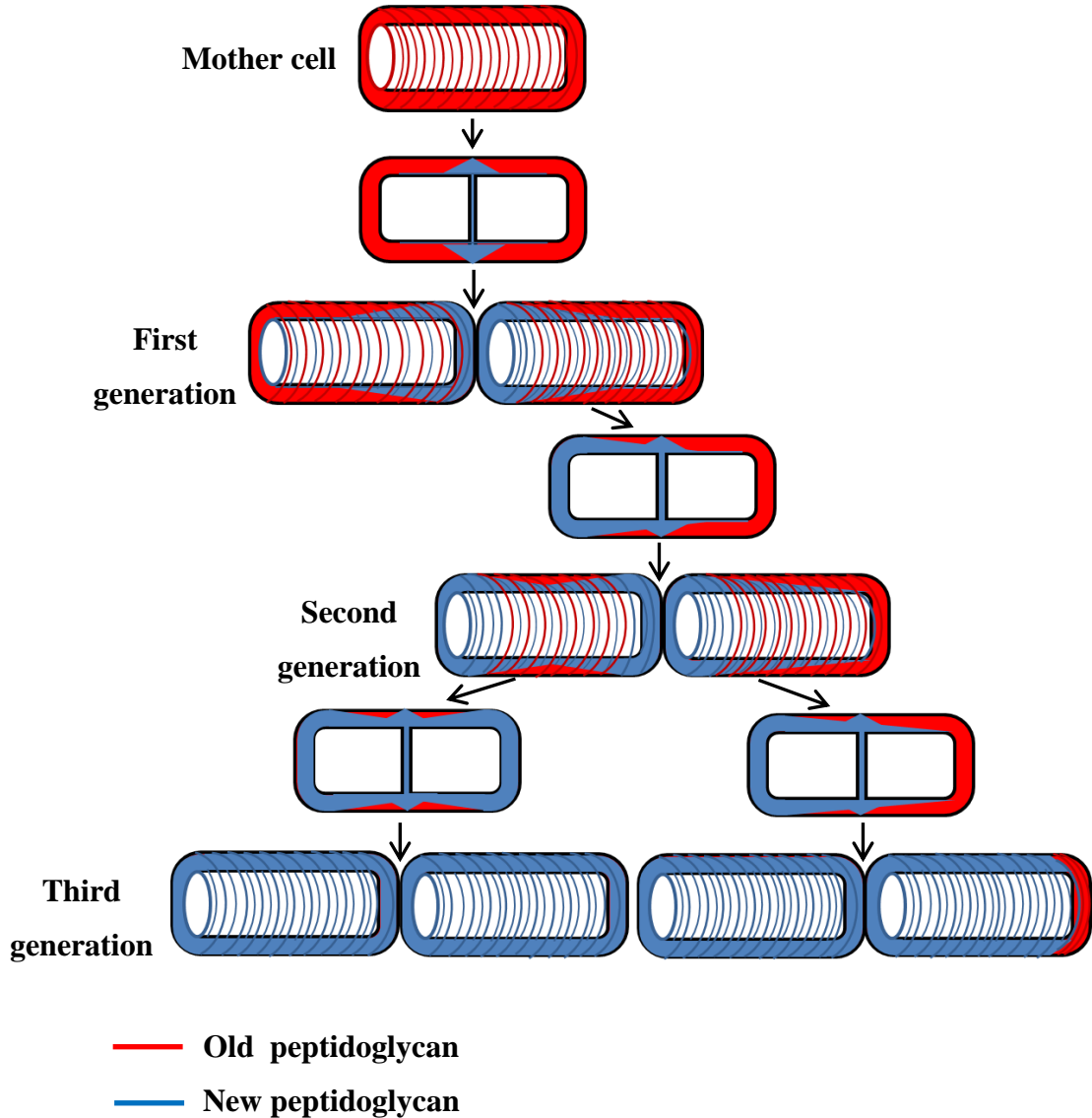


Figure 5.18 A schematic diagram showing the pattern of peptidoglycan synthesis and turnover throughout generations of *B. subtilis*. This diagram was generated based on the microscopic images and surface plots in Figure 5.14, which shows the NADA labelling of peptidoglycan in KS15 (*AdacA::spc*) strain. The red colour represents multiple layers of old peptidoglycan, which coiled around the cell shaft. The blue colour represents multiple layers of new peptidoglycan, which are synthesised in the middle of the cell and moved in helical patterns towards the cell poles.

Chapter 6. General discussion and future directions

Almost nothing was known about bacterial cell wall composition until 1950 (Martin, 1966). After several decades of cell wall investigations, there are hopefully great knowledge about cell wall structure and metabolism in bacteria. However, the studies have primarily focused on the cell wall of Gram-negative model bacterium, *E. coli*. The cell wall synthesis and turnover have also been studied in rod shaped Gram-positive bacteria, but the coordination of the cell wall metabolic processes and the fate of cell wall degraded materials have been paid little attention. Also, the dynamics or mechanistic details of cell wall assembly are still not clearly understood in the multi-layered wall of Gram-positives. This study set out to further understand the cell wall metabolic processes (synthesis, modification, turnover, recycling and dynamics of peptidoglycan assembly) in a Gram-positive model bacterium, *B. subtilis*. Exploiting the fact that D-alanine is an essential and a global component of bacterial cell wall, we did genetic manipulations in D-alanine biosynthetic pathway and in D-alanine involved cell wall processes to approach the aims of the study.

We firstly characterised a *B. subtilis* D-alanine auxotroph (*alrA*) in rich medium as a starting point of the study. It was found that the *alrA* strain requires 500 μM of D-alanine to obtain good growth in rich medium. Through deletion of *dlt* operon to prevent D-alanylation of teichoic acids, we found that teichoic acids contain almost the same amount of D-alanine as much as peptidoglycan during exponential growth (chapter 3). This result is in agreement with a previous study by (Hyyrylainen *et al.*, 2000), who observed rapid increase in D-alanylation of WTA during exponential phase of *B. subtilis*. These can suggest that Gram-positive bacteria require sufficient amount of D-alanine for the biosynthesis of peptidoglycan and modification of teichoic acids. Our result also supports a previous study, which reported the complete absence of D-alanine in the teichoic acids of a *dlt* strain (Perego *et al.*, 1995). We also observed a significant difference between the amount of radioactive D-alanine consumed from the medium and the amount incorporated into the cells of D-alanine prototroph strains, but not the D-alanine auxotroph (*alrA*) strain (chapter 3 and 4), suggesting that the exogenous D-alanine is used for cell wall synthesis as well as energy production. Moreover, it was previously shown that *alrA* strain of *B. subtilis* is able to grow in MM without D-alanine and the growth is inhibited by L-alanine (Ferrari *et al.*, 1985), but this observation was not followed up beyond suggesting a second D-alanine racemase (AlrB) in *B. subtilis*

(Pierce *et al.*, 2008). Whilst approaching the submission of this thesis we managed to identify that D-alanine aminotransferase (Dat), which produces D-alanine from D-glutamate and vice versa (Figure 1.3B and 6.1), supports the growth of *alrA* strain in MM (discussed in chapter 3). We suggest that Dat could act to ensure the balance between D-alanine and D-glutamate production under some conditions. The inhibition of *alrA* growth by L-alanine might be related to the preference of Dat to convert L-alanine to L- or D-glutamate rather than making D-alanine (Thorne *et al.*, 1955). This is the first *in vivo* evidence about the role of Dat in D-alanine synthesis in *B. subtilis*. This finding would be really important to further understand alanine metabolic pathway and to investigate cell wall metabolism in MM. The role of Dat in D-alanine synthesis was already reported in D-alanine auxotroph (*dal*) *L. monocytogenes* as well (Thompson *et al.*, 1998). In addition, the transport of D-alanine by *alrA* strain also inspired us to identify a D-alanine transporter (DatA, formerly YtnA) in *B. subtilis*. The genetic experiments (chapter 3) strongly suggested that DatA has high specificity to D-alanine, because the growth of *alrA* strain depends on DatA protein in rich media, supplemented with D-alanine. The *datA* gene seemed to be transcribed in an operon, but the proposed function of its upstream and downstream genes are not related to amino acid transport and D-alanine metabolism. Following our genetic data, the bioinformatics analysis (chapter 4) suggested that DatA protein is a member of amino acid-polyamine-organocations superfamily and the general features of DatA are similar to those of secondary carriers (permease) (Poolman and Konings, 1993). The proteins homologous to DatA are also found in many bacterial species, and the most interesting protein is D-alanine/glycine/D-serine transporter (CycA) of *E. coli*, which showed 41.7 % identity to DatA.

In the published literature, it is reported that D-alanine, D-serine, D-cycloserine, glycine and to some extent L-alanine are relatively transported through a common uptake system in bacteria. We firstly wanted to investigate the amino acid specificity of DatA, using *in vitro* system (e.g liposomes) and heterogeneous hosts (e.g *E. coli* and frog oocytes), but these attempts were not successful (discussed in section 4.3). Alternatively, we were able to indirectly examine the specificity of D-alanine transporter in *alrA* strain, using amino acid competition assay (see chapter 4 for details). We observed that only L-alanine inhibits the growth of *alrA* strain, which did not manage to grow when the ratio of L-alanine to D-alanine is 20:1. This observation indirectly suggested that either L- and D-alanine are transported via the same uptake

system or D-alanine transporter is distracted by L-alanine due to the structural identity of L- and D-alanine. This observation may suggest that the *alrA* strain actually requires less than the observed amount of D-alanine (500 μ M) for growth, but the normal L-alanine content of rich medium reduces the transport of the supplemented D-alanine. The above result could be consistent with the kinetics and amino acid inhibition study of Clark and Young (1974), who proposed a specific high-affinity transport system for both L- and D- alanine in *B. subtilis* 168. Similarly, the transport of L- and D-alanine via a common transporter was also suggested in *M. tuberculosis* (David, 1971), *Bacillus sp.* PB3 (Kanamori *et al.*, 1999) and an archaea bacterium, *Methanococcus maripaludis* (Moore and Leigh, 2005). In contrast to the above suggestions, we detected evidence for the transport of L-alanine by the *datA* strain, when it was grown in rich and minimal media (chapter 3 and 4). These observations directly suggest that *B. subtilis* has two separate uptake systems for L-and D-alanine. This suggestion can be supported by some studies, which suggested two separate transport systems for L-and D-alanine in *E. coli* K-12 (Wargel *et al.*, 1970; Wargel *et al.*, 1971; Cosloy, 1973; Robbins and Oxender, 1973). Moreover, we found that D-cycloserine was able to inhibit the growth of *datA* strain. This suggested that D-cycloserine is normally taken up in the absence of DatA protein; hence D-alanine and D-cycloserine must have separate uptake systems in *B. subtilis*. This result is in agreement with Clark and Young (1977), who did not observe any reduction in the rate of D-alanine transport in D-cycloserine resistant *B. subtilis* 168, which was less efficient in D-cycloserine transport. In contrast, in *E. coli* a common transport system for D-cycloserine and D-alanine was suggested (Wargel *et al.*, 1970; Wargel *et al.*, 1971; Baisa *et al.*, 2013) and similarly for *M. tuberculosis* (David, 1971). Thus based on the above direct and indirect experimental observations regarding the specificity of DatA to L-alanine, D-alanine, glycine and D-cycloserine, we believe that DatA is a D-alanine specific transporter.

It is known that the uncross-linked D-alanine residues in peptidoglycan are trimmed by DD- and LD- carboxypeptidases in *B. subtilis*, for unclear reasons. Interestingly, Lam *et al.* (2009) already used HPLC to analyse the accumulation of D-amino acids in the exhausted LB culture of some bacteria, but D-alanine was not detected in the culture of *B. subtilis*. From this result it seems that the released D-alanine from cell wall is re-utilised, so this prompted us to investigate the roles of carboxypeptidases. We firstly asked why peptidoglycan is processed by carboxypeptidases or what are the physiological roles of carboxypeptidases in peptidoglycan metabolism?. Interestingly,

our radioactive labelling data showed that the lack of carboxypeptidases (DacA and LdcB) does not alter the rate of cell wall synthesis and turnover but increased the requirement of D-alanine for peptidoglycan synthesis in *dacA* and *lcdB* mutants (chapter 3 and 5). This observation suggested that the carboxypeptidases apparently do not have a role in peptidoglycan biosynthesis and hypothesised that the trimmed D-alanine molecules from peptidoglycan might be recycled. The removal of D-alanine esters in the teichoic acids (deletion of *dlt* genes) and the identification of D-alanine transporter (DatA) were really useful to investigate the unclear role of carboxypeptidases and the fate of the cell wall derived D-alanine in *B. subtilis*. These were investigated by performing cross-feeding assay and RP-HPLC analysis (chapter 4). It was found that the released D-alanine molecules from peptidoglycan by carboxypeptidases and from teichoic acids by spontaneous breaking are recycled through DatA, suggesting that both DatA and carboxypeptidases establish a recycling pathway for cell wall derived D-alanine (Figure 6.1). This finding can be supported by the presence of a 22 nm periplasmic space between plasma membrane and cell wall in *B. subtilis* (Matias and Beveridge, 2005), because this space might accommodate the released D-alanine molecules and facilitate D-alanine recycling via DatA. Surprisingly, the RP-HPLC analysis showed that the accumulated D-alanine is disappeared even in the stationary culture of *datA* strain, suggesting that D-alanine is still transported (or recycled) in the absence of DatA protein. This observation is also consistent with Lam *et al.* (2009), who did not detect D-alanine in the stationary culture of *B. subtilis*. The transport of D-alanine into *datA* strain was furthered confirmed by growing the wild type and *datA* strain in MM, supplemented with radioactive D-alanine, and by exploiting the poor growth of *alaT* mutant in MM (chapter 4). From our analyses (chapter 3 and 4) it was evident that even in a *datA* strain D-alanine uptake occurs, which can only be observed in MM and during stationary phase in rich medium, where the amino acid contents of the medium is predominantly consumed. This might suggest that *datA* strain presumably transports D-alanine via non-specific amino acid uptake systems in poor growth media.

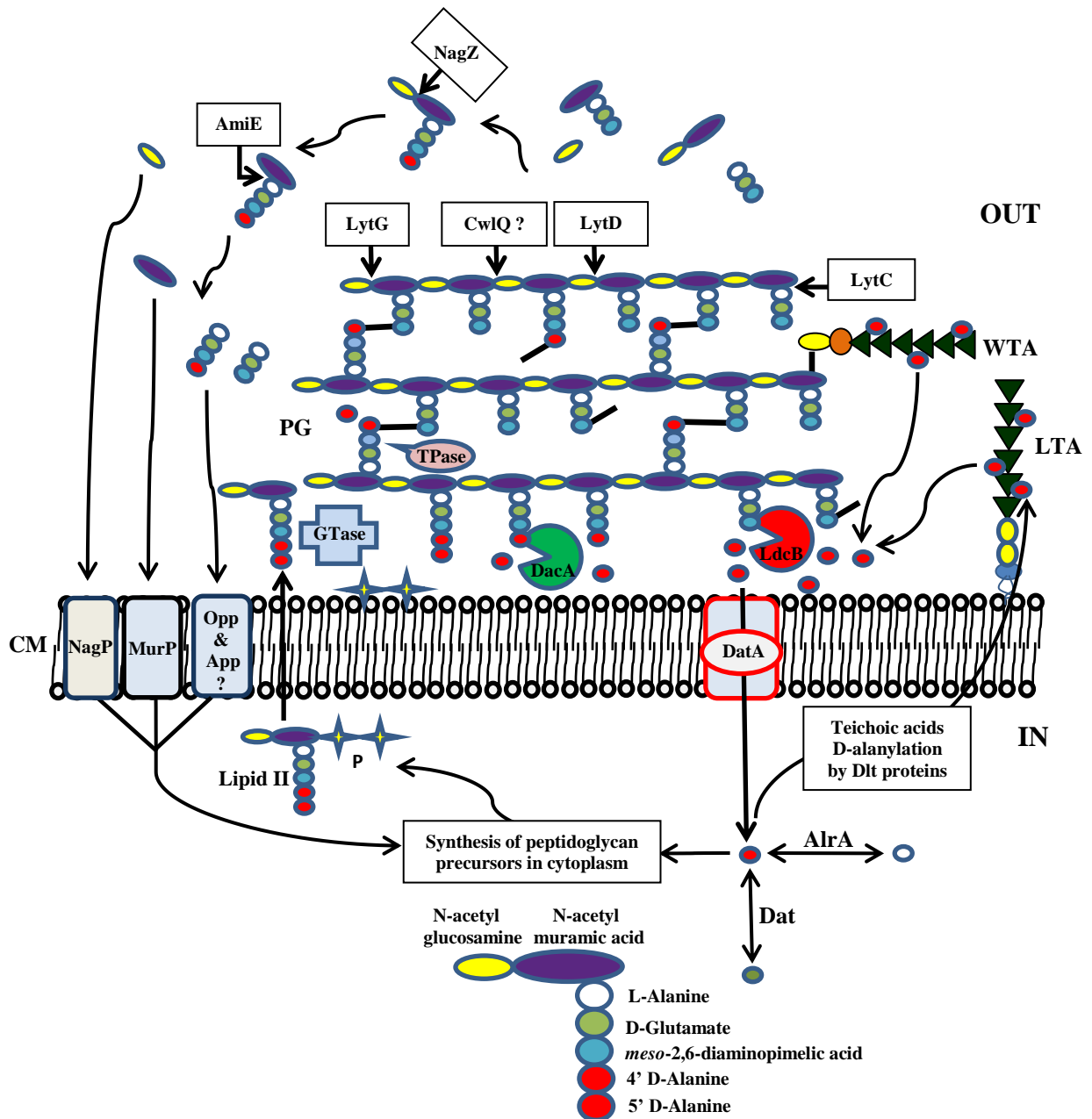


Figure 6.1 Proposed D-alanine and peptidoglycan recycling pathways in *B. subtilis*. The diagram clarifies cell wall metabolism during vegetative growth. The newly synthesised peptidoglycan layers are processed by carboxypeptidases (DacA and LdcB) soon after cross-linking. The released D-alanine molecules from both peptidoglycan and teichoic acids are re-taken up via DatA for *de novo* synthesis of peptidoglycan precursor. Meanwhile, the peptidoglycan hydrolases (muramidase (CwlQ ?), exo- and endo- β -N-acetyl glucosaminidase (LytG, lytD) and amidase (LytC)) degrade the old peptidoglycan at the outermost layers. The released muropeptides are then hydrolysed by a β -N-acetyl glucosaminidase (NagZ) and an amidase (AmiE). The amino sugars (MurNAc and GlcNAc) and detached stem peptides are probably taken up through their specific uptake systems. The muropeptide recycling pathway (NagZ, AmiE, NagP and MurP) is adapted from (Litzinger *et al.*, 2010a; Reith and Mayer, 2011)

CM: plasma membrane; PG: Peptidoglycan; P: Phosphate; LTA: Lipoteichoic acid; WTA: Wall teichoic acids.

Previously, different techniques were used to study the assembly and architecture of cell wall in Gram-positive bacteria (see introduction of chapter 5). However, the ability to understand the mechanistic details of assembly of multi-layered peptidoglycan was limited, because of the potential artifacts generated through the atomic force and electron microscopic techniques and the radioactive experiments only provided indirect explanation. We took the advantage of the development of a cell wall labelling fluorescent probe (NADA) to visualise different peptidoglycan metabolic processes (synthesis, modification and turnover) (chapter 5). Cell wall synthesis and turnover were firstly investigated, using radioactive D-alanine and NADA, which is extracellularly exchanged with the 5th D-alanine residues on some stem peptides in the peptidoglycan of *B. subtilis* “D-alanine swapping”. It was found that the complete shedding of old peptidoglycan and its replacement by new peptidoglycan take about three generations. This observation is consistent with the previous studies, which investigated cell wall turnover over, using radioactive GlcNAc and D-glutamic acid (Mauck *et al.*, 1971; Mobley *et al.*, 1984; Blackman *et al.*, 1998). Our radioactive data also suggested that either the D-alanine residues of teichoic acids are spontaneously released, which is consistent with (Ellwood and Tempest, 1972; Archibald *et al.*, 1973; Koch *et al.*, 1985b; Hyyrylainen *et al.*, 2000) or teichoic acids undergo turnover as much as peptidoglycan. This is in agreement with Mauck *et al.* (1971), who used radioactive phosphate (³²P) for monitoring teichoic acids turnover in *B. subtilis* and with Wong *et al.* (1974), using radioactive GlcNAc for cell wall investigation in *S. aureus*. Unlike the radioactive studies, we visualized and tracked the coordinated peptidoglycan synthesis and turnover in growing cells, in which the incorporation of new and the degradation of old peptidoglycan started at the cell division site and continued towards the cell poles (chapter 5). However, peptidoglycan synthesis and turnover were not observed at the cell poles, which is consistent with the studies by Mobley *et al.* (1984) and Merad *et al.* (1989) (see introduction section of chapter 5). Moreover, radioactive and fluorescent data demonstrated that the degraded cell wall materials are released into the culture medium during exponential growth, suggesting that the efficient recycling of old cell wall material does not occur in exponential phase. This observation is consistent with Mauck *et al.* (1971), who analyzed the composition of culture supernatant of *B. subtilis* W-23, growing in minimal medium. The absence of cell wall recycling during exponential growth could be due to catabolic repression of cell wall recycling pathway by nutrients in the medium as suggested by (Reith and Mayer, 2011). However, we observed the transport of D-alanine in both exponential and

stationary growth phases (chapter 4), suggesting that the recycling of simple cell wall derived molecules (e.g amino acids) are possible during exponential phase. The repression of cell wall recycling could have impact on both quantity and quality of biotechnological products because of a massive loss of nutrients through cell wall turnover (Reith and Mayer, 2011) and the induction of innate immune response by the soluble cell wall contaminants (e.g muropeptides) (Boudreau *et al.*, 2012; Johnson *et al.*, 2013; Bertsche *et al.*, 2015). The synthetic inhibition of cell wall recycling pathway might have clinical importance, because the released cell wall material from pathogenic bacteria could activate host immune system to control the bacterial infection with the aid of antibiotics.

Regarding the modification of peptidoglycan, we proposed the dynamics of peptidoglycan carboxypeptidation in *B. subtilis* based on immunofluorescence microscopy and GFP tagging (see discussion of chapter 5). We also studied D-alanine swapping and found that the swapping reaction can be catalysed by some of the PBPs (PBP2a, PBP3, PBP4, PBP4* and PBP1), but more potentially by PBP2a. In contrast, Fura *et al.* (2015) suggested that D-alanine swapping is primarily catalysed by PBP4, using flow cytometry (see discussion in chapter 5). Unlike in *E. coli*, we also found that the 4th D-alanine residues on the stem peptides in *ldcB* strain are not swapped with NADA, using microscopic analysis. This observation is in agreement with the previous studies (Lam *et al.*, 2009; Cava *et al.*, 2011; Kuru *et al.*, 2012), which reported the swapping of only 5th D-alanine residues in the peptidoglycan of *B. subtilis*, using muropeptides analysis. The physiological role of D- amino acid swapping in peptidoglycan is unclear, we assume that D-alanine swapping occurs during glycan strand polymerization by the transpeptidase domains of PBP2a, PBP3, PBP4, PBP4* and PBP1. It is possible the swapped 5th D-alanine residues on some stem peptides guide the transpeptidases to only cross-link the modified stem peptides, in other words, D-alanine swapping might play role in controlling the percentage of peptidoglycan cross-links because only 30-40 % of stem peptides are found to be cross-linked in the peptidoglycan of *B. subtilis* (Atrih *et al.*, 1999).

The interpretation of the fluorescent microscopic data all together led to the development of an interesting model, illustrating the coordination and mechanistic details of cell wall assembly in single cell and throughout generations of *B. subtilis* (see chapter 5). Briefly, we proposed that the polymerisation of new glycan strands successively starts at the cell division site and are extended around the cylindrical part

of the cell towards the cell poles, in other words, new peptidoglycan layers are incorporated close to the cell membrane in a cascade manner and are polymerised in helical pattern around the cell shaft. In the meantime, the corresponding outermost layers of old peptidoglycan are coordinately degraded and released to the surrounding environment (see discussion section of chapter 5). The developed model integrates the inside-to-outside model of cell wall growth (Pooley, 1976a; Pooley, 1976b; Koch and Doyle, 1985a) and supports the murein layered model of cell wall architecture (Holtje, 1998; Vollmer and Holtje, 2001; Vollmer and Holtje, 2004). In the model, the peptidoglycan layers are arranged in a helical pattern around the cylindrical part of the cell, which is consistent with the observations made using fluorescent vancomycin labelling of cell wall (Daniel and Errington, 2003; Tiyanont *et al.*, 2006). In contrast to the old models (Pooley, 1976b; Mobley *et al.*, 1984), which proposed even distribution of new and old peptidoglycan along the cylindrical part of the cell, our model suggests that the area of lateral cell wall close to the cell division site contains more new peptidoglycan than the area close to the cell poles. This means that the rates of peptidoglycan synthesis and turnover varied along the cylindrical part of the cell (see section 5.2.6 and Figure 5.18).

Taken together, the investigation of D-alanine metabolism and its involvement in different cell wall metabolic processes in *B. subtilis* led to the identification of a D-alanine transporter (DatA), which functions with carboxypeptidases (DacA and LdcB) as a recycling pathway for cell wall derived D-alanine. Despite our characterisation of D-alanine transporter (DatA), more biochemical and structural investigations should be done. We also found that D-alanine aminotransferase (Dat) can act to synthesis D-alanine when *alrA* strain is grown in MM. Interestingly, a model with regard to the mechanistic details of peptidoglycan assembly has been proposed as well. As our microscopic data showed obvious coordination between peptidoglycan synthesis and turnover, it is still unclear how the peptidoglycan synthases and hydrolases coordinate in the multi-layered peptidoglycan of Gram-positive bacteria. It is increasingly suggested that teichoic acids are turned over as much as peptidoglycan, but it is still unclear how the turnover of teichoic acids occurs and what is the fate of the released teichoic acid material. The suggested role of PBP2a in D-alanine swapping should also be investigated at structural level.

References

- Abachin, E., Poyart, C., Pellegrini, E., Milohanic, E., Fiedler, F., Berche, P. and Trieu-Cuot, P. (2002) 'Formation of D-alanyl-lipoteichoic acid is required for adhesion and virulence of *Listeria monocytogenes*', *Mol Microbiol*, 43(1), pp. 1-14.
- Abhayawardhane, Y. and Stewart, G.C. (1995) '*Bacillus subtilis* possesses a second determinant with extensive sequence similarity to the *Escherichia coli mreB* morphogene', *Journal of Bacteriology*, 177(3), pp. 765-773.
- Abusubel, M.F., Brent, R., Kingston, R.E., Moore, D.D., Seidman, J.G., Smith, J.A. and Struhl, K.e. (2003) 'Current Protocols in Molecular biology', *John Wiley & Sons, Inc. All rights reserved.*, Unit 1.8 , Section II.
- Allison, S.E., D'Elia, M.A., Arar, S., Monteiro, M.A. and Brown, E.D. (2011) 'Studies of the genetics, function, and kinetic mechanism of TagE, the wall teichoic acid glycosyltransferase in *Bacillus subtilis* 168', *J Biol Chem*, 286(27), pp. 23708-16.
- Anagnostopoulos, C. and Spizizen, J. (1961) 'Requirements for Transformation in *Bacillus subtilis*', *J Bacteriol*, 81(5), pp. 741-6.
- Archibald, A.R., Baddiley, J. and Heptinstall, S. (1973) 'The alanine ester content and magnesium binding capacity of walls of *Staphylococcus aureus* H grown at different pH values', *Biochim Biophys Acta*, 291(3), pp. 629-34.
- Arminjon, F., Guinand, M., Vacheron, M.-J. and Michel, G. (1977) 'Specificity Profiles of the Membrane-Bound γ -d-Glutamyl-(l)meso-diaminopimelate Endopeptidase and l-d-Carboxypeptidase from *Bacillus sphaericus* 9602', *European Journal of Biochemistry*, 73(2), pp. 557-565.
- Ashiuchi, M., Soda, K. and Misono, H. (1999) 'Characterization of *yprC* gene product of *Bacillus subtilis* IFO 3336 as glutamate racemase isozyme', *Biosci Biotechnol Biochem*, 63(5), pp. 792-8.
- Ashiuchi, M., Tani, K., Soda, K. and Misono, H. (1998) 'Properties of glutamate racemase from *Bacillus subtilis* IFO 3336 producing poly-gamma-glutamate', *J Biochem*, 123(6), pp. 1156-63.
- Atrih, A., Bacher, G., Allmaier, G., Williamson, M.P. and Foster, S.J. (1999) 'Analysis of Peptidoglycan Structure from Vegetative Cells of *Bacillus subtilis* 168 and Role of PBP 5 in Peptidoglycan Maturation', *Journal of Bacteriology*, 181(13), pp. 3956-3965.

- Azua, I., Goiriena, I., Bana, Z., Iriberry, J. and Unanue, M. (2014) 'Release and consumption of D-amino acids during growth of marine prokaryotes', *Microb Ecol*, 67(1), pp. 1-12.
- Baisa, G., Stabo, N.J. and Welch, R.A. (2013) 'Characterization of *Escherichia coli* D-cycloserine transport and resistant mutants', *J Bacteriol*, 195(7), pp. 1389-99.
- Barendt, S.M., Sham, L.-T. and Winkler, M.E. (2011) 'Characterization of Mutants Deficient in the L,d-Carboxypeptidase (DacB) and WalRK (VicRK) Regulon, Involved in Peptidoglycan Maturation of *Streptococcus pneumoniae* Serotype 2 Strain D39', *Journal of Bacteriology*, 193(9), pp. 2290-2300.
- Barreteau, H., Kovac, A., Boniface, A., Sova, M., Gobec, S. and Blanot, D. (2008) 'Cytoplasmic steps of peptidoglycan biosynthesis', *FEMS Microbiol Rev*, 32(2), pp. 168-207.
- Beeby, M., Gumbart, J.C., Roux, B. and Jensen, G.J. (2013) 'Architecture and assembly of the Gram-positive cell wall', *Mol Microbiol*, 88(4), pp. 664-72.
- Berg, J.M., Tymoczko, J.L. and Stryer, L. (2002) 'Amino Acids Are Made from Intermediates of the Citric Acid Cycle and Other Major Pathways ', *Biochemistry. 5th edition. New York: W H Freeman; Section 24.2.*
- Bertran, J., Werner, A., Stange, G., Markovich, D., Biber, J., Testar, X., Zorzano, A., Palacin, M. and Murer, H. (1992) 'Expression of Na(+)-independent amino acid transport in *Xenopus laevis* oocytes by injection of rabbit kidney cortex mRNA', *Biochemical Journal*, 281(Pt 3), pp. 717-723.
- Bertsche, U., Mayer, C., Gotz, F. and Gust, A.A. (2015) 'Peptidoglycan perception--sensing bacteria by their common envelope structure', *Int J Med Microbiol*, 305(2), pp. 217-23.
- Bhavsar, A.P. and Brown, E.D. (2006) 'Cell wall assembly in *Bacillus subtilis*: how spirals and spaces challenge paradigms', *Molecular Microbiology* 60(5), pp. 1077-1090.
- Bhavsar, A.P., Erdman, L.K., Schertzer, J.W. and Brown, E.D. (2004) 'Teichoic acid is an essential polymer in *Bacillus subtilis* that is functionally distinct from teichuronic acid', *J Bacteriol*, 186(23), pp. 7865-73.
- Bisicchia, P., Noone, D., Lioliou, E., Howell, A., Quigley, S., Jensen, T., Jarmer, H.Ø. and Devine, K.M. (2007) 'The essential YycFG two-component system controls cell wall metabolism in *Bacillus subtilis*', *Molecular Microbiology*, 65(1), pp. 180-200.

- Blackman, S.A., Smith, T.J. and Foster, S.J. (1998) 'The role of autolysins during vegetative growth of *Bacillus subtilis* 168', *Microbiology*, 144, pp. 73-82.
- Boudreau, M.A., Fisher, J.F. and Mobashery, S. (2012) 'Messenger Functions of the Bacterial Cell Wall-derived Muropeptides', *Biochemistry*, 51, pp. 2974-2990.
- Bouhss, A., Trunkfield, A.E., Bugg, T.D. and Mengin-Lecreux, D. (2008) 'The biosynthesis of peptidoglycan lipid-linked intermediates', *FEMS Microbiol Rev*, 32(2), pp. 208-33.
- Boyd, D.A., Cvitkovitch, D.G., Bleiweis, A.S., Kiriukhin, M.Y., Debabov, D.V., Neuhaus, F.C. and Hamilton, I.R. (2000) 'Defects in D-alanyl-lipoteichoic acid synthesis in *Streptococcus mutans* results in acid sensitivity', *J Bacteriol*, 182(21), pp. 6055-65.
- Brown, S., Meredith, T., Swoboda, J. and Walker, S. (2010) '*Staphylococcus aureus* and *Bacillus subtilis* W23 make polyribitol wall teichoic acids using different enzymatic pathways', *Chem Biol*, 17(10), pp. 1101-10.
- Caparrós, M., Pisabarro, A.G. and de Pedro, M.A. (1992) 'Effect of D-amino acids on structure and synthesis of peptidoglycan in *Escherichia coli*', *Journal of Bacteriology*, 174(17), pp. 5549-5559.
- Carballido-Lopez, R. and Errington, J. (2003a) 'The bacterial cytoskeleton: *in vivo* dynamics of the actin-like protein Mbl of *Bacillus subtilis*', *Dev Cell*, 4(1), pp. 19-28.
- Carballido-Lopez, R. and Errington, J. (2003b) 'A dynamic bacterial cytoskeleton', *Trends Cell Biol*, 13(11), pp. 577-83.
- Carballido-Lopez, R., Formstone, A., Li, Y., Ehrlich, S.D., Noirot, P. and Errington, J. (2006) 'Actin homolog MreBH governs cell morphogenesis by localization of the cell wall hydrolase LytE', *Dev Cell*, 11(3), pp. 399-409.
- Casagrande, F., Ratera, M., Schenk, A.D., Chami, M., Valencia, E., Lopez, J.M., Torrents, D., Engel, A., Palacin, M. and Fotiadis, D. (2008) 'Projection structure of a member of the amino acid/polyamine/organocation transporter superfamily', *J Biol Chem*, 283(48), pp. 33240-8.
- Cava, F., de Pedro, M.A., Lam, H., Davis, B.M. and Waldor, M.K. (2011) 'Distinct pathways for modification of the bacterial cell wall by non-canonical D-amino acids', *Embo j*, 30(16), pp. 3442-53.

- Chaloupka, J., Kreckova, P. and Rihova, L. (1962) 'The mucopeptide turnover in the cell walls of growing cultures of *Bacillus megaterium* KM', *Experientia*, 18, pp. 362-3.
- Chen, J.M., Uplekar, S., Gordon, S.V. and Cole, S.T. (2012) 'A point mutation in *cycA* partially contributes to the D-cycloserine resistance trait of *Mycobacterium bovis* BCG vaccine strains', *PLoS One*, 7(8), p. e43467.
- Cheng, Q., Li, H., Merdek, K. and Park, J.T. (2000) 'Molecular characterization of the beta-N-acetylglucosaminidase of *Escherichia coli* and its role in cell wall recycling', *J Bacteriol*, 182(17), pp. 4836-40.
- Clark, V.L. and Young, F.E. (1974) 'Active transport of D-alanine and related amino acids by whole cells of *Bacillus subtilis*', *J Bacteriol*, 120(3), pp. 1085-92.
- Clark, V.L. and Young, F.E. (1977) 'D-Cycloserine-induced alterations in the transport of D-alanine and glycine in *Bacillus subtilis* 168', *Antimicrob Agents Chemother*, 11(5), pp. 877-80.
- Cohen, G.N. and Monod, J. (1957) 'Bacterial permeases', *Bacteriological Reviews*, 21(3), pp. 169-194.
- Cosloy, S.D. (1973) 'D-serine transport system in *Escherichia coli* K-12', *J Bacteriol*, 114(2), pp. 679-84.
- Courtin, P., Miranda, G., Guillot, A., Wessner, F., Mezange, C., Domakova, E., Kulakauskas, S. and Chapot-Chartier, M.P. (2006) 'Peptidoglycan structure analysis of *Lactococcus lactis* reveals the presence of an L,D-carboxypeptidase involved in peptidoglycan maturation', *J Bacteriol*, 188(14), pp. 5293-8.
- Curtiss, R., Charamella, L.J., Berg, C.M. and Harris, P.E. (1965) 'Kinetic and Genetic Analyses of d-Cycloserine Inhibition and Resistance in *Escherichia coli*', *Journal of Bacteriology*, 90(5), pp. 1238-1250.
- D'Elia, M.A., Millar, K.E., Beveridge, T.J. and Brown, E.D. (2006b) 'Wall teichoic acid polymers are dispensable for cell viability in *Bacillus subtilis*', *J Bacteriol*, 188(23), pp. 8313-6.
- D'Elia, M.A., Pereira, M.P., Chung, Y.S., Zhao, W., Chau, A., Kenney, T.J., Sulavik, M.C., Black, T.A. and Brown, E.D. (2006a) 'Lesions in teichoic acid biosynthesis in *Staphylococcus aureus* lead to a lethal gain of function in the otherwise dispensable pathway', *J Bacteriol*, 188(12), pp. 4183-9.

- Dahl, U., Jaeger, T., Nguyen, B.T., Sattler, J.M. and Mayer, C. (2004) 'Identification of a phosphotransferase system of *Escherichia coli* required for growth on N-acetylmuramic acid', *J Bacteriol*, 186(8), pp. 2385-92.
- Daniel, R.A. and Errington, J. (2003) 'Control of cell morphogenesis in bacteria: two distinct ways to make a rod-shaped cell', *Cell*, 113(6), pp. 767-76.
- Daniel, R.A., Harry, E.J. and Errington, J. (2000) 'Role of penicillin-binding protein PBP 2B in assembly and functioning of the division machinery of *Bacillus subtilis*', *Molecular Microbiology*, 35 (2), pp. 299-311.
- Daniel, R.A., Harry, E.J., Katis, V.L., Wake, R.G. and Errington, J. (1998) 'Characterization of the essential cell division gene *ftsL(yIID)* of *Bacillus subtilis* and its role in the assembly of the division apparatus', *Mol Microbiol*, 29(2), pp. 593-604.
- Daniel, R.A., Williams, A.M. and Errington, J. (1996) 'A complex four-gene operon containing essential cell division gene *pbpB* in *Bacillus subtilis*', *J Bacteriol*, 178(8), pp. 2343-50.
- Das, D., Herve, M., Elsliger, M.A., Kadam, R.U., Grant, J.C., Chiu, H.J., Knuth, M.W., Klock, H.E., Miller, M.D., Godzik, A., Lesley, S.A., Deacon, A.M., Mengin-Lecreulx, D. and Wilson, I.A. (2013) 'Structure and function of a novel LD-carboxypeptidase a involved in peptidoglycan recycling', *J Bacteriol*, 195(24), pp. 5555-66.
- David, H.L. (1971) 'Resistance to D-cycloserine in the tubercle bacilli: mutation rate and transport of alanine in parental cells and drug-resistant mutants', *Appl Microbiol*, 21(5), pp. 888-92.
- de Jong, I.G., Beilharz, K., Kuipers, O.P. and Veening, J.W. (2011) 'Live Cell Imaging of *Bacillus subtilis* and *Streptococcus pneumoniae* using Automated Time-lapse Microscopy', *J Vis Exp*, (53).
- de Pedro, M.A., Quintela, J.C., Hölftje, J.V. and Schwarz, H. (1997) 'Murein segregation in *Escherichia coli*', *Journal of Bacteriology*, 179(9), pp. 2823-2834.
- Debabov, D.V., Kiriukhin, M.Y. and Neuhaus, F.C. (2000) 'Biosynthesis of lipoteichoic acid in *Lactobacillus rhamnosus*: role of DltD in D-alanylation', *J Bacteriol*, 182(10), pp. 2855-64.
- Decatur, A., Kunkel, B. and Losick, R.H.U. (1993) ': In Abhayawardhane, Y. and Stewart, G. C. (1995) *Bacillus subtilis* possesses a second determinant with extensive

- sequence similarity to the *Escherichia coli mreB* morphogene', *J Bacteriol*, 177(3), pp. 765-73.
- Defeu Soufo, H.J. and Graumann, P.L. (2006) 'Dynamic localization and interaction with other *Bacillus subtilis* actin-like proteins are important for the function of MreB', *Mol Microbiol*, 62(5), pp. 1340-56.
- Dmitriev, B., Toukach, F. and Ehlers, S. (2005) 'Towards a comprehensive view of the bacterial cell wall', *Trends Microbiol*, 13(12), pp. 569-74.
- Dmitriev, B.A., Ehlers, S. and Rietschel, E.T. (1999) 'Layered murein revisited: a fundamentally new concept of bacterial cell wall structure, biogenesis and function', *Med Microbiol Immunol*, 187(3), pp. 173-81.
- Dmitriev, B.A., Toukach, F.V., Schaper, K.J., Holst, O., Rietschel, E.T. and Ehlers, S. (2003) 'Tertiary structure of bacterial murein: the scaffold model', *J Bacteriol*, 185(11), pp. 3458-68.
- Doi, M., Wachi, M., Ishino, F., Tomioka, S., Ito, M., Sakagami, Y., Suzuki, A. and Matsubishi, M. (1988) 'Determinations of the DNA sequence of the *mreB* gene and of the gene products of the *mre* region that function in formation of the rod shape of *Escherichia coli* cells', *J Bacteriol*, 170(10), pp. 4619-24.
- Dominguez-Cuevas, P., Porcelli, I., Daniel, R.A. and Errington, J. (2013) 'Differentiated roles for MreB-actin isologues and autolytic enzymes in *Bacillus subtilis* morphogenesis', *Mol Microbiol*, 89(6), pp. 1084-98.
- Duggin, I.G., Andersen, P.A., Smith, M.T., Wilce, J.A., King, G.F. and Wake, R.G. (1999) 'Site-directed mutants of RTP of *Bacillus subtilis* and the mechanism of replication fork arrest', *J Mol Biol*, 286(5), pp. 1325-35.
- Dul, M.J. and Young, F.E. (1973) 'Genetic Mapping of a Mutant Defective in D, L-Alanine Racemase in *Bacillus subtilis* 168', *Journal of Bacteriology*, 15(3), pp. 1212-1214.
- Egan, A.J.F. and Vollmer, W. (2013) 'The physiology of bacterial cell division', *Ann. N.Y.Acad.Sci.*, 1277, pp. 8-28.
- Ellwood, D.C. and Tempest, D.W. (1972) 'Influence of culture pH on the content and composition of teichoic acids in the walls of *Bacillus subtilis*', *J Gen Microbiol*, 73(2), pp. 395-402.

- Estrela, A.I., Pooley, H.M., de Lencastre, H. and Karamata, D. (1991) 'Genetic and biochemical characterization of *Bacillus subtilis* 168 mutants specifically blocked in the synthesis of the teichoic acid poly(3-O-beta-D-glucopyranosyl-N-acetylgalactosamine 1-phosphate): *gneA*, a new locus, is associated with UDP-N-acetylglucosamine 4-epimerase activity', *J Gen Microbiol*, 137(4), pp. 943-50.
- Fang, Y., Jayaram, H., Shane, T., Kolmakova-Partensky, L., Wu, F., Williams, C., Xiong, Y. and Miller, C. (2009) 'Structure of a prokaryotic virtual proton pump at 3.2 Å resolution', *Nature*, 460(7258), pp. 1040-3.
- Ferrari, E., Henner, D.J. and Yang, M.Y. (1985) 'Isolation of an alanine racemase gene from *Bacillus subtilis* and its use for plasmid maintenance in *Bacillus subtilis*', *Bio/technology*, 3, pp. 1003-1007.
- Feucht, A. and Lewis, P.J. (2001) 'Improved plasmid vectors for the production of multiple fluorescent protein fusions in *Bacillus subtilis*', *Gene*, 264(2), pp. 289-97.
- Fischer, W. (1994) 'Lipoteichoic acid and lipids in the membrane of *Staphylococcus aureus*', *Med Microbiol Immunol*, 183(2), pp. 61-76.
- Fischer, W. and Rosel, P. (1980) 'The alanine ester substitution of lipoteichoic acid (LTA) in *Staphylococcus aureus*', *FEBS Lett*, 119(2), pp. 224-6.
- Formstone, A., Carballido-López, R., Noirot, P., Errington, J. and Scheffers, D.-J. (2008) 'Localization and Interactions of Teichoic Acid Synthetic Enzymes in *Bacillus subtilis*', *Journal of Bacteriology*, 190(5), pp. 1812-1821.
- Formstone, A. and Errington, J. (2005) 'A magnesium-dependent *mreB* null mutant: implications for the role of *mreB* in *Bacillus subtilis*', *Mol Microbiol*, 55(6), pp. 1646-57.
- Foster, S.J. and Popham, D.L. (2002) 'Structure and synthesis of cell wall, spore cortex, teichoic acids, S-layers, and capsules. In *Bacillus subtilis* and Its Closest Relatives: From Genes to Cells. Sonenshein, A.L., Losick, R., and Hoch, J.A. (eds). Washington, DC: American Society for Microbiology Press, pp', pp. 21-41.
- Fotheringham, I.G., Bledig, S.A. and Taylor, P.P. (1998) 'Characterization of the genes encoding D-amino acid transaminase and glutamate racemase, two D-glutamate biosynthetic enzymes of *Bacillus sphaericus* ATCC 10208', *J Bacteriol*, 180(16), pp. 4319-23.

- Freymond, P.P., Lazarevic, V., Soldo, B. and Karamata, D. (2006) 'Poly(glucosyl-N-acetylgalactosamine 1-phosphate), a wall teichoic acid of *Bacillus subtilis* 168: its biosynthetic pathway and mode of attachment to peptidoglycan', *Microbiology*, 152(Pt 6), pp. 1709-18.
- Fridrich, E., Vermeulen, J., Biboy, J., Soares, F., Taveirne, M.E., Johnson, J.G., DiRita, V.J., Girardin, S.E., Vollmer, W. and Gaynor, E.C. (2014) 'Peptidoglycan Id-Carboxypeptidase Pgp2 Influences *Campylobacter jejuni* Helical Cell Shape and Pathogenic Properties and Provides the Substrate for the dl-Carboxypeptidase Pgp1', *The Journal of Biological Chemistry*, 289(12), pp. 8007-8018.
- Fura, J.M., Kearns, D. and Pires, M.M. (2015) 'D-Amino Acid Probes for Penicillin Binding Protein-based Bacterial Surface Labeling', *J Biol Chem*.
- Gan, L., Chen, S. and Jensen, G.J. (2008) 'Molecular organization of Gram-negative peptidoglycan', *Proc Natl Acad Sci U S A*, 105(48), pp. 18953-7.
- Gao, X., Lu, F., Zhou, L., Dang, S., Sun, L., Li, X., Wang, J. and Shi, Y. (2009) 'Structure and mechanism of an amino acid antiporter', *Science*, 324(5934), pp. 1565-8.
- Gao, X., Zhou, L., Jiao, X., Lu, F., Yan, C., Zeng, X., Wang, J. and Shi, Y. (2010) 'Mechanism of substrate recognition and transport by an amino acid antiporter', *Nature*, 463(7282), pp. 828-32.
- Glaser, P., Kunst, F., Arnaud, M., Coudart, M.P., Gonzales, W., Hullo, M.F., Ionescu, M., Lubochinsky, B., Marcelino, L., Moszer, I. and et al. (1993) '*Bacillus subtilis* genome project: cloning and sequencing of the 97 kb region from 325 degrees to 333 degrees', *Mol Microbiol*, 10(2), pp. 371-84.
- Goodell, E.W. (1985) 'Recycling of murein by *Escherichia coli*', *Journal of Bacteriology*, 163(1), pp. 305-310.
- Goodell, E.W. and Schwarz, U. (1985) 'Release of cell wall peptides into culture medium by exponentially growing *Escherichia coli*', *J Bacteriol.*, 162(1), pp. 391-397.
- Grisshammer, R. and Tate, C.G. (1995) 'Overexpression of integral membrane proteins for structural studies', *Q Rev Biophys*, 28(3), pp. 315-422.
- Gross, M., Cramton, S.E., Götz, F. and Peschel, A. (2001) 'Key Role of Teichoic Acid Net Charge in *Staphylococcus aureus* Colonization of Artificial Surfaces', *Infection and Immunity*, 69(5), pp. 3423-3426.

- Guinand, M., Vacheron, M.J., Michel, G. and Tipper, D.J. (1979) 'Location of peptidoglycan lytic enzymes in *Bacillus sphaericus*', *Journal of Bacteriology*, 138(1), pp. 126-132.
- Haas, R., Koch, H.U. and Fischer, W. (1984) 'Alanyl turnover from lipoteichoic acid to teichoic acid in *Staphylococcus aureus*', *FEMS Microbiology Letters*, 21(1), pp. 27–31.
- Halpern, Y.S. (1974) 'Genetics of amino acid transport in bacteria', *Annu Rev Genet*, 8, pp. 103-33.
- Hashimoto, M., Ooiwa, S. and Sekiguchi, J. (2012) 'Synthetic lethality of the *lytE cw10* genotype in *Bacillus subtilis* is caused by lack of D,L-endopeptidase activity at the lateral cell wall', *J Bacteriol*, 194(4), pp. 796-803.
- Hashimoto, M., Seki, T., Matsuoka, S., Hara, H., Asai, K., Sadaie, Y. and Matsumoto, K. (2013) 'Induction of extracytoplasmic function sigma factors in *Bacillus subtilis* cells with defects in lipoteichoic acid synthesis', *Microbiology*, 159(Pt 1), pp. 23-35.
- Hayhurst, E.J., Kailas, L., Hobbs, J.K. and Foster, S.J. (2008) 'Cell wall peptidoglycan architecture in *Bacillus subtilis*', *Proceedings of the National Academy of Sciences of the United States of America*, 105(38), pp. 14603-14608.
- Heaton, M.P. and Neuhaus, F.C. (1994) 'Role of the D-alanyl carrier protein in the biosynthesis of D-alanyl-lipoteichoic acid', *J Bacteriol*, 176(3), pp. 681-90.
- Holtje, J.V. (1998) 'Growth of the stress-bearing and shape-maintaining murein sacculus of *Escherichia coli*', *Microbiol Mol Biol Rev*, 62(1), pp. 181-203.
- Hosie, A.H. and Poole, P.S. (2001) 'Bacterial ABC transporters of amino acids', *Res Microbiol*, 152(3-4), pp. 259-70.
- Hoyland, C.N., Aldridge, C., Cleverley, R.M., Duchene, M.C., Minasov, G., Onopriyenko, O., Sidiq, K., Stogios, P.J., Anderson, W.F., Daniel, R.A., Savchenko, A., Vollmer, W. and Lewis, R.J. (2014) 'Structure of the LdcB LD-carboxypeptidase reveals the molecular basis of peptidoglycan recognition', *Structure*, 22(7), pp. 949-60.
- Hurst, A., Hughes, A., Duckworth, M. and Baddiley, J. (1975) 'Loss of D-alanine during sublethal heating of *Staphylococcus aureus* S6 and magnesium binding during repair', *J Gen Microbiol*, 89(2), pp. 277-84.
- Hyyrylainen, H.L., Vitikainen, M., Thwaite, J., Wu, H., Sarvas, M., Harwood, C.R., Kontinen, V.P. and Stephenson, K. (2000) 'D-Alanine substitution of teichoic acids as a

- modulator of protein folding and stability at the cytoplasmic membrane/cell wall interface of *Bacillus subtilis*', *J Biol Chem*, 275(35), pp. 26696-703.
- Illana Kolodkin-Gal, D.R., Shugeng Cao, Jon Clardy, Roberto Kolter, and Richard Losick (2010) 'D-Amino Acids Trigger Biofilm Disassembly', *Science*, 328(5978), pp. 627-629.
- Izaki, K., Matsushashi, M. and Strominger, J.L. (1968) 'Biosynthesis of the peptidoglycan of bacterial cell walls. 8. Peptidoglycan transpeptidase and D-alanine carboxypeptidase: penicillin-sensitive enzymatic reaction in strains of *Escherichia coli*', *J Biol Chem*, 243(11), pp. 3180-92.
- Jacobs, C., Huang, L.J., Bartowsky, E., Normark, S. and Park, J.T. (1994) 'Bacterial cell wall recycling provides cytosolic muropeptides as effectors for beta-lactamase induction', *Embo j*, 13(19), pp. 4684-94.
- Jacobs, C., Joris, B., Jamin, M., Klarsov, K., Van Beeumen, J., Mengin-Lecreulx, D., van Heijenoort, J., Park, J.T., Normark, S. and Frere, J.M. (1995) 'AmpD, essential for both beta-lactamase regulation and cell wall recycling, is a novel cytosolic N-acetylmuramyl-L-alanine amidase', *Mol Microbiol*, 15(3), pp. 553-9.
- Johnson, J.W., Fisher, J.F. and Mobashery, S. (2013) 'Bacterial cell-wall recycling', *Ann N Y Acad Sci*, 1277, pp. 54-75.
- Jones, L.J., Carballido-Lopez, R. and Errington, J. (2001) 'Control of cell shape in bacteria: helical, actin-like filaments in *Bacillus subtilis*', *Cell*, 104(6), pp. 913-22.
- Jung, H., Pirch, T. and Hilger, D. (2006) 'Secondary transport of amino acids in prokaryotes', *J Membr Biol*, 213(2), pp. 119-33.
- Kamata, H., Akiyama, S., Morosawa, H., Ohta, T., Hamamoto, T., Kambe, T., Kagawa, Y. and Hirata, H. (1992) 'Primary structure of the alanine carrier protein of thermophilic bacterium PS3', *J Biol Chem*, 267(30), pp. 21650-5.
- Kanamori, M., Kamata, H., Yagisawa, H. and Hirata, H. (1999) 'Overexpression of the alanine carrier protein gene from thermophilic bacterium PS3 in *Escherichia coli*', *J Biochem*, 125(3), pp. 454-9.
- Kawai, Y., Asai, K. and Errington, J. (2009b) 'Partial functional redundancy of MreB isomers, MreB, Mbl and MreBh, in cell', *Molecular Microbiology*, 73(4), pp. 719-731.

- Kawai, Y., Daniel, R.A. and Errington, J. (2009a) 'Regulation of cell wall morphogenesis in *Bacillus subtilis* by recruitment of PBP1 to the MreB helix', *Mol Microbiol*, 71(5), pp. 1131-44.
- Kennedy, D.J., Leibach, F.H., Ganapathy, V. and Thwaites, D.T. (2002) 'Optimal absorptive transport of the dipeptide glycylsarcosine is dependent on functional Na⁺/H⁺ exchange activity', *Pflugers Arch*, 445(1), pp. 139-46.
- Kimura, K., Tran, L.S. and Itoh, Y. (2004) 'Roles and regulation of the glutamate racemase isogenes, *racE* and *yrpC*, in *Bacillus subtilis*', *Microbiology*, 150(Pt 9), pp. 2911-20.
- Kiriukhin, M.Y. and Neuhaus, F.C. (2001) 'D-alanylation of lipoteichoic acid: role of the D-alanyl carrier protein in acylation', *J Bacteriol*, 183(6), pp. 2051-8.
- Koch, A.L. (2006) 'The exocytoskeleton', *J Mol Microbiol Biotechnol*, 11(3-5), pp. 115-25.
- Koch, A.L. and Doyle, R.J. (1985a) 'Inside-to-outside growth and turnover of the wall of Gram-positive rods', *J Theor Biol*, 117(1), pp. 137-57.
- Koch, H.U., Döker, R. and Fischer, W. (1985b) 'Maintenance of D-alanine ester substitution of lipoteichoic acid by reesterification in *Staphylococcus aureus*', *J Bacteriol.*, 164(3), pp. 1211-1217.
- Koide, A. and Hoch, J.A. (1994) 'Identification of a second oligopeptide transport system in *Bacillus subtilis* and determination of its role in sporulation', *Mol Microbiol*, 13(3), pp. 417-26.
- Koide, A., Perego, M. and Hoch, J.A. (1999) 'ScoC regulates peptide transport and sporulation initiation in *Bacillus subtilis*', *J Bacteriol*, 181(13), pp. 4114-7.
- Konings, W.N. and Freese, E. (1972) 'Amino Acid Transport in Membrane Vesicles of *Bacillus subtilis*', *The Journal of Biological Chemistry*, 247, pp. 2408-2418.
- Korza, H.J. and Bochtler, M. (2005) '*Pseudomonas aeruginosa* LD-carboxypeptidase, a serine peptidase with a Ser-His-Glu triad and a nucleophilic elbow', *J Biol Chem*, 280(49), pp. 40802-12.
- Kovacs, M., Halfmann, A., Fedtke, I., Heintz, M., Peschel, A., Vollmer, W., Hakenbeck, R. and Bruckner, R. (2006) 'A functional *dlt* operon, encoding proteins required for incorporation of d-alanine in teichoic acids in gram-positive bacteria,

confers resistance to cationic antimicrobial peptides in *Streptococcus pneumoniae*', *J Bacteriol*, 188(16), pp. 5797-805.

Kramer, R. (1994) 'Systems and mechanisms of amino acid uptake and excretion in prokaryotes', *Arch Microbiol*, 162(1-2), pp. 1-13.

Kristian, S.A., Datta, V., Weidenmaier, C., Kansal, R., Fedtke, I., Peschel, A., Gallo, R.L. and Nizet, V. (2005) 'D-alanylation of teichoic acids promotes group A streptococcus antimicrobial peptide resistance, neutrophil survival, and epithelial cell invasion', *J Bacteriol*, 187(19), pp. 6719-25.

Kunst, F., Ogasawara, N., Moszer, I., Albertini, A.M., Alloni, G., Azevedo, V., Bertero, M.G., Bessieres, P., Bolotin, A., Borchert, S., Borriss, R., Boursier, L., Brans, A., Braun, M., Brignell, S.C., Bron, S., Brouillet, S., Bruschi, C.V., Caldwell, B., Capuano, V., Carter, N.M., Choi, S.K., Cordani, J.J., Connerton, I.F., Cummings, N.J., Daniel, R.A., Denziot, F., Devine, K.M., Dusterhoft, A., Ehrlich, S.D., Emmerson, P.T., Entian, K.D., Errington, J., Fabret, C., Ferrari, E., Foulger, D., Fritz, C., Fujita, M., Fujita, Y., Fuma, S., Galizzi, A., Galleron, N., Ghim, S.Y., Glaser, P., Goffeau, A., Golightly, E.J., Grandi, G., Guiseppi, G., Guy, B.J., Haga, K., Haiech, J., Harwood, C.R., Henaut, A., Hilbert, H., Holsappel, S., Hosono, S., Hullo, M.F., Itaya, M., Jones, L., Joris, B., Karamata, D., Kasahara, Y., Klaerr-Blanchard, M., Klein, C., Kobayashi, Y., Koetter, P., Koningstein, G., Krogh, S., Kumano, M., Kurita, K., Lapidus, A., Lardinois, S., Lauber, J., Lazarevic, V., Lee, S.M., Levine, A., Liu, H., Masuda, S., Mauel, C., Medigue, C., Medina, N., Mellado, R.P., Mizuno, M., Moestl, D., Nakai, S., Noback, M., Noone, D., O'Reilly, M., Ogawa, K., Ogiwara, A., Oudega, B., Park, S.H., Parro, V., Pohl, T.M., Portelle, D., Porwollik, S., Prescott, A.M., Presecan, E., Pujic, P., Purnelle, B., et al. (1997) 'The complete genome sequence of the gram-positive bacterium *Bacillus subtilis*', *Nature*, 390(6657), pp. 249-56.

Kuramitsu, H.K. and Snoke, J.E. (1962) 'The biosynthesis of D-amino acids in *Bacillus licheniformis*', *Biochimica et Biophysica Acta*, 62(1), pp. 114-121.

Kuru, E., Hughes, H.V., Brown, P.J., Hall, E., Tekkam, S., Cava, F., de Pedro, M.A., Brun, Y.V. and VanNieuwenhze, M.S. (2012) 'In Situ probing of newly synthesized peptidoglycan in live bacteria with fluorescent D-amino acids', *Angew Chem Int Ed Engl*, 51(50), pp. 12519-23.

- Lam, H., Oh, D.-C., Cava, F., Takacs, C.N., Clardy, J., Pedro, M.A.d. and Waldor, M.K. (2009) 'D-amino acids govern stationary phase cell wall remodeling in bacteria.', *Science*, 325(5947), pp. 1552-1555.
- Lebar, M.D., May, J.M., Meeske, A.J., Leiman, S.A., Lupoli, T.J., Tsukamoto, H., Losick, R., Rudner, D.Z., Walker, S. and Kahne, D. (2014) 'Reconstitution of Peptidoglycan Cross-Linking Leads to Improved Fluorescent Probes of Cell Wall Synthesis', *Journal of the American Chemical Society*, 136(31), pp. 10874-10877.
- LeDeaux, J.R., Solomon, J.M. and Grossman, A.D. (1997) 'Analysis of non-polar deletion mutations in the genes of the *spo0K* (*opp*) operon of *Bacillus subtilis*', *FEMS Microbiol Lett*, 153(1), pp. 63-9.
- Lewis, P.J. and Marston, A.L. (1999) 'GFP vectors for controlled expression and dual labelling of protein fusions in *Bacillus subtilis*', *Gene*, 227(1), pp. 101-10.
- Liman et al. (1992), *Neuron* 9:861 (with modification by E. Goulding and S. Siegelbaum of Columbia University P&S).
- Litzinger, S., Duckworth, A., Nitzsche, K., Risinger, C., Wittmann, V. and Mayer, C. (2010a) 'Muropeptide Rescue in *Bacillus subtilis* involves Sequential Hydrolysis by β -N-Acetylglucosaminidase and N-Acetylmuramyl-L-Alanine Amidase', *J. Bacteriol.*, 192(12), pp. 3132-3143.
- Litzinger, S., Fischer, S., Polzer, P., Diederichs, K., Welte, W. and Mayer, C. (2010b) 'Structural and kinetic analysis of *Bacillus subtilis* N-acetylglucosaminidase reveals a unique Asp-His dyad mechanism', *J Biol Chem*, 285(46), pp. 35675-84.
- Lupoli, T.J., Tsukamoto, H., Doud, E.H., Wang, T.-S.A., Walker, S. and Kahne, D. (2011) 'Transpeptidase-mediated incorporation of D-Amino Acids into bacterial peptidoglycan', *Journal of the American Chemical Society*, 133(28), pp. 10748-10751.
- MacArthur, A.E. and Archibald, A.R. (1984) 'Effect of culture pH on the D-alanine ester content of lipoteichoic acid in *Staphylococcus aureus*', *Journal of Bacteriology*, 160(2), pp. 792-793.
- MacLeod, P.R. and MacLeod, R.A. (1992) 'Identification and sequence of a Na(+)-linked gene from the marine bacterium *Alteromonas haloplanktis* which functionally complements the *dagA* gene of *Escherichia coli*', *Mol Microbiol*, 6(18), pp. 2673-81.

- Marfey, P. (1984) 'Determination of D-amino acids. II. Use of a bifunctional reagent, 1,5-difluoro-2,4-dinitrobenzene', *Carlsberg Research Communications*, 49(6), pp. 591-596.
- Martin, H.H. (1966) 'Biochemistry of bacterial cell walls', *Annu Rev Biochem*, 35, pp. 457-84.
- Martinez-Carrion, M. and Jenkins, W.T. (1965) 'D-Alanine-D-glutamate Transaminase (I. Purification and Characterization)', *The Journal of Biological Chemistry*, 240(9), pp. 3538-3546.
- Matias, V.R. and Beveridge, T.J. (2005) 'Cryo-electron microscopy reveals native polymeric cell wall structure in *Bacillus subtilis* 168 and the existence of a periplasmic space', *Mol Microbiol*, 56(1), pp. 240-51.
- Matias, V.R.F., Al-Amoudi, A., Dubochet, J. and Beveridge, T.J. (2003) 'Cryo-Transmission Electron Microscopy of Frozen-Hydrated Sections of *Escherichia coli* and *Pseudomonas aeruginosa*', *Journal of Bacteriology*, 185(20), pp. 6112-6118.
- Mauck, J., Chan, L. and Glaser, L. (1971) 'Turnover of the cell wall of Gram-positive bacteria', *J Biol Chem*, 246(6), pp. 1820-7.
- May, J.J., Finking, R., Wiegeshoff, F., Weber, T.T., Bandur, N., Koert, U. and Marahiel, M.A. (2005) 'Inhibition of the D-alanine: D-alanyl carrier protein ligase from *Bacillus subtilis* increase the bacterium's susceptibility to antibiotics that target the cell wall', *FEBS*, 272, pp. 2993-3003.
- Mayer, C. (2012) 'Bacterial Cell Wall Recycling.', In: eLS. John Wiley & Sons Ltd, Chichester. <http://www.els.net> [doi: 10.1002/9780470015902.a0021974].
- McPherson, D.C., Driks, A. and Popham, D.L. (2001) 'Two Class A High-Molecular-Weight Penicillin-Binding Proteins of *Bacillus subtilis* Play Redundant Roles in Sporulation', *Journal of Bacteriology*, 183(20), pp. 6046-6053.
- McPherson, D.C. and Popham, D.L. (2003) 'Peptidoglycan synthesis in the absence of class A penicillin-binding proteins in *Bacillus subtilis*', *J Bacteriol*, 185(4), pp. 1423-31.
- Meisner, J., Montero Llopis, P., Sham, L.T., Garner, E., Bernhardt, T.G. and Rudner, D.Z. (2013) 'FtsEX is required for CwlO peptidoglycan hydrolase activity during cell wall elongation in *Bacillus subtilis*', *Mol Microbiol*, 89(6), pp. 1069-83.

- Mendelson, N.H. (1976) 'Helical growth of *Bacillus subtilis*: a new model of cell growth', *Proceedings of the National Academy of Sciences of the United States of America*, 73(5), pp. 1740-1744.
- Merad, T., Archibald, A.R., Hancock, I.C., Harwood, C.R. and Hobot, J.A. (1989) 'Cell wall assembly in *Bacillus subtilis*: visualization of old and new wall material by electron microscopic examination of samples stained selectively for teichoic acid and teichuronic acid', *J Gen Microbiol*, 135(3), pp. 645-55.
- Metz, R., Henning, S. and Hammes, W.P. (1986) 'LD-carboxypeptidase activity in *Escherichia coli*. II. Isolation, purification and characterization of the enzyme from *E. coli* K 12', *Arch Microbiol*, 144(2), pp. 181-6.
- Miroux, B. and Walker, J.E. (1996) 'Over-production of proteins in *Escherichia coli*: mutant hosts that allow synthesis of some membrane proteins and globular proteins at high levels', *J Mol Biol*, 260(3), pp. 289-98.
- Mobley, H.L., Koch, A.L., Doyle, R.J. and Streips, U.N. (1984) 'Insertion and fate of the cell wall in *Bacillus subtilis*', *J Bacteriol*, 158(1), pp. 169-79.
- Moore, B.C. and Leigh, J.A. (2005) 'Markerless mutagenesis in *Methanococcus maripaludis* demonstrates roles for alanine dehydrogenase, alanine racemase, and alanine permease', *J Bacteriol*, 187(3), pp. 972-9.
- Muchová, K., Wilkinson, A.J. and Barák, I. (2011) 'Changes of lipid domains in *Bacillus subtilis* cells with disrupted cell wall peptidoglycan', *FEMS Microbiol Lett.*, 325(1), pp. 92-98.
- Murray, T., Popham, D.L. and Setlow, P. (1996) 'Identification and characterization of *pbpC*, the gene encoding *Bacillus subtilis* penicillin-binding protein 3', *J Bacteriol*, 178(20), pp. 6001-5.
- Murray, T., Popham, D.L. and Setlow, P. (1997) 'Identification and characterization of *pbpA* encoding *Bacillus subtilis* penicillin-binding protein 2A', *Journal of Bacteriology*, 179(9), pp. 3021-3029.
- Murray, T., Popham, D.L. and Setlow, P. (1998) '*Bacillus subtilis* cells lacking penicillin-binding protein 1 require increased levels of divalent cations for growth', *J Bacteriol*, 180(17), pp. 4555-63.

- Neuhaus, F.C. and Baddiley, J. (2003) 'A Continuum of Anionic Charge: Structures and Functions of D-Alanyl-Teichoic Acids in Gram-Positive Bacteria', *MICROBIOL. MOL. BIOL. REV.*, 67(4), pp. 686-723.
- Neuhaus, F.C. and Lynch, J.L. (1964) 'The Enzymatic Synthesis of D-alanyl-D-alanine. III. On the Inhibition of D-alanyl-D-alanine synthase by the Antibiotic D-cycloserine', *Biochemistry*, 3, pp. 471-80.
- Nicolas, P., Mader, U., Dervyn, E., Rochat, T., Leduc, A., Pigeonneau, N., Bidnenko, E., Marchadier, E., Hoebeke, M., Aymerich, S., Becher, D., Bisicchia, P., Botella, E., Delumeau, O., Doherty, G., Denham, E.L., Fogg, M.J., Fromion, V., Goelzer, A., Hansen, A., Hartig, E., Harwood, C.R., Homuth, G., Jarmer, H., Jules, M., Klipp, E., Le Chat, L., Lecointe, F., Lewis, P., Liebermeister, W., March, A., Mars, R.A., Nannapaneni, P., Noone, D., Pohl, S., Rinn, B., Rugheimer, F., Sappa, P.K., Samson, F., Schaffer, M., Schwikowski, B., Steil, L., Stulke, J., Wiegert, T., Devine, K.M., Wilkinson, A.J., van Dijl, J.M., Hecker, M., Volker, U., Bessieres, P. and Noirot, P. (2012) 'Condition-dependent transcriptome reveals high-level regulatory architecture in *Bacillus subtilis*', *Science*, 335(6072), pp. 1103-6.
- Nouaille, S., Commissaire, J., Gratadoux, J.J., Ravn, P., Bolotin, A., Gruss, A., Le Loir, Y. and Langella, P. (2004) 'Influence of lipoteichoic acid D-alanylation on protein secretion in *Lactococcus lactis* as revealed by random mutagenesis', *Appl Environ Microbiol*, 70(3), pp. 1600-7.
- Oggioni, M.R., Pozzi, G., Valensin, P.E., Galieni, P. and Bigazzi, C. (1998) 'Recurrent Septicemia in an Immunocompromised Patient Due to Probiotic Strains of *Bacillus subtilis*', *Journal of Clinical Microbiology*, 36(1), pp. 325-326.
- Osborne, S.E., Tuinema, B.R., Mok, M.C., Lau, P.S., Bui, N.K., Tomljenovic-Berube, A.M., Vollmer, W., Zhang, K., Junop, M. and Coombes, B.K. (2012) 'Characterization of DalS, an ATP-binding cassette transporter for D-alanine, and its role in pathogenesis in *Salmonella enterica*', *J Biol Chem*, 287(19), pp. 15242-50.
- Oxender, D.L. (1972) 'Membrane transport', *Annu Rev Biochem*, 41(10), pp. 777-814.
- Park, J.T. (1993) 'Turnover and recycling of the murein sacculus in oligopeptide permease-negative strains of *Escherichia coli*: indirect evidence for an alternative permease system and for a monolayered sacculus', *J Bacteriol*, 175(1), pp. 7-11.

- Park, J.T., Raychaudhuri, D., Li, H., Normark, S. and Mengin-Lecreulx, D. (1998) 'MppA, a periplasmic binding protein essential for import of the bacterial cell wall peptide L-alanyl-gamma-D-glutamyl-meso-diaminopimelate', *J Bacteriol*, 180(5), pp. 1215-23.
- Park, J.T. and Uehara, T. (2008) 'How bacteria consume their own exoskeletons (turnover and recycling of cell wall peptidoglycan)', *Microbiol. Mol. Biol. Rev.*, 72, pp. 211-227.
- Pedersen, L.B., Angert, E.R. and Setlow, P. (1999) 'Septal Localization of Penicillin-Binding Protein 1 in *Bacillus subtilis*', *Journal of Bacteriology*, 181(10), pp. 3201-3211.
- Pedersen, L.B., Murray, T., Popham, D.L. and Setlow, P. (1998) 'Characterization of *dacC*, which encodes a new low-molecular-weight penicillin-binding protein in *Bacillus subtilis*', *J Bacteriol*, 180(18), pp. 4967-73.
- Perego, M., Glaser, P., Minutello, A., Strauch, M.A., Leopold, K. and Fischer, W. (1995) 'Incorporation of D- Alanine into Lipoteichoic Acid and Wall Teichoic Acid in *Bacillus subtilis*. Identification of Genes and Regulation', *The journal of Biological Chemistry*, 270(26), pp. 15598-15606.
- Peschel, A., Vuong, C., Otto, M. and Gotz, F. (2000) 'The D-alanine residues of *Staphylococcus aureus* teichoic acids alter the susceptibility to vancomycin and the activity of autolytic enzymes', *Antimicrob Agents Chemother*, 44(10), pp. 2845-7.
- Pierce, K.J., Salifu, S.P. and Tangney, M. (2008) 'Gene cloning and characterization of a second alanine racemase from *Bacillus subtilis* encoded by *yncD*', *FEMS Microbiol Lett*, 283(1), pp. 69-74.
- Pooley, H.M. (1976a) 'Layered distribution, according to age, within the cell wall of *Bacillus subtilis*', *Journal of Bacteriology*, 125(3), pp. 1139-1147.
- Pooley, H.M. (1976b) 'Turnover and spreading of old wall during surface growth of *Bacillus subtilis*', *Journal of Bacteriology*, 125(3), pp. 1127-1138.
- Poolman, B. and Konings, W.N. (1993) 'Secondary solute transport in bacteria', *Biochim Biophys Acta*, 1183(1), pp. 5-39.
- Popham, D.L. (2013) 'Visualizing the production and arrangement of peptidoglycan in Gram-positive cells', *Mol Microbiol*, 88(4), pp. 645-9.

- Popham, D.L., Gilmore, M.E. and Setlow, P. (1999) 'Roles of low-molecular-weight penicillin-binding proteins in *Bacillus subtilis* spore peptidoglycan synthesis and spore properties', *J Bacteriol*, 181(1), pp. 126-32.
- Popham, D.L. and Setlow, P. (1996) 'Phenotypes of *Bacillus subtilis* mutants lacking multiple class A high-molecular-weight penicillin-binding proteins', *Journal of Bacteriology*, 178(7), pp. 2079-2085.
- Radkov, A.D. and Moe, L.A. (2014) 'Bacterial synthesis of D-amino acids', *Appl Microbiol Biotechnol*, 98(12), pp. 5363-74.
- Reeve, J.N., Mendelson, N.H., Coyne, S.I., Hallock, L.L. and Cole, R.M. (1973) 'Minicells of *Bacillus subtilis*', *J Bacteriol*, 114(2), pp. 860-73.
- Reichmann, N.T., Picarra Cassona, C. and Grundling, A. (2013) 'Revised mechanism of D-alanine incorporation into cell wall polymers in Gram-positive bacteria', *Microbiology*.
- Reith, J. and Mayer, C. (2011) 'Peptidoglycan turnover and recycling in Gram-positive bacteria', *Appl Microbiol Biotechnol*, 92, pp. 1-11.
- Robbins, J.C. and Oxender, D.L. (1973) 'Transport Systems for Alanine, Serine, and Glycine in *Escherichia coli* K-12', *Journal of Bacteriology*, 116(1), pp. 12-18.
- Roze, U. and Strominger, J., L. (1966) 'Alanine Racemase from *Staphylococcus aureus*: Conformation of its substrates and its inhibitor, D-cycloserine', *Mol. Pharmacol.*, 2, pp. 92-94.
- Russell, R.R.B. (1972) 'Mapping of a d-Cycloserine Resistance Locus in *Escherichia coli* K-12', *Journal of Bacteriology*, 111(2), pp. 622-624.
- Saar-Dover, R., Bitler, A., Ravit Nezer, Shmuel-Galia, L., Firon, A., Shimoni, E., Trieu-Cuot, P. and Shai, Y. (2012) 'D-Alanylation of Lipoteichoic acid Confers Resistance to Cationic Peptides in Group B *Streptococcus* by increasing the cell wall density.', *PLOS Pathogens*, 8(9).
- Saier, M.H. (2000) 'Families of transmembrane transporters selective for amino acids and their derivatives', *Microbiology*, 146, pp. 1775-1795.
- Sauvage, E., Kerff, F., Terrak, M., Ayala, J.A. and Charlier, P. (2008) 'The penicillin-binding proteins: structure and role in peptidoglycan biosynthesis', *FEMS Microbiol Rev*, 32(2), pp. 234-58.

- Scheffers, D.-J. and Errington, J. (2004) 'PBP1 Is a Component of the *Bacillus subtilis* Cell Division Machinery', *Journal of Bacteriology*, 186(15), pp. 5153-5156.
- Scheffers, D.J., Jones, L.J. and Errington, J. (2004) 'Several distinct localization patterns for penicillin-binding proteins in *Bacillus subtilis*', *Mol Microbiol*, 51(3), pp. 749-64.
- Schirner, K. and Errington, J. (2009) 'The Cell Wall Regulator σ (I) Specifically Suppresses the Lethal Phenotype of *mbl* Mutants in *Bacillus subtilis*', *Journal of Bacteriology*, 191(5), pp. 1404-1413.
- Schirner, K., Marles-Wright, J., Lewis, R.J. and Errington, J. (2009) 'Distinct and essential morphogenic functions for wall- and lipo-teichoic acid in *Bacillus subtilis*', *The EMBO Journal*, 28, pp. 830-842.
- Sekiguchi, J. and Yamamoto, H. (2012) 'Cell wall structure of *E. coli* and *B. subtilis*', p 115–148 In Sadaie Y, Matsumoto K, editors. (ed), *Escherichia coli and Bacillus subtilis: the frontiers of molecular microbiology revisited*. Research Signpost, Kerala, India.
- Sharpe, A., Blumberg, P.M. and Strominger, J.L. (1974) 'D- Alanine Carboxypeptidase and Cell wall Cross-Linking in *Bacillus subtilis*', *Journal of Bacteriology*, 117(2), pp. 926-927.
- Shockman, G.D. (1959) 'Reversal of cycloserine inhibition by D-alanine', *Proc Soc Exp Biol Med*, 101, pp. 693-5.
- Shockman, G.D. and Barrett, J.F. (1983) 'Structure, function, and assembly of cell walls of Gram-positive bacteria', *Annu Rev Microbiol*, 37, pp. 501-27.
- Sierro, N., Makita, Y., de Hoon, M. and Nakai, K. (2008) 'DBTBS: a database of transcriptional regulation in *Bacillus subtilis* containing upstream intergenic conservation information', *Nucleic Acids Res*, 36(Database issue), pp. D93-6.
- Sigel, E. (2010) 'Microinjection into *Xenopus* Oocytes', In: eLS. John Wiley & Sons Ltd, Chichester. <http://www.els.net> [doi: 10.1002/9780470015902.a0002658.pub2].
- Smith, T.J., Blackman, S.A. and Foster, S.J. (1996) 'Peptidoglycan hydrolases of *Bacillus subtilis* 168', *Microb Drug Resist*, 2(1), pp. 113-8.
- Smith, T.J., Blackman, s.A. and Foster, S.J. (2000) 'Autolysins of *Bacillus subtilis*: multiple enzymes with multiple functions', *Microbiology*, 146, pp. 249-262.

- Soldo, B., Lazarevic, V. and Karamata, D. (2002a) '*tagO* is involved in the synthesis of all anionic cell-wall polymers in *Bacillus subtilis* 168', *Microbiology*, 148(Pt 7), pp. 2079-87.
- Soldo, B., Lazarevic, V., Pagni, M. and Karamata, D. (1999) 'Teichuronic acid operon of *Bacillus subtilis* 168', *Mol Microbiol*, 31(3), pp. 795-805.
- Soldo, B., Lazarevic, V., Pooley, H.M. and Karamata, D. (2002b) 'Characterization of a *Bacillus subtilis* thermosensitive teichoic acid-deficient mutant: gene *mnaA* (*yvyH*) encodes the UDP-N-acetylglucosamine 2-epimerase', *J Bacteriol*, 184(15), pp. 4316-20.
- Soper, T.S. and Manning, J.M. (1981) 'Different modes of action of inhibitors of bacterial D-amino acid transaminase. A target enzyme for the design of new antibacterial agents', *J Biol Chem*, 256(9), pp. 4263-8.
- Soufo, H.J. and Graumann, P.L. (2003) 'Actin-like proteins MreB and Mbl from *Bacillus subtilis* are required for bipolar positioning of replication origins', *Curr Biol*, 13(21), pp. 1916-20.
- Steen, A., Buist, G., Leenhouts, K.J., El Khattabi, M., Grijpstra, F., Zomer, A.L., Venema, G., Kuipers, O.P. and Kok, J. (2003) 'Cell wall attachment of a widely distributed peptidoglycan binding domain is hindered by cell wall constituents', *J Biol Chem*, 278(26), pp. 23874-81.
- Strominger, J.L., Threnn, R. H. and Scott, S. S. (1959) 'Oxamycin, a competitive antagonist of the incorporation of D-alanine into a uridine nucleotide in *Staphylococcus aureus*', *J. Am. Chem. Soc.*, 81, pp. 3803-3804.
- Sudiarta, I.P., Fukushima, T. and Sekiguchi, J. (2010) '*Bacillus subtilis* CwlQ (previous YjbJ) is a bifunctional enzyme exhibiting muramidase and soluble-lytic transglycosylase activities', *Biochem Biophys Res Commun*, 398(3), pp. 606-12.
- Swoboda, J.G., Campbell, J., and, T.C.M. and Longwood, S. (2010) 'Wall Teichoic Acid Function, Biosynthesis, and Inhibition', *Chembiochem*, 11, pp. 35-45.
- Sycuro, L.K., Wyckoff, T.J., Biboy, J., Born, P., Pincus, Z., Vollmer, W. and Salama, N.R. (2012) 'Multiple peptidoglycan modification networks modulate *Helicobacter pylori*'s cell shape, motility, and colonization potential', *PLoS Pathog*, 8(3), p. e1002603.

- Tam, N.K.M., Uyen, N.Q., Hong, H.A., Duc, L.H., Hoa, T.T., Serra, C.R., Henriques, A.O. and Cutting, S.M. (2006) 'The Intestinal Life Cycle of *Bacillus subtilis* and Close Relatives', *Journal of Bacteriology*, 188(7), pp. 2692-2700.
- Tamehiro, N., Okamoto-Hosoya, Y., Okamoto, S., Ubukata, M., Hamada, M., Naganawa, H. and Ochi, K. (2002) 'Bacilysocin, a novel phospholipid antibiotic produced by *Bacillus subtilis* 168', *Antimicrob Agents Chemother*, 46(2), pp. 315-20.
- Templin, M.F., Ursinus, A. and Holtje, J.V. (1999) 'A defect in cell wall recycling triggers autolysis during the stationary growth phase of *Escherichia coli*', *EMBO J*, 18(15), pp. 4108-17.
- Thompson, R.J., Bouwer, H.G., Portnoy, D.A. and Frankel, F.R. (1998) 'Pathogenicity and immunogenicity of a *Listeria monocytogenes* strain that requires D-alanine for growth', *Infect Immun*, 66(8), pp. 3552-61.
- Thorne, C.B., Gómez, C.G. and Housewright, R.D. (1955) 'Transamination of D-Amino acids by *Bacillus subtilis*', *Journal of Bacteriology*, 69(3), p. 357.
- Tiyanont, K., Doan, T., Lazarus, M.B., Fang, X., Rudner, D.Z. and Walker, S. (2006) 'Imaging peptidoglycan biosynthesis in *Bacillus subtilis* with fluorescent antibiotics', *Proc Natl Acad Sci U S A*, 103(29), pp. 11033-8.
- Todd, J.A., Roberts, A.N., Johnstone, K., Piggot, P.J., Winter, G. and Ellar, D.J. (1986) 'Reduced heat resistance of mutant spores after cloning and mutagenesis of the *Bacillus subtilis* gene encoding penicillin-binding protein 5', *J Bacteriol*, 167(1), pp. 257-64.
- Tsuruoka, T., Tamura, A., Miyata, A., Takei, T., Iwamatsu, K., Inouye, S. and Matsubashi, M. (1984) 'Penicillin-insensitive incorporation of D-amino acids into cell wall peptidoglycan influences the amount of bound lipoprotein in *Escherichia coli*', *Journal of Bacteriology*, 160(3), pp. 889-894.
- Uehara, T. and Park, J.T. (2007) 'An anhydro-N-acetylmuramyl-L-alanine amidase with broad specificity tethered to the outer membrane of *Escherichia coli*', *J Bacteriol*, 189(15), pp. 5634-41.
- Ursinus, A., Steinhaus, H. and Holtje, J.V. (1992) 'Purification of a nocardicin A-sensitive LD-carboxypeptidase from *Escherichia coli* by affinity chromatography', *J Bacteriol*, 174(2), pp. 441-6.
- van Heijenoort, J. (2001) 'Formation of the glycan chains in the synthesis of bacterial peptidoglycan', *Glycobiology*, 11(3), pp. 25R-36R.

- Varley, A.W. and Stewart, G.C. (1992) 'The divIVB region of the *Bacillus subtilis* chromosome encodes homologs of *Escherichia coli* septum placement (*minCD*) and cell shape (*mreBCD*) determinants', *J Bacteriol*, 174(21), pp. 6729-42.
- Vollmer, W., Blanot, D. and de Pedro, M.A. (2008a) 'Peptidoglycan structure and architecture', *FEMS Microbiol Rev*, 32(2), pp. 149-67.
- Vollmer, W. and Holtje, J.V. (2001) 'Morphogenesis of *Escherichia coli*', *Curr Opin Microbiol*, 4(6), pp. 625-33.
- Vollmer, W. and Holtje, J.V. (2004) 'The architecture of the murein (peptidoglycan) in gram-negative bacteria: vertical scaffold or horizontal layer(s)?', *J Bacteriol*, 186(18), pp. 5978-87.
- Vollmer, W., Joris, B., Charlier, P. and Foster, S. (2008b) 'Bacterial peptidoglycan(murein) hydrolases', *FEMS Microbiol Rev*, 32, pp. 259-286.
- Votsch, W. and Templin, M.F. (2000) 'Characterization of a beta -N-acetylglucosaminidase of *Escherichia coli* and elucidation of its role in muropeptide recycling and beta -lactamase induction', *J Biol Chem*, 275(50), pp. 39032-8.
- Walsh, C.T. (1989) 'Enzymes in the D-Alanine Branch of Bacterial Cell Wall Peptidoglycan Assembly', *The journal of Biological Chemistry*, 264(5), pp. 2393-2396.
- Ward, J.B. (1981) 'Teichoic and Teichuronic Acids: Biosynthesis, Assembly, and Location', *Microbiological Reviews*, 45(2), pp. 211-243.
- Ward, J.B. and Perkins, H.R. (1973) 'The direction of glycan synthesis in a bacterial peptidoglycan', *Biochem J*, 135(4), pp. 721-8.
- Ward, J.B. and Zahler, S.A. (1973) 'Genetic studies of leucine biosynthesis in *Bacillus subtilis*', *J Bacteriol*, 116(2), pp. 719-26.
- Wargel, R.J., Shadur, C.A. and Neuhaus, F.C. (1970) 'Mechanism of D-cycloserine action: transport systems for D-alanine, D-cycloserine, L-alanine, and glycine', *J Bacteriol*, 103(3), pp. 778-88.
- Wargel, R.J., Shadur, C.A. and Neuhaus, F.C. (1971) 'Mechanism of d-Cycloserine Action: Transport Mutants for d-Alanine, d-Cycloserine, and Glycine', *Journal of Bacteriology*, 105(3), pp. 1028-1035.
- Warth, A.D. and Strominger, J.L. (1971) 'Structure of the peptidoglycan from vegetative cell walls of *Bacillus subtilis*', *Biochemistry*, 10(24), pp. 4349-58.

- Wecke, J., Madela, K. and Fischer, W. (1997) 'The absence of D-alanine from lipoteichoic acid and wall teichoic acid alters surface charge, enhances autolysis and increases susceptibility to methicillin in *Bacillus subtilis*', *Microbiology*, 143(9), pp. 2953-2960.
- Wecke, J., Perego, M. and Fischer, W. (1996) 'D-alanine deprivation of *Bacillus subtilis* teichoic acids is without effect on cell growth and morphology but affects the autolytic activity', *Microb Drug Resist*, 2(1), pp. 123-9.
- Wei, Y., Havasy, T., McPherson, D.C. and Popham, D.L. (2003) 'Rod shape determination by the *Bacillus subtilis* class B penicillin-binding proteins encoded by *pbpA* and *pbpH*', *J Bacteriol*, 185(16), pp. 4717-26.
- Wientjes, F.B., van 't Piet, J. and Nanninga, N. (1979) 'Formation of inside-out vesicles of *Bacillus licheniformis*. Dependence on buffer composition and lysis procedure', *Biochim Biophys Acta*, 553(2), pp. 213-23.
- Wong, W., Young, F.E. and Chatterjee, A.N. (1974) 'Regulation of Bacterial Cell Walls: Turnover of Cell Wall in *Staphylococcus aureus*', *Journal of Bacteriology*, 120(2), pp. 837-843.
- Wormann, M.E., Corrigan, R.M., Simpson, P.J., Matthews, S.J. and Grundling, A. (2011) 'Enzymatic activities and functional interdependencies of *Bacillus subtilis* lipoteichoic acid synthesis enzymes', *Mol Microbiol*, 79(3), pp. 566-83.
- Yanouri, A., Daniel, R.A., Errington, J. and Buchanan, C.E. (1993) 'Cloning and sequencing of the cell division gene *pbpB*, which encodes penicillin-binding protein 2B in *Bacillus subtilis*', *Journal of Bacteriology*, 175(23), pp. 7604-7616.
- Yonaha, K., Misono, H., Yamamoto, T. and Soda, K. (1975) 'D-amino acid aminotransferase of *Bacillus sphaericus*. Enzymologic and spectrometric properties', *J Biol Chem*, 250(17), pp. 6983-9.
- Yoshida, K., Fujita, Y. and Ehrlich, S.D. (1999) 'Three asparagine synthetase genes of *Bacillus subtilis*', *J Bacteriol*, 181(19), pp. 6081-91.
- Yoshimura, T. and Esak, N. (2003) 'Amino acid racemases: functions and mechanisms', *J Biosci Bioeng*, 96(2), pp. 103-9.
- Young, F.E. and Spizizen, J. (1961) 'Physiological and genetic factors affecting transformation of *Bacillus subtilis*', *J Bacteriol*, 81, pp. 823-9.

Zhang, G. and Sun, H.J. (2014) 'Racemization in Reverse: Evidence that D-Amino Acid Toxicity on Earth Is Controlled by Bacteria with Racemases', *PLoS ONE*, 9(3), p. e92101.

Zimbro, M.J., Power, D.A., Miller, S.M., Wilson, G.E. and Johnson, J.A. (2009) 'Difco™ & BBL™ Manual: Manual of Microbiological Culture Media, 2nd ed.', *BD Diagnostics-Diagnostic system 7 Loeton Cicle, Sparks, MD 21152-0999 USA*.

Zygmunt, W.A. (1962) 'Reversal of D-Cycloserine Inhibition of Bacterial growth by Alanine.', *J Bacteriol*, 84(1), pp. 154-6.

Appendices

Appendix A. Solutions and buffers

<u>Name</u>	<u>Composition</u>
DNA loading dye	0.04 % Bromphenol blue in 50 % glycerol
50× TAE buffer	2.0 M Tris pH 8.0 50 mM Acetic acid 100 mM EDTA
SSC	0.15 M Sodium chloride 0.01 M Sodium tricitrate pH 7.0
Protein gel fixation solution	10 % Methanol 10 % Acetic acid 10 % Isopropanol 5.0 % Glycerol
Coomassie brilliant blue (G) stain	1.6 %
1X MES SDS running buffer (Stock solution: 20X)	50 mM MES 50 mM Tris Base 0.1 % SDS 1.0 mM EDTA pH 7.3
Transfer Buffer (Wet transfer)	0.5X MES SDS running buffer 20 % Methanol
Protein membrane blocking buffer	3.0 % Milk powder 0.1 % Tween in PBS
PBST buffer	0.1 % Tween 20 in PBS
HPLC solution A	0.05M Triethylamine phosphate pH3
HPLC solution B	99.9 % Acetonitrile 0.1 % Formic acid
HPLC suspension solution	90 % 0.05M Triethylamine phosphate pH 3 9.99 % Acetonitrile 0.01 % Formic acid
Spizizen minimal medium (SMM)	0.2 % Ammonium sulphate 1.4 % Dipotassium phosphate 0.6 % Potassium dihydrogen phosphate 0.1 % Sodium citrate dihydrate

	0.02 %	Magnesium sulphate
Casamino acids (CAA)	20 %	Casamino acids
Solution D	0.1 M	CaCl ₂
Solution E	40 %	D-glucose
Solution F	1.0 M	MgSO ₄
Solution H	0.065 M	MnSO ₄
Solution P	5.0 ml 25 ml 0.1 ml	solution D solution F solution H filled up to 100 ml with d H ₂ O and autoclaved.
Universal buffer	300 mM 20 mM	NaCl Tris-HCl pH 8.0
Extraction buffer	300 mM 20 mM 1.5% 10%	NaCl Tris-HCl pH 8.0 DDM or 2% Triton X-100 Glycerol
Column equilibration buffer	300 mM 20 mM 0.2 % 10 %	NaCl Tris-HCl pH 8.0 DDM or 1.0 % Triton X-100 Glycerol
Column wash buffer	300 mM 20 mM 0.2% 10% 25 mM	NaCl Tris-HCl pH 8 DDM or 0.2 % Triton X-100 Glycerol Imidazole
Elution buffer	300 mM 20 mM 0.2 % 10 % 300 mM	NaCl Tris-HCl pH 8 DDM or 0.2 % Triton X-100 Glycerol Imidazole
Protoplast formation buffer	0.1 M 0.5 M 200µg/m	Potassium phosphate Sucrose Lysozyme pH7.3
TE buffer	10 mM 1.0 mM	Tris pH 8.0 EDTA

GTE buffer	50 mM	Glucose
	25 mM	Tris pH 8.0
	10 mM	EDTA pH 8.0
Cell fixation solution	3.0 %	Paraformaldehyde in PBS
Cell blocking solution	2.0 %	Bovine serum albumin in PBS

Appendix B. Growth media

<u>Name</u>	<u>Composition</u>
Pre-transformation medium (PTM)	10 ml SMM 0.25 ml solution E 0.1 ml Tryptophan 0.1 ml solution P 0.2 ml CAA
Transformation medium (TM)	10 ml SMM 0.15 ml solution E 0.05 ml solution F 5.0 µl CAA
LB medium	10 gm Tryptone 5 gm Yeast extract 10 gm NaCl adjusted to pH 7.0, filled up to 1.0 L with dH ₂ O and autoclaved.
Nutrient Agar	28 gm Oxoid Nutrient Agar filled up to 1.0 L with dH ₂ O and autoclaved.
PAB medium	17.5 gm Oxoid antibiotic medium no. 3 filled up to 1.0 L with dH ₂ O and autoclaved.
Minimal medium	0.2 % Ammonium sulphate 1.4 % Dipotassium phosphate 0.6 % Potassium dihydrogen phosphate 0.1 % Sodium citrate dihydrate 0.02 % Magnesium sulphate filled up to 97 ml with dH ₂ O and autoclaved, then the following solutions added. 1.5 ml solution E 0.6 ml solution F 0.05 ml solution D 1.0 ml Tryptophan for solid medium 1.5 % agar no.1 added.

Appendix C. Oligonucleotides

Name	Sequence	Restriction site	Purpose
oKS01	5'-AAGGAACAGATGATGCGCACG-3'	-----	For deletion of <i>dltA-D</i> genes
oKS02	5'AGT TCTAGAT CCGCATGTGTTTGAA TAGC-3'	<i>XbaI</i>	
oKS03	5'ATAT TCTAGAAAGATCT AGCGAAGGG CTTCCAGGTTGC-3'	<i>XbaI</i> and <i>BglII</i>	
oKS04	5'-TGCGATTTCTCCTGTTTCACCG-3'	-----	
oKS05	5'-ATGTACGCATAGGCCATTCCG-3'	-----	For deletion of <i>dacA</i> gene
oKS06	5'ATAG GGATCC GCCGTTAAGGACATT TTCAATGC-3'	<i>BamHI</i>	
oKS07	5'ATAG GGATCC TGATGGATGTTAGGG CTCTTTCG-3'	<i>BamHI</i>	
oKS08	5'-TCGCCTTTGTGTACAAGCTTTGC-3'	-----	
oKS09	5'-CAGGTTGCTCATCGTAA TCGCC-3'	-----	For deletion of <i>ldcB</i> gene
oKS10	5'-ATAG GGATCC CGCTTACACTAGATA AGCGGGC-3'	<i>BamHI</i>	
oKS11	5'TGC GGATCC TATCAATCGTTTCCG CATGC-3'	<i>BamHI</i>	
oKS12	5'-TAGTATTCGGCACAGATCGGC-3'	-----	
oKS13	5'-TATCATGGACATATGACGGCG-3'	-----	For checking <i>alrA</i> gene deletion
oKS14	5'-TGCTTCGTTTCTCCCGCATCGC-3'	-----	
oKS15	5'-TAGCTCCGGTCGGCGGAGGGC-3'	-----	For checking <i>ldcB</i> gene deletion
oKS16	5'-AAGCCCTGTCAATTCTCACCG-3'	-----	
oKS17	5'-CGCGAAAGCCATCCGCATGACG-3'	-----	For checking <i>dacA</i> gene deletion
oKS18	5'-TGTTTGAGCCATTCTTGGTC-3'	-----	
oKS19	5'-GTTTCTGCTTTCACCTGAACG-3'	-----	For checking <i>dltAD</i> genes Deletion
oKS20	5'-ATTGCCAAGTTCCAGCAGGCG-3'	-----	

oKS21	5'ATC <u>TCTAGA</u> AATGATATTTTTTTCTA GGGGAGAAGAAGC-3	<i>XbaI</i>	For pKS1 construction
oKS22	5'TGAT <u>TCTAGAT</u> TCAGCTGATATTTTCGT TCGCTGGC-3	<i>XbaI</i>	
oKS23	5'ACG <u>CTCGAG</u> ATGCAAAAACAAAA CAAGAGCTGC-3	<i>XhoI</i>	For pKS2 and pKS3 construction
oKS24	5'ATAG <u>GAATTC</u> GCTGATATTTTCGTTTCG CTGGCAGCAGC-3	<i>EcoRI</i>	
oKS25	5'ATC <u>TCTAGA</u> AAAATTTAAAAGGAGG TCATCAGCCTATGCAAAAACAAAAAC AAGAGCTGCACCGC-3	<i>XbaI</i>	For pKS6 construction
oKS26	5'TGA <u>AGATCT</u> TCAGCTGATATTTTCGT TCGCTGGC-3	<i>BglII</i>	
oKS27	5'ATA <u>CCATGGG</u> CATGCAAAAACAAA AACAAGAGC-3	<i>NcoI</i>	For pKS7 construction
oKS28	5'ATAG <u>GGATCC</u> GCTGATATTTTCGTTTCG CTGGC-3	<i>BamHI</i>	
oKS29	5'ATAG <u>GCTAGC</u> ATGCAAAAACAAAA CAAGAGC-3	<i>NheI</i>	For pKS8 construction
oKS30	5'ATA <u>CTCGAG</u> TCAGCTGATATTTTCGT TCGCTGGC-3	<i>XhoI</i>	
oKS31	5'-CAGCCGTAAAATTTGGACTGTGC-3	-----	For checking <i>datA</i> gene deletion
oKS32	5'-CAACAAACATAAGACCTGCTTCG-3	-----	
oKS33	5'-TGAAGTGGCGGAACGGATTTACC G-3	-----	For checking <i>alaT</i> gene deletion
oKS34	5'-ATATCACACATGTCTTATTTCCGC-3	-----	
oKS35	5'-TGGA ACTACTGGTTTTT TATGGG-3	-----	For checking the sequence of cloned <i>datA</i> gene, it binds to 300 bases downstream of start codon

oKS36	5'-AACCCGCAAAAATCGTTAGCC-3'	-----	For checking the sequence of cloned <i>datA</i> gene, it binds to 700 bases downstream of start codon
oKS37	5'-TACAAAATGCCTTTATTTCCG-3'	-----	For checking the sequence of cloned <i>datA</i> gene, it binds to 1200 bases downstream of start codon
oKS38	5'-AACGGCTCGGTGACATGTAT-3'	-----	oKS38 to oKS69 used for transcription analysis of <i>datA</i> gene
oKS39	5'-TGTTCAATGGCTTTGATCGT-3'	-----	
oKS40	5'-GGACTTGGACCAGCAAACAG-3'	-----	
oKS41	5'-CGGAAAACCTCCCTTTTCT-3'	-----	
oKS42	5'-AGCGGTGCTTTCTGTGAAAT-3'	-----	
oKS43	5'-GTGCGGCTATTATTGCGATT-3'	-----	
oKS44	5'-TGTCCAGCTCTTGATGAACG-3'	-----	
oKS45	5'-CAGAGAGTGGGAAGGGCTTT-3'	-----	
oKS46	5'-GCATCACAAGAAGCGGAAC-3'	-----	
oKS47	5'-TCGCTCCGTCACTTAAGGTT-3'	-----	
oKS48	5'-ACTTGCCCCGTGAATGATTA-3'	-----	
oKS49	5'-TTCTCCGATCACGACATCAC-3'	-----	
oKS50	5'-CGGAGAACAGTCCAGCATTT-3'	-----	
oKS51	5'-ATCCCGATTAAGGCGTTCTT-3'	-----	
oKS52	5'-CGCCCTGCAAAAGTCATC-3'	-----	
oKS53	5'-TTGCTGGCTGTGTACTATGGA-3'	-----	
oKS54	5'-TTTCTTTTCTTCCGGCTTCA-3'	-----	
oKS55	5'-ATCCCGGGTAAAGCTGTTCT-3'	-----	
oKS56	5'-GCGGTGCAGCTCTTGTTT-3'	-----	
oKS57	5'-AGCTGAGCCATCAGCCTAAA-3'	-----	
oKS58	5'-CCGTTCTTCGTTTTTCAGCTC-3'	-----	
oKS59	5'-CGCGATGTGACGAAGACTTA-3'	-----	
oKS60	5'-GCTTGTTAAAAACCCCGACA-3'	-----	
oKS61	5'-GGAGCAGCTGCGTAAAGAAG-3'	-----	

oKS62	5'-GGGCAAGTGAAATTGGAAGA-3'	-----	oKS38 to oKS69 used for transcription analysis of <i>datA</i> gene
oKS63	5'-ATCGGATACACACGTGCAAAA-3'	-----	
oKS64	5'-GCCCCTCCGTAACAGATTC-3'	-----	
oKS65	5'-TGAAAGGCACAAAGACCAAAA-3'	-----	
oKS66	5'-TCGTAAAAGGGTTTGCAATG-3'	-----	
oKS67	5'-CAGCGGTCAAATCAACTGAG-3'	-----	
oKS68	5'-AGCGGCTGTACACGAAAGTT-3'	-----	
oKS69	5'-AACGGCTGCTCAACTGTTTT-3'	-----	
oKS70	5'-ATCATCAATAAACCGACAGC-3'	-----	For checking the sequence of cloned <i>datA</i> gene, it binds to 500 bases downstream of <i>datA</i> start codon
oKS71	5'-GCGC <u>GAATTC</u> CCACCATGGCAAAA CAAAAACAAGAGCTGCACCGCGGACT CG-3'	<i>EcoRI</i>	For construction of pKS9 and pKS11
oKS72	5'GCGC <u>TCTAG</u> ACCTTAGCTGATATTT CGTTCGCTGGCAGCAGCCGC-3'	<i>XbaI</i>	For construction of pKS9 and pKS10
oKS73	5'-GCGC <u>GAATTC</u> CCACCATGGC TAC CCATACGATGTTCCAGATTACGCTCA AAAACAAAACAAGAGCTGCACCGC GGACTCG-3'	<i>EcoRI</i>	For pKS10 construction
oKS74	5'-GCGC <u>TCTAG</u> ACCTTA AGCGTAATC TGGAACATCGTATGGGTAGCTGATAT TTCGTTCGCTGGCAGCAGCCGC-3'	<i>XbaI</i>	For pKS11 construction

- The restriction sites are bolded and underlined.
- The red highlighted nucleotides represent the coding sequence of HA-epitope.

Appendix D. Distribution of DatA (formerly YtnA) homologous proteins

The following data are generated by STRING 9.1 bioinformatics database. The coloured cells represent the families and groups of the organisms (see the end of the table).

Families	Organisms	Protein	Function	Bit score
Enterobacteriaceae	<i>Escherichia coli</i>	ProY	Putative proline-specific permease	603.4
	<i>Escherichia fergusonii</i>			600.9
	<i>Salmonella enterica</i>			600.9
	<i>Yersinia pestis</i>			606.5
	<i>Yersinia pseudotuberculosis</i>			605.5
	<i>Yersinia enterocolitica</i>			616.6
	<i>Shigella flexneri</i>			597.4
	<i>Shigella boydii</i>			603.4
	<i>Shigella dysenteriae</i>			603.4
	<i>Shigella sonnei</i>			603.4
	<i>Klebsiella pneumoniae</i>			598.5
	<i>Dickeya zeae</i>			611.4
	<i>Hamiltonella defensa</i>			589.7
	<i>Pectobacterium spp</i>			616.6
	<i>Cronobacter spp</i>			599.2
	<i>Edwardsiella</i>			614.9
	<i>Photobacterium spp</i>			573.0
	<i>Erwinia pyrifoliae</i>			605.1
	<i>Proteus mirabilis</i>			566.7
	<i>Enterobacter sp</i>			595.0
	<i>Dickeya dadantii</i>	Dd703_2910		617.0
	<i>Citrobacter koseri</i>	CKO_02767		596.7
	<i>Serratia proteamaculans</i>	Spro_1046		618.7
Pseudomonadaceae	<i>Pseudomonas aeruginosa</i>	PA0789	Amino acid permease	739.5
	<i>Pseudomonas putida</i>	PputW619_1089		728.3
	<i>Pseudomonas fluorescens</i>	PFL_4906		736.4
	<i>Pseudomonas entomophila</i>	PSEEN1179	Amino acid permease	729.4
	<i>Pseudomonas syringae</i>	ProY	Proline-specific permease	568
	<i>Pseudomonas stutzeri</i>	AroP1	Aromatic amino acid transport protein	479.8
	<i>Sodalis glossinidius</i>	SG0465		480.5
Thiotrichales	<i>Francisella tularensis</i>	FTF1633c	Amino acid transporter	356.9
	<i>Francisella novicida</i>	LysP	Lysine:H ⁺ symporter	357.6
	<i>Francisella philomiragia</i>	Fphi_0529		359.7

Families	Organisms	Protein	Function	Bit score
Moraxellaceae	<i>Acinetobacter baumannii</i>	ProY	Proline-specific permease	552.7
	<i>Acinetobacter sp.</i>	ACIAD1168	Amino acid APC transporter	549.6
Xanthomonadaceae	<i>Xanthomonas oryzae</i>	PXO_04173	D-alanine/D-serine/glycine permease	467.2
	<i>Xanthomonas campestris</i>	XCC3533		488.8
	<i>Xanthomonas axonopodis</i>	XAC0600		488.1
	<i>Xanthomonas campestris</i>	CycA		481.2
	<i>Stenotrophomonas maltophilia</i>	Smlt0526		466.5
Legionellales	<i>Legionella pneumophila</i>	LPC_2317	Amino acid permease	321.6
Unclassified Gammaproteobacteria	<i>Baumannia cicadellinicola</i>	LysP	Lysine-specific permease	338.4
Aeromonadaceae	<i>Aeromonas hydrophila</i>	AroP	Aromatic amino acid transport protein	512.9
	<i>Aeromonas salmonicida</i>	ASA_2547		512.9
	<i>Tolumonas auensis</i>	Tola_2345	Amino acid permease-associated region	491.6
Rhizobiaceae	<i>Rhizobium etli</i>	AnsP	L-asparagine permease protein	398.8
	<i>Agrobacterium radiobacter</i>			403.3
	<i>Agrobacterium tumefaciens</i>			398.8
	<i>Rhizobium sp.</i>	NGR_b23020		436.1
	<i>Rhizobium leguminosarum</i>	Rleg2_5754	Amino acid permease-associated region	396.3
Brucellaceae	<i>Brucella melitensis</i>	BAWG_1429	D-serine/D-alanine/glycine transporter	462.0
	<i>Brucella abortus</i>	BruAb2_0056	Amino acid permease family protein	462.0
	<i>Brucella suis</i>	BRA0056		462.0
	<i>Brucella microti</i>	BMI_II58		458.1
	<i>Brucella ovis</i>	BOV_A0051		464.4
	<i>Ochrobactrum anthropi</i>	Oant_4275	Amino acid permease-associated region	467.9
Methylobacterium	<i>Methylobacterium nodulans</i>	Mnod_4992	Amino acid permease-associated region	608.9












Families	Organisms	Protein	Function	Bit score	
Bertonella	<i>Bartonella quintana</i>	BQ06710	Amino acid permease	505.9	
	<i>Bartonella grahamii</i>	Bgr_12560		500.4	
	<i>Bartonella tribocorum</i>	BT_1464		494.4	
	<i>Bartonella henselae</i>	BH06520		500.7	
	<i>Bartonella bacilliformis</i>	AroP	Aromatic amino acid transport protein	479.1	
Xanthobacteraceae	<i>Azorhizobium caulinodans</i>	AZC_1994	Putative amino acid permease	471.7	
Acetobacteraceae	' <i>Gluconobacter oxydans</i> '	GOX0699	L-asparagine permease	448.0	
	<i>Acetobacter pasteurianus</i>	APA01_02480	Amino acid transporter	438.9	
	<i>Gluconacetobacter diazotrophicus</i>	AapA	Putative amino acid permease	383.1	
Sphingomonadaceae	<i>Sphingomonas wittichii</i>	Swit_0683	Amino acid permease	386.2	
Caulobacteraceae	<i>Caulobacter sp</i>	Caul_5252	Amino acid permease	467.9	
Berkholderiaceae	<i>Burkholderia pseudomallei</i>	ProY	Proline-specific permease	767.1	
	<i>Burkholderia mallei</i>	BMA_2796	Amino acid permease	764.7	
	<i>Burkholderia thailandensis</i>	BTH_I3129	Amino acid permease-associated region	764.7	
	<i>Burkholderia cenocepacia</i>	Bcen2424_4371		750.7	
	<i>Burkholderia ambifaria</i>	BamMC4_06_1095		550.6	
	<i>Burkholderia vietnamiensis</i>	Bcep1808_4336		647.3	
	<i>Burkholderia phytofirmans</i>	Bphyt_3123		513.6	
	<i>Burkholderia phymatum</i>	Bphy_0601		508.4	
	<i>Burkholderia glumae</i>	bglu_2g11350		533.9	
	<i>Ralstonia eutropha</i>	Reut_B4894		761.5	
	<i>Burkholderia sp</i>	Bcep1819_4_B1646		Amino acid transporter	747.2
	<i>Burkholderia multivorans</i>	Bmul_4250		AAT family amino acid transporter	754.2
	<i>Burkholderia xenovorans</i>	Bxe_A0842	Aromatic amino acid/H ⁺ symporter	509.4	
	<i>Ralstonia eutropha</i>	H16_B2165	Amino acid ABC transporter permease	752.8	

Families	Organisms	Protein	Function	Bit score
Berkholderiaceae	<i>Cupriavidus taiwanensis</i>	ProY	Proline transport protein, APC family	746.2
	<i>Ralstonia metallidurans</i>	Rmet_5046	Histidine transport protein	580.0
	<i>Ralstonia pickettii</i>	Rpic12D_0905	Amino acid permease-associated region	575.4
	<i>Polynucleobacter necessarius</i>	Pnuc_0665		632.3
	<i>Ralstonia solanacearum</i>	LysP	Lysine-specific permease	369.1
Comamonadaceae	<i>Acidovorax citrulli</i>	Aave_2608	D-alanine/D-serine/glycine permease	495.8
	<i>Delftia acidovorans</i>	Daci_3739		484.3
	<i>Comamonas testosteroni</i>	CtCNB1_0951		601.3
	<i>Verminophrobacter eiseniae'</i>	Veis_2830	Amino acid permeas	383.4
Bordetella	<i>Bordetella avium</i>	BAV1610	Lysine-specific permease	370.1
	<i>Bordetella parapertussis</i>	LysP		356.5
	<i>Bordetella petrii</i>			365.2
	<i>Bordetella bronchiseptica</i>	cadR		359.7
Neisseriaceae	<i>Laribacter hongkongensis</i>	LysP	Lysine-specific permease	354.1
	<i>Chromobacterium violaceum</i>	ProY	Proline-specific permease	792.2
Desulfovibrionaceae	<i>Desulfovibrio desulfuricans</i>	Ddes_0172	Amino acid permease	662.7
Campylobacteraceae	<i>Campylobacter fetus</i>	LysP	Lysine-specific permease	363.5
	<i>Sulfurospirillum deleyianum</i>	Sdel_0552	Amino acid permease-region	464.8
Helicobacteraceae	<i>Helicobacter pylori</i>	HP_1017	Amino acid permease	359.7
	<i>Helicobacter acinonychis</i>	rocE		359.7
Leuconostocaceae	<i>Leuconostoc citreum</i>	LCK_00446	Gamma-aminobutyrate permease	479.8
	<i>Leuconostoc mesenteroides</i>	LEUM_0515	Amino acid transporter	501.4
Staphylococcaceae	<i>Staphylococcus aureus</i>	SAR2400	Putative amino acid permease	542.3
	<i>Staphylococcus epidermidis</i>	SERP1902	Amino acid permease	534.2
Listeria	<i>Listeria monocytogenes</i>	ProY	Proline-specific permease	586.6
Paenibacillaceae	<i>Brevibacillus brevis</i>	BBR47_14760	Amino acid permease	567.0
Veillonella	<i>Veillonella parvula</i>	Vpar_1627	Amino acid permease	582.1

Families	Organisms	Protein	Function	Bit score
Streptococcaceae	<i>Streptococcus pyogenes</i>	M5005_Spy_1359	Amino acid permease	400.2
	<i>Streptococcus suis</i>	SSU98_2026		336.6
	<i>Streptococcus equi</i>	SZO_03910		401.6
	<i>Streptococcus dysgalactiae</i>	SDEG_1715		402.3
	<i>Streptococcus agalactiae</i>	SAG1480		415.9
	<i>Streptococcus uberis</i>	SUB1411		390.4
	<i>Streptococcus mutans</i>	SMU_1450	Putative amino acid permease	399.1
	<i>Streptococcus thermophilus</i>	CycA	D-Serine/D-alanine/glycine: H ⁺ symporter	388.3
	<i>Lactococcus lactis</i>	LysP	Lysine specific permease	374.0
Lactobacillaceae	<i>Lactobacillus reuteri</i>	lr0024	Amino acid permease-associated region	497.9
	<i>Lactobacillus rhamnosus</i>	ProY	Amino acid permease	495.5
	<i>Lactobacillus delbrueckii</i>	Ldb1796		370.8
	<i>Lactobacillus johnsonii</i>	LJ_0507		488.8
	<i>Lactobacillus plantarum</i>	lp_0120	Amino acid transport protein	497.2
	<i>Lactobacillus casei</i>	LSEI_0642	amino acid transporter	496.5
	<i>'Pediococcus pentosaceus'</i>	PEPE_1230	Gamma-aminobutyrate permease related permease	505.2
Exiguobacterium	<i>Exiguobacterium sibiricum</i>	Exig_0221	Amino acid permease	715.1
Clostridiaceae	<i>Clostridium botulinum Eklund</i>	CLL_A1399	D-serine/D-alanine/glycine transporter	552.0
	<i>Clostridium botulinum</i>	CLK_3428	Lysine-specific permease	385.5
	<i>Clostridium novyi</i>	NT01CX_2354	Lysine-specific permease	390.0
	<i>Clostridium perfringens</i>	CPE1166		383.4
	<i>Clostridium kluyveri</i>	CKL_0647	Putative amino acid permease	638.3
	<i>Clostridium acetobutylicum</i>	YifK		559.7
Lysinibacillus	<i>Lysinibacillus sphaericus</i>	Bsph_0500	Hypothetical protein	638.6

Families	Organisms	Protein	Function	Bit score
Bacillaceae	<i>Bacillus cereus</i>	ProY	Proline-specific permease	796.4
	<i>Bacillus thuringiensis</i>			796.8
	<i>Bacillus anthracis</i>	BAS0659	Amino acid permease family protein	796.4
	<i>Bacillus weihenstephanensis</i>	BcerKBA B4_0608		796.8
	<i>Bacillus licheniformis</i>	YdgF	-----	571.9
	<i>Bacillus amyloliquefaciens</i>	YtnA	-----	943.8
	<i>Bacillus pumilus</i>	YbxG	APC family amino acid-polyamine-organocation transporter	566.0
	<i>Geobacillus spp</i>	GK3461	Amino acid transporter	845.3
	<i>Bacillus subtilis</i>	YtnA	Putative amino acid permease	1059.7
Peptococcaceae	<i>Desulfitobacterium hafniense</i>	Dhaf_2459	Amino acid permease-associated region	605.8
	<i>Desulfotomaculum reducens</i>	Dred_3225		600.2
Thermoanaerobacteraceae	<i>Carboxydotherrnus hydrogenoformans</i>	CHY_2456	Amino acid permease	582.1
Corynebacterineae	<i>Mycobacterium tuberculosis</i>	CycA	D-serine/alanine/glycine transporter protein	459.9
	<i>Mycobacterium bovis</i>			463.0
	<i>Mycobacterium ulcerans</i>			392.5
	<i>Mycobacterium marinum</i>			459.5
	<i>Mycobacterium leprae</i>			AnsP
	<i>Mycobacterium smegmatis</i>	MSMEG_3587	457.4	
	<i>Corynebacterium spp</i>	cu0683	Putative transporter	473.8
	<i>Rhodococcus erythropolis</i>	ProY	Proline-specific permease	549.9
	<i>Nocardia farcinica</i>	NFA_12290	Putative amino acid transporter	551.0
	<i>Gordonia bronchialis</i>	Gbro_2751	Amino acid permease	352.0
	Micrococcaceae	<i>Arthrobacter spp</i>	Arth_0369	Amino acid permease
<i>Micrococcus luteus</i>		Mlut_01910	Gamma-aminobutyrate permease-like transporter	484.7
<i>Kocuria rhizophila</i>		proY	Putative proline-specific permease	532.8

Families	Organisms	Protein	Function	Bit score
Microbacteriaceae	<i>Clavibacter michiganensis</i>	CMS0688	Putative L-asparagine permease	399.1
	<i>Leifsonia xyli</i>	ansP		400.2
Frankineae	<i>Nakamurella multipartita</i>	Namu_1301	Amino acid permease	430.9
Pseudonocardiaceae	<i>Saccharopolyspora erythraea</i>	SACE_5703	Amino acid permease-associated region	568.8
Streptosporangineae	<i>Streptosporangium roseum</i>	Sros_2891	L-asparagine permease	478.7
Streptomyces	<i>Streptomyces spp</i>	SGR_4625	Putative proline permease	536.0
Propionibacterineae	<i>Propionibacterium acnes</i>	PPA1069	Aromatic amino acid transport protein	549.2
-----	<i>Catenulispora acidiphila</i>	Caci_3270	Amino acid permease	476.3
-----	<i>Kineococcus radiotolerans</i>	Krad_4431	Amino acid permease	432.6
Bifidobacterium	<i>Bifidobacterium longum</i>	aroP	Aromatic amino acid transport protein	470.3
Flavobacteriaceae	<i>Flavobacterium johnsoniae</i>	Fjoh_3147	Amino acid permease	458.5
Elusimicrobia	<i>Uncultured bacterium</i>	TGRD_007	Aromatic amino acid transport protein	435.8
Arthropoda	<i>Apis mellifera</i>	GB13584	Similar to CG12531-PA	396.7
Caenorhabditis	<i>Caenorhabditis japonica</i>	CJA29188	-----	398.1
	<i>Caenorhabditis remanei</i>	CRE09959		450.4
Trichocomaceae	<i>Aspergillus spp</i>	-----	Putative amino acid permease	331.4
Saccharomycetaceae	<i>Pichia stipitis</i>	GAP1.2	General amino acid permease	316.4
	<i>Saccharomyces cerevisiae</i>	LYP1	High-affinity Lysine-specific permease	317.4
Poaceae	<i>Oryza sativa Indica</i>	BGIOSIB SE037819	-----	473.5

 Protobacteria-G	 Protobacteria-E	 Others	 Bacteria
 Protobacteria-A	 Firmicutes		 Eukaryot
 Protobacteria-B	 Actinobacteria		
 Protobacteria-D	 Bacteroidetes		

Appendix E. Transport of D-alanine by DataA protein translated in oocytes of *Xenopus laevis*.

- ***Making complimentary ribonucleic acid (cRNA)***

The pKS9 construct (pGH19 Ω *dataA*) (table 2.2) was firstly linearised by restriction digestion with *XhoI*. The linear construct was used as template in making cRNA, using *in vitro* transcription system (mMessage mMachine T7 transcription kit, Ambion™).

- ***Microinjection of cRNA into the oocytes***

A 50 μ l of cRNA (50 ng) was injected into the recovered *Xenopus laevis* oocytes in Barth's solution, using a Nanoject II automated injector (Drummond Scientific Company, Broomall, USA). The injected oocytes were kept at 18 °C for three days before use.

- ***D-alanine transport in oocytes.***

The transport of D-alanine into the oocytes was done according to (Bertran *et al.*, 1992) and (Kennedy *et al.*, 2002). The prepared oocytes were incubated in transport solution for 2.0 min. The oocytes were washed and suspended in 200 μ l of transport solutions (pH 5.5 and 7.0) plus [³H] D-alanine (1.0 μ M, 5.0 μ Ci/ml). The transport suspension was incubated at 22 °C for 40 min, and then the oocytes were washed 3.0 times with ice-cold transport solution. The oocytes were lysed with 200 μ l of 10 % SDS in scintillation vials (n=10), and then 1.0 ml of Optiphase HiSafe scintillation cocktail (PerkinElmer, Beaconsfield, UK) was added. The mixture was vortexed and the radioactivity (DPM) was measured, using an LS6500 liquid scintillation counter (Beckman Coulter, High Wycombe, UK).

Solutions composition

Barth's solution: 88 mM NaCl, ; 1.0 mM KCl; 0.41 mM CaCl₂; 0.82 mM MgSO₄; 0.33 mM Ca(NO₃)₂; 2.4 mM NaHCO₃; 10 mM HEPES; pH 7.5 with Tris base.

Transport solution: 100 mM NaCl; 2.0 mM KCl; 1.0 mM CaCl₂; 1.0 mM MgCl₂; 10 MES (pH 5.5 with Tris base) or HEPES (pH 7.0 with Tris base).

Publications

Hoyland, C.N., Aldridge, C., Cleverley, R.M., Duchene, M.C., Minasov, G., Onopriyenko, O., Sidiq, K., Stogios, P.J., Anderson, W.F., Daniel, R.A., Savchenko, A., Vollmer, W. and Lewis, R.J. (2014) 'Structure of the LdcB LD-carboxypeptidase reveals the molecular basis of peptidoglycan recognition', *Structure*, 22(7), pp. 949-60.